THE UNIVERSITY OF MANITOBA

UNIT CONNECTION OF GENERATORS TO HVDC CONVERTERS

BY

MALAKONDAIAH NAIDU

A Thesis

Submitted to the Faculty of Graduate Studies

in Partial Fullfilment of the Requirements for the Degree

of Doctor of Philosophy

DEPARTMENT OF ELECTRICAL ENGINEERING

WINNIPEG, MANITOBA R3T 2N2

CANADA

April 1987

ISBN 0-315-37408-X

UNIT CONNECTION OF GENERATORS TO HVDC CONVERTERS

BY

MALAKONDAIAH NAIDU

A thesis submitted to the Faculty of Graduate Studies of
the University of Manitoba in partial fulfillment of the requirements
of the degree of

DOCTOR OF PHILOSOPHY

ABSTRACT

If the power is solely for transmission from remote generating stations to the load centres, by adopting HVDC unit connection schemes, considerable savings can be achieved at the sending end terminal. A methodology has been developed to operate hydroturbine under variable speed operation to maximize the efficiency under variable loading and water head conditions. A six phase generator is modeled in d-q-o co-ordinates and harmonic currents flowing in the stator and the rotor windings are computed by simulating the generator directly connected to a 12-pulse converter.

A 500 MW unit connection scheme has been simulated in time domain using EMTDC program. The recovery of the system for different faults have been studied. Also generator derating factors for 60 Hz and 70 Hz operations have been evaluated. It has been found that a generator designed for 60 Hz operation at 0.85 pf has to be derated to 86.3% to operate at 70 Hz operation with 12-pulse converter load.

A small signal model of a generator with diode bridge rectifier is developed to study the controller response in order to control the dc voltage through generator field voltage. A 500 MW, 250 kV diode rectifier scheme has been simulated in time domain and it was found that the total recovery time from a dc line fault is about 3.0 s.

Economic evaluation of a 10X100 MW hydro power station and a 1000 MW nuclear power station has been performed based on the available data and it was found that by adopting unit connection schemes C$ 50x 10^6 can be saved for hydrostation and C$ 20 x 10^6 for back-to-back and C$ 13 x 10^6 for point-to-point schemes for nuclear stations with six phase generators.

In conclusion, unit connection schemes can emerge as viable economical alternatives to conventional HVDC current collector schemes.

ACKNOWLEDGEMENTS

The author expresses deep sense of gratitude to Professors R.M.Mathur, M.Z.Tarnawecky, D. Card of the University of Manitoba and Professor Dennis Woodford of the Manitoba HVDC Research Centre for serving on his Advisory Committee.

The author is indebted to Dr. R.M.Mathur, the author's thesis supervisor for the stimulating guidance and useful suggestions as a scholar and educator to accomplish this endeavor. The author has immensely benefited from his association with Dr. R.M.Mathur for continuous encouragement, perennial approachability in spite of administrative schedules being the Department Head and absolute freedom of thought and action and will appreciate such relationship for many years to come.

A special word of thanks reserved to Dr. A.M.Gole , Dr. R.W.Menzies and Prof. M.Z.Tarnawecky for sparing their time for useful discussions.

The author is very much grateful to Manitoba HVDC Research Centre for financing the first phase of this investigation, Manitoba Hydro and National Research Council of Canada for financing the second phase of this investigation.

The author expresses profound gratitude to Mr C.V.Thio, John Mc Nichol, Jack Heidrick of Manitoba Hydro for their bounteous assistance rendered in providing useful system data and also for useful discussions during this investigation.

Finally, the author expresses sincere appreciation to his wife Padma, and children Madhavi and Sridhar for their encouragement, patience and understanding for the many months of neglect during the execution of this endeavor.

TABLE OF CONTENTS

	page
ABSTACT	ii
ACKNOWLEDGEMENTS	iii
TABLE OF CONTENTS	iv
LIST OF FIGURES	ix
LIST OF TABLES	xv
LIST OF MOST USED SYMBOLS	xvii
CHAPTER I : INTRODUCTION	
1.1 General	1
1.2 Problem definition	4
1.3 Primary objective	7
1.4 Scope of the thesis	7
1.5 State–of–the–art of the unit connection schemes	10
CHAPTER II : CONFIGURATIONS FOR UNIT CONNECTION SCHEMES	
2.1 Introduction	14
2.2 Summary of advantages and disadvantages of unit connection schemes	15
2.3 Selection of candidate configurations	19
2.4 Candidate configurations for nuclear power plants	20
2.5 Candidate configurations for hydro power plants	27
2.6 Summary	32
CHAPTER III : PERFORMANCE EVALUATION OF HYDRAULIC TURBINES	
3.1 Introduction	33
3.2 Parameters governing the operation of the hydraulic turbines	34
3.2.1 Cavitation phenomenon	36
3.2.2 Unit power and fuctional relationship	37
3.3 Hydroturbine efficiency evaluation	38
3.3.1 Efficiency evaluation with fixed speed operation	39

3.3.2 Efficiency evaluation with variable speed operation . . 41
3.4 Performance evaluation of a 10X100 MW hydro station under variable speed operation 53
3.5 Summary and conclusions 59
CHAPTER IV : GENERATORS FOR UNIT CONNECTION SCHEMES
4.1 Introduction 61
4.2 Six phase generators 66
4.3 Harmonic analysis of the air gap mmf of a six phase generator connected to a 12–pulse converter 71
4.3.1 Analysis of the air gap mmf of a Y–Y connected armature windings 71
4.3.2 Analysis of the air gap mmf of a Y–Δ connected armature windings 75
4.3.3 Conclusions 77
4.4 Performance of a six phase generator connected to a 12–pulse converter 78
4.4.1 Six phase generator model 78
4.4.2 Digital simulation of a six phase generator connected to a 12–pulse converter 86
4.4.2.1 Interface of a six phase generator with the EMTDC program 86
4.4.3 Simulation results 90
4.4.3.1 Commutation reactance 90
4.4.3.2 Additional losses in the generator . . . 96
4.4.3.3 Evaluation of derating factor 98
4.5 Special design and operating features of generators for unit connection schemes. 101
4.6 Commutation reactance and its effect on the generator performance 105
4.6.1 Equivalent circuits for Block and Double Block

connection 105
4.6.2 Significance of commutation reactance
on the generator performance 107
4.7 Three phase generators 113
4.7.1 Additional losses and derating factor
for 60 Hz operation 114
4.7.2 Additional losses and derating factor
for 70 Hz operation 119
4.8 Summary and conclusions 123
CHAPTER V : DC SYSTEM ASPECTS OF UNIT
CONNECTION SCHEMES
5.1 Introduction 124
5.2 Hydro power station interface with dc system 126
5.2.1 Determination of the ratings of converters and
converter transformers 128
5.2.2 Determination of the ratings of converters and converter
transformers with unequal bridge ratings at the inverter 136.
5.3 Interface of a 1000 MW nuclear power station
with dc system 140
5.4 Discussions . . . . . .
5.5 Digital simulation of unit connection scheme. 143
5.5.1 DC controls 145
5.5.2 System startup – simulation 146
5.5.3 Simulation results 150
5.5.4 Discussions 161
5.6 Unit connection schemes with diode bridge rectifiers . . 164
5.6.1 Introduction 164
5.7 Digital simulation of a diode rectifier
unit connection scheme 165
5.7.1 System startup 165
5.7.2 Simulation results 167

5.7.3 Conclusions 171

CHAPTER VI : ECONOMIC EVALUATION OF UNIT CONNECTION SCHEMES

6.1 Introduction 172

6.2 A 10X100 MW hydro power station with conventional current collector scheme 172

6.2.1 Economic evaluation of a 10X100 MW conventional current collector scheme 174

6.2.1 Economic evaluation of a 10X100 MW unit connection scheme 177

6.3 Economic evaluation of a 1000 MW nuclear power station . . 182

6.3.1 Economic Evaluation of a 1000 MW point-to-point conventional current collector scheme for nuclear power station 182

6.3.2 Economic Evaluation of a 1000 MW nuclear power power station with unit connection scheme . . . 185

6.4 Economic evaluation of a 1000 MW nuclear power station with back-to-back scheme 186

6.4.1 Economic Evaluation of a 1000 MW conventional nuclear power station 189

6.4.2 Economic Evaluation of a 1000 MW nuclear station with conventional back-to-back scheme 189

6.4.3 Economic Evaluation of a 1000 MW unit connected nuclear power station with back-to-back scheme . 191

6.4.4 Discussions 192

6.5 Summary and conclusions 193

CHAPTER VII : CONCLUSIONS AND RECOMMENDATIONS

7.1 Major conclusions 194

7.2 Recommendations for future work 196

BIBLIOGRAPHY 197
APPENDIXI 203
APPENDIXII 207
APPENDIXIII 220
APPENDIXIV 226
APPENDIXV 229

LIST OF FIGURES

Figure		page
1.1	Essential features of a conventional current collector HVDC transmission scheme.	6
1.2	Unit connection of generator converters for HVDC transmission scheme.	6
2.1a	1000 MW bipolar transmission scheme for nuclear power station with a three phase generator and three–winding transformers.	21
2.1b	1000 MW bipolar back–to–back scheme for nuclear power station with a three phase generator and three–winding transformers.	21
2.1c	1000 MW bipolar transmission scheme for nuclear power station with a three phase generator and three–winding transformers.	22
2.1d	1000 MW bipolar back–to–back scheme for nuclear power station with a three phase generator and two–winding transformers.	22
2.2a	1000 MW transmission scheme with metalic return for nuclear power station with a six phase generator and two–winding transformers with one twelve pulse valve group.	24
2.2b	1000 MW back–to–back scheme with metalic return for nuclear power station with a six phase generator and two–winding transformers with two pulse valve groups. .	24
2.2c	1000 MW transmission scheme with metalic return for nuclear power station with a six phase generator	

	and three–winding transformers with two twelve pulse valve groups.	24
2.2d	1000 MW bipolar transmission scheme for nuclear power station with six phase generator and two–winding transformers.	25
2.2e	1000 MW bipolar transmission scheme for nuclear power station with a six phase generator and three–winding transformers.	25
2.2f	1000 MW bipolar transmission scheme for nuclear power station with a six phase generator and three–winding transformers.	26
2.2g	1000 MW back–to–back scheme for nuclear power station with a six phase generator without converter transformers.	26
2.3a	10X100 MW bipolar transmission scheme for hydro power station with three phase generators and three–winding transformers.	30
2.3b	10X100 MW bipolar transmission scheme for hydro power station with groups of three phase genera–tors and three–winding transformers per unit.	30
2.3c	10X100 MW bipolar transmission scheme for hydro power station with five three phase generators per pole with three–winding transformers.	31
2.3d	10X100 MW back–to–back scheme for hydro power station with groups of three phase generator per unit. . . .	31
3.1	A typical model turbine performance curves	40
3.2	Variation of efficiency with water head at 105% load.	42

3.3	Variation of efficiency with water head at 100% load.	43
3.4	Variation of efficiency with water head at 95% load.	44
3.5	Variation of efficiency with water head at 90% load.	45
3.6	Variation of speed with water head at different loads.	46
3.7	Variation of efficiency with load at water head of 80 ft. . .	48
	water head of 80 ft.	48
3.8	Variation of efficiency with load duration at	
3.9	Variation of turbine efficiency for different loads at	
	different water heads with fixed speed operation. . .	49
3.10	Variation of turbine efficiency for different loads at	
	different water heads with variable speed operation. . .	50
3.11	Loading curve of turbines with equal loading criteria. . . .	51
3.12	Annual load curve of a 10X100 MW hydrostation.	54
3.13	Annual water head variation curve of a 10X100 MW	
	hydrostation	55
3.14	Averaged annual water head variation of a 10X100 MW	
	hydrostation	56
3.15	Averaged annual load curve of a 10X100 MW hydrostation. .	56
3.16	Increase in turbine efficiency with load under–	
	variable speed operation	57
4.1	Phase current of a 5 phase generator fed with	
	10 pulse converter.	63
4.2	Losses at the surface of the rotor due limited	68
	number of phases.	68
4.3	Variation of losses with the air gap for 3–phase generator. .	69
4.4	Variation of losses with air gap for six phase generator. .	69
4.5	Y–Y windings configuration with 12–pulse converter. . .	74

4.6	Generator currents for Y−Y windings configuration with 30° phase shift.	74
4.7	Y−Δ windings configuration with 12−pulse converter. . . .	76
4.8	Generator phase currents for Y−Δ windings configuration. .	76
4.9	Six phase generator with equivalent damper windings.	79
4.10	D−axis flux model of a six phase generator.	81
4.11	Six phase generator equivalent circuits.	82
4.12	System configuration for digital simulation.	87
4.13	Constant current control at the inverter.	87
4.14	Interface of a sysnchronous machine with EMTDC network. .	88
4.15	Steady state performance of a six phase generator directly connected to a 12−pulse converter.	91
4.16	Generator rotor currents under steady state.	92
4.17	Dynamic response of a six phase generator directly connected to a 12−pulse converter.	93
4.18	Capacity per unit volume of 2−pole generators at different base speeds.	102
4.19	Capacity per unit volume of 4−pole generators at different base speeds.	102
4.20	Electrical loading of 2−pole generators at different base speeds.	103
4.21	Electrical loading of 4−pole generators at different base speeds.	103
4.22	Block connection; (a) Single line diagram, (b) Equivalent circuit	106
4.22	Double Block connection; (a) Single line diagram, (b) Equivalent circuit	106

5.1	Interface of unit connected hydrostation with dc system. .	127
5.2	Schematic diagram for digital simulation of unit connection scheme.	144
5.3a	Block diagram of pole controller (POL1C6).	147
5.3b	Block diagram of valve group controller (VG1C18).	148
5.3c	Block diagram of the static exciter model.	149
5.4	Block diagram of DC controls.	151
5.5a	DC line fault at the rectifier (60 Hz operation).	152
5.5b	DC line fault at the rectifier (70 Hz operation).	153
5.6a	Permanent dc block (60 Hz operation).	154
5.6b	Permanent dc block (70 Hz operation).	155
5.7a	3–phase to ground fault at the rectifier(60 Hz operation). .	157
5.7b	3–phase to ground fault at the rectifier (70 Hz operation). .	158
5.8a	Single line to ground fault at the rectifier (60 Hz operation). .	159
5.8b	Single line to ground fault at the rectifier (70 Hz operation). .	160
5.19	Simulation setup with diode bridge rectifiers for unit connection scheme.	166
5.20	Steady state performance of the diode bridge rectifier unit connection scheme.	168
5.21a	Performance of the diode rectifier unit connection scheme for dc line fault.	169
5.21b	Performance of the diode bridge rectifier unit connection scheme for dc line fault.	170
6.1	Single line diagram of a 10X100 MW hydro power station with conventional current collector scheme.	173
6.2	Single line diagram of a 10X100 MW hydro power station with unit connection scheme.	178

6.3 Single line diagram of a 1000 MW nuclear power station with conventional current collector scheme. 183

6.4 Single line diagram of a 1000 MW nuclear power station with unit connection scheme. 187

6.5 Variation of the price per terminal per kW with HVDC terminal size. 188

6.6 1000 MW conventional nuclear generating station. . . . 190

6.7 1000 MW conventional HVDC back–to–back scheme for nuclear power station. 190

6.8 1000 MW unit connected back–to–back scheme with six phase generator for nuclear power station. 190

LIST OF TABLES

Table		page
4.1	Harmonic winding factors of a six phase generator	74
4.2	Magnitude and direction of space harmonics generated by time harmonic currents in Y−Y windings with 30° phase shift. . .	74
4.3	Magnitude and direction of space harmonics generated by time harmonic currents in Y−Δ windings configuration.	76
4.4	Magnitude of harmonic currents in six phase generator with 12−pulse converter load at α = 15.18°for 60 Hz operation. .	96
4.5	Variation of commutation angle at different frequencies for various delay angles with a hydrogenerator.	107
4.6	Variation of commutation angle at different frequencies for various delay angles with a turbogenerator.	109
4.7	Variation of power factor at different frequencies for various delay angles with a hydrogenerator.	110
4.8	Variation of power factor at different frequencies for various delay angles with a turbogenerator.	111
4.9	Magnitude of harmonic currents in the generator with 12−pulse converter load at α = 13.7° for 60 Hz operation. . .	112
4.10	Magnitude of harmonic currents in the generator with 12−pulse converter load at α = 19.5° for 70 Hz operation.	119
5.1	Efficiency variation of a 120 MVA 0.85 pf salient pole synchronous generator with load.	131
5.2	Loading sequence of generators and converters of a 10X100 MW unit connected station depending upon the load demand. . .	134

5.3 Loading sequence of generators and converters of a 8X125 MW unit connected station depending upon the load demand. . . 135

5.4 Loading sequence of generators and converters of a 10X100 MW unit connected station depending upon the load demand. . . 139

5.5 System parameters under fault conditions for 60/70 Hz operation. 162

6.1 Cost break down in C$ per kW of HVDC terminal equipment. . . 175

6.2 Cost break down in US $ per Terminal per kW. 180

LIST OF MOST USED SYMBOLS

E_c = Line to line commutation voltage.

E = Electromotive force.

Δe_f = Incremental field voltage.

f = Frequency in Hz.

$F(p)$ = Direct axis operational impedance.

F_a, F_b, F_c = Armature m.m.fs of a, b and c phases.

F_x, F_y, F_z = Armature m.m.fs of x, y and z phases.

F_p, F_q, F_c = Armature m.m.fs of p, q and r phases.

F_{abc}, F_{xyz} = Total armature m.m.fs due a, b and c and x, y and z phases respectively.

F_{pqr} = Total armature m.m.f of p, q and r phases.

F_{Y-Y} = Total air gap m.m.f of Y-Y windings of the armature.

$F_{Y-\Delta}$ = Total air gap m.m.f of Y-Δ windings of the armature.

$G(p)$ = Excitation factor (operational impedance).

g = Acceleration due to gravity, ft/s^2.

h = A posive integer.

$H(p)$ = Quadrature axis operational impedance.

H = Water head in ft.

H_{sv} = Absolute head at the outlet of turbine, ft.

h_a = Atmospheric head, ft.

i_a, i_b, i_c = Instantaneous armature phase currents in 3-phase Y connected windings.

i_x, i_y, i_z = Instantaneous armature phase currents in 3-phase Y connnected windings displaced by 30 degrees with respect to the above winding set.

i_p, i_q, i_r = Instantaneous armature phase currents in 3- phase Δ connected windings.

i_s, i_t, i_u = Instantaneous armature line currents of Δ connected 3-phase windings.

i_{d1} , i_{d2} = D-axis currents for winding sets 1 and 2.

i_{q1}, i_{q2} = Q-axis currents for winding sets 1 and 2.

i_f = Field current.

I_{dc} = DC current.

J = Moment of inertia.

k = Any positive integer.

K_{dm} = Dstribution factor for m th space harmonic winding.

K_{pm} = Pitch factor for m th space harmonic winding.

K_{wm} = $K_{dm} . K_{pm}$ = Winding factor for m th harmonic.

L_a = Self inductance of the generator.

L_{md} = Direct axis magnetizing reactance.

L_{12} = Mutual inductance between ABC and XYZ phases on d and q axis equivalent coils.

L_{mq} = Quadrature axis magnetizing inductance.

L_{kd}, L_{kq} = Self inductances of damper windings.

L_F = Self inductance of the field winding.

L_s = Smoothing inductor.

L_{o1}, L_{o2} = Zero sequence inductances.

M_t = Shaft torque.

m = $(2h + 1)$ = Order of space harmonic.

N_s = Specific speed of the hydraulic turbine.

N = Speed in rpm.

N_a = Number of turns per pole per phase.

n = $(6k \pm 1)$ = Order of time harmonic.

p = Laplace operator.

P = Horsepower

P_{11} = Unit power of the model turbine.

Q = Water discharge, ft^3/s.

q = Number of slots per pole per phase.

T_{do}' = Direct axis subtransient open-circuit time constant.

T_d' = Direct axis transient short circuit time constant.

T_{do}'' = Direct axis subtransient open circuit time constant.

T_d'' = Direct axis subtransient short circuit time constant.

T_q'' = Quadrature axis short circuit time constant.

T_{kd} = Direct axis damper (leakage) time constant.

U = Voltage behind subtansient reactance per phase.

V_{dc} = DC voltage.

v_{d1} , v_{d2} = D-axis voltages for winding sets 1 and 2.

v_{q1}, v_{q2} = Q-axis voltages for winding sets 1 and 2.

ω_n = Un damped natural frequency, radians /s.

ω_d = Damped natural frequency, radians /s

ω = Angular frequency, radians /s.

x_d = Direct axis synchronous reactance.

x_d' = Direct axis transient reactance.

x_d'' = Direct axis subtransient reactance.

X_t = Leakage reactance of the transformer.

t_r = Rise time in, s.

θ = Phase shift between E and V.

θ' = Phase shift between E and U.

γ = Slot angle.

ϵ = Chording angle.

ψ_{d1}, ψ_{d2} = D-axis fluxlinkages of winding sets 1 and 2.

ψ_{q1}, ψ_{q2} = Q-axis fluxlinkages of winding sets 1 and 2.

CHAPTER I

INTRODUCTION

1.1 General

Electrical energy consumption continues to increase all over the world. Gradually, the energy resources near load centres are being exhausted. Consequently there is greater emphasis on developing remote hydro stations, mine mouth thermal stations and super nuclear stations far removed from the populated areas for fear of health hazards. Development of remote power stations require provision of appropriate electric power transmission capacity. In this regard EHV ac and HVDC transmission systems have lately attracted the attention of power system planners and designers.

There are several situations where HVDC transmission is justified over EHV ac transmission on the basis of economy and technical advantages. Some important advantages of the application of HVDC transmission are:

1. Fast controllability and power reversal capacity.
2. Asynchronous coupling of sending end and receiving end ac systems.
3. Lower transmission line cost and lower transmission line losses.
4. Smaller right-of-way requirements.

5. No line compensation is required.

Some of the situations where HVDC is found to be more attractive are as follows:

(1) Transmission of bulk power over long distances

To transmit bulk power generated from remote hydro stations, or from remote mine mouth thermal stations, or from remotely located nuclear stations to load centers, where long distances are involved, HVDC transmission is more economical alternative.

The following are some of the examples of such schemes:

(a) *Remote Hydro Stations :*

(i) Nelson River scheme in Manitoba, Canada, for 1600 MW, ± 450 kV, and 2000 MW, ± 500 kV, transmitted over 895 km.

(ii) Cobora Bassa - Appolo scheme in Zaire, Africa, for 1920 MW, ± 533 kV, over 1414 km.

(b) *Mine mouth Thermal Stations :*

(i) Ekibastuz Centre Plant in USSR, with ultimate capacity of 6000 MW, ± 750 kV, over 2500 km.

(2) Connecting two large ac systems of different frequencies:

Power can be interchanged between two large ac systems operating at different frequencies only by connecting these two systems through asynchronous HVDC interconnection. For example, between Shin and Shinano in Japan, 300 MW, ± 125 kV, HVDC tie is in operation.

(3) Cables crossing bodies of water:

Due to the requirement of large charging current, power transfer capability of ac cables depends upon the distance involved. Where as, in the case of dc cables no charging current is required and hence power can be transferred for long distances. For example, Cross Channel I and II between Great Britain and France with 160 MW, ± 100 kV and 2000 MW, ± 270 kV are in operation.

In HVDC transmission considerable saving is made in the cost of transmission lines for a given power as compared to ac lines. The HVDC schemes however require additional investment at the converting stations. It is when the savings from the transmission exceed the added expenditure at the converters that the HVDC schemes become economically justifiable. In situations where cables are required (water crossings) the savings in transmission cost in the case of dc as compared to ac are larger.

In situations where the HVDC starts from a generating station, it is possible to reduce the generating station-switch yard- HVDC rectifier station cost further by utilizing the unit connection of generators with HVDC converters. By doing so the ac switch yard can be almost totally eliminated and several components such as ac filters, generator circuit breakers and at least one level of transformers can be eliminated. In addition, by virtue of direct connection of generators with converters restrictions of fixed power frequency generation and fixed speed operation of turbines can be sacrificed which result in further savings.

This thesis examines various aspects of unit connection of HVDC converters with variable frequency generators driven by variable speed turbines.

1.2 Problem definition

Modern power systems are standardized to operate at 50 Hz or 60 Hz. Standardization of operating frequency imposes speed restrictions on turbines and generators which once designed must operate under very tight speed tolerances. Because of turbine characteristics and number of pairs of poles in turbogenerators, all steam turbines operate at 1500/1800 or 3000/3600 rpm for 50/60 Hz generation. Hydro turbines on the other hand operate in the wider range of lower but fixed speeds.

In a conventional scheme, usually called current collector scheme, all generators of a station and those from nearby stations are connected to a common ac bus. The HVDC transmission system which is separately optimized for current and voltage levels is then connected to this collector bus. The collector bus operates almost like an ideal voltage source by connecting to it appropriate tuned ac filters and where necessary a separate controllable reactive power source.

Fig. (1.1) shows the essential components of a current collector HVDC transmission scheme. The sending end converter station comprises typically one or two twelve pulse valve groups per pole (C), converter transformer (TC) between the collector ac bus and converters. Tuned ac filters are installed on the ac bus to absorb harmonic currents generated by the converters. At the fundamental power frequency the filters also supply a part of the reactive power required for the the converters. Each generator (G)

driven by a turbine (T) is connected to a common current collector ac bus through a generator breaker (B) and the generator transformer (TG). Additional controllable reactive power sources if required can be connected to the common ac bus (not shown in the Fig. (1.1) as they are not normally required).

If the power generated at the generating station is exclusively for transmission to a remote load centre, considerable simplification can be achieved at the sending end by intergrating generating and converting stations. The connection of each turbine and generator to 12-pulse converters is called " Unit Connection of Generator to Converters ". The main aim of this thesis is to investigate the application of unit connection schemes for HVDC transmission.

Fig. (1.2) shows the essential elements of the unit connection of generator to converters. The generator (G) driven by a turbine (T) is connected to a 12-pulse converter (C) through converter transformers (TC). Considerable simplification at the sending end station is achieved by dispensing ac filters, ac switch yard and associated protection equipment, generator transformer and generator breakers. Converters can be located in the proximity of the generator, in which case terminal faults on the ac side of the generator can be minimized. Since each generator in the station is separately connected to converters, operation of turbines and generators at fixed speed/frequency may not be meaningful. Tight speed restrictions on the part of the turbine-governor can be relaxed. Turbines can be operated under variable speeds or at higher base speeds for economic advantages. For example, in the case of a hydro power station where variations in water head and load normally occur during the year, operating turbines under fixed speeds dictated by the system frequency results in loss of turbine efficiency. If the system frequency is not a criteria, where station

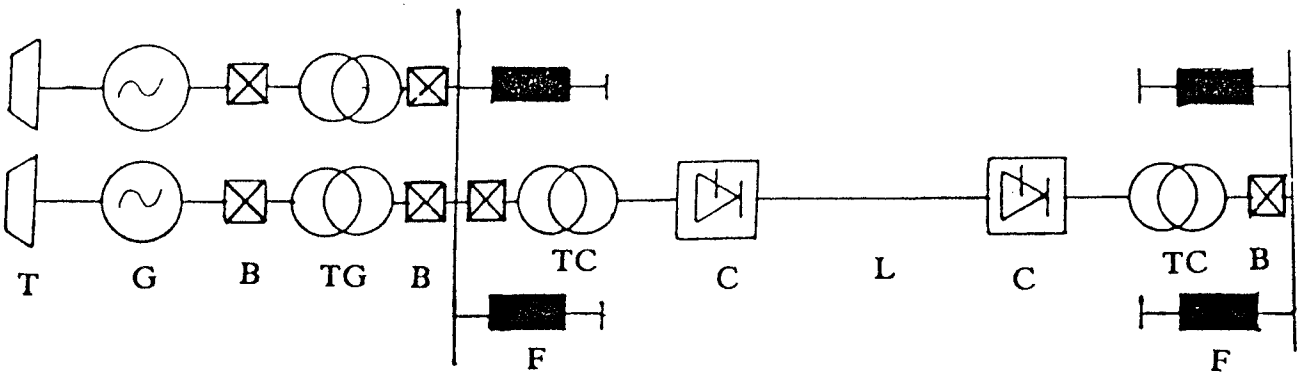

Fig. 1.1 Essential features of a conventional current collector HVDC transmission scheme.

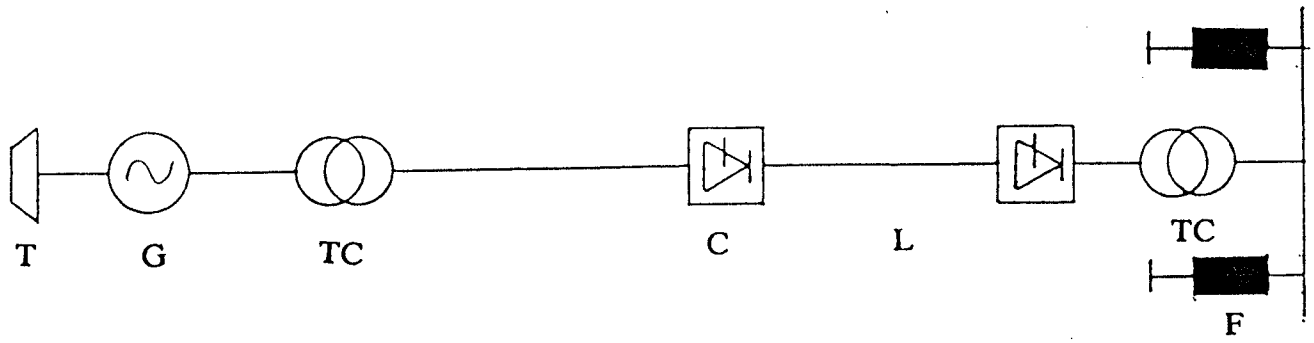

Fig. 1.2 Unit connection of generator to converter for HVDC transmission scheme.

T : Turbine
G : Generator
B : Generator Breaker
TG: Generator Transformer
TC: Converter Transformer
F : Filter Circuits
C : Converter Station
L : Transmission Line

auxiliaries are to be fed from a separate power source, there is a possibility of operating turbine under variable speeds to obtain maximum efficiency depending upon the available water head and load demand.

In the case of thermal or nuclear power stations turbines and generators can be designed at higher base speed operation to minimize the capital cost. Moreover it is not necessary to restrict to conventional three phase generators. Multiphase generators can be designed with compact sizes at improved efficiencies. Diode rectifiers converters can be employed instead of thyristor converters for further savings. But due to the lack of controllability of the diode rectifiers, the applicability of these schemes need further investigation.

All those promising features of unit connection schemes mentioned above need detailed investigation. Most of the important features of unit connection schemes are analyzed in this thesis.

1.3 Primary objective

To conduct a systematic study of the technical aspects of the performance of turbine-generator-converter unit connection schemes. As well to conduct a preliminary economic viability of unit connection schemes.

1.5 Scope of the thesis

This thesis covers broadly the following important aspects :

(1) At first, pros and cons of unit connection schemes are broadly identified on the basis of technical, economical and reliability aspects.

A systems approach is used to select possible configurations of unit connection schemes for hydro, thermal and nuclear power stations for detailed study [Chapter II].

(2) A methodology has been developed to operate hydraulic turbines under variable speeds depending upon the available water head and loading conditions to maximize the turbine efficiency [Chapter III].

(3) The application of multiphase generators for unit connection schemes is studied. It is found that for larger sizes, six phase generators have technical and economical advantages as compared to three phase generators.

The air gap mmf of a six phase generator connected to a 12-pulse converter is analyzed for Y-Y and Y- Δ windings configurations taking real distribution of armature windings. It is found that Y-Y windings configuration with 30^{o} space displacement between winding sets resulted in less mmf harmonics as compared to that of Y- Δ windings configuration [Chapter IV].

(4) A six phase generator is modelled in d-q-o co-ordinates and simulated in time domain to study the steady state and dynamic behaviour of a 2X588 MW generator directly connected to a 12-pulse converter. The effective commutation reactance of the generator directly connected to a 12-pulse converter is evaluated based on the simulation results.

Harmonic currents flowing in the stator and the rotor circuits are computed to evaluate additional losses and the derating factor of the generator [Chapter V].

(5) The effect of variable frequency operation of the generator is studied with respect to the commutation reactance, overlap angle, power factor and reactive power requirements [Chapter V].

(6) Interface of generators to converters is studied for a 10X100 MW and 8X125 MW hydro power stations taking into account all possible loading conditions and contingencies to evaluate number of converters and converter transformers and their ratings on the rectifier and the inverter ends. A 1000 MW nuclear station with single generator is analyzed for the above [Chapter V].

(7) A 500 MW, 250 kV unit connection scheme is simulated in time domain using Electromagnetic Transient Program (EMTDC) to study the dynamic behaviour of the system for different fault conditions for 60 Hz and 70 Hz operation.

Harmonic currents flowing in a 120 MVA, 3-phase generator connected to a 12-pulse converter are computed to evaluate additional losses and thereby derating factor of the generator for 60 Hz and 70 Hz operation [Chapter V].

(8) A small signal model of the generator connected to a 12-pulse diode bridge rectifier is developed based on Park's equations to study the dc voltage control at the rectifier terminal through generator field excitation. A voltage regulator is designed with lead compensation using root locus technique for optimum performance of the system.

A 500 MW, 250 kV, unit connection scheme with diode rectifiers is simulated in time domain using EMTDC program to study the recovery of the system for dc line fault. In this case current control is modelled at the inverter end and voltage control by means of generator excitation [Chapter V].

(9) A typical 10X100 MW hydro station and a 1000 MW nuclear station is analyzed for economic evaluation [Chapter VI].

1.5 State-of-the-art of unit connection schemes

The concept of the unit connection of generators to HVDC converters was conceived in 1973 by Kauferle, J. [1] and subsequently many authors [2,3,4] discussed the economical and technical advantages of unit connection schemes as compared to the conventional current collector schemes. Hausler, M. and Kanngiesser, K.W. [3] studied these schemes with thyristor and also to some extent with diode rectifiers with conventional three phase generators operating at fixed power frequency. Even though Kanngiesser [4] indicated that hydro turbines can be operated under variable speeds (in order to maximize the turbine efficiency) no detailed study has yet been reported. Krishnayya [5] has evaluated additional losses in the generator

due to harmonic currents when fed with six and twelve pulse converter loads and evaluated the equivalent negative sequence loading of the generator due to the above loads based on the stator harmonic currents for power frequency operation. Bajwa and Mathur [6] showed that a conventionally designed three phase generator with 10% negative sequence loading capability has to be derated to 86% when feeding 6- pulse converter load; whereas no derating is necessary with 12-pulse converter load. All these studies have been conducted at fixed power frequency operation of generators.

Dynamic analysis of the isolated generator connected to HVDC converters has been reported by Arrilaga, J., et al. with and without ac filters connected to the generator bus [7]. EL-Serafi, A.M. and Sheheta, S.A. also modelled a three phase generator in direct phase quantities and studied the effect of harmonic currents on the generator performance connected to a 6-pulse converter with and without ac filters [8]. No attempt has been made in evaluating additional losses in the generator.

Diode rectifier schemes are also proposed by Bowles, J.P. for their cost effectiveness [9]. But, due to the lack of controllability of diodes on the rectifier side, dc circuit breaker has been proposed in the dc line to protect against the dc line faults. This proposition may nullify the savings attainable in choosing diodes instead of thysistors. However, these schemes may be economical for multiterminal schemes where the role of dc circuit breaker can be justifiable. These diode rectifier schemes may be attractive for dc taps to feed power to the nearby existing dc line [10]. Machida et. al [11] studied the protection and control aspects of diode rectifier schemes for HVDC transmission. However these studies were conducted with ac filters on the generator bus. It has been found that a large change in the current reference on the inverter side to meet the power demand causes

undesirable disturbances in the generator frequency and the terminal voltage. These deviations are minimized by means of co-ordinated power control of the generator and the dc system. A method has been proposed to bring down the dc current in the dc line to zero at a faster rate after dc line fault by switching a resistor in series with dc line and at the same time bypassing the smoothing inductor. Even though this proposal works well for smaller capacity systems, while in the case of bulk power transmission the cost and cooling arrangements for the switching resistor and the associated thyristors has to be worked out. In the case of unit connection schemes, where ac filters are removed from the generator bus, the voltage and the frequency fluctuations may not pose any serious problems.

It has been reported in the literature that one hydro power station in USSR is being operated under variable speed operation for maximizing the turbine efficiency [14]. It has also been reported that the performance improvement in terms of plant output by adopting variable speed operation of turbines is about 5%. Advantage of variable speed operation of hydraulic turbines has been reported recently by Sheldon [16] . The efficiency was calculated by varying parameters such as head, load, specific speed etc. one at a time. But, in actual practice all these parameters may vary simultaneously and hence it may be required to consider all the variables simultaneously for the efficiency evaluation.

Richert et al. [17] studied the unit connection scheme with a six phase generator directly connected to a 12-pulse converter. It is mentioned that steam turbines can be designed for higher base speed operation to reduce the cost by about 30%. The dynamic analysis showed that stability of a system with six phase generator connected to a 12-pulse converter improved considerably as compared to the three phase generator of the same capacity directly connected to the ac system. Even though the cost of the converter

fed system is higher than that of a normal one, these schemes are recommended where system stability is the major criterion. It is also mentioned that generator windings required higher insulation since the generator is directly connected to the converters. However the technical and economical advantages of six phase generators have not been mentioned. It has been reported that six phase generators can improve system stability as compared to three phase generators [18]. Successful operation of an isolated generator connected to HVDC converters has been reported by Last, F.H., et al. [43].

Most of the available literature gives the general idea of unit connection schemes and their relative advantages as compared to the conventional current collector schemes. This thesis bridges some of the technical gaps existing in the literature and analyzes the important aspects of the unit connection scheme for their applicability for HVDC transmission.

CHAPTER II

CONFIGURATIONS FOR UNIT CONNECTION SCHEMES

2.1 Introduction

Unit connection configuration of generators and HVDC converters offers several advantages. At the same time it suffers from many draw backs. In order to justify a serious systematic analysis, a preliminary investigation describing the potential advantages and disadvantages of unit connected schemes is undertaken. Advantages and disadvantages are identified on the basis of technical, economical and reliability aspects. Having found that there are many advantages which may outweigh the disadvantages possible configurations of unit connected schemes are listed. In order to carry out detailed investigation of unit connection schemes, from the possible configurations, a number of candidate configurations are selected. The selected configurations correspond to a nuclear power station having large size generators and a hydro power station comprising a large number of smaller size generators. A typical thermal station would lie in between the range of hydro and nuclear stations. It is presumed that appropriate conclusions can be extended from those drawn from hydro and nuclear stations. Such procedure is important from the point of view of the limitation on time imposed by the Ph.D work.

2.2 Summary of advantages and disadvantages of unit connection schemes

In order to discuss briefly the advantages and disadvantages of unit connection schemes, each salient difference from the conventional scheme is taken up, one by one, and discussed below.

Description : (1) Removal of ac filters

Advantages:

(1) Saving in the capital cost.

(2) Elimination of system resonance problems at non characteristic harmonics.

(3) Reduced risk of self excitation of generators.

(4) Capitalized savings of filter losses.

Disadvantages:

(1) Harmonic currents flow into the generators lead to increase in losses and ac voltage waveform distortion.

(2) Generators have to be designed to meet additional reactive power demand.

(3) Commutation reactance may increase which may lead to increase in the voltage stresses on the valves.

(4) Distortion in the ac voltage waveform at the converter bus may lead to added complexity to the converter controls.

Description : (2) Removal of generator breakers

Advantages:

(1) Savings in the capital cost.

Disadvantages:

(1) No protection for the generator or converter terminal faults.

Description : (3) Removal of generator transformer and combining the duties of the generator and converter transformers into one

Advantages:

(1) Savings in the capital cost.

(2) A three phase generator can still be used for 12-pulse operation of converters.

(3) Possibility of eliminating on-load tap changer if the generator excitation can provide the required voltage control.

(4) High availability of the system because of less number of transformers.

(5) Capitalized savings in transformer losses.

Description : (4) Total elimination of transformers

Advantages:

(1) Further savings in capital costs.

(2) Greater savings in capitalized transformer losses.

(3) If the size of the generator is above 1000 MW, six phase generators can be economically designed for 12-pulse operation.

Disadvantages:

(1) Requirement of higher voltages on the generators.

(2) Low voltage and high current operation of converters may necessitate paralleling of thyristors and converters.

(3) In the case of generators directly connected to the converters, generator windings have to be designed for higher voltages.

(4) Generator neutrals are subjected to the dc potential. Protection against internal faults may require special consideration.

Description : (5) Generators for unit connection schemes

Advantages:

(1) Flexibility in choosing higher base speed of operation which may reduce the cost of the generators.

(2) Possibility of variable speed operation.

(3) Reduction in the cost and increase in the efficiency.

Disadvantages:

(1) Special design requirements may be necessary to avoid mechanical resonance under variable speed operation and higher base speed operation.

Description : (6) Turbines for unit connection schemes

Advantages:

(1) Flexibility in choosing in higher base speeds.

(2) Possibility of variable speed operation.

(3) Possible reduction in the cost and increase in the efficiency.

Disadvantages:

(1) Special design requirements may be necessary to avoid mechanical resonance under variable speed operation.

Description : (7) Converters for unit connection schemes

Advantages:

(1) Possibility of using diode bridge rectifiers for savings in converters cost.

(2) Fast telecommunication link can be eliminated for further savings.

(3) Possibility of eliminating the generator circuit breaker with thyristor converters.

Disadvantages:

(1) No protection against dc line faults and hence require dc or ac circuit breakers for protection.

(2) For hydrostation multiplicity of converters and controls may be required.

Description : (8) Station auxiliaries

Disadvantage:

(1) A separate power source may be required to feed station auxiliaries, but this may not be different from a conventional requirement.

Description : (9) Substation elimination

Advantage:

(1) Savings in the capital cost.

2.3 Selection of candidate configurations

In order to arrive at suitable configurations for unit connection schemes, the following situations are examined.

(1) Nuclear power station with typical generator size of 1000 MW which can justify a bipole.
(2) A hydro power station typically 10 units each of 100 MW.

The above situation can exists for:

(a) Point-to-point scheme (for long distance transmission) or;
(b) back-to back HVDC interconnection with ac transmission / distribution.

From the above, four distinct possibilities emerge. These are combination of (1) or (2) with (a) or (b). These schemes are as follows :

(i) Nuclear station with point-to-point dc transmission.

(ii) Nuclear station with back-to-back dc link.

(iii) Hydro station with point-to-point dc transmission.

(iv) Hydro station with back-to-back dc link.

The candidate schemes for the above four are presented here. The only other situation which warrants additional inclusion is that of a thermal station which may have several units each of approximately 500 MW capacity. It is believed that the basic discussion of hydro station will apply here too, except economic considerations which must be dealt with separately.

2.4 Candidate configurations for nuclear power stations

Figs. (2.1a) to (2.1d) show the possible configurations of 1000 MW nuclear station with three phase generator. In order to optimally use the current ratings of thyristors and also to minimize the line losses in the case of the point-to-point schemes, it is necessary to use significant dc voltage. For example, for 2000 A dc current, ± 250 kV dc system voltage is required. This is beyond the limit of the maximum voltage obtainable from the generators. Moreover to minimize the characteristic harmonics flowing into the generator, higher pulse operation of the converters is necessary. Hence, converter transformers are mandatory for point-to-point transmission schemes. One three-winding transformer (Figs. 2.1a and 2.1b) connected to a 12-pulse bridge, or two two-winding transformers (Figs. 2.1c and 2.1d), each connected to a 6-pulse converter bridge can be used for 12- pulse operation of converters. In the event of the failure of one

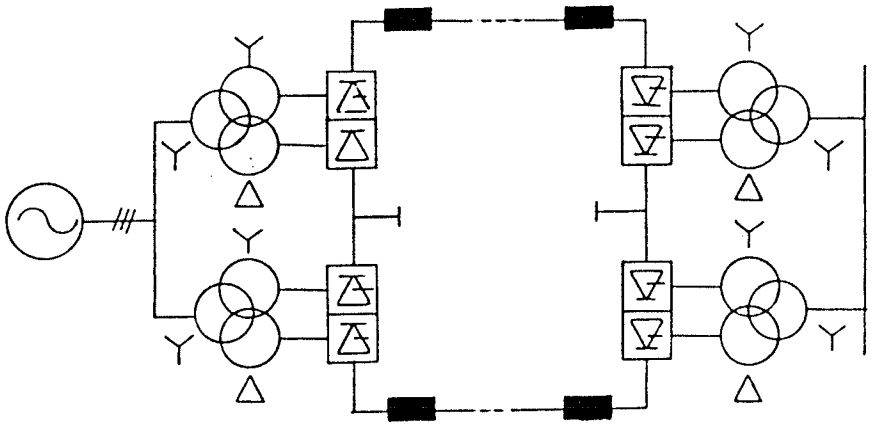

Fig. 2.1a : 1000 MW bipolar transmission scheme for nuclear power station with a three phase generator and three-winding transformers.

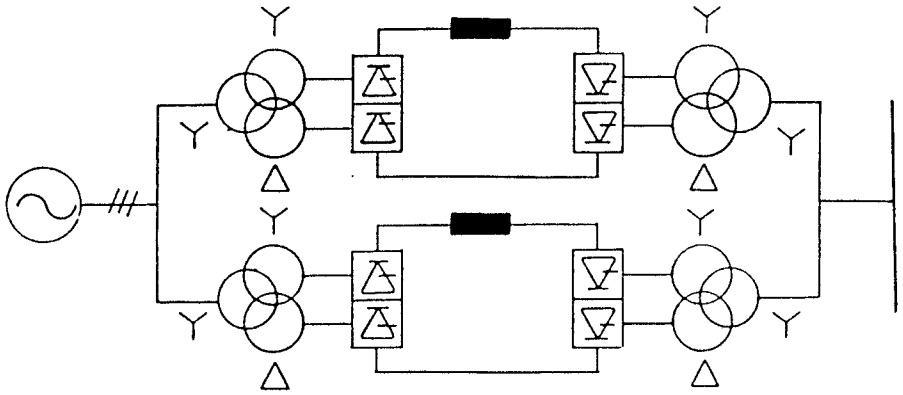

Fig. 2.1b : 1000 MW bipolar back-to-back scheme for nuclear power station with a three phase generator and three-winding transformers.

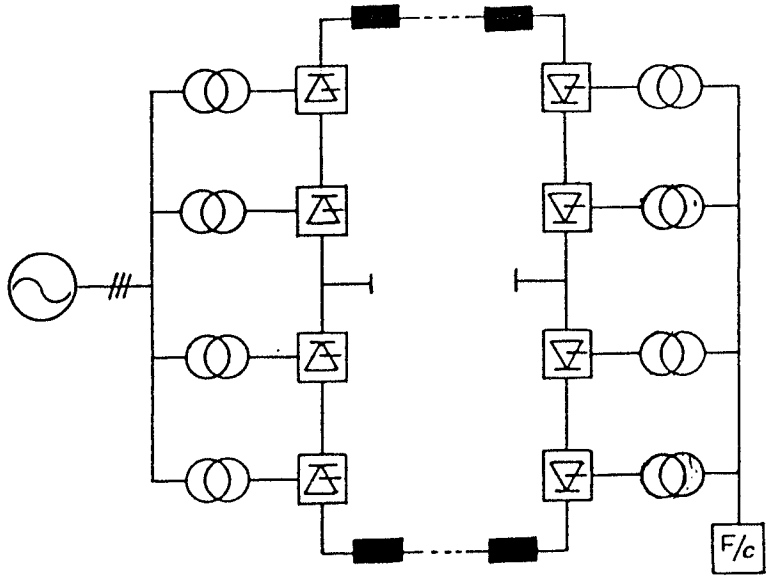

Fig. 2.1c : 1000 MW bipolar transmission scheme for nuclear power station with a three phase generator and three-winding transformers.

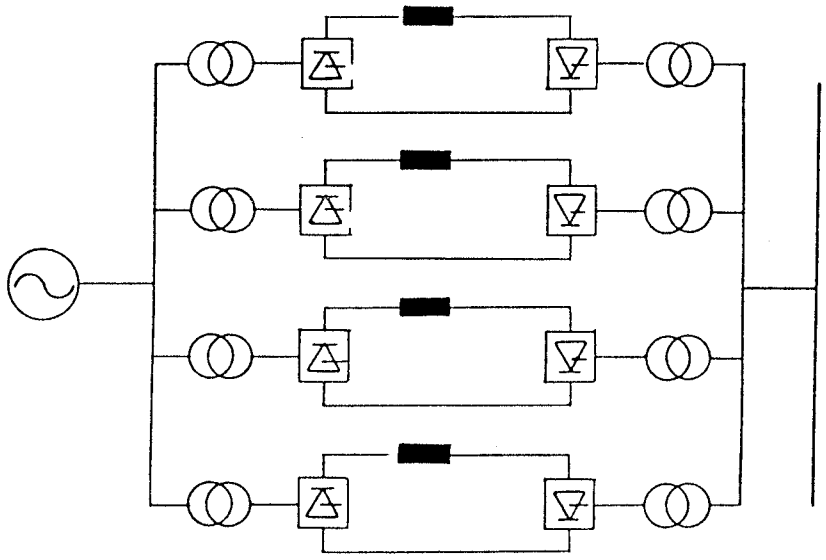

Fig. 2.1d : 1000 MW bipolar back-to-back scheme for nuclear power station with a three phase generator and two-winding transformers.

converter, it results in 50% outage of the total capacity in all the cases. In the case of Fig. (2.1c) and (2.1d), two three phase two-winding transformers are used to connect to 6-pulse converters connected in series for 12-pulse operation. In this case the spare capacity of the transformer is less than that of the three-windings transformer of Figs. (2.1a) and (2.1b). Moreover there may be transportation limitations in manufacturing single 500 MW three-winding transformer. However this limitation can be over come by using three single phase three-winding transformers which may result in more number of transformers.

Figs. (2.2a) to (2.2g) show the 1000 MW nuclear station configuration with six phase generator for point-to-point and back-to-back schemes. In the case of Fig. (2.2a) two sets of generator windings are connected to two 6- pulse converters through two two-winding transformers for 12-pulse operation. In this case ($6k \pm 1$) harmonic currents flow into the stator windings as compared to ($12k \pm 1$) harmonic currents in the case of Figs. (2.2b) to (2.2f). Failure of a converter or a converter transformer in the above case results in the outage of the total power. But, the number of converter transformers and converters are less in this case.

In the case of Figs. (2.2b) and (2.2c), if one converter bridge is out of service, paralleling of the generator windings are possible. About 75% of the power can be transmitted by paralleling the generator windings if converters are rated for 25% excess capacity. In the case of Fig. (2.2b) spare capacity of the transformer is reduced as compared to Fig. (2.2c), but the number of transformers are more which may lead to increase in the cost. Figs. (2.2d) to (2.2f) are shown with bipolar arrangement. In these cases, if two six pulse converters connected to transformers of the same windings configuration one in each pole is out of service, each pole can be operated at 50% of is capacity, since 12-pulse operation possible. In the case of

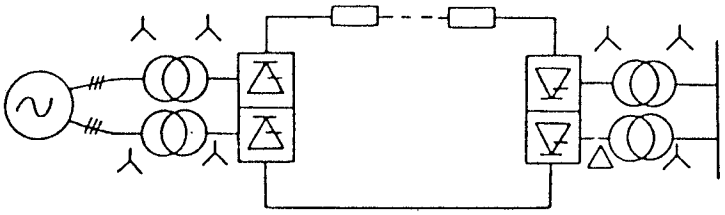

Fig. 2.2a : 1000 MW transmission scheme with metalic return for nuclear power station with a six phase generator and two-winding transformers with one twelve-pulse valve group.

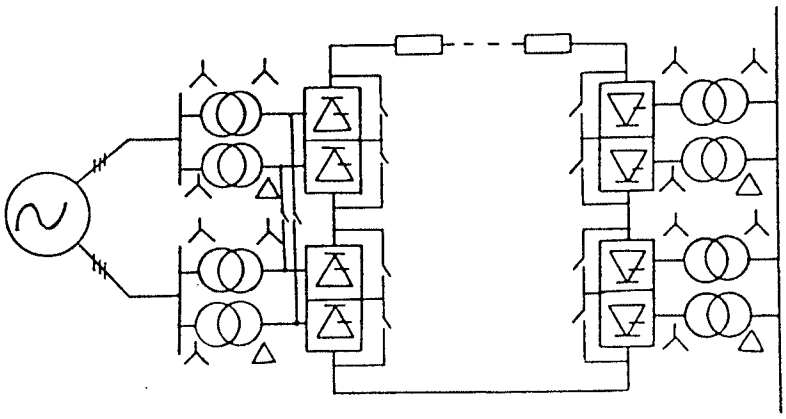

Fig. 2.2b : 1000 MW back-to-back scheme with metalic return for nuclear power station with a six phase generator and two-winding transformers with two twelve pulse valve groups.

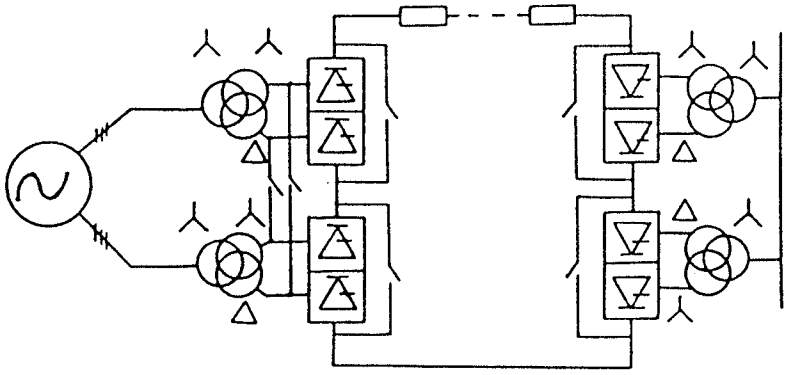

Fig. 2.2c : 1000 MW transmission scheme with metalic return for nuclear power station with a six phase generator and three-winding transformers with two twelve pulse valve groups.

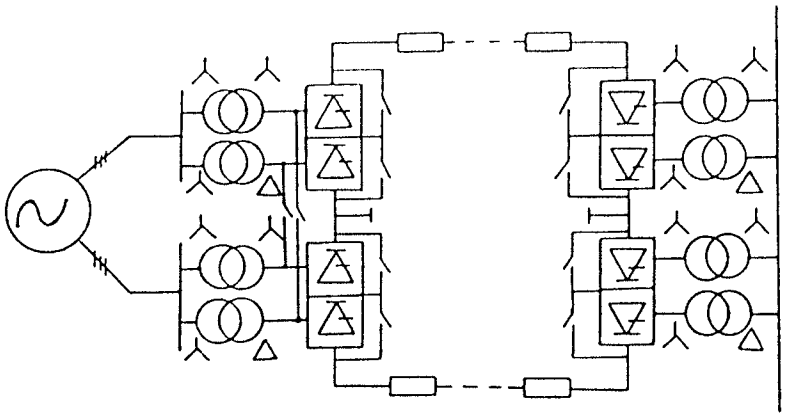

Fig. 2.2d : 1000 MW bipolar transmission scheme for nuclear power station with six phase generator and two-winding transformers.

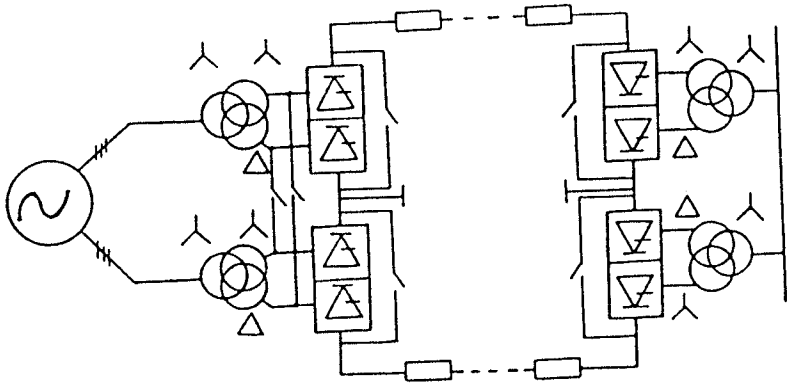

Fig. 2.2e : 1000 MW bipolar transmission scheme for nuclear power station with a six phase generator and three-winding transformers.

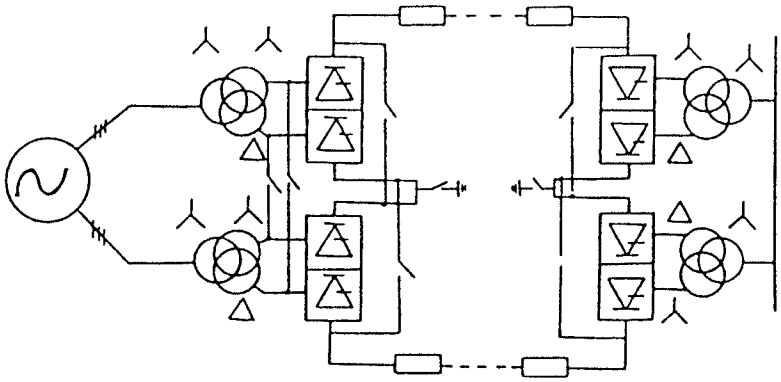

Fig. 2.2f : 1000 MW bipolar transmission scheme for nuclear power station with a six phase generator and three-windings transformers.

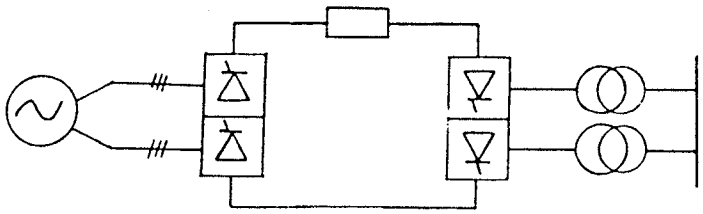

Fig. 2.2g : 1000 MW back-to-back scheme for nuclear power station with a six phase generator without converter transformers.

outage of a converter or a pole paralleling of generator windings are possible. In the case of Fig. (2.2f), in the event a of dc line fault on one pole, paralleling of generator windings and also paralleling of converters are possible to transmit about 75% of the total power if the converters are designed for 25% excess capacity. Paralleling of generator windings reduces the harmonic currents entering into the generator, since each set of armature windings carry (12k ± 1) harmonics. The magnitudes of 12k harmonic currents induced in the rotor circuits are less due to 30^0 space displacement between the winding sets.

Fig. (2.2g) shows the back-to-back scheme without transformers, where considerable savings can be achieved in the capital cost. But, the generator windings are to be designed for higher voltages as these are subjected to the dc potential. The generator neutrals are also subjected to dc potential hence require special protection schemes for detecting internal faults of the generator.

2.5 Candidate configurations for hydro power stations

Variety of combinations arise in this case. Connection of a single 100 MW generator to a 6-pulse or a 12-pulse appears to be possible. Due to the limitations of harmonic currents entering into the generator, only 12-pulse connection is considered. If it is a point-to-point scheme, it becomes apparent that the dc transmission voltage must be built up by series connection of converter bridges. Series connection of bridges introduces a dc voltage bias to the generator windings. It being highest for the generator farthest from the ground end. It is seen to be impracticable design restraint on the generator from the view point of slot insulation. Hence total

elimination of transformers are not considered any further.

Fig (2.3a) shows the bipolar arrangement of the unit connection of 10X100 MW generator, each one connected asynchronously to a 12-pulse converter through a three-winding converter transformer. The converters are connected in series to obtain the desired high dc voltage. Considerable operating flexibility can be achieved by connecting units in series which will be discussed in the Chapter V. Since the size of each unit is 100 MW selection of three-winding transformer is the best choice for minimizing the capital cost as compared to two two-winding transformers. Since each unit requires one transformer, the total number of the transformers in the station increases, which may result in higher cost, but the spare capacity of the transformer is reduced. In the event of the fault on the generator, complete unit has to be isolated by blocking and bypassing the converter. Hence, the generator breaker can be replaced by an isolator which may result in saving in the cost. When more than one unit is taken out of service, the dc voltage at the sending end decreases. Since the link operates under constant current mode, the line losses are constant at full load value. Therefore the transmission efficiency will decrease under this condition. Normally hydrostation is operated under light loads in the night time. For example, in the case of a 10X100 MW Longspruce generating station on the Nelson River, in Canada, only 4 units are in operation for a period of 9 hours. Under this situation if 6 units out of 10 are taken out of service, the transmission efficiency decreases. In order to improve the overall efficiency of the system, all units are operated under partial load condition in which case transmission efficiency can increase. The efficiency of the turbine can be improved by adopting variable speed operation. Since the generator efficiency would not change much from 105% load to 25% load, the overall efficiency of the system can be improved.

In Fig. (2.3b) total number of transformers are reduced as compared to Fig. (2.3a). Out of five generators per pole, three generator are connected to a common bus, therefrom to a 12-pulse converter through a single three-winding transformer. Other two generators are grouped to a second bus and then connected to another 12-pulse converter through three-winding transformer. These two buses can be interconnected through an isolator for flexibility of operation. If each bridge is rated to 60% of a pole capacity, then in the event of failure of one bridge, or a transformer on a pole, 60% power can be transmitted. Savings in the cost of the transformers is more than that of Fig. (2.3a). The generator circuit breaker capacity is more in the case of a group scheme with three generators than that of a scheme with two generators. If the fault occur on the ac bus of a three generator group scheme, only 40% power can be transmitted on that pole. Whereas if the fault occurs on the ac bus of two generators group scheme, 60% power on the pole can be transmitted.

Fig. (2.3c) is similar to a conventional arrangement except that ac filters are removed from the common ac bus. It has the same flexibility of operation of schemes as shown in Figs. (2.3a) and (2.3b). In the event of a fault on the ac bus, the total system has to be shut down. The capacity of the generator breaker is more than that of the previous group scheme. The above configurations can also be used for back-to-back schemes. Fig. (2.3d) shows one of the back-to-back schemes. In this case, groups of three and two generators are connected to separate ac buses, therefrom to a 12-pulse converter. If each converter is rated to the capacity of three generators, then interconnection of generators is possible from one group to another, should there be an outage of a bridge or a generator in a particular group. This arrangement can facilitate to transmit maximum possible power in the case of contingencies.

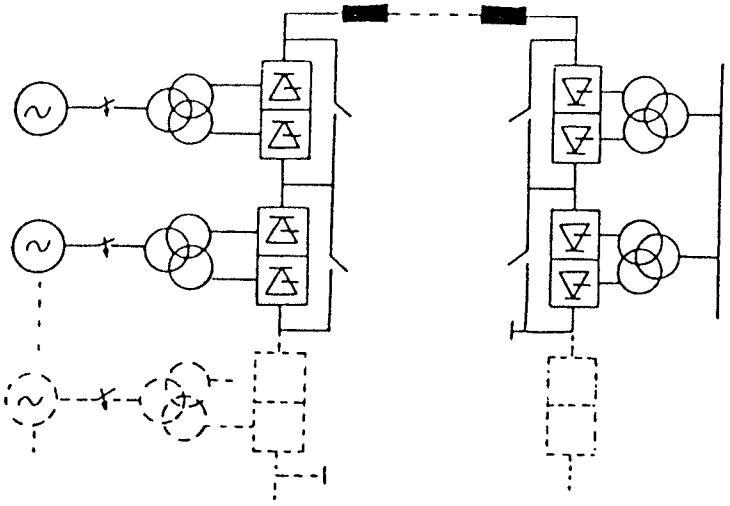

Fig. 2.3a : 10X100 MW bipolar transmission scheme for hydro power station with three phase generators and three-winding transformers.

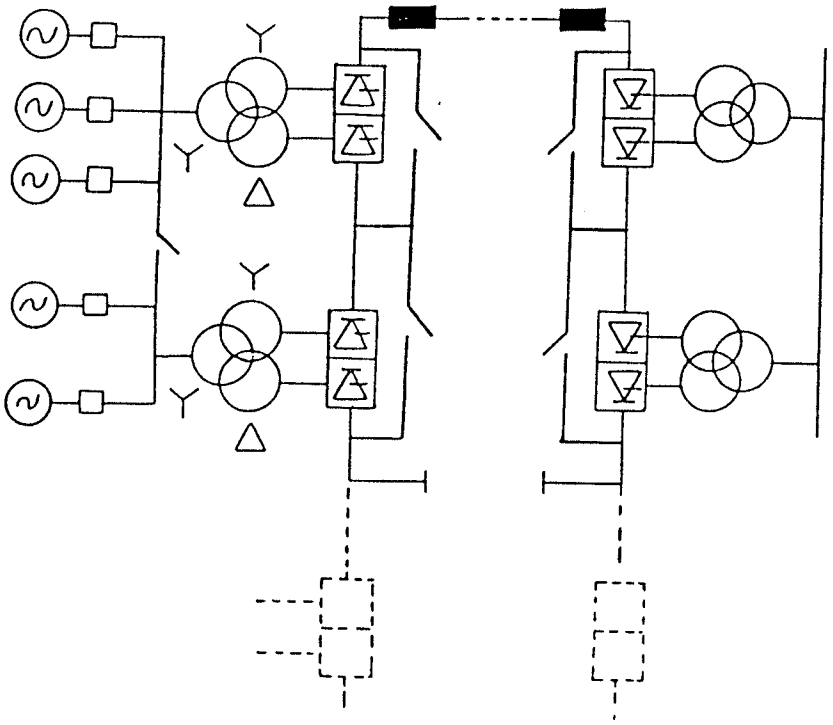

Fig. 2.3b : 10X100 MW bipolar transmission scheme for hydro power station with groups of three phase generators and three-winding transformers per unit.

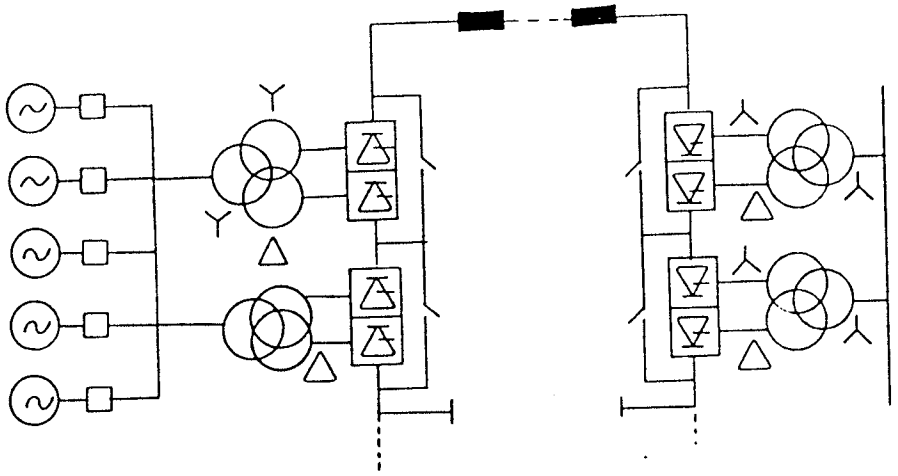

Fig. 2.3c : 10X100 MW bipolar transmission scheme for hydro power station with five three phase generators per pole with three-windingtransformers.

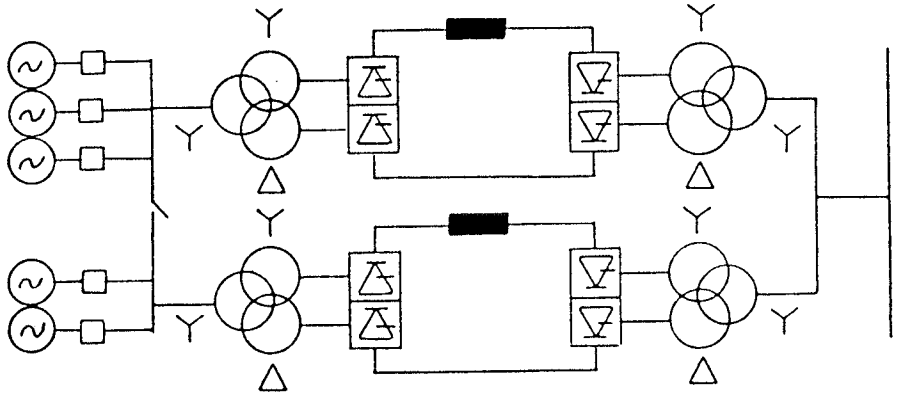

Fig. 2.3d : 10X100 MW back-to-back scheme for hydro power station with groups of three phase generator per unit.

2.6 Summary:

Pros and cons of unit connected schemes are identified on the basis of technical, economical and reliability aspects. Possible candidate configurations for nuclear and hydro power stations are shown for point-to-point and back-to-back schemes and their merits and demerits are discussed. Configurations with six phase generators for nuclear power stations are also shown and their merits and demerits based on technical, economical and operational aspects are discussed.

CHAPTER III

PERFORMANCE EVALUATION OF HYDRAULIC TURBINES

3.1 Introduction

In hydro power stations, turbines are designed to operate at maximum efficiency under full load condition with nominal water head at the nominal speed which is selected based on the hydraulic conditions. Sophisticated turbine governor controls are used to keep the frequency fluctuations within the tolerable limits. In hydro power stations seasonal water flow variations cause deviation in operating head. If the turbine operates at a fixed speed when the head or the load deviates from the nominal value, its efficiency decreases. This disadvantage can be over come by operating the turbine at an optimum speed for a given water head and load. This may not be possible in the case of a conventional HVDC scheme, where all the generators generate a fixed power frequency and are connected to a common ac bus, to which HVDC converters and station auxiliaries are connected.

If instead, a unit connection scheme is employed, each generator or a group of generators in a unit can be operated at an independent frequency. If the common power frequency is not to be maintained and as the station auxiliaries are supplied by another source, hydro turbines can be operated under variable speeds to maximize the efficiency. This is a promising application of unit connection for a remote generating station from where the power is transmitted to the load centre through a HVDC link.

It has been reported that Toktogulsk HES Power Plant in USSR is being operated under variable speed operation and transmitting power through HVDC link [14]. L.H.Sheldon [16] showed the improvement in the efficiency of a hydraulic turbine from a prototype model, under different water head conditions by keeping constant discharge, constant peripheral speed coefficient and also constant power. But, in a real situation, both water head and load may vary simultaneously. In this chapter, the performance of hydraulic turbines is analyzed under fixed speed and variable speed operation for different loading conditions with corresponding water head to evaluate the efficiency benefits due to variable speed operation. A 1000 MW hydro power station which is typical for Manitoba Hydro's Nelson River Scheme, is used as a sample system to quantize the efficiency benefits occurring from variable speed operation.

3.2 Parameters governing the operation of hydraulic turbines

In this section, some of the important parameters governing the operation of hydraulic turbines are discussed. One of such parameters is the specific speed. It is the common basis for comparison between the runners of different type and different characteristics. It is defined as the number of revolutions per minute at which a given runner will revolve if it were reduced in proportion such that it would develop 1 hp under 1 foot head [15]. Since the most of the data pertaining to hydraulic turbines are in British System, the same is adopted in this chapter. Since $N \alpha H^{1/2}$ and $P \alpha H^{3/2}$, the specific speed of any runner operating under head H is given by (as shown in Appendix I)

$$N_s = \frac{N P^{1/2}}{H^{5/4}} \qquad (3.1)$$

The output power (hp) of the turbine is given by

$$P = \frac{H \cdot Q \cdot \rho \cdot \eta}{550} \tag{3.2}$$

Where

η = Overall efficiency.

ρ = Density of water, lb/ft^3.

Most of the hydro turbines are generally designed to operate at the highest possible efficiency at full load and at nominal water head. The operating speed, N (rpm) of the turbine is chosen to maximize the efficiency based on the water head, by choosing maximum possible specific speed without causing cavitation. Then, the poles of the synchronous generator are selected from (3.3) for a given system frequency.

$$N = \frac{120\ f}{\text{No. poles}} \tag{3.3}$$

Where f is the frequency of the generator in Hz. Hydro turbines are generally operated at low speeds (about 100 to 200 rpm). Since the number of poles of the generator is even, considerable flexibility exists in choosing the operating speed of the turbine. As the operating speed is selected higher, the turbine and the generator sizes and therefore their costs reduce. At higher specific speeds the cavitation phenomenon takes place in the turbines which may damage the turbine blades. Hence, the maximum allowable operating speed of the turbine is determined by the maximum allowable specific speed of the turbine at a given head without causing cavitational problems.

3.2.1 Cavitation phenomenon

If the pressure of the turbine falls below the vapor pressure of the water, pitting action on the blades takes place. This is called ' cavitation '. To avoid cavitation taking place in the turbine, proper cavitation coefficient should be selected.

For Francis turbine the Thoma cavitation coefficient σ should be [13]

$$\sigma \geq 0.625 \left(\frac{N_s}{100}\right)^2 \tag{3.4}$$

For Propeller type turbine:

$$\sigma \geq 0.28 + \frac{1}{7.5}\left(\frac{N_s}{100}\right)^3 \tag{3.5}$$

Should the value of σ falls below those given in eqns. (3.4) and (3.5), cavitation takes place. The Thoma cavitation coefficient can be calculated as

$$\sigma = \frac{H_{sv}}{H} \tag{3.6}$$

where:

$H_{sv} = h_a - h_s - h_v$

H_{sv} = Absolute head at the outlet of the turbine, ft.

h_a = Atmosperic head, ft.

h_s = Draft head, ft.

h_v = Vapour pressure head, ft.

The convenient way of determining the highest operating speed of the turbine is given by the relation of the specific speed to the head. The empirical relation for maximum specific speed to avoid cavitation problems are given by

For Francis turbine:

$$N_{s\,(max)} = \frac{800}{\sqrt{H}} \tag{3.7}$$

For Propeller type turbine:

$$N_{s\,(max)} = \frac{1125}{\sqrt{H}} \tag{3.8}$$

3.2.2 Unit power and its functional relationship

The unit power is defined as the output of the model turbine of 1 foot diameter operating at 1 foot water head. This is given by

$$P_{11} = \frac{P}{D^2 \,.\, H^{3/2}} \tag{3.9}$$

The peripheral speed coefficient Φ is given by

$$\Phi = \frac{\pi \,.\, D \,.\, N}{60 \;\; (2\,g\,H)^{\frac{1}{2}}} \tag{3.10}$$

By substituting H from (3.10) into (3.9)

$$P_{11} = \frac{P}{\pi^3} \cdot \frac{(60)^3 \,.\, (2g)^3}{D^3 \,.\, N^3} \cdot \Phi^3$$

$$= K \cdot \frac{P}{N^3} \cdot \Phi^3 \qquad (3.11)$$

Where:

$$K = 3.57 \times \frac{10^6}{D^5}$$

3.3 Hydro turbine efficiency evaluation

In hydro power stations, seasonal water flow variations cause deviation in water head from the nominal value at which the turbines are designed for maximum efficiency at nominal speed. If many hydro stations are located on the same river, it is necessary to regulate the water flow such that the head variation is kept to a minimum (less than 5% in the case of Nelson River stations). Many hydro stations are operated not only as base load stations but also as peak load stations permitting up to 5% overload. For example, broadly speaking hydro power stations on the Nelson River operate at 105% load for a period of about 37% in a year. Overload operation and the deviation of water head from the nominal value cause loss in turbine efficiency if operated at fixed speed. If unit connection schemes are adopted for these stations as discussed earlier, the operating speed can be selected such that the turbines operate at the maximum attainable efficiency depending upon load and the available water head.

In this Section, a 10X100 MW Long Spruce hydro station of Manitoba Hydro has been analyzed for fixed and variable speed operations using model turbine performance curves to evaluate efficiency benefits for variable speed operation.

3.3.1 Efficiency evaluation with fixed speed operation

Recalling operating relations for the specific speed and unit power from (3.10) and (3.11) respectively, a constant speed turbine therefore operates on constant power curves as shown in Fig. (3.1). It can be observed that as the operating head varies changes occur in both Φ and P_{11} , which in turn lead to changes in efficiency. The procedure used for calculating the efficiency for a given power output and the water head is as follows:

(1) Find P_{11} for a given power output from (3.9).

(2) Find peripheral speed coefficient Φ from (3.10).

(3) Calculate the specific speed $N_{s\,(cal)}$ by

$$N_{s\,(cal)} = \frac{N \cdot D \cdot \sqrt{P_{11}}}{\sqrt{H}} \qquad (3.12)$$

(4) Check the calculated value of N_s with the permissible value from the relation given in (3.8).

(5) If the $N_{s\,(cal)}$ is greater than $N_{s\,(max)}$, fix the allowable specific speed as $N_{s\,(max)}$ to avoid cavitational problems and recalculate P_{11} .

(6) From the model turbine performance curves, the efficiency can be obtained corresponding to the value of P_{11} and Φ .

Efficiencies are calculated based on the above procedure for 135 000 hp hydraulic turbine in Long Spruce generating station under fixed speed operation at different loads with wide variation of water head from 75 ft. to 90 ft. The design data of the 135 000 hp hydraulic turbine is also given in Appendix I. The variation of efficiency with different water heads for different loads of 105%, 100%, 95% and 90% is shown in Figs. (3.2) to

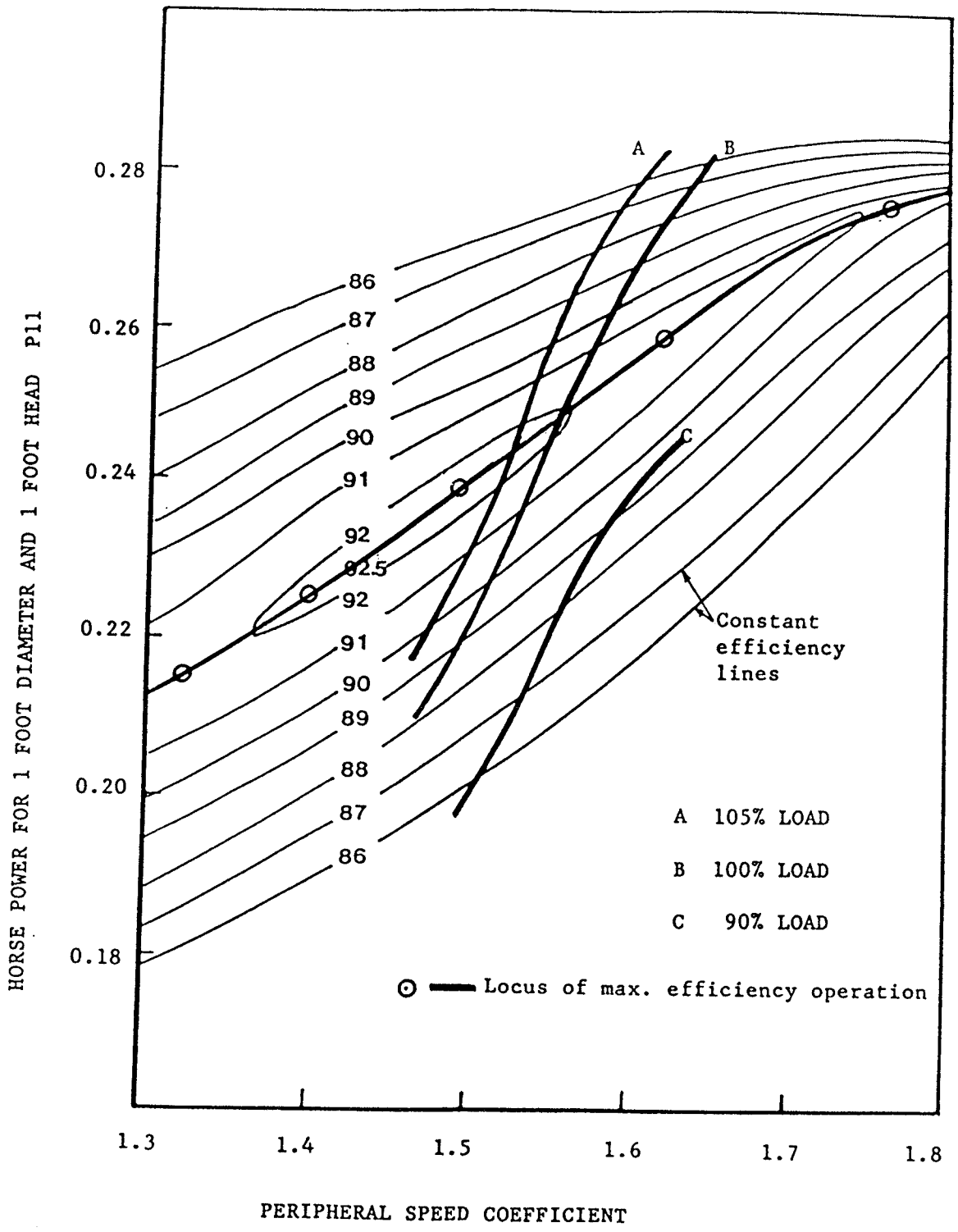

Fig. 3.1 : A typical model turbine performance curves

(3.5) respectively.

3.3.2 Efficiency evaluation with variable speed operation

By suitably selecting the operating speed of the turbine depending upon the available water head for a given load, the efficiency can be improved. A methodology has been developed for calculating the efficiency of a turbine under variable speed operation for a given load and water head. The procedure is as follows:

(1) Calculate P_{11} for a given power output and water head using (3.9).

(2) From the model turbine performance curves, find the peripheral speed coefficient Φ corresponding to the maximum possible efficiency.

(3) Calculate the required operating speed corresponding to this value of Φ using (3.10).

(4) Calculate the specific speed $N_{s\,(cal)}$ from (3.12).

(5) If the $N_{s\,(cal)}$ is more than the $N_{s\,(max)}$ given by (3.8), fix $N_{s\,(max)}$ as the allowable specific speed and recalculate the operating speed by using

$$N = \frac{N_{s\,(cal)} \cdot \sqrt{H}}{D \cdot \sqrt{P_{11}}}$$

(6) Calculate the new value of the peripheral speed coefficient Φ from (3.10).

(7) Find the efficiency form the model turbine performance curves shown in Fig. (3.1) corresponding to P_{11} and Φ.

Efficiencies are calculated based on the above developed procedure

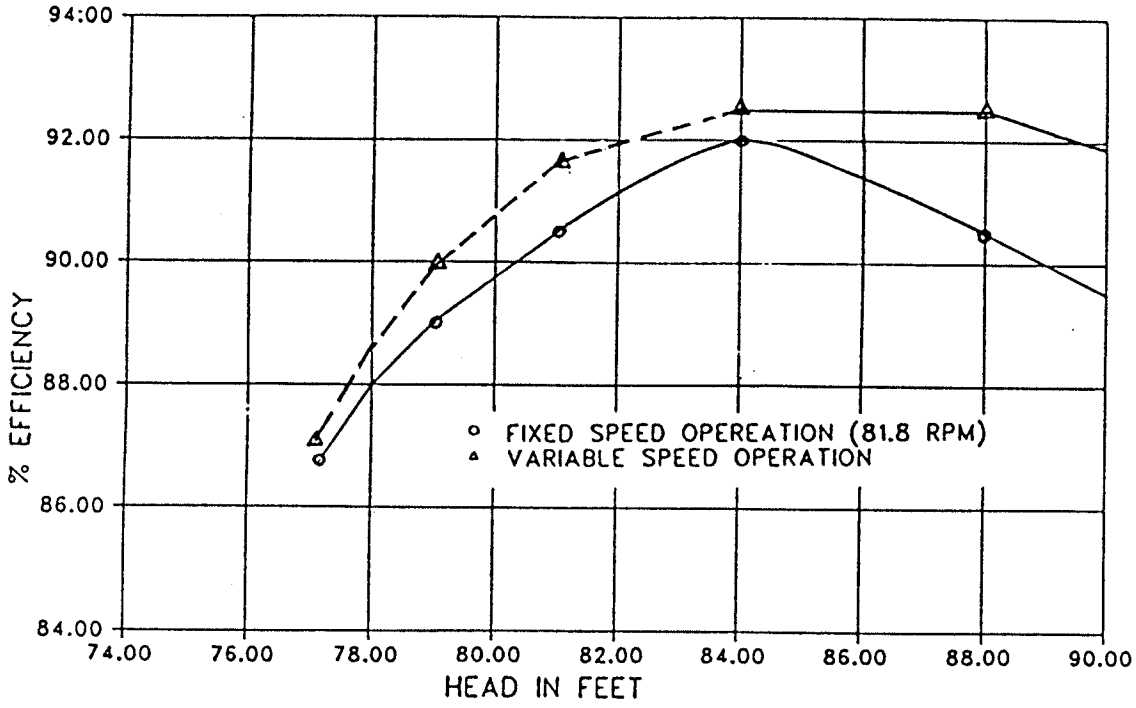

Fig. 3.2 : Variation of efficiency with water head at 105% load.

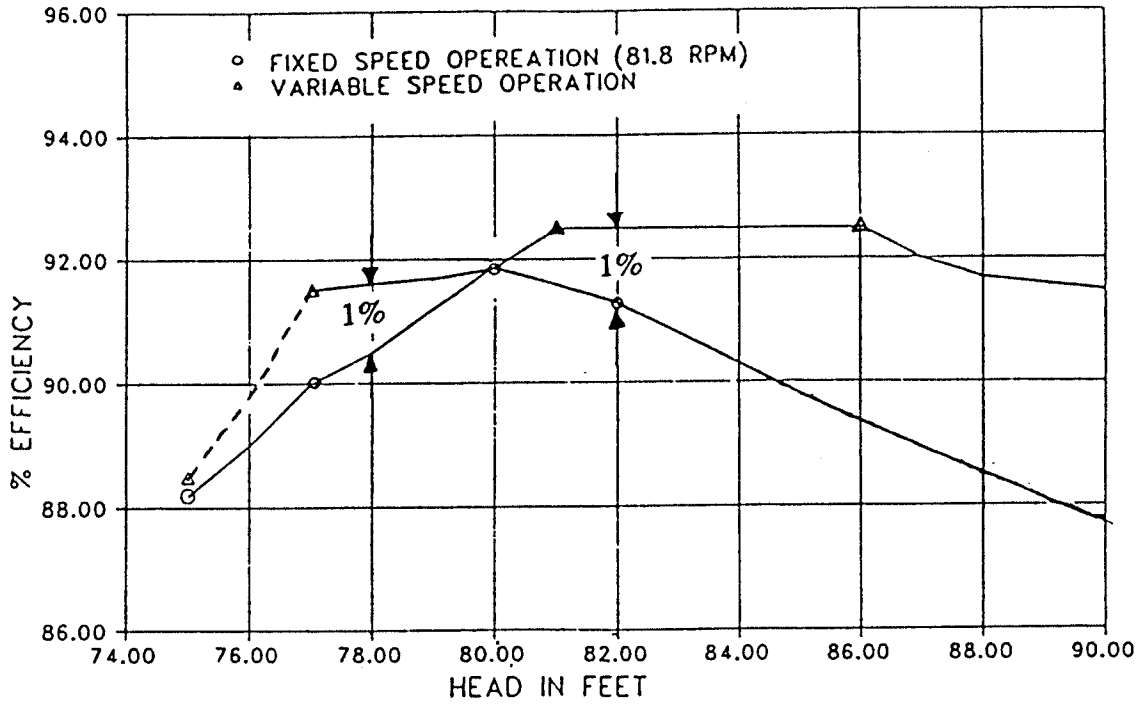

Fig. 3.3 : Variation of efficiency with water head at 100% load.

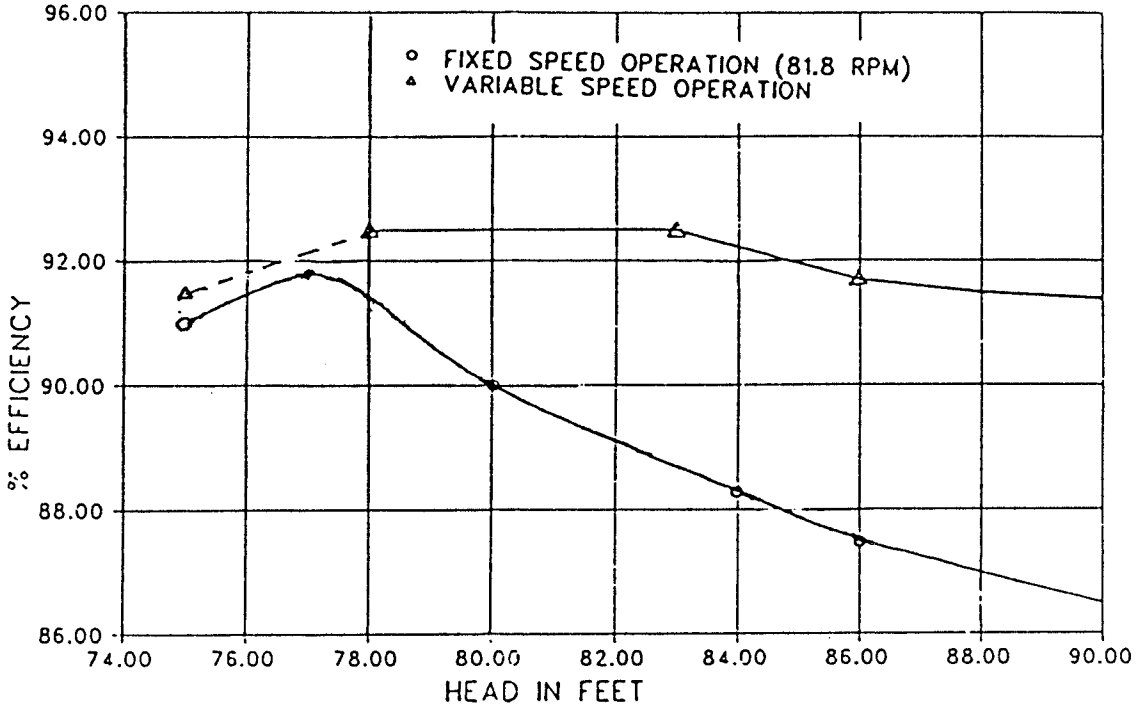

Fig. 3.4 : Variation of efficiency with water head at 95% load.

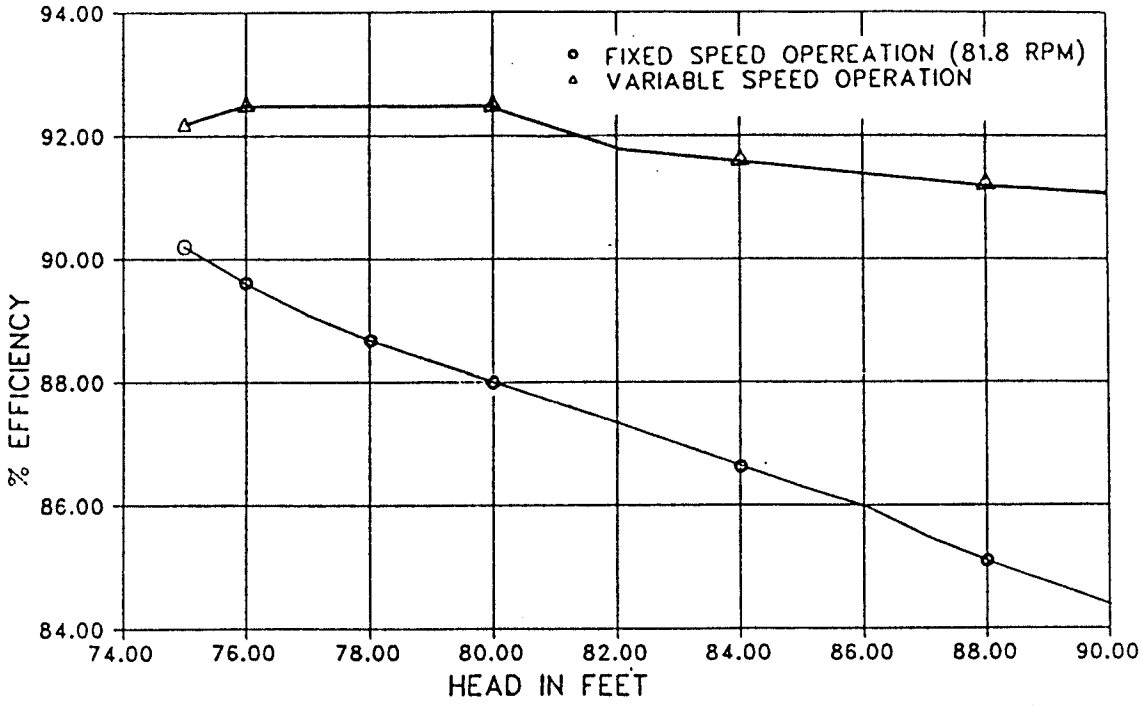

Fig. 3.5 : Variation of efficiency with water head at 90% load.

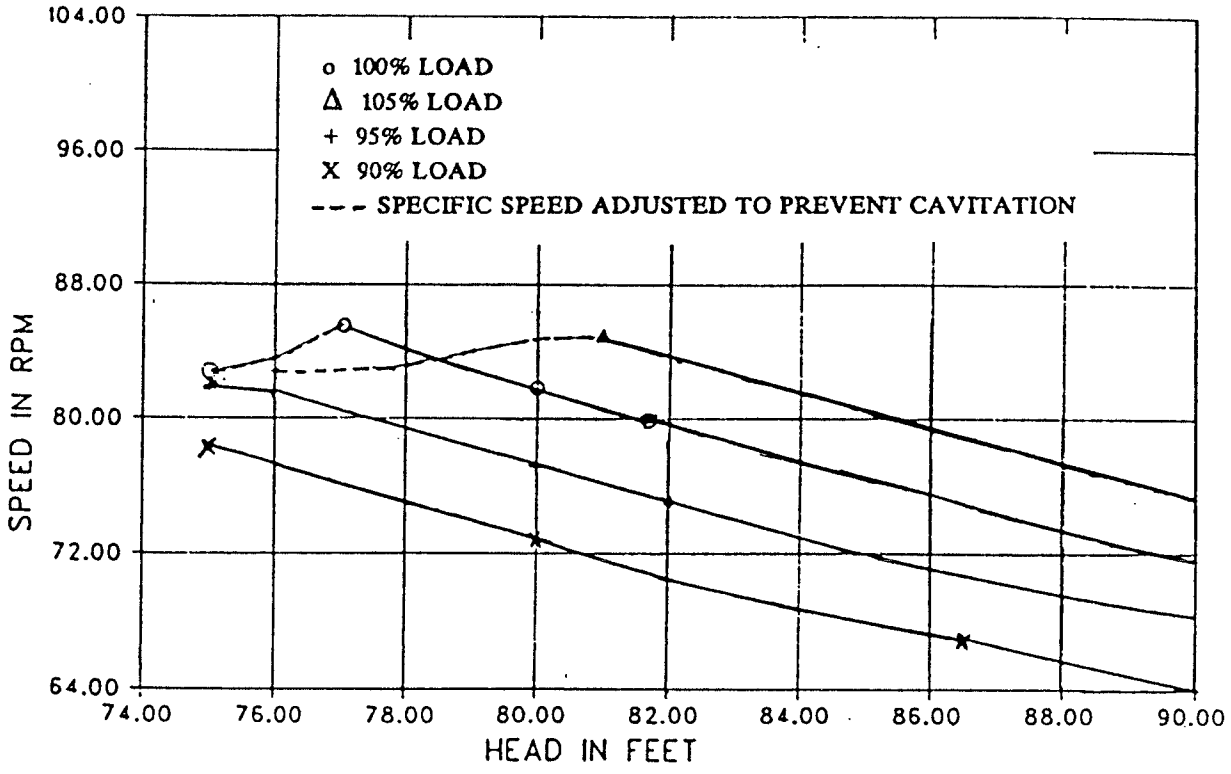

Fig. 3.6 : Variation of speed with water head at different loads.

for a 135,000 hp turbine in the Longspruce generating station for different loads of 105%, 100%, 95% and 90% with water head variation from 75 ft. to 90 ft. and are shown in Figs. (3.2) to (3.5) respectively. The variation of the speed for the above loading and water head conditions are shown in Fig. (3.6). The variation of the efficiency under different loads at the constant nominal head of 80 ft. is shown in Fig. (3.7) for both fixed and variable speed operations.

Since the Longspruce generating station operates about 37% of the time at 105% full load in a year, it is assumed that for the remaining 63% period the station operates at 100% load, in order to evaluate savings due to the increase in the efficiency under variable speed operation. Fig. (3.8) shows the variation of the efficiency under fixed and variable speed operations for the above loading conditions at fixed nominal head of 80 ft.

The variation of turbine efficiency for different water heads and different loading conditions at fixed speed operation is shown in Fig. (3.9) in three dimensional view. As seen from the above figure, P is the operating point of the turbine which has been designed for maximum efficiency at nominal load and water head conditions. If there is a variation in water head; or in load; or in both; the efficiency of the turbine decreases as seen from the above figure. If the turbine is operated under variable speed then the efficiency can be maintained at the maximum possible value if variations in load and water head occur. Fig. (3.10) shows the variation of turbine efficiency at different load and water head conditions under variable speed operation shown in three dimensional view. It can be observed from the above figure that any deviation in water head or load the efficiency is maintained to the maximum possible value taking specific speed limitations into account. Fig. (3.11) shows the loading curve of units. Equal loading criteria is adopted in loading the turbines based on the load

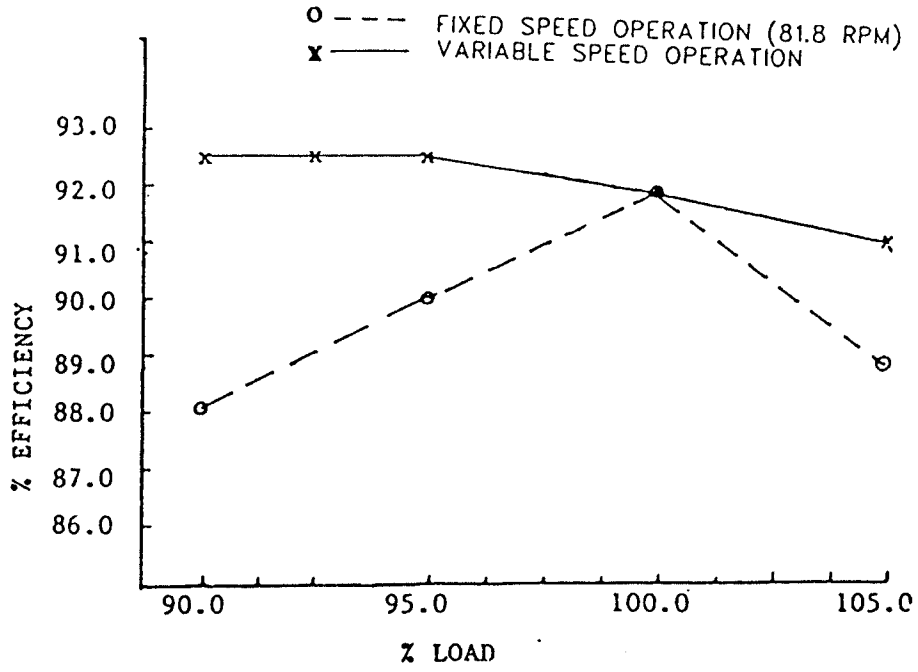

Fig. 3.7 : Variation of efficiency with load at nominal water head of 80 ft.

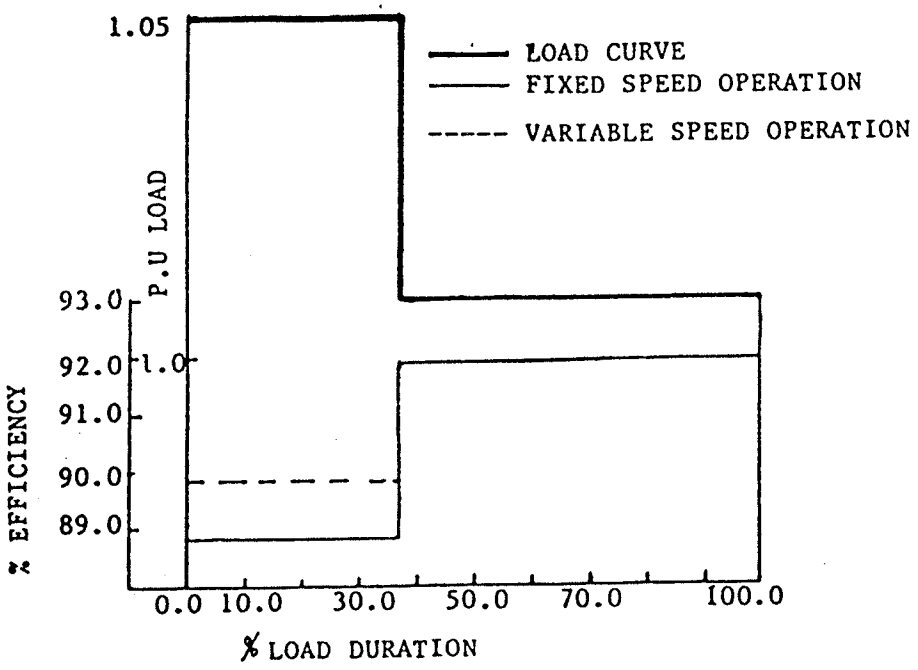

Fig. 3.8 : Variation of efficiency with load duration at nominal head of 80 ft.

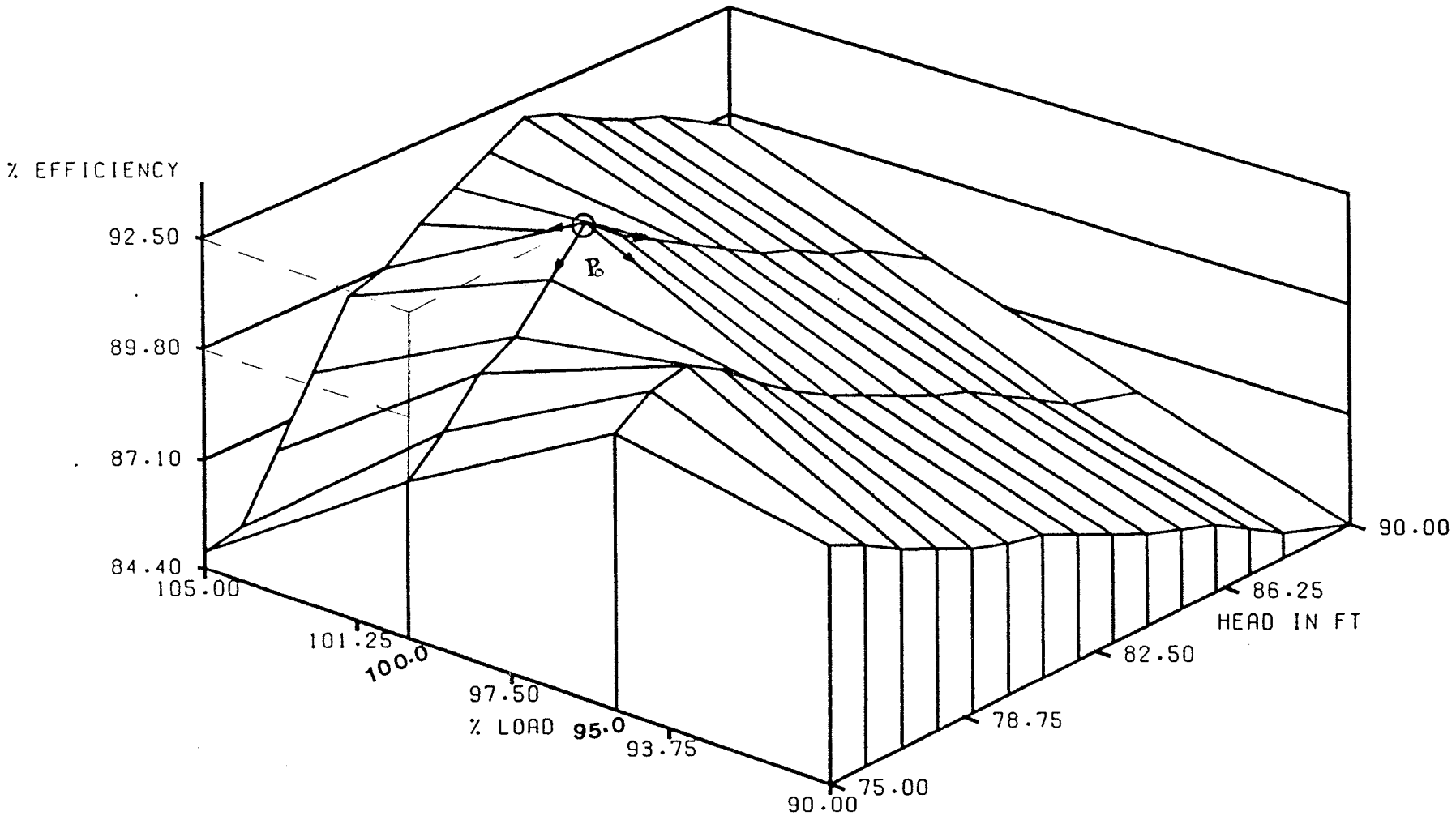

Fig. 3.9 : Variation of turbine efficiecy for different loads at different water heads with fixed speed operation.

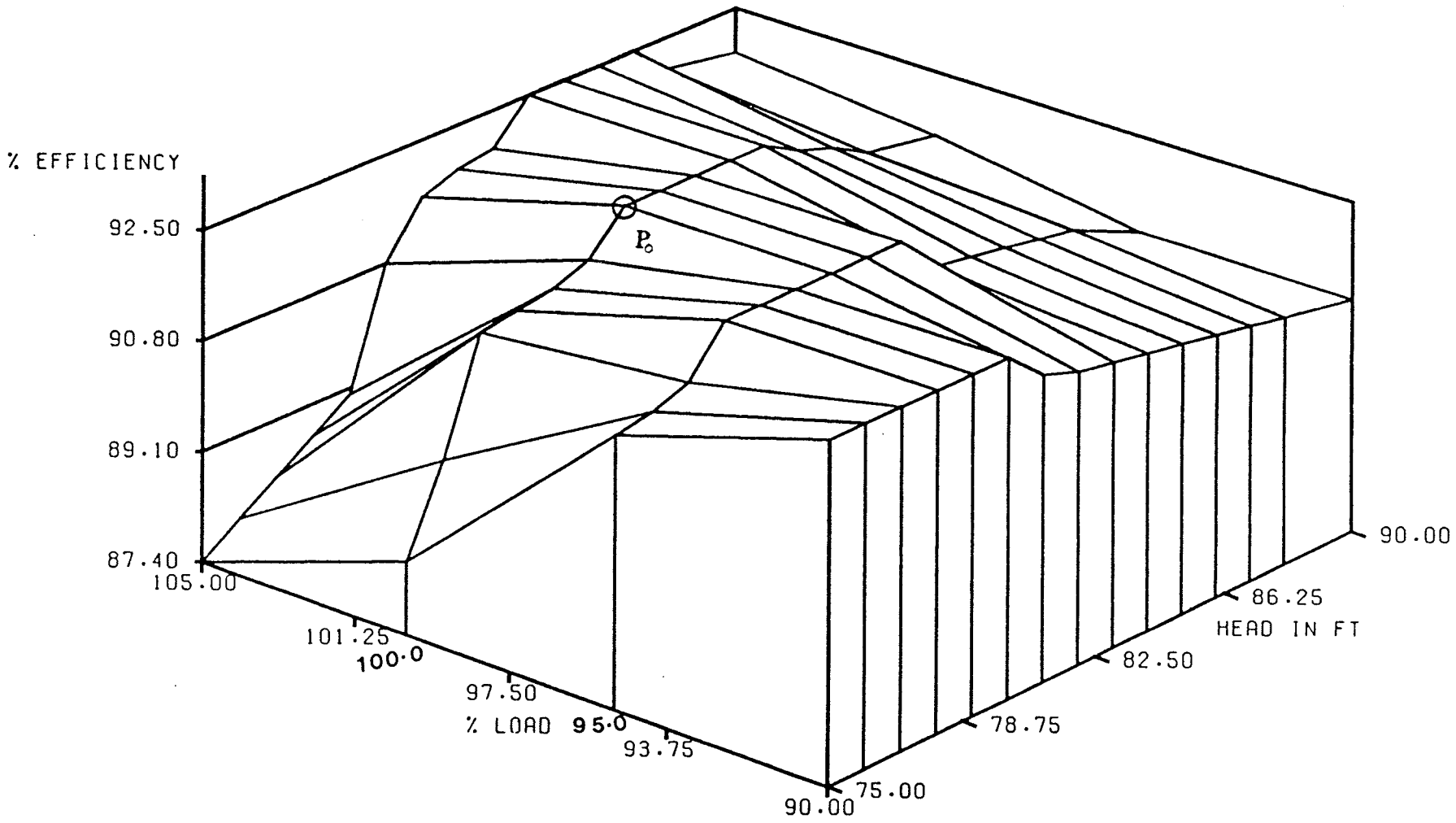

Fig. 3.10 : Variation of turbine efficiency for different loads at different water heads with variable speed operation.

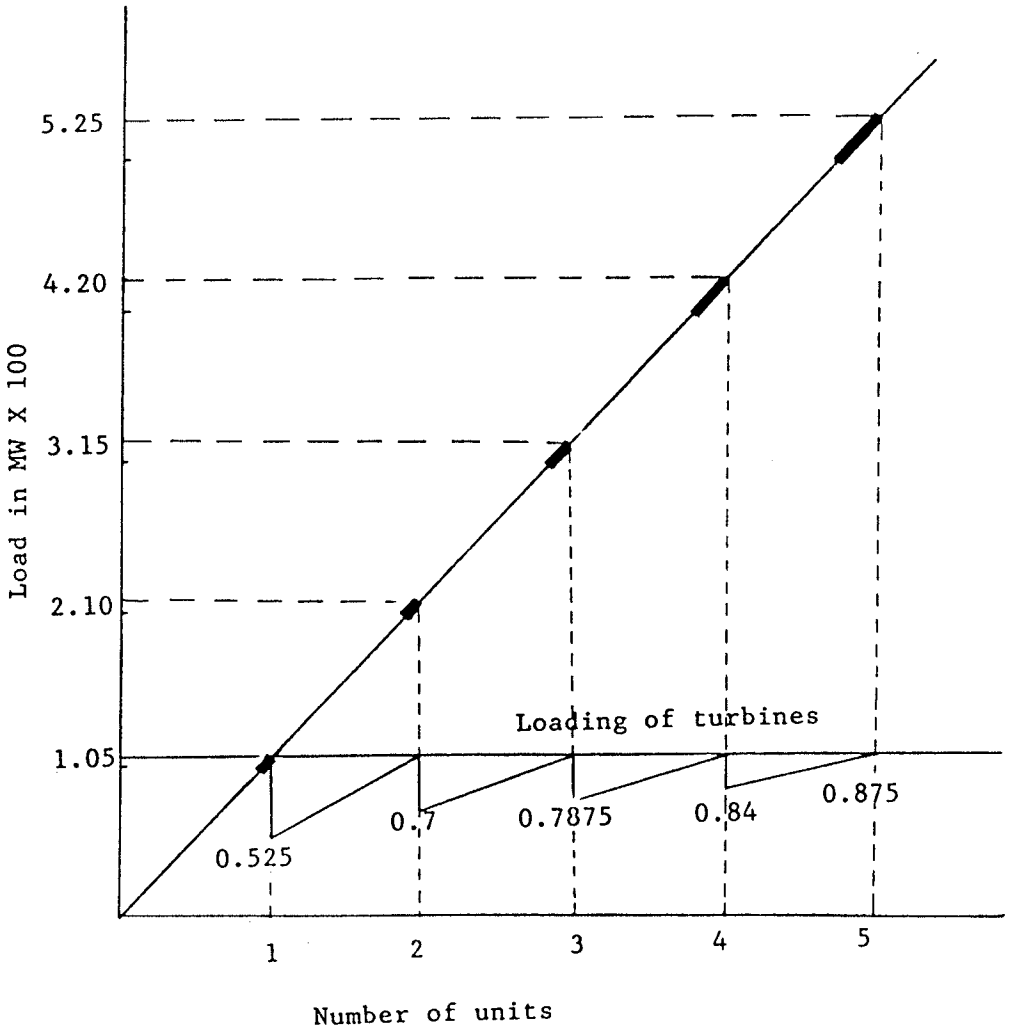

Fig. 3.11 : Loading curve of turbines with equal loading criteria.

demand. The turbine can be loaded to 105% of its rated capacity as indicated in the above figure.

Based on Fig. (3.8) for a 1000 MW station, energy saving with variable speed operation due to increase in the efficiency is given by

$$\Delta E = \left[\int_0^{100} P_{\Delta T} \cdot \frac{\Delta\eta}{100} \cdot \frac{\Delta T}{100} \right] . T . 10^3 \quad kWh \qquad (3.13)$$

Where

$P_{\Delta T}$ = Load in MW during the period ΔT

$\Delta\eta$ = % increase in efficiency.

ΔT = % duration of load.

T = Total duration in hours.

Therefore

$$\Delta E = \left(1.05 \text{ X } 10^3\right) \left(\frac{1.1}{100}\right) \left(\frac{3.7}{100}\right) \text{ x } 8760 \text{ x } 10^3$$

The capitalized savings at the rate of \$ 0.016 per kWh is given by

$$\Delta E \cdot \frac{1.6}{100} = \$ \, 0.598 \text{ x } 10^6$$

In these calculations, the deviations of water head from the nominal value are not taken into account. Generally the water head varies 2.5% either way from the nominal value. At 100% load, the variation of water head of 2 ft. (2.5 %) either way will lead to nearly 1% gain in the efficiency as shown in Fig. (3.3). This alone for 63% operating time will result in \$ 0.88 x 10^6 savings. For 105% load, the variation of the water

head of 2 ft. (2.5%) either way from the nominal value will lead to nearly 0.8% gain in the efficiency as shown in Fig. (3.2). This operation for 37% time will result in a further $ 0.436 x 10^6 saving.

The total savings due to variable speed operation of 1000 MW Longspruce generating station with the load duration curve shown in the Fig. (3.8) is estimated to be $ 1.914 x 10^6 . Since this value is not based on the actual load curve and hence may not be true value. Therefore it is necessary to evaluate actual savings based on the annual load duration curve and water head variation curve.

3.4 Performance evaluation of 10X100 MW hydro station under variable speed operation

In order to evaluate savings due to variable speed operation of 1000 MW Longspruce generating station, actual load duration and water variation curves for one year period should be taken into account. Since the variations of load demand and water head are expressed in percentage duration as shown in Figs. (3.12) and (3.13) respectively, it may not be possible to find the actual water head corresponding to the load in a particular duration. It is so because chronological data records are not available. Hence, the water head duration curve has been approximated into three segments with its average head in each segment. The load duration curve has been divided into five segments with its average load in each segment. The actual load and water duration curves are shown in Figs. (3.12) and (3.13) respectively, and the corresponding averaged curves are shown in Figs. (3.14) and (3.15) respectively.

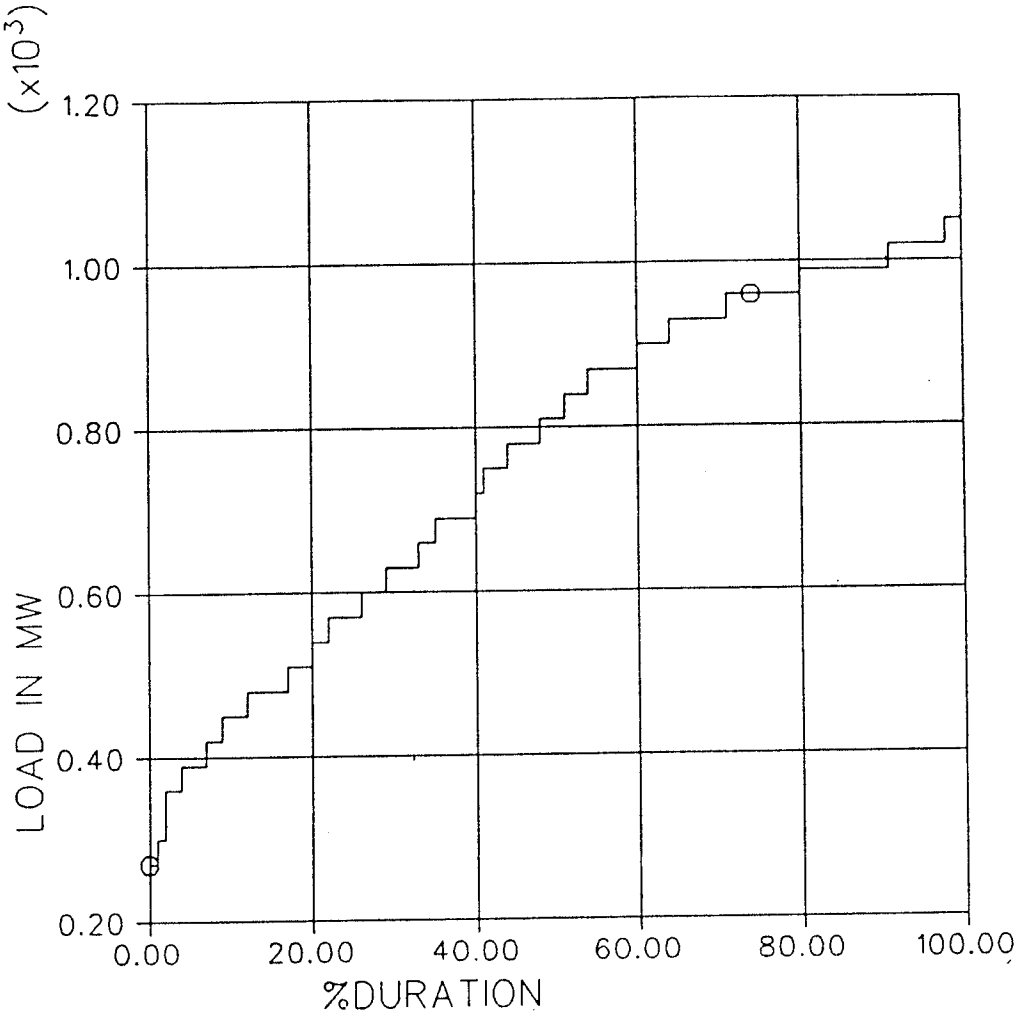

Fig. 3.12 : Annual load curve of a 10X100 MW hydrostation.

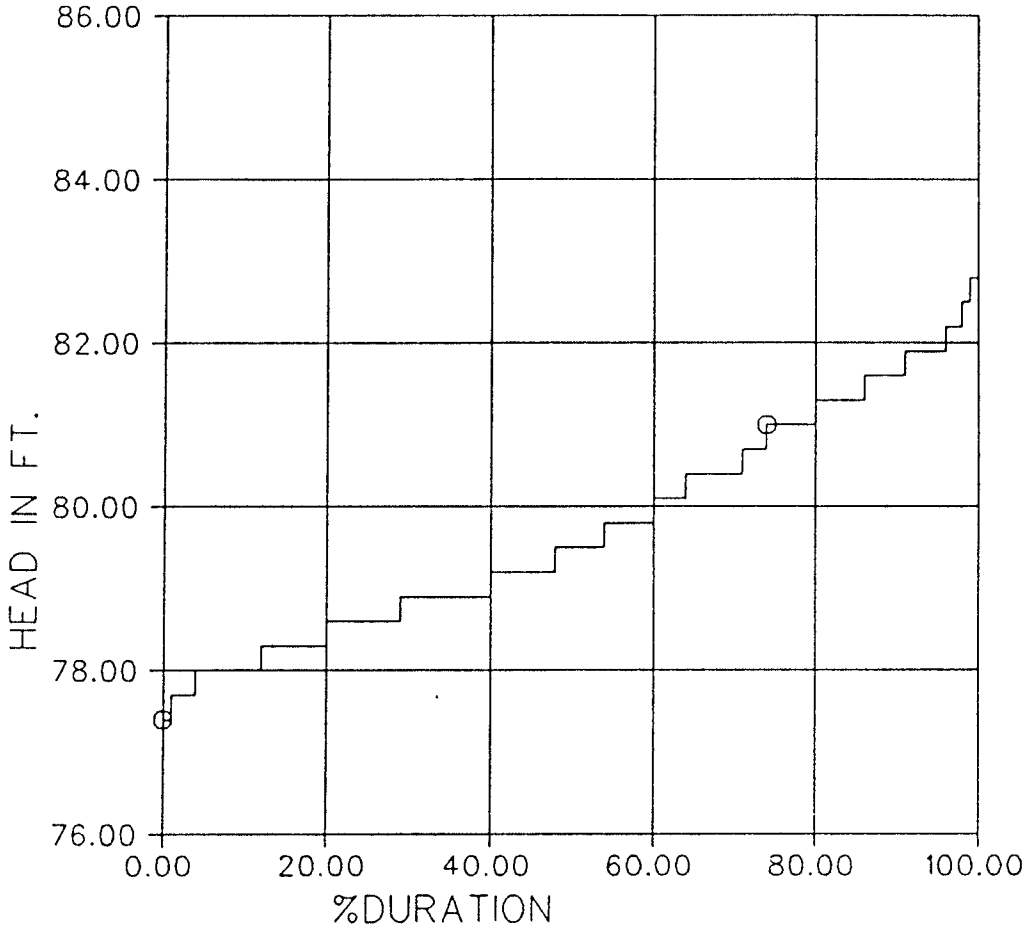

Fig. 3.13 : Annual water head variation curve of a 10X100 MW hydrostation.

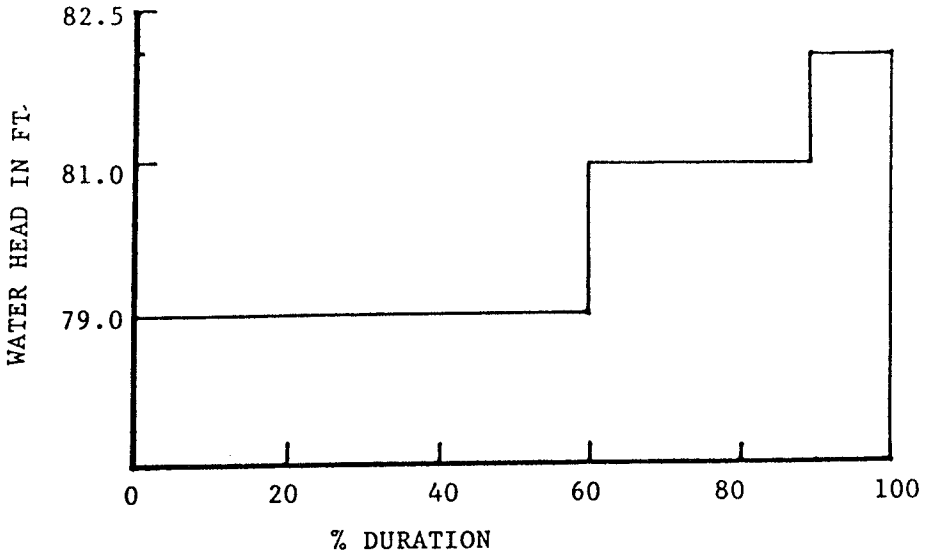

Fig. 3.14 : Averaged annual water head variation of a 10X100 MW hydrostation.

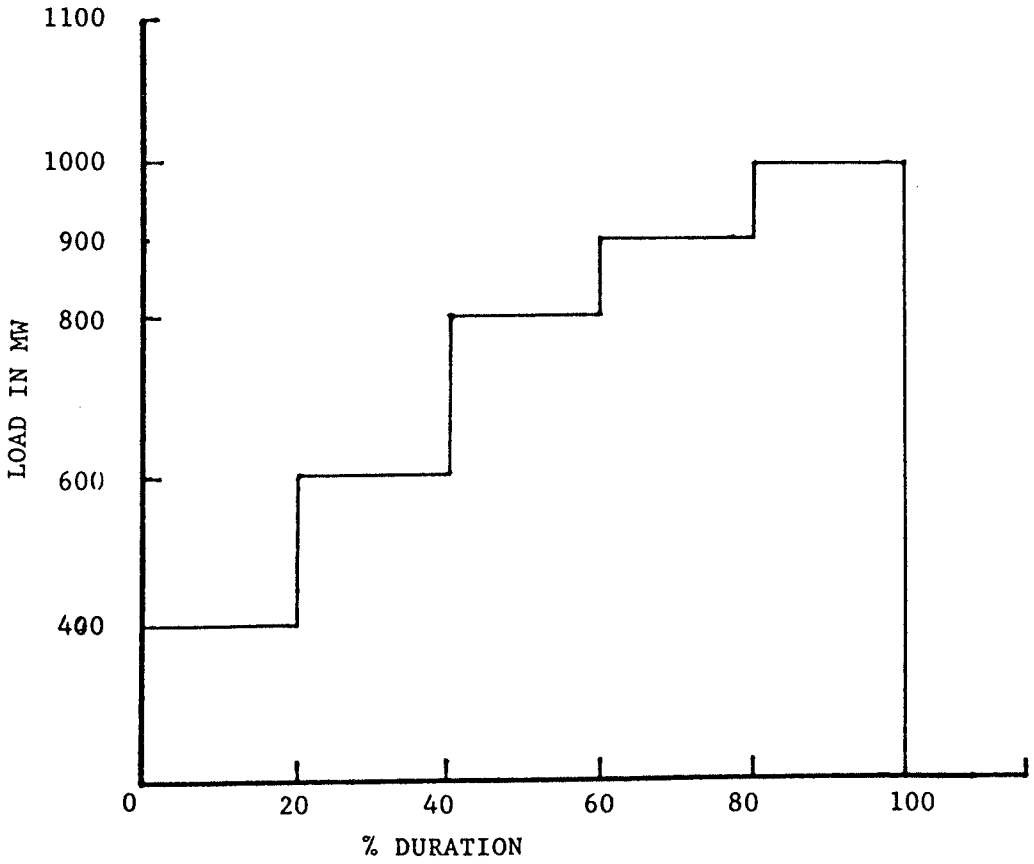

Fig. 3.15 : Averaged annual load curve of a 10X100 MW hydrostation.

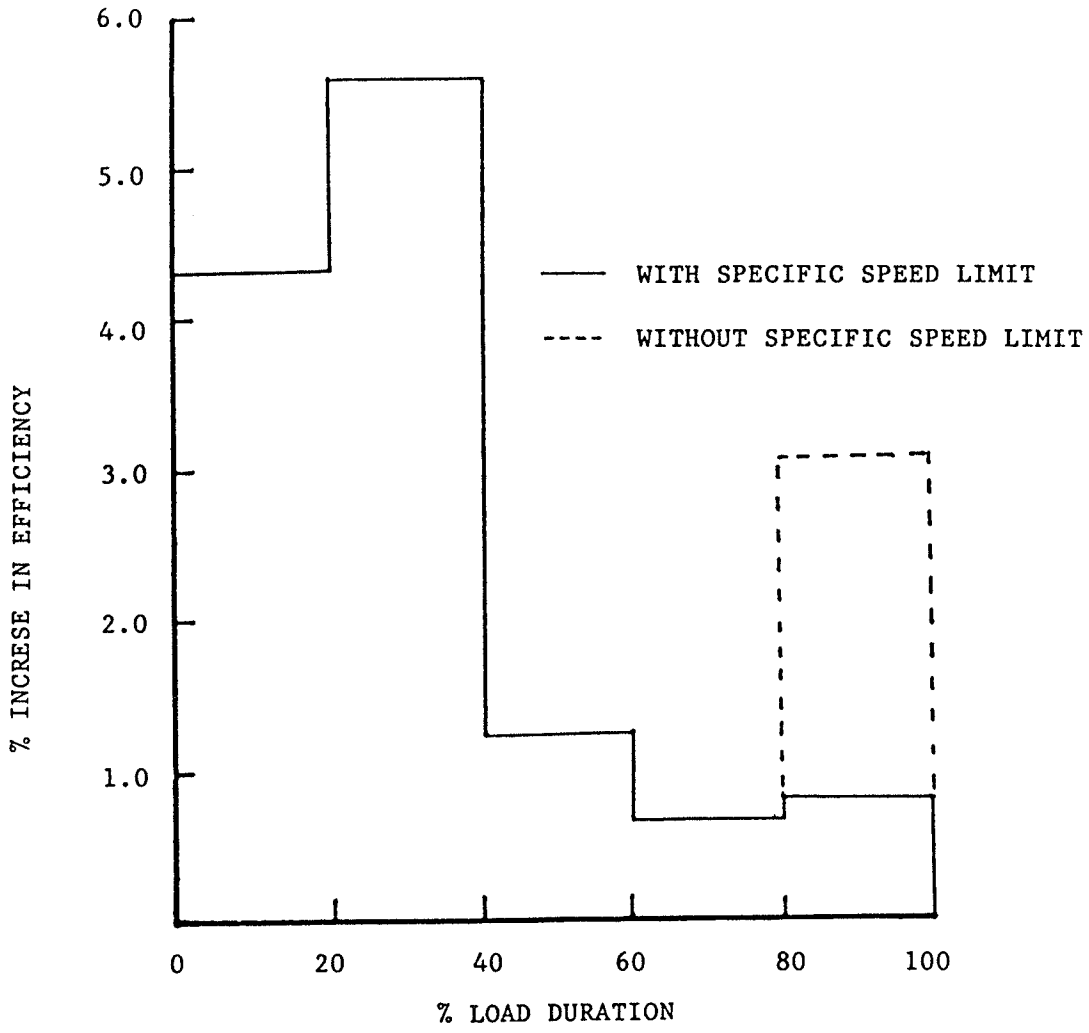

Fig. 3.16 : Increase in turbine efficiency with load under variable speed operation.

In the absence of chronological data, all segments of water head are considered for each segment of the load duration curve to evaluate the efficiencies under fixed and variable speed operation. Efficiency evaluation is done taking into account the specific speed limitation and also without taking specific speed limitation into account. The later condition can be reasonably valid if the turbine blades are stainless steel material with non corrosive coating. Fig. (3.16) shows the increase in the efficiency due to variable speed operation taking specific speed limitations into account. The energy savings due to variable speed operation due to increase in efficiency is calculated using Eqn. (3.18).

The net savings in energy taking
specific speed limitations into account = 130.87×10^6 kWh

With the energy rate factor of \$ 0.016 / kWh,
the net savings with variable speed operation
taking specific speed limitations into account = \$ 2.1×10^6

If the turbine blades are made of stainless steel material, the specific speed limitations can be relaxed. The increase in the efficiency without specific speed limitation is shown in the Fig. (3.16).

The net savings due to increase in the efficiency
without specific speed limitations taken into account = \$ 2.71×10^6

3.5 Summary and conclusions

A methodology has been developed to calculate the efficiency of the turbine under variable speed operation. In order to illustrate the relative advantage of variable speed operation, efficiencies are calculated for a typical 135,000 hp hydraulic turbine under both fixed and variable speed operation for different loads of 105%, 100%, 95% and 90% taking reasonably wide variation of water head from 75 ft to 90 ft and shown in Figs. (3.2) to (3.5).

A constant speed turbine operates on constant power curves marked for 105%, 100% and 90% loads in Fig. (3.1). It can be observed that as the operating head changes, changes occur in both Φ and P_{11} which in turn lead to change in the operating efficiency. On the other hand if the speed is allowed to change as permitted by the unit connection scheme, it could always be chosen such that its efficiency can be kept at its maximum value. For example, for constant output power, if changes occur in the P_{11} between 0.22 and 0.245 due to changes in head (Eqn. 3.9), the operating speed N should always be chosen such that the operating point always lie within the closed curve for $\eta = 90\%$ in $P_{11} - \Phi$ plane as shown in Fig. (3.1).

As observed from the Fig. (3.3) and Fig. (3.4), as the water head drops below 77 ft and 78 ft respectively, the operating speed is held at its maximum possible value without violating specific speed limitations and therefore below these water heads, the turbine operates at fixed speed. Fig. (3.7) shows another important comparison of the turbine for the fixed and the variable speed operation as a function of load with the nominal water head of 80 ft. It can be observed that there is an improvement of 4.2% and 1.1% in efficiency at 90% and 105% loads respectively under variable speed operation. It means that the improvement in efficiency under low load

conditions is more than that of the over load condition for fixed water head. The variation of turbine efficiency for different loads at different heads is shown in Fig. (3.9) and Fig. (3.10) for fixed and variable speed operations respectively. It can be clearly seen from the above three dimensional figures, that maximum possible efficiency can be achieved by adopting variable speed operation of turbine as compared to fixed speed operation for variable load and water head conditions.

A typical yearly load duration curve for 1000 MW hydro station shown in Fig. (3.8) with 100% load for 63% of time and 105% load for the remaining 37% of time is evaluated for variable speed operation taking 2.5% variation in water head. It has been found that an annual gains of $ 1.914 x 10^6 is expected due to variable speed operation.

Annual load and water head variation curves of 1000 MW Long Spruce hydro station of Manitoba Hydro are analyzed for variable speed operation with and without specific speed limitations. The expected gains due to variable speed operation with and without taking specific speed limitations into account are $ 2.1 x 10^6 and $ 2.71 x 10^6 respectively.

In conclusion, if turbines in hydro power station are operated under variable speed depending upon the available water head and load, as permitted by the unit connection scheme, considerable gains can result due to increase in the operating efficiency.

CHAPTER IV

GENERATORS FOR UNIT CONNECTION SCHEMES

4.1 Introduction

In conventional HVDC schemes a group of generators are connected to a common ac bus, therefrom to converter transformers and converters. Tuned ac filters are installed on the ac bus to absorb ac harmonics generated by converters. Increase in the pulse number of converters reduces the harmonic generation, which is normally achieved by connecting transformers of different configurations to converters. For example, 12-pulse operation of converters is obtained by connecting a three phase supply through Y-Y and Y- Δ transformers to two 6-pulse converters connected in series. In unit connection schemes, ac filters are removed and the generated harmonic currents are allowed to flow into generator. These harmonics cause additional losses and may result in a loss of capacity of the generator.

Multiphase generators can be designed for unit connection schemes to increase the pulse number to reduce the harmonic generation. This chapter deals with the design aspects and analysis of generators for unit connection schemes. If 5 phase generators are designed for the above schemes, 10-pulse operation can be achieved by connecting the generator to 10-pulse converter. If the scheme is intended for the dc power transmission, the required dc voltage can be obtained by connecting the generator to the

converter through 5 phase transformer or five single phase transformers. The 5 phase transformer requires five limb core of which the design may be complex. Other alternative is to use five single phase transformers which may increase the cost. Increase in pulse number by more than three legs on the converter influences the harmonic generation and therefore injection into the system. Large pulse number means more cost, e.g 10-pulse converter cost will increase by a factor of $\left(\frac{5}{3}\right)$ / kW.

In order to examine the harmonic currents injected into the 5 phase generator connected to a 10-pulse converter, the phase current as shown in Fig. (4.1) is analyzed. Each valve in the converter bridge conducts for a period of $\frac{2\pi}{5}$ radians. The Fourier analysis of the current waveform shown in Fig. (4.1) is given by

$$i_{a5}(\omega t) = 0.7485\, I_{dc} \Big\{ \sin(\omega t) - 0.539 \sin 3(\omega t) + 0.231 \sin 7(\omega t) - 0.111 \sin 9(\omega t) - 0.091 \sin 11(\omega t) + 0.0124 \sin 13(\omega t) - 0.095 \sin 17(\omega t) + 0.041 \sin 21(\omega t) - \ldots\ldots \Big\} \qquad (4.1.1)$$

It can be observed from the above equation that the generator phase current contains all odd harmonics. For balanced 5 phase generator with star connection, the 5th harmonic is of zero sequence and hence all harmonics multiples of 5 cancel in the machine. The 3rd and the 7th harmonics are predominant in the phase current with magnitudes of 54% and 23% of the fundamental respectively. These harmonics induce currents in the rotor circuits and cause not only additional losses but also produce pulsating torques in the machine. The negative sequence 9 th harmonic current

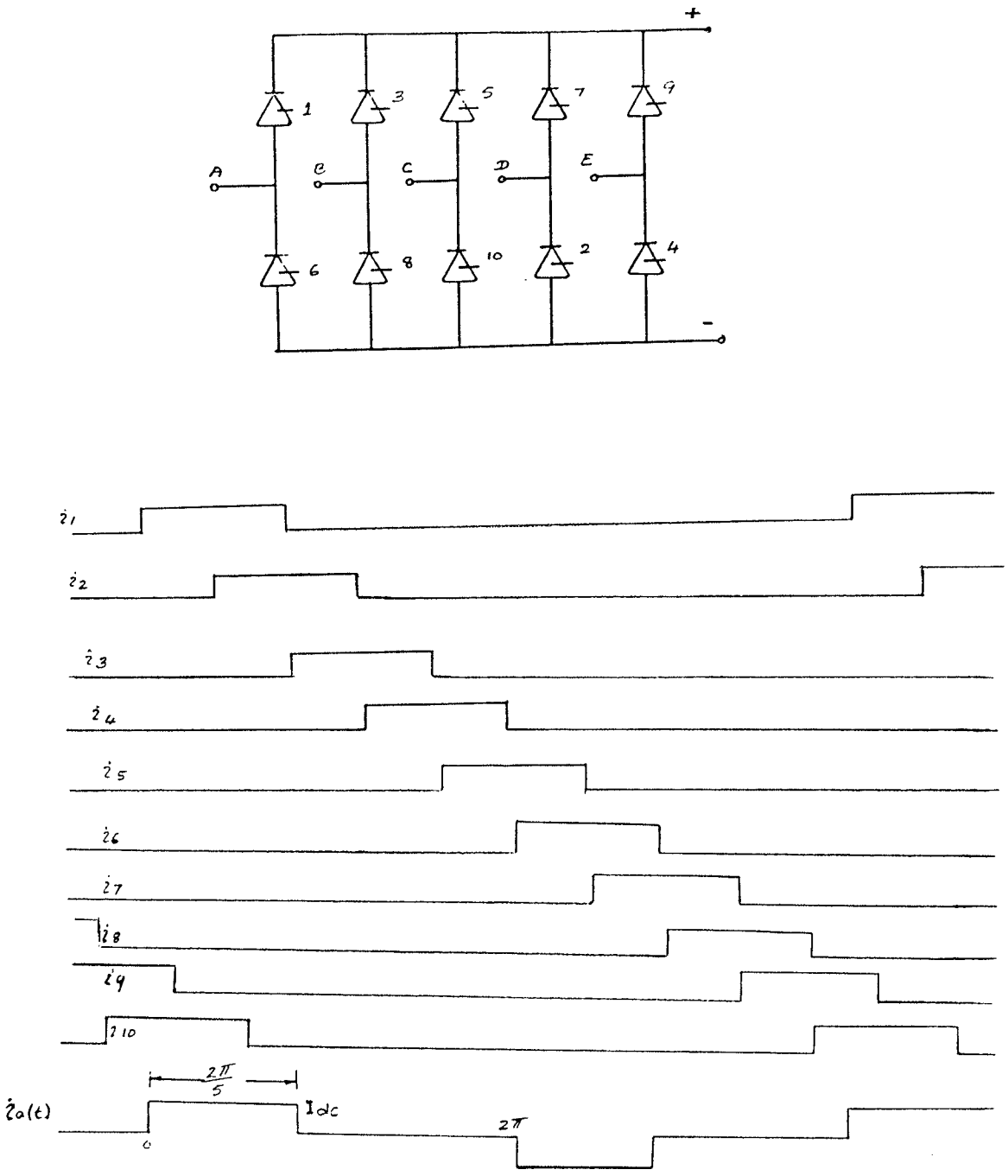

Fig. 4.1 : Phase current of a 5 phase generator fed with 10 pulse converter.

of 11.1% magnitude induces 10 th harmonic currents in the rotor circuits. These currents produce breaking torques in the machine.

In the case of 7 phase generator, 7 leg converter required to achieve 14-pulse operation which may increase the cost by a factor of $(\frac{7}{3})$ / kW. The expression for the phase current is given by

$$i_{a7}(\omega t) = \frac{\sqrt{3} \cdot I_{dc}}{\pi} \left\{ \sin(\omega t) - 0.75 \sin 3(\omega t) + 0.361 \sin 5(\omega t) \right.$$

$$- 0.2 \sin 9(\omega t) - 0.091 \sin 11(\omega t) + 0.0124 \sin 13(\omega t)$$

$$\left. - 0.095 \sin 17(\omega t) + 0.041 \sin 21(\omega t) - \cdots \right\} \qquad (4.1.2)$$

It can be observed from the above expression that all odd harmonics are present in the generator phase current. The 3rd and the 5th harmonic currents are predominant with magnitudes of 75% and 36.1% of fundamental respectively. These harmonic currents cause additional losses in the stator and the rotor. If these generators are to be used in point-to-point transmission schemes, the required dc voltage can be achieved by connecting to the converter either by a 7 phase transformer or by seven single phase transformers. The seven phase transformer design may be complex as it requires 7 limb core. If seven single phase transformers are employed, the cost of the terminal may increase.

Since the harmonic currents in the 5 phase and 7 phase generators are higher and involves high cost transformers, these are discarded for unit connection application. The next viable alternative in multiphase generators is the 6 phase generator. If the generator is designed with two sets of Y-connected three phase windings spatially displaced by 30° to each other,

12 pulse operation can be achieved by connecting these two winding sets to two six pulse converters. Six phase generators have technical and economical advantages when compared with conventional three phase generators if the rating the generator is large. These advantages are discussed in the section [4.2] of this chapter. These generators are applicable for thermal and nuclear power stations either with point-point schemes or back-to-back schemes.

In back-to-back schemes, there is a possibility of eliminating converter transformers by connecting generators directly to converters. In this situation ($6k \pm 1$) harmonic currents flow in the stator windings, where k is any positive integer. The 5th and 7th harmonic m.m.fs cancel in the air gap due to 30^{o} space displacement between winding sets. The 11th, the 13th etc., harmonic mmfs induce the 12th, the 24th etc., harmonic currents in rotor circuits. This type of schemes are more applicable to improve stability of the system where a large generating station is to be connected to the nearby ac systems [17]. However the main draw backs of these schemes are as follows:

(a) The generator windings are subjected to different dc potentials, since they are directly connected to two six pulse converters connected in series. In this case one set of windings is to be designed to half the dc voltage and the other set to full dc voltage.

(b) The generator neutrals are also elevated to higher dc potentials which may increase the complexity of protection schemes for the generator internal faults.

If these schemes are contemplated aiming at the system stability, it may be

worthwhile analyzing different possible windings configurations of the generator to adopt the best possible one. In this chapter, the effect of time harmonic currents in the air gap mmf of a six phase generator directly connected to a 12-pulse converter is analyzed taking the real distribution of the stator windings into account for Y-Y and Y- Δ configurations. It is found that magnitudes of mmf space harmonics generated by the time harmonics currents are less in the case of a Y-Y windings configuration than Y- Δ windings configuration.

Harmonic currents flowing in the stator and the rotor circuits of a six phase generator with Y-Y windings configuration directly connected to a 12-pulse converter are computed by modelling the generator in d-q-o coordinates and simulated by using EMTDC Program. The additional losses are calculated in order to evaluate the derating factor of the generator. Design aspects of large rating generators for thermal and nuclear power stations are discussed with respect to higher base speed operation. The effect of variable speed operation of hydro generators is also discussed with respect to the commutation reactance, reactive power requirements and power factor.

4.2 Six phase generators

If the size of the generator is large, six phase generators have the following advantages as compared to that of a three phase generator of the same rating.

(a) *Increased utilization of active material :*

when the number of phases increases, the winding distribution factor increases as the slots per pole per phase decreases. Due to increase in the winding factor, for its design, the generator require less number of turns which in turn reduce both the copper and iron volume and therefore result in less active material requirement per kVA. For example, in the case of three phase machine, with 5/6 winding pitch, the winding factor is 0.922. Whereas in the case of a six phase generator with 11/12 winding pitch, the winding factor is 0.977. The increase in the winding factor in the case of a six phase generator is 6.1% which means that the reduction in the active material is in the same proportion.

(b) *Reduction in rotor surface losses :*

The rotor surface losses in the machine are produced by the pulsation of the flux density in the rotor pole surface. These are caused by :

(i) The harmonics of the magnetomotive ampere-turns of the armature reaction produced due to the use of limited number of phases. The higher the number of phases the lower the harmonic content.

(ii) The harmonics of the magnetomotive ampere-turns of the armature reaction due to limited number of slots.

(iii) The variation of permeance of the air gap due to the slotting of the stator.

The increase in number of phases therefore reduces the rotor surface losses.

Robert, P. et al. [18] compared losses of three phase and six phase

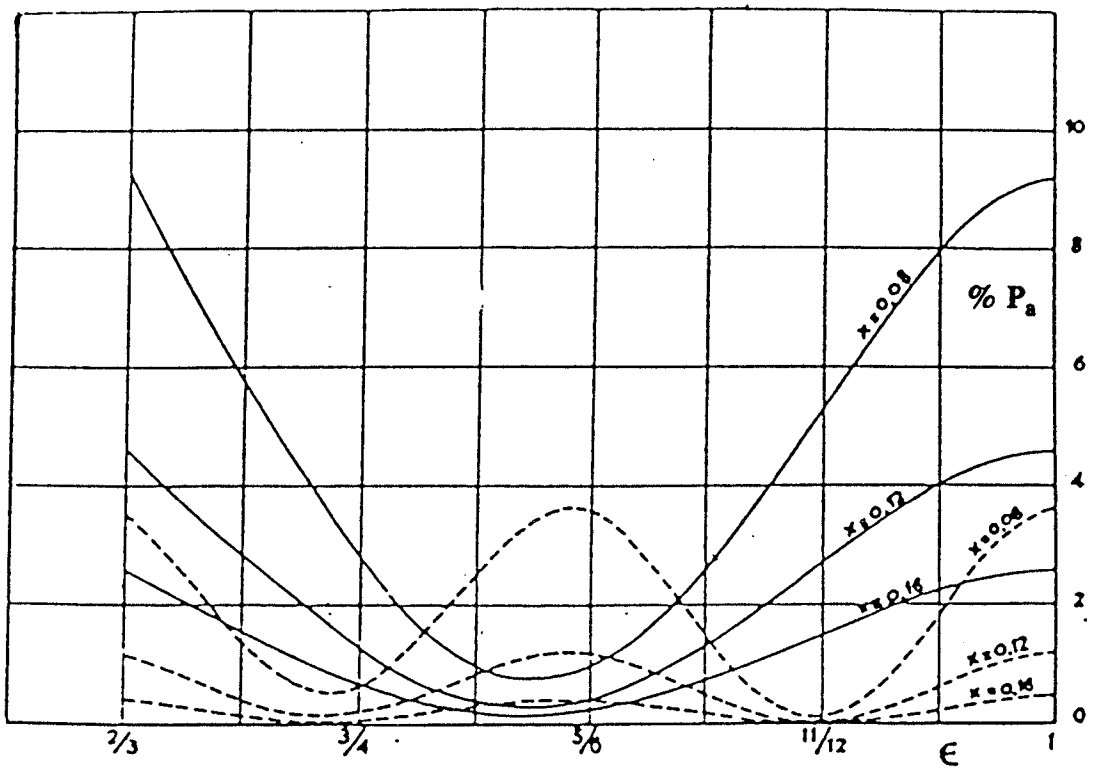

Fig. 4.2 : Losses at the surface of the rotor due to limited number of phases.

ϵ : pitch factor.

x : air gap ratio.

P_a : Losses expressed as % of apparent power.

---- : losses in 3-phase machine expressed as 10^{-3} of rated power.

---- : losses in 6-phase machine expressed as 10^{-4} of the rated power.

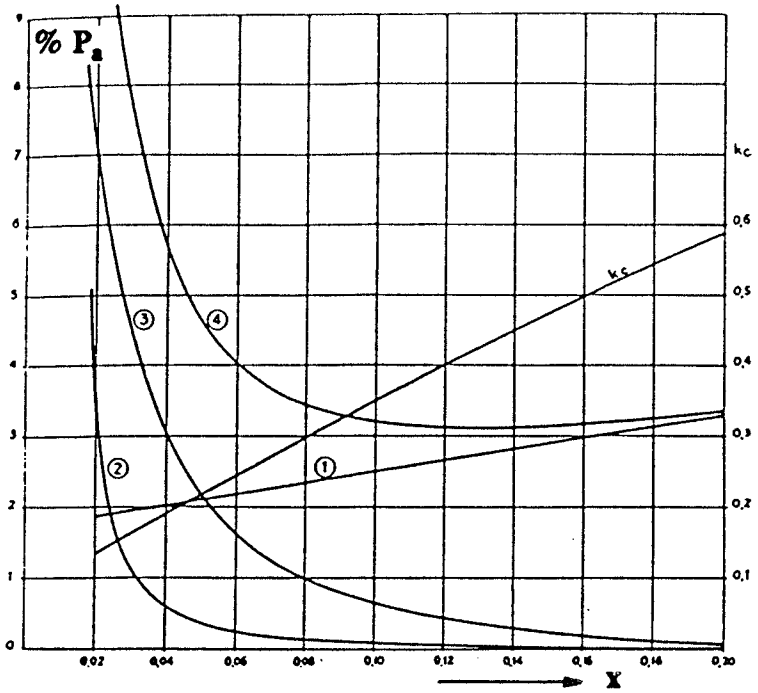

Fig. 4.3 : Variation of losses with the air gap for 3-phase generator.

$x = \frac{2l}{D_s}$, air gap ratio.

l = length of the air gap.

P_a = losses expressed as % of the apparent power.

k_c = short circuit ratio of the machine.

(1) ohmic losses in the windings.
(2) rotor surface losses due to limited number of slots.
(3) rotor surface losses due to limited number of phases.
(4) sum of the above losses.

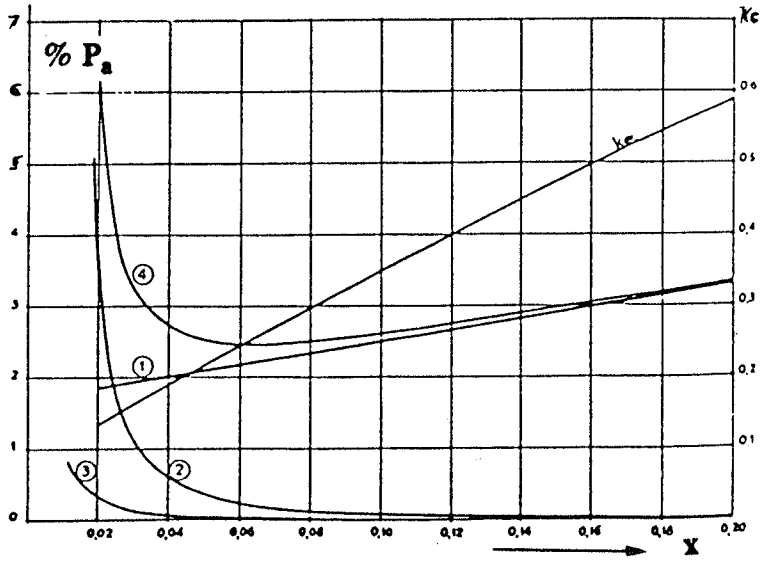

Fig. 4.4 : Variation of losses with air gap for six phase generator.

generators of 1200 MW rating as shown in Figs. (4.2) to (4.4). Fig. (4.2) shows the variation of the rotor surface losses as a function of the winding pitch. It can be seen that the rotor surface losses in the case of a six phase machine with 11/12 winding pitch are less than that of a three phase machine with 5/6 pitch for a given air gap ratio, where air gap ratio is defined as the ratio of twice air gap length to bore diameter. As seen from Fig.(4.3) and Fig.(4.4), for the normal design range of air gap ratios varying from 0.06 to 0.16, the losses in the case of a six phase generator are found to be smaller than an equivalent size three phase generator. Yhis happens because of the reduction in the rotor surface losses.

Therefore due to the reduction in losses and the active material, six phase generators can be designed for higher efficiency with compact sizes as compared to three phase generators. It is also shown that a six phase generator of 1200 MW capacity with Y Δ - Y three phase transformer is cheaper than a conventional three phase machine of the same capacity [18]. This may enhance the applicability of six phase generators to unit connection schemes.

4.3 Harmonic analysis of the air gap mmf of a six phase generator connected to a 12-pulse converter

If the stator windings in the generator are not distributed sinusoidally, the space harmonics are generated in the air gap mmf due to currents flowing in these windings. This section deals with the analysis of the air gap mmf of a six phase generator with Y-Y windings configuration displaced by 30° from each other and Y- Δ windings configuration. Real distribution of stator windings when connected to a 12-pulse load is examined. The overlap angle and delay angle are neglected in this analysis for the sake of brevity. This, however is not to be regarded as a shortcoming because when taken into account they only modify the relative content of the harmonic currents injected into the machine. The magnitude of harmonic currents are maximum when the overlap angle is zero for a given delay angle and subsequently decreases as the overlap angle increases up to $\frac{360}{p}$, where p is a pulse number [19]. This analysis assumes a pessimistic condition on the generator.

4.3.1 Analysis of air gap mmf of a Y-Y connected armature windings with 30° phase shift

The generator with Y-Y windings configuration with 30° phase shift between axes is connected directly to two six pulse rectifiers as shown in Fig. (4.5). The armature phase currents are shown in Fig. (4.6). The explicit equations for the mmf due to currents in different windings are derived in Appendix II.

The total armature mmf due to currents in Y-Y windings displaced in space by 30° is given by :

$$F_{Y-Y}(\theta, t) = F_{abc} + F_{xyz}$$

$$= \frac{24\sqrt{3}}{\pi^2} N_a I_{dc} \left(kw_1 \left[\cos(\omega t-\theta) - \frac{1}{11}\cos(11\omega+\theta) + \frac{1}{13}\cos(13\omega t-\theta) - .. \right] \right.$$

$$+ \frac{kw_5}{5} \left[-\frac{1}{5}\cos(5\omega t-5\theta) + \frac{1}{7}\cos(7\omega t+5\theta) \right]$$

$$- \frac{kw_7}{7} \left[\cos(-\frac{1}{5}\cos(5\omega t+7\theta) + \frac{1}{7}\cos(7\omega t-7\theta) \right]$$

$$+ \frac{kw_{11}}{11} \left[\cos(\omega t+11\theta) - \frac{1}{11}\cos(11\omega t-11\theta) + \frac{1}{13}\cos(13\omega t+11\theta) - .. \right]$$

$$- \frac{kw_{13}}{13} \left[\cos(\omega t-13\theta) - \frac{1}{11}\cos(11\omega t+13\theta) \right]$$

$$\left. + \frac{1}{13}\cos(13\omega t-13\theta) - ..... \right] \qquad (4.3.1)$$

It can be observed from the above equation that the air gap mmf contains both time and space harmonics. In general, $F_{(m,n)} \cos (n\omega t \pm m\theta)$ is the armature mmf of the m th space harmonic generated by n th time harmonic current in the stator windings. This mmf wave rotates at $\pm \frac{n}{m}$ times the synchronous speed with respect to the stator and its magnitude is $F_{(m,n)}$. The direction of rotation of the field structure with respect to the armature is taken as positive. The harmonic currents induced in the rotor rotate at $[1- (\pm \frac{n}{m})]$ times the synchronous speed with respect to the rotor. These currents cause additional losses in the rotor circuits. A 125

MVA, 2 pole round rotor generator with Y-Y windings configuration has been analyzed for mmf harmonics when connected to a 12-pulse converter load. The parameters of the machine are also shown in Appendix II. The harmonic winding factors are calculated and shown in Table (4.1). The Table (4.2) shows the magnitude and the direction of air gap mmf space harmonics generated by the time harmonic currents.

It can be seen from the Table (4.2) that the components of the fundamental space wave produced by the 11 th and 13 th time harmonic currents are predominant with the magnitudes of 9.1% and 7.7% respectively. These harmonics rotate at -11 and +13 times the fundamental frequency with respect to the stator. When referred to the rotor these components rotate at 12 times the fundamental frequency. The mmf also contains the 5th and the 7th space harmonics produced by the 5th time harmonic current and also 7th time harmonic current. The magnitude of the 5th space harmonic produced by the 5th time harmonic is 2.4% and it rotates at the fundamental frequency with respect to the stator. Hence this component would not induce currents in the rotor circuits. It means that this component causes additional losses only in the stator, but not in the rotor. The 5th space harmonic mmf caused by the 7th time harmonic current has the magnitude of 1.73% and rotates at -7/5 times the fundamental frequency with respect to the stator. This will induce rotor currents at 12/5 times fundamental frequency. The magnitude of other mmf space harmonics produced by time harmonic currents are very small.

All these harmonics in the air gap mmf cause additional losses both in the stator and the rotor circuits. The significant loss contribution is due to fundamental space harmonics produced by 11th and 13th time harmonic currents and the effect of other harmonic currents are not very significant.

Harmonic number, m	1	3	5	7	11	13
Winding factor K_{wm}	0.98	0.83	0.59	0.326	0.012	0.01

Table 4.1 : Harmonic winding factors of a six phase generator.

$\%F_{m-n}$ (rotation)	Order of the time harmonic 'n'.				
Order of the space harmonic 'm'	1	5	7	11	13
1	100 (ω)			9.1 (-11ω)	1.7 (13ω)
5		2.4 ($+\omega$)	1.73 ($-\frac{7}{5}\omega$)		
7		0.95 ($-\frac{5}{7}\omega$)	0.66 ($+\omega$)		
11	0.09 ($-\frac{1}{11}\omega$)			0.01 (ω)	0.008 ($-\frac{13}{11}\omega$)
13	0.078 ($+\frac{1}{13}\omega$)			0.007 ($-\frac{11}{13}\omega$)	0.006 ($+\omega$)

Table 4.2 : Magnitude and direction of space harmonics generated by time harmonic currents in Y-Y windings with 30° phase shift.

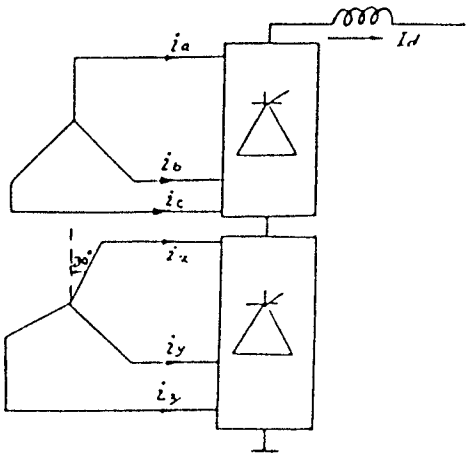

Fig. 4.5 : Y-Y windings configuration with 12-pulse converter.

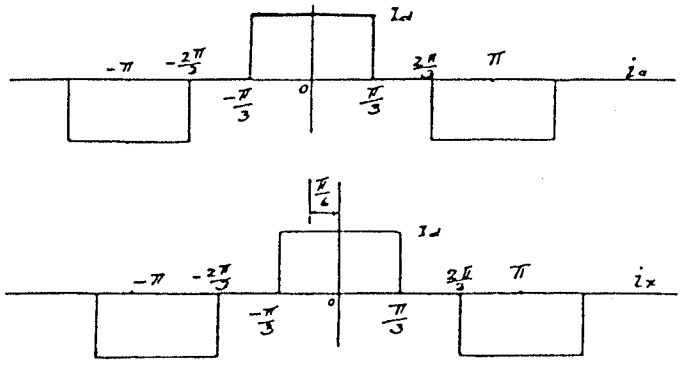

Fig. 4.6 : Generator currents for Y-Y winding configuration with 30° phase shift.

4.3.2 Analysis of air gap mmf of a Y- Δ connected armature windings

As shown in the Appendix II, the air gap mmf due to currents flowing in the armature windings of Y- Δ configuration is given by :

$$F_{Y-\Delta} = \frac{24\sqrt{3}}{\pi^2} I_{dc}\, N_a \left(kw_1 \left[\cos(\omega t-\theta)-\frac{1}{11}\cos(11\omega t+\theta)+\frac{1}{13}\cos(13\omega t-\theta)-..\right] \right.$$

$$+\frac{kw_5}{5}\left[\cos(\omega t+5\theta)-\frac{1}{11}\cos(11\omega t-5\theta)+\frac{1}{13}\cos(13\omega t+5\theta)-..\right]$$

$$+\frac{kw_7}{5}\left[\cos(\omega t-7\theta)-\frac{1}{11}\cos(11\omega t+7\theta)+\frac{1}{13}\cos(13\omega t-7\theta)-..\right]$$

$$+\frac{kw_{11}}{11}\left[\cos(\omega t+11\theta)-\frac{1}{11}\cos(11\omega t-11\theta)+\frac{1}{13}\cos(13\omega t+11\theta)-..\right]$$

$$+\frac{kw_{13}}{5}\left[\cos(\omega t-13\theta)-\frac{1}{11}\cos(11\omega t+11\theta)\right.$$

$$\left. \left. +\frac{1}{13}\cos(13\omega t-11\theta)-..\right] \right) \qquad (4.3.2)$$

The magnitude and direction of harmonics in the air gap mmf are shown in the Table (4.3). It can be observed form the above equation that the predominant components in the air gap mmf are as follows:

(1) The components of the fundamental space wave produced by the 11th and 13th harmonic currents are of the magnitude 9.1% and 1.7% respectively. The fundamental component of the space mmf produced by the negative sequence 11th harmonic current rotate at -11 times the fundamental frequency with respect to the stator. This component

$\%F_{m-a}$ (rotation)	Order of the time harmonic ' n '				
Order of the space harmonic 'm'	1	5	7	11	13
1	100 $(+\omega)$			9.1 $(-11\ \omega)$	1.7 $(+13\omega)$
5	12.0 $(-\frac{\omega}{5})$			1.1 $(+\frac{11}{5}\omega)$	0.93 $(-\frac{13}{5}\omega)$
7	4.7 $(+\frac{\omega}{7})$			0.43 $(-\frac{11}{7}\omega)$	0.365 $(+\frac{13}{7}\omega)$
11	0.111 $(-\frac{\omega}{11})$			0.01 $(+\omega)$	0.009 $(-\frac{13}{11}\omega)$
13	0.078 $(+\frac{\omega}{13})$			0.007 $(-\frac{11}{13}\omega)$	0.006 $(+\omega)$

Table 4.3 : Magnitude and direction of space harmonics generated by time harmonic currents in Y-Δ windings configuration.

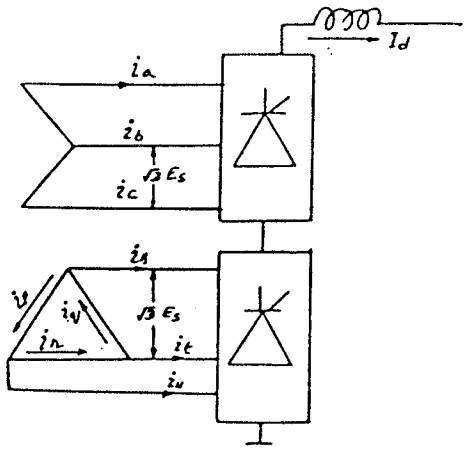

Fig. 4.7 : Y- Δ windings configuration with 12-pulse converter.

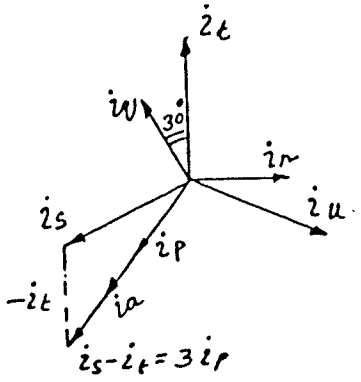

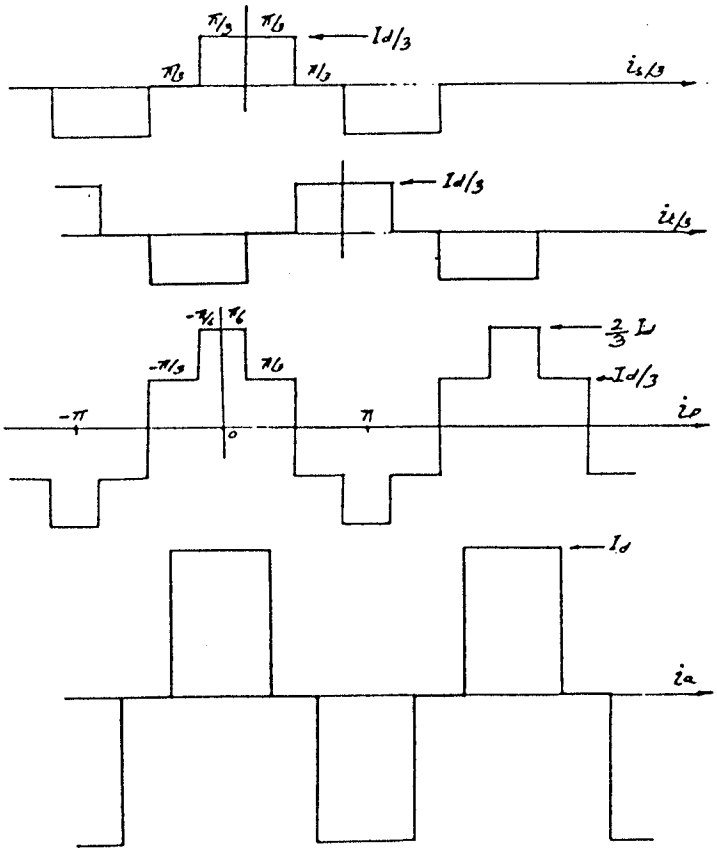

Fig. 4.8 : Generator phase currents for Y- Δ windings configuration.

induces 12th harmonic currents in the rotor circuits. Similarly, the fundamental component of the space mmf produced by the positive sequence 13th harmonic current rotates at 13 times the fundamental frequency with respect to the stator and induces 12th harmonic currents in the rotor circuits. These components are of same magnitudes as in the previous configuration.

(2) The space mmf also contains predominant 5th and 7th harmonics produced by the fundamental time harmonic current. It is interesting to note that the 5th space harmonic produced by the fundamental current is the most predominate component with 12% magnitude. This rotates at -1/5 times the fundamental frequency with respect to the stator. When referred to the rotor this component rotates at 6/5 times the rotor speed and produces braking torques and causes additional losses. The 7th space harmonic has 4.7% magnitude and rotates at an angular speed of + 1/7 times the stator speed and induces the currents in the rotor at 6/7 times the fundamental frequency. The magnitudes of other space harmonics are not significant.

4.3.3 Conclusions

It can be observed from the above analysis that the six phase generator with Y-Y windings configuration has less space harmonics in the air gap mmf as compared to that of Y- Δ windings configuration. Hence it is recommended that the six phase generator with Y-Y windings configuration is more suitable for unit connection schemes as compared to Y- Δ configuration.

4.4 Performance of a six phase generartor connected to a 12-pulse converter

When the six phase generator with Y-Y windings configuration with 30^0 space dispalcement between winding sets is directly connected to a 12-pulse converter, 5th, 7th, 11th,t13th etc., harmonic currents flow into the stator windings and 12th, 24th, etc., harmonic currents are induced in the rotor circuits. In order to calculate harmonic currents in the stator and rotor windings, the generator is modelled in d-q-o co-ordinates and simulated the system as shown in Fig. (4.12) using EMTDC program. Harmonic currents in the stator and the rotor windings are computed in order to calculate the additional losses in the generator for evaluating the derating factor.

4.4.1 Six phase generator model

The generator with equivalent damper windings is shown in Fig. (4.9). The armature consists of two sets of windings ABC and XYZ displaced in space by 30^0 . The rotor is represented by lumped equivalent damper windings one in each axis and the field winding on the d-axis. The following assumptions are made in this analysis :

(1) All armature windings are sinusoidally distributed around the periphery of the stator with equal number of turns.

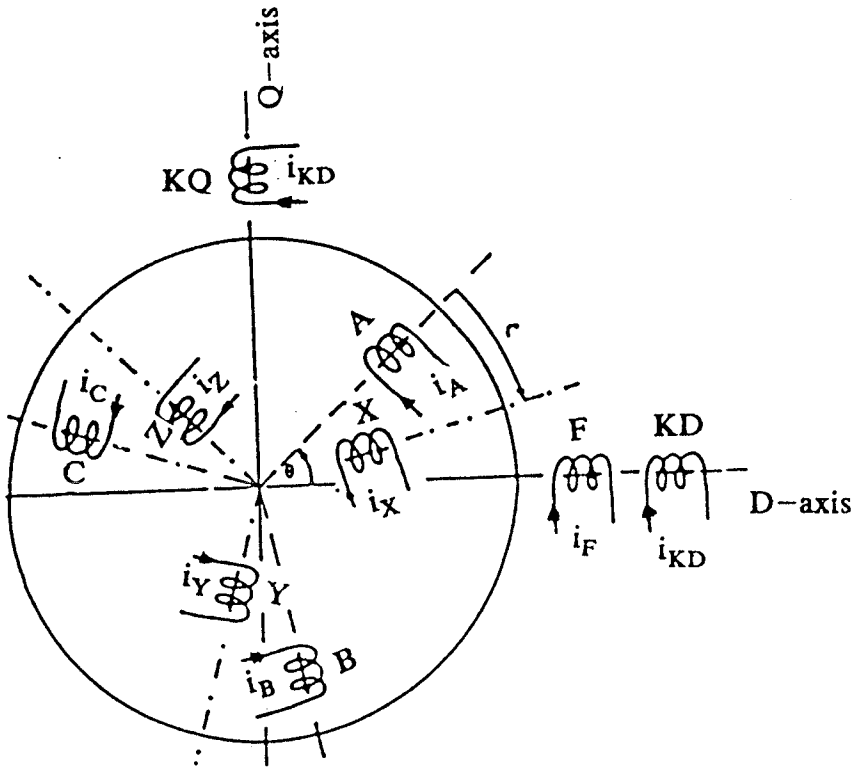

Fig. 4.9 : Six phase generator with equivalent damper windings.

(2) The mutual coupling of the flux which does not cross the air gap between phases of one set of windings is equal to that of the corresponding phases in the other set.

The axis equations for voltages and fluxlinkages are derived in the Appendix III. From the equations (C.30) to (C.36) from the above Appendix the d and q axes equivalent are derived and shown in Fig.(4.11) The simplified q-q-o axis equations are as follows.

Winding set 1 :

$$v_{d1} = p\,\psi_{d1} + \omega\,\psi_{q1} + r_a\,i_{d1} \tag{4.4.1}$$

$$v_{q1} = p\,\psi_{q1} - \omega\,\psi_{d1} + r_a\,i_{d1} \tag{4.4.2}$$

$$v_{o1} = (p\,L_o + r_a)\,i_{o1} \tag{4.4.3}$$

$$\psi_{d1} = \psi_{md} + L_a\,i_{d1} + L_{12}\,(i_{d1} + i_{d2}) \tag{4.4.4}$$

$$\psi_{q1} = \psi_{mq} + L_a\,i_{q1} + L_{12}\,(i_{q1} + i_{q2}) \tag{4.4.5}$$

Winding set 2 :

$$v_{d2} = p\,\psi_{d2} + \omega\,\psi_{q2} + r_a\,i_{d2} \tag{4.4.6}$$

$$v_{q2} = p\,\psi_{q2} - \omega\,\psi_{d2} + r_a\,i_{d2} \tag{4.4.7}$$

$$v_{o2} = (p\,L_o + r_a)\,i_{o2} \tag{4.4.8}$$

$$\psi_{d2} = \psi_{md} + L_a\,i_{d2} + L_{12}\,(i_{d1} + i_{d2}) \tag{4.4.9}$$

$$\psi_{q2} = \psi_{mq} + L_a\,i_{q2} + L_{12}\,(i_{q1} + i_{q2}) \tag{4.4.10}$$

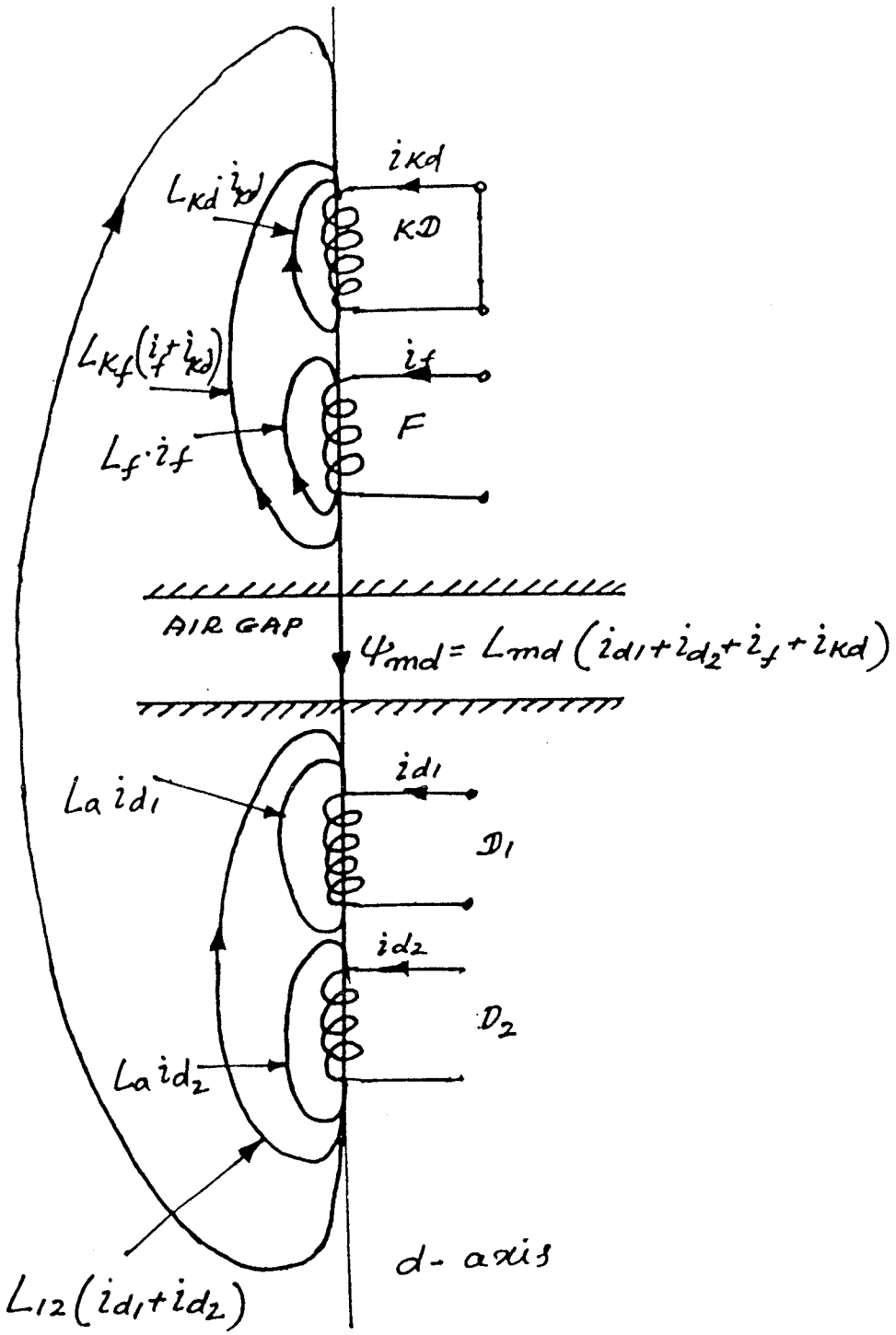

Fig. 4.10 : D-axis flux model of a six phase generator.

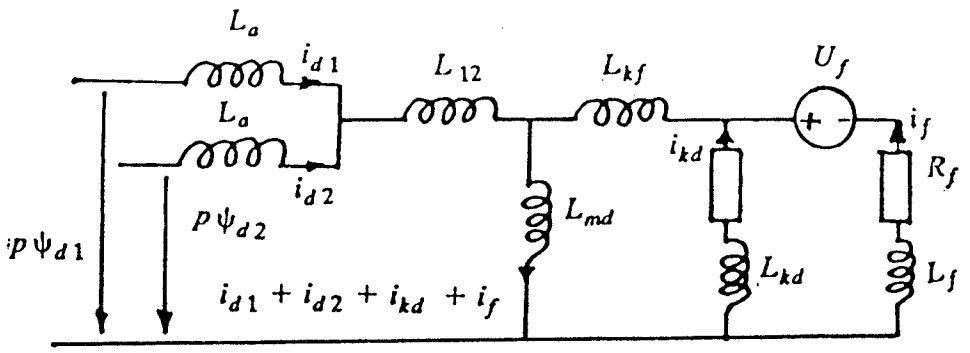

d−axis equivalent circuit

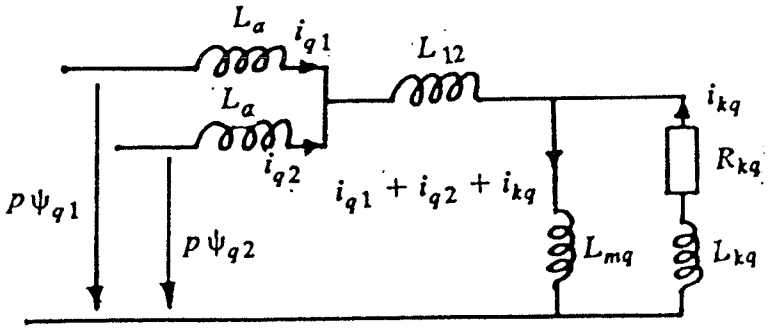

q−axis equivalent circuit

Fig. 4.11 : Six phase generator equivalent circuits.

Where:

$$\psi_{md} = L_{md} (i_{d1} + i_{d2} + i_f + i_{kd})$$

$$\psi_{mq} = L_{mq} (i_{q1} + i_{q2} + i_{kq})$$

$$L_{12} = \sqrt{3}\, L_{m2}$$

$$L_a = L_1 + L_{m1} - L_{12}$$

$$L_o = L_1 - 2\, L_{m1}$$

The d-axis flux model of the generator is shown in Fig. (4.10) and the equivalent circuits are shown in Fig. (4.11).

The generator equations are represented in the following state space form for simulation on the digital computer.

$$\dot{x} = [A]\, \bar{x} + [B]\, \bar{u}$$

d-axis equations :

$$\frac{d}{dt} \begin{bmatrix} i_{d1} \\ i_{d2} \\ i_f \\ i_{kd} \end{bmatrix} = [\, L_d \,]^{-1} \begin{bmatrix} -\omega\, \psi_{q1} - r_a\, i_{d1} \\ -\omega\, \psi_{q2} - r_a\, i_{d2} \\ - r_f\, i_f \\ - r_{kd}\, i_{kd} \end{bmatrix} + [\, L_d]^{-1} \begin{bmatrix} v_{d1} \\ v_{d2} \\ v_f \\ o \end{bmatrix} \qquad (4.4.11)$$

Where :

$$[\,L_d\,] =$$

$$\begin{bmatrix} L_{md}+L_a+L_{12} & L_{md}+L_{12} & L_{md} & L_{md} \\ L_{md}+L_{12} & L_{md}+L_a+L_{12} & L_{md} & L_{md} \\ L_{md} & L_{md} & L_{md}+L_f+L_{kf} & L_{md}+L_{kf} \\ L_{md} & L_{md} & L_{md}+L_{kf} & L_{md}+L_{kd}+L_{kf} \end{bmatrix}$$

q-axis equations :

$$\frac{d}{dt}\begin{bmatrix} i_{q1} \\ i_{q2} \\ i_{kq} \end{bmatrix} = [\,L_q\,]^{-1}\begin{bmatrix} -\omega\,\psi_{d1} - r_a\,i_{q1} \\ -\omega\,\psi_{d2} - r_a\,i_{q2} \\ -r_{kq}\,i_{kq} \end{bmatrix} + [\,L_q]^{-1}\begin{bmatrix} v_{q1} \\ v_{q2} \\ o \end{bmatrix} \qquad (4.4.12)$$

Where :

$$[\,L_q\,] = \begin{bmatrix} L_{mq}+L_a+L_{12} & L_{mq}+L_{12} & L_{mq} \\ L_{md}+L_{12} & L_{mq}+L_a+L_{12} & L_{mq} \\ L_{mq} & L_{mq} & L_{mq}+L_{kq} \end{bmatrix}$$

o-axis equations :

$$\frac{d}{dt}\begin{bmatrix} i_{o1} \\ i_{o2} \end{bmatrix} = [\,L_{oo}\,]^{-1}\begin{bmatrix} -r_a\,i_{o1} \\ -r_a\,i_{o2} \end{bmatrix} + [\,L_{oo}]^{-1}\begin{bmatrix} v_{o1} \\ v_{o2} \end{bmatrix} \qquad (4.4.13)$$

Where :

$$[\,L_{oo}\,] = \begin{bmatrix} L_o & o \\ o & L_o \end{bmatrix}$$

Mechanical System :

$$M_t = T_e - J \frac{d\omega}{dt} - K \omega \qquad (4.4.13)$$

Where :

M_t = Shaft toruqe.

T_e = Electrical torque.

K = Damping constant.

J = Moment of Inertia of the rotor.

Therefore

$$\frac{d\omega}{dt} = \frac{T_e}{J} - \frac{K}{J} \omega - \frac{M_t}{J} \qquad (4.4.15)$$

Where :

$$T_e = \frac{\omega_o}{4} (\psi_{d1} i_{q1} + \psi_{d2} i_{q2} - \psi_{q1} i_{d1} - \psi_{q2} i_{d2}) \qquad (4.4.15)$$

4.4.2 Digital simulation of six phase generator connected to a 12-pulse converter

A 2X588 MVA, 22 kV six phase generator directly connected to two six pulse converters as shown in Fig. (4.12) is simulated in time domain using EMTDC program. As the data of large size six phase generator is not available, a three phase 588 MVA generator data is converted for six phase generator and used in this simulation. Since the primary interest of the study is mainly restricted to the generator and the rectifier, the inverter is modelled as constant current source. The realization of the constant current control is shown in Fig. (4.13). The measured current is passed through the time delay circuit and compared with the reference value. The error signal is amplified through proportional and integral controller to obtain the output voltage. This voltage is devided by the Norton's equivalent resistance of the inverter to obtain the current signal to be injected at the inverter side.

4.4.2.1 Interfacing of a six phase generator model with EMTDC program

The six phase generator model descibed in the section [4.4.1] interfaces with EMTDC program as a current source as shown in Fig. (4.14). The machine model makes use of the terminal voltages of the sytem in the previous time step to calculate the currents to be injected into the EMTDC network. Since the machine is represented by a current source which is dependent on the the voltage of the previous time step, any sudden change in the voltage causes change in the current response only in the next time step. Hence, for the previous time step, the machine looks like an open

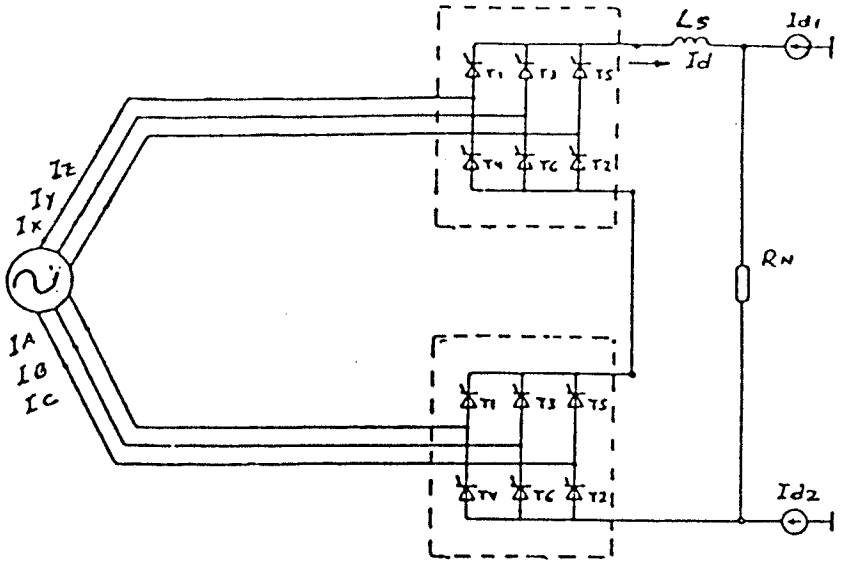

Fig. 4.12 : System configuration for digital simulation.

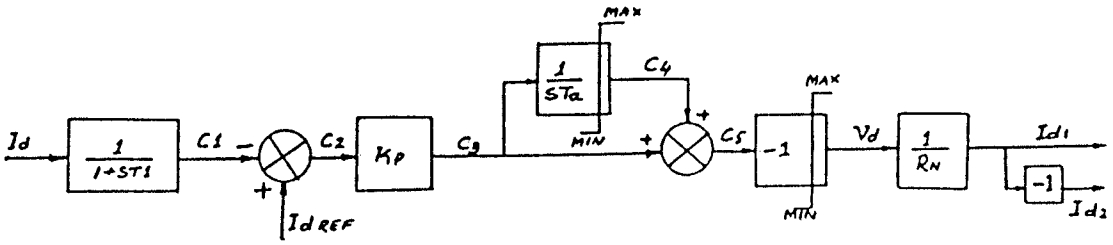

Fig. 4.13 : Constant current control at the inverter.

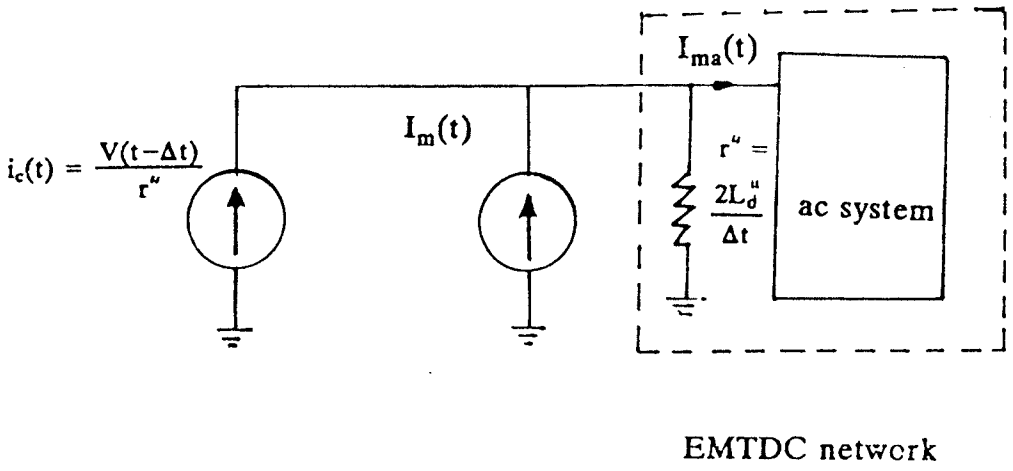

Fig. 4.14 : Interface of a sysnchronous machine with EMTDC network.

circuit. This means that it does not respond with the new current until the next time step, hence spurious spikes may appear in the terminal voltage. In order to overcome this draw back, the machine is terminated to the network through its characteristic impedance as shown in Fig. (4.14) [20]. For a synchronous machine the characteristic impedance is chosen as its subtransient reactance. A resitor $r'' = \frac{2L_d''}{\Delta t}$ is calculated, where L_d'' is the subtransient inductance of the machine and Δt is the time step of the main program. If there be N coherent machines operating in parallel, then $r'' = \frac{2L_d''}{N\,\Delta t}$. This resistance is placed from each node of the machine terminal to the ground in the EMTDC network. Then, instead of injecting the calculated machine currents $I_m(t)$, a compensated current $I_m(t) + I_c(t)$ is injected into the system.

Where, $\quad I_c = \frac{V(t-\Delta t)}{r''}$

$V(t-\Delta t)$ is the terminal voltage of the previous time step.

Thus, the actual current injected into the network is :

$$I_{ma}(t) = I_m(t) + \frac{V(t-\Delta t) - V(t)}{r''}$$

Since Δt is small, r'' is large. For small time step $V(t-\Delta t) \approx V(t)$ and thus $I_{ma}(t) \approx I_m(t)$. The error introduced vanishes in the limit when Δt is small. However, for sudden voltage changes, $I_m + I_c$ is not calculated until the next time step, the network sees an impedance r'' for this instant intead of an open circuit as discussed earlier. This is the actual impedance it would have seen if this would have been represented in the EMTDC program.

4.4.3 Simulation results

A 2 X 588 MVA, 22 kV, 0.85 pf, 3600 rpm six phase generator directly connected to two 6-pulse converter is simulated in time domain using EMTDC program to give 56 kV, 18.5 kA dc output. The steady state generator phase currents, commutation voltage of upper bridge and the dc voltage are shown in Fig. (4.15). The generator rotor currents are shown in Fig. (4.16). The system response for 50% change in current order is shown in Fig. (4.17). It can be observed from the Fig. (4.17) that the dc current settled down to 50% set value in 0.1 s after changing the current reference. The harmonics contents in the stator and rotor currents are computed to calculate additional losses in the machine. The time step Δ t of 25 μ was used in the digital simulation to ensure an accurate calculation of upto 24 th order harmonic.

4.4.3.1 Commutation Reactance

If the synchronous generator is directly connected to a converter, the commutation point shifts to the internal voltage of the generator. During commutation period the generator is subjected to the line to line short circuit. As seen in the literature, for a three phase generator connected to a six pulse converter, some authors have taken the effective commutation reactance as subtransient reactance of the generator [4-5], and in another paper it is represented as the arithmetic mean of direct axis and quadrature axis subtransient reactances [21].

In order to investigate this, the commutation reactance is calculated from the simulation results. For I_{dc} = 18.5 kA, α = 15.18° the measured overlap angle is 26.4° , and the voltage behind the subtransient reactance is 24.4 kV. The commutation reactance is calculated using the following

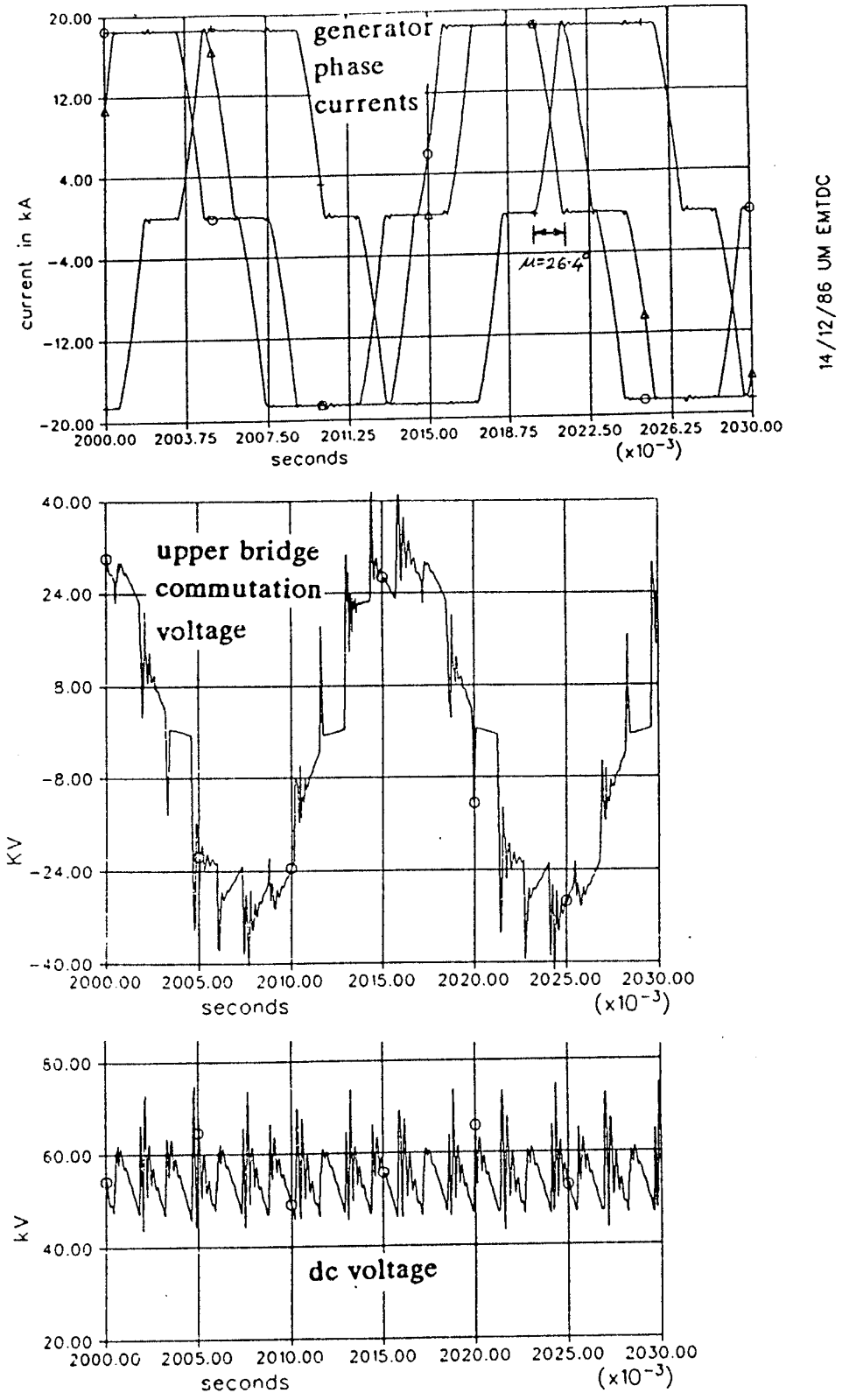

Fig. 4.15 : Steady state performance of a six phase generator directly connected to a 12-pulse converter.

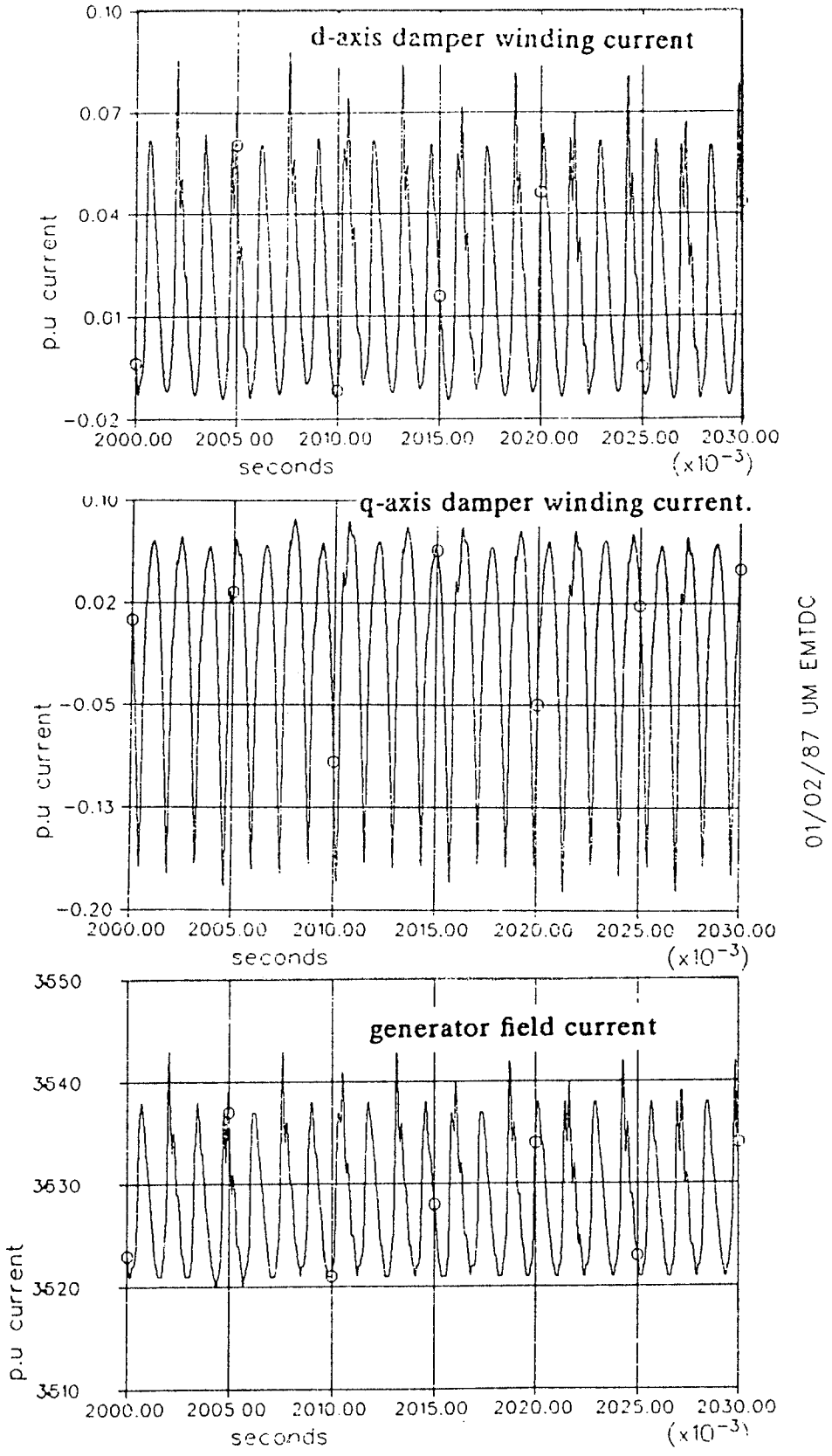

Fig. 4.16 : Generator rotor currents under steady state.

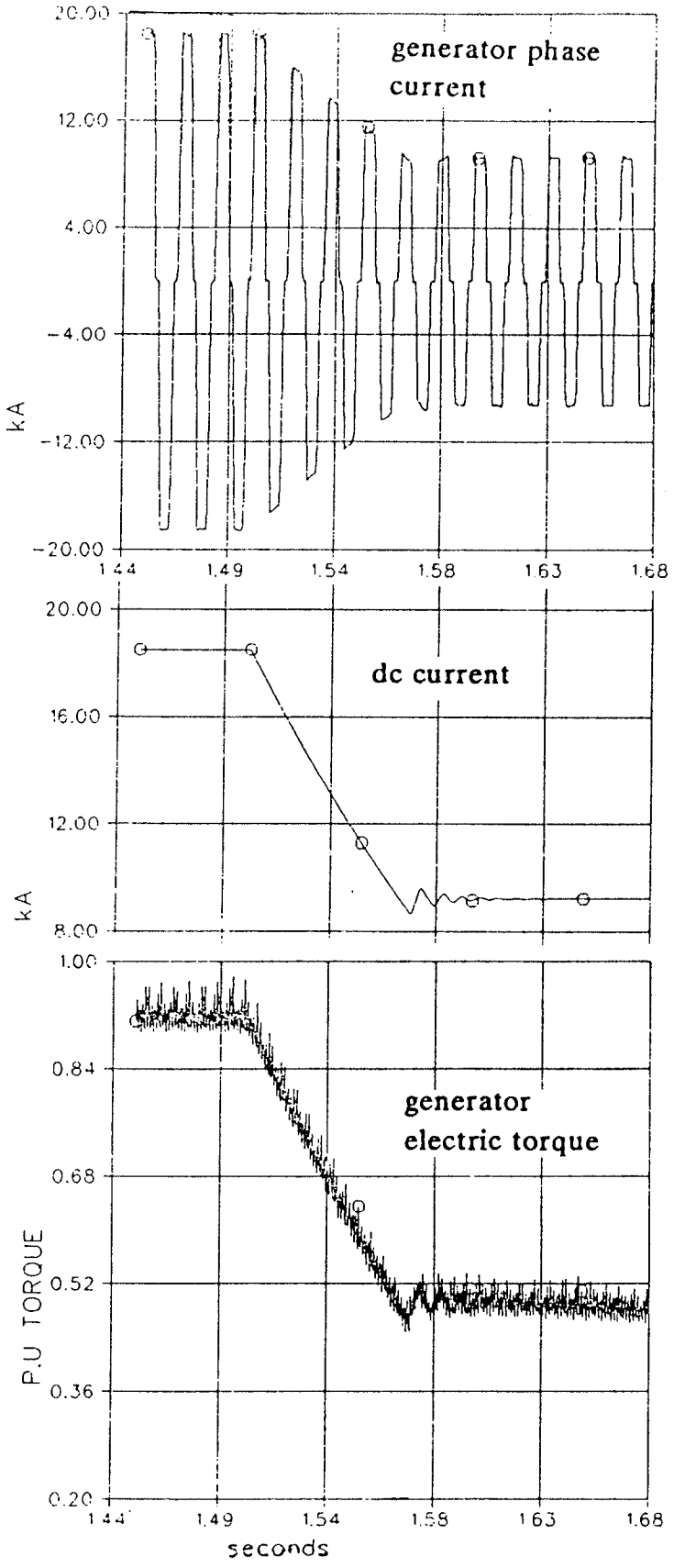

Fig. 4.17 : Dynamic response of a six phase generator directly connected to a 12-pulse converter for 50% step change in current order.

equation.

$$I_{dc} = \frac{E_c}{\sqrt{2}\, X_c} \left(\cos \alpha - \cos (\alpha + \mu) \right) \qquad (4.4.17)$$

Where :

I_{dc} = DC current.

α = Delay angle.

μ = Overlap angle.

E_c = Line-line voltage behind subtransient reactance.

X_c = Commutation reactance.

A 2 X 588 MVA generator parameters and base quantities are shown in Appendix III. For $\alpha = 15.18^{\circ}$, the measured value of μ is 26.4° and the E_c is 24.4 kV. The calculated value of the commutation reactance from the equation (4.4.17) is 0.1986 Ω .

Three possible alternatives for commutation reactance in terms of machine reactances are examined to select the best possible one which is in close agreement with the simulated value.

For the above machine with $x_d'' = 0.208\ \Omega$ and $x_q'' = 0.1875\ \Omega$

(a) If $X_c = x_d''$ then , $X_c = 0.208\ \Omega$.

(b) If $X_c = \dfrac{x_d'' + \sqrt{x_d'' \cdot x_q''}}{2}$ then , $X_c = 0.203\ \Omega$.

(c) If $X_c = \frac{x_d'' + x_q''}{2}$ then, $X_c = 0.1977\ \Omega$.

From these possible alternatives for X_c , the value of X_c equal to $\frac{x_d'' + x_q''}{2}$ which is equal to $0.1977\ \Omega$ is in close agreement with the calculated value of $0.1986\ \Omega$ from the simulated results. If the subtransient saliency is neglected, then $X_c = x_d''$. Hence the effective commutation reactance of the six phase generator taking subtransient saliency into account can be taken as the arithmetic mean of d and q axes subtransient reactances.

The p.u value of X_c is given by :

$$X_c\ (pu) = \cos\alpha - \cos(\alpha + \mu)$$

$$= 0.2129\ pu.$$

The total effective MVA of the generator $= \frac{\pi}{3} \cdot V_{do} \cdot I_{dc} = 1276$ MVA.

The base impedance , $Z_b = \frac{E_c^2}{1276} = \frac{(24.4)^2}{1276} = 0.46647\ \Omega$

With the above base impedance, the p.u values of $x_d'' = 0.446$
and $x_q'' = 0.402$

If $X_c(pu) = \frac{x_d'' + x_q''}{4} = 0.2128$ pu , it is close agreement with calculated value of pu commutation reactance of 0.2129. Therefore, the p.u commutation reactance of a six phase generator connected to a 12-pulse converter can be represented as $\frac{x_d'' + x_q''}{4}$

4.4.3.2 Additional losses in the generator

Since each set of three phase windings are directly connected to a six pulse converter, the 5th, 7th, 11th,13th etc., harmonic currents flow into stator windings. But the 5th and the 7th, the 17th and the 19th harmonic mmfs cancel in the air gap due to 30° phase displacement between the two sets of windings, The 12th, 24th etc., harmonic currents flow in the field and damper windings. These harmonic currents cause additional losses in the stator and rotor circuits. The harmonic currents flowing in the generator are computed for $\alpha = 15.18°$ and $I_{dc} = 18.5$ kA and shown in Table (4.4).

Harmonic number n	Stator phase current I_{an} p.u	Stator phase current I_{xn} p.u	d-axis damper winding current I_{kdn} p.u	q-axis damper winding current I_{kqn} p.u	Field winding current I_{fn} p.u
0	-	-	-	-	3.537
1	0.5	0.5	-	-	-
5	0.0817	0.0817	-	-	-
7	0.0459	0.0459	-	-	-
11	0.01295	0.01295	-	-	-
12	-	-	0.02478	0.06869	0.003523
13	0.0059	0.0059	-	-	-
17	0.00525	0.00525	-	-	-
19	0.0057	0.0057	-	-	-
23	0.00397	0.00397	-	-	
24	-	-	0.007027	0.0226	0.004032
25	0.002	0.002	-	-	-

Table 4.4 : Magnitude of harmonic currents in the six phase generator with 12-pulse converter load at $\alpha = 15.18°$ for 60 Hz operation.

The harmonic power loss in the rotor circuits is given by :

$$P_H = \sum_n r \sqrt{n} I_{rn}^2 \qquad (4.4.18)$$

Where :

P_H = Rotor power loss due to harmonic currents.

n = p.q , where p is the pulse number and q is any positive integer.

r = Effective rotor resistance at the fundamental frequency.

$r \sqrt{n}$ = Effective frequency dependent resistance [5]

I_{rn} = Magnitude of the n th harmonic current in the rotor circuits.

Considering one damper winding in each axis, the power loss due to harmonic currents is given by :

$$P_H = \sum_n \sqrt{n} r_{kd1} I_{kdn}^2 + \sum_n \sqrt{n} r_{kq1} I_{kqn}^2 + \sum_n \sqrt{n} r_{f1} I_{fn}^2 \qquad (4.4.19)$$

Where r_{kd1} , r_{kq1} and r_{f1} are the effective resistances at the fundamental frequency.

Using the harmonic currents shown in Table (4.4), the calculated value of the harmonic power loss in the rotor circuits is 0.482×10^{-4} p.u. The heating effect in the rotor due to harmonic currents can be represented by an equivalent negative sequence current, I_{EN} , which causes equal rotor heating as the rectifier load,

i.e $P_{EN} = P_H$, where $P_{EN} = r \sqrt{2} I_{EN}^2$

which is power loss due to I_{EN} . Therefore, the equivalent negative sequence current is given by :

$$I_{EN} = \sqrt{\sqrt{n}\,[\,\sum I_{kdn}^2 + \sum I_{kqn}^2 + \sum I_{fn}^2\,]/\sqrt{2}} \qquad (4.4.20)$$

The calculated value of I_{EN} = 0.1228 p.u

For the above machine 2.3 p.u field current is required to produce 1.0 p.u open circuit terminal voltage. If this value is taken as 100%, then I_{EN} = 5.34% . In the case of round rotor turbogenerators, the negative sequence current withstand capability depends upon the size of the generator. Normally generators of about 1000 MW capacity are designed to withstand up to 8% continuous negative sequence current [17]. If its value is between 8% to 12%, suitable design modifications and cooling methods need to be adopted. If the value is about 12%, it may not be acceptable. Since the calculated value of the negative sequence current is 5.34%, the generator can withstand this duty without design modifications.

4.4.3.3 Evaluation of derating factor

The harmonic currents in the stator and rotor circuits cause additional losses which in turn cause overheating of the machine. In order to accommodate additional losses without derating the machine, the generator rating has to be lowered. The derating factor is defined as the ratio of the actual rating of the machine with rectifier load to the normal designed rating.

(a) Generator under normal operation :

Rated capacity = 1176 MVA

Rated power factor = 0.85 lag

Rated field current = 3.54 p.u

Rated reactive power = 620 Mvar

Rated active power = 1000 MW

Stator copper losses = 0.0008 p.u

Field copper losses = 0.004386 p.u

The equivalent loss resistance of the generator, r_e = 0.005186 p.u

(b) Generator under 12-pulse rectifier load operation :

Additional stator copper losses are given by :

$$P_{SH} = \sum_{n} r_{a1} \sqrt{n}\, I_{an}^2 \qquad (4.4.21)$$

Where :

r_{a1} = Fundamental frequency resistance of the stator winding.

I_{an} = n th harmonic stator phase current.

The calculated value of P_{SH} = 0.0000689 p.u

It is assumed that the fundamental frequency resistance of the stator winding is equal to that of a dc resistance since conductors in each bar are transposed to minimize the eddy current losses. Since the the harmonic currents have been computed from the generator model represented by constant resistances in the stator and rotor circuits, the effect of the variation of the magnitude of harmonic currents due to change in the resistance caused by harmonic frequency currents can not be taken into account. However, as the reactance of the machine predominates the resistance at higher frequencies, the bove effect may not be very significant. This effect is duly taken into account while evaluating the losses in the machine.

Additional losses in the rotor circuits, P_H

calculated using the Eqn. (4.4.18) = 0.0000482 p.u

Total additional losses in the generator = $P_{SH} + P_H$

= 0.0001171 pu

Total losses in the generator = 0.005186 + 0.00001171

= 0.0051978 p.u

The equivalent loss resistance of the generator, r_{eh} = 0.0051978 p.u

The power factor under this load is given by :

$$\cos \phi = \frac{1}{2} [\cos \alpha + \cos (\alpha + \mu)$$

For $\alpha = 15.18^{\circ}$ and $\mu = 26.4$, $\cos \phi = 0.855$

In order to keep power losses in the machine same as under the normal load operation, the generator current has to be reduced.

New value of the current, $I_N = \sqrt{\frac{r_e}{r_{eh}}} I_a = 0.99886 \ I_a$

Where I_a is the normal full load current = 1.0 p.u

The new rating of the generator = $(MVA)_{rated} . I_N . \cos \phi$

= 1176 x 0.99886 x 0.885

= 1004 MW

But the designed rating of the generator = 1000 MW

Hence, the generator need not be derated since it is designed for 0.85 pf.

4.5 Special design and operating features of generators for unit connection schemes

In the case of HVDC transmission schemes, high dc voltage is required to minimize the transmission line losses. In order to achieve this converter transformers are necessary. Converter transformers also isolate generators from the dc system thereby eliminating problems such as flow of galvanic currents into the surrounding metal parts as the neutrals are subjected to the dc potential if transformers are not connected.

Normally 2 pole or 4 pole generators are used for nuclear or thermal power stations depending upon the rating of the station. For higher capacity (1200 - 2000 MW), the condition of steam supplied by the light water reactor calls for reduction in speed of the turbine and accordingly the use of 4-pole generators [22]. In conventional HVDC schemes the generator speed is fixed by the system frequency resulting in 3600 rpm for 2-pole machine and 1800 rpm for 4-pole machines at 60 Hz frequency. In unit connection schemes if the system frequency is not a criteria, turbines and generators can be designed for higher base speeds thus minimizing their sizes and the cost. In order to illustrate this point, consider the governing relation for the output of the generator which is given by :

$$S = K D_s^2 L n \qquad (4.5.1)$$

Where :

D_s= Diameter of the stator bore.

L = Length of the stator core.

n = Speed of the machine.

K = output coefficient.

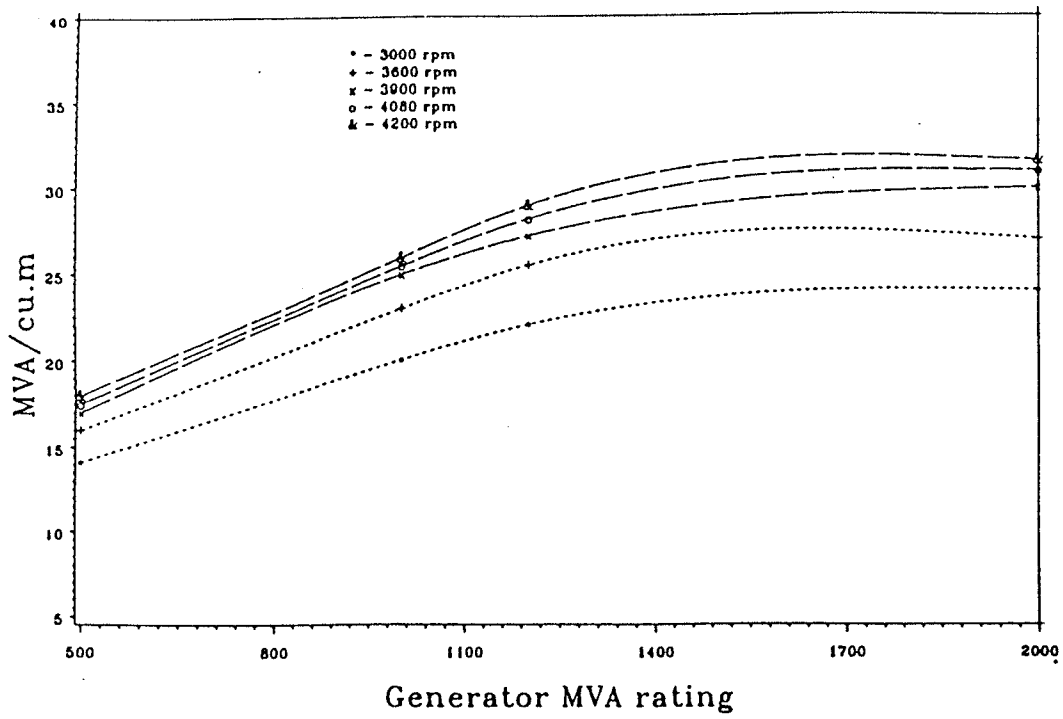

Fig. 4.18 : Capacity per unit volume of 2-pole generators at different base speeds.

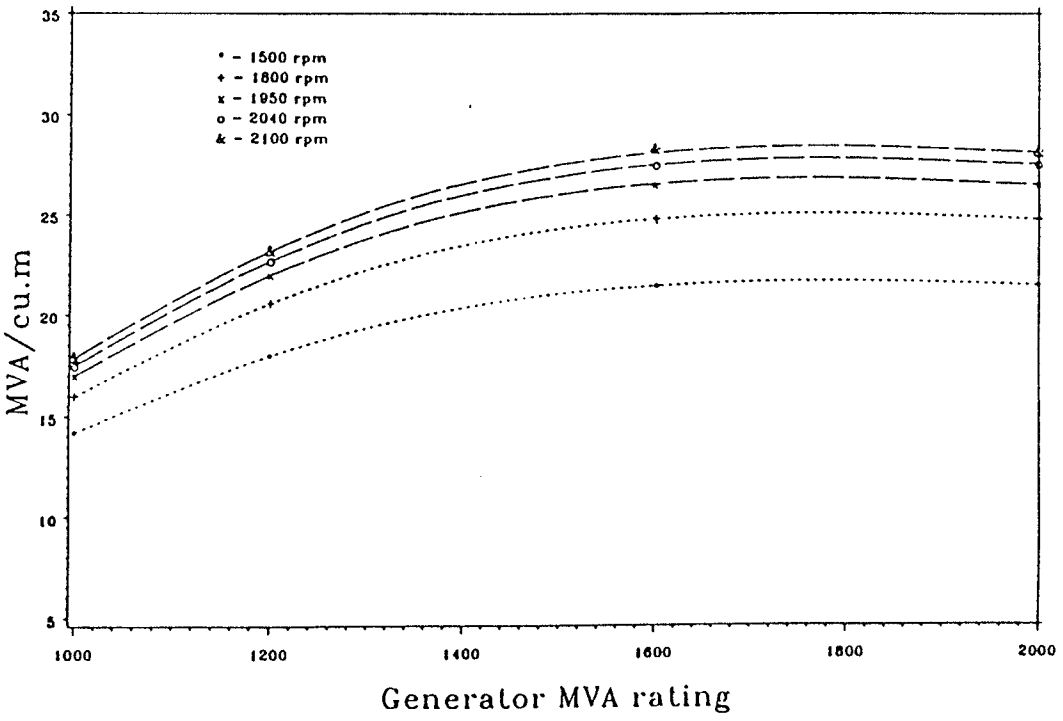

Fig. 4.19 : Capacity per unit volume of 4-pole generators at different base speeds.

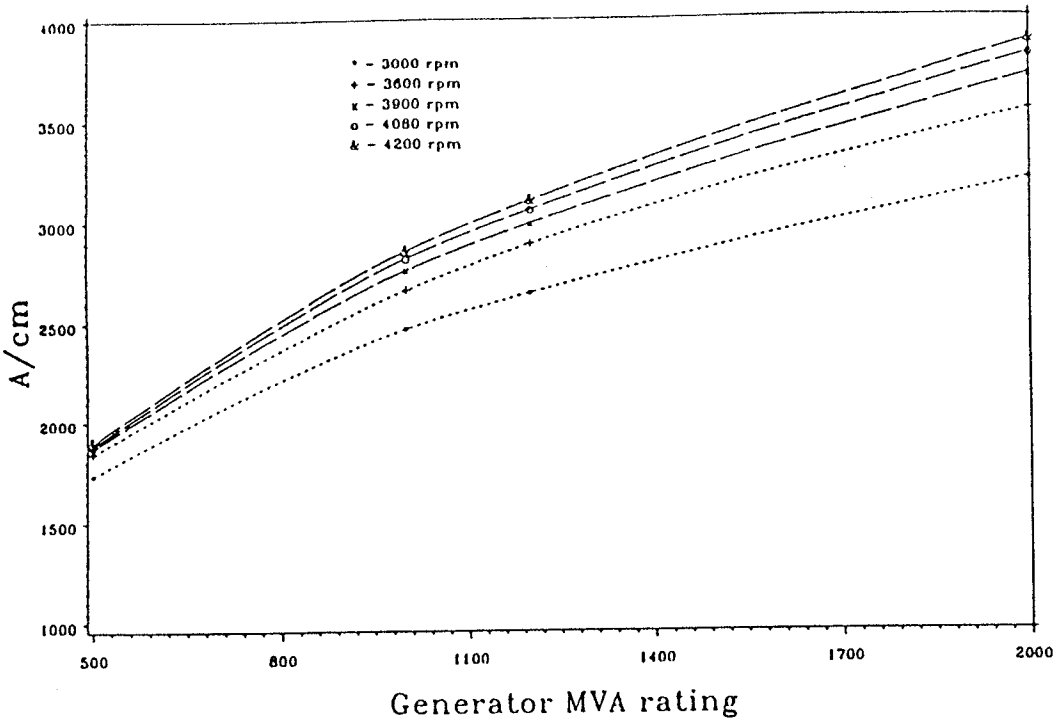

Fig. 4.20 : Electrical loading of 2-pole generators at different base speeds.

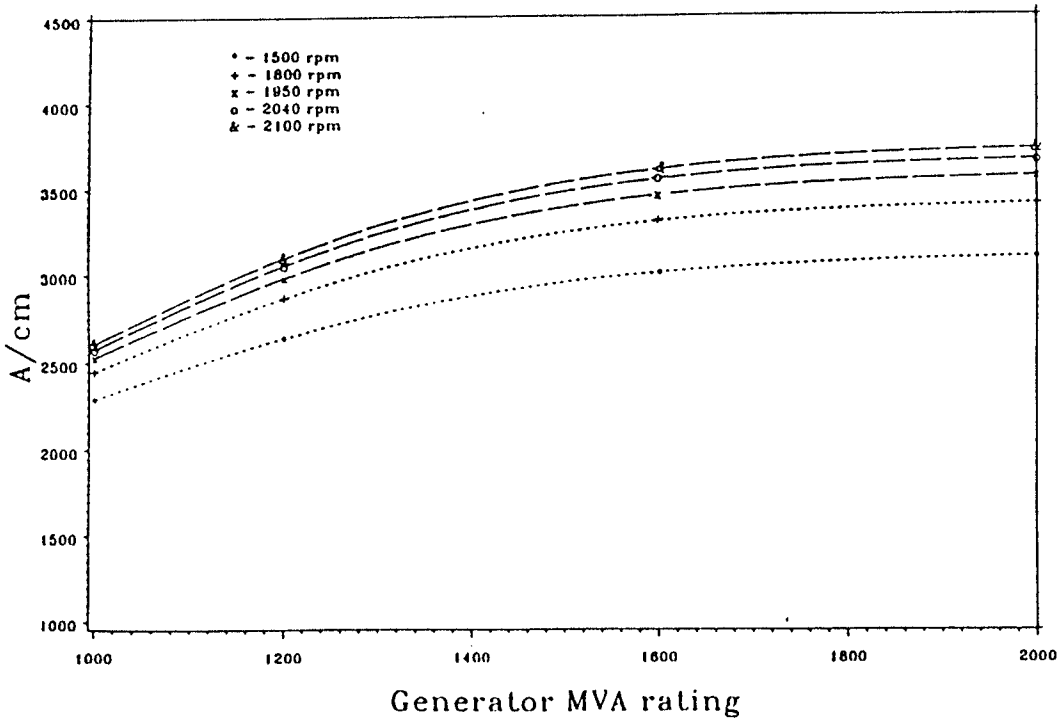

Fig. 4.21 : Electrical loading of 4-pole generators at different base speeds.

It can be observed from the above relation that by increasing the speed of the machine, the output of the generator can be increased. It means that for a given rating of a machine the size can be reduced by increasing the speed. This is shown in Figs. (4.18) and (4.19) for a 2 pole and a 4 pole generators respectively [23]. It can be observed from the above figures that the specific volume of the machine decreases with the increase in the operating base speed for a given rating of the machine. The electrical loading of the machine also decreases with the increase in the speed as shown in Figs. (4.20) and (4.21). In the case of hydro power stations as discussed in the Chapter III, the turbines can be operated under variable speed operation to maximize the efficiency under variable loading and water head conditions.

Steam turbines can be built with optimum designs for speeds between 2100 rpm and 4200 rpm [17]. The maximum frequency of operation of the generator for unit connection scheme can be limited to about 70 to 75 Hz mainly due to mechanical constraints. As the frequency increases the subtransient reactances of the generator may increase. This may lead to increase in the commutation reactance. However, by adopting special design procedures for the generator rotor, it may be possible to reduce the commutation reactance at higher frequency of operation. In view of the above considerations, the frequency of operation is limited to 70 Hz in this study.

By operating at higher base speeds the cost of the turbine and the generator can be reduced. If the base frequency is higher, the cost of the transformers, smoothing reactors and the ac filters may also be reduced. Hence, the unit connection scheme offers the flexibility of operating hydraulic turbines under variable speed operation and steam turbines at higher base speeds.

4.6 Commutation reactance and its effect on the generator performance

This section deals with the equivalent circuits of a three phase generator connected to a six pulse and twelve pulse bridges through converter transformers and the effect of commutation reactance on the generator performance.

4.6.1 Equivalent circuits for Block and Double Block connections

If a generator is connected to a six pulse converter through a converter transformer,then it is called Block connection [5]. The effective commutation reactance of the Block connection is given by

$$X_{c\,(pu)} = \frac{x_d'' + x_q''}{2} + X_t \qquad (4.6.1)$$

Where :

x_d'' , x_q'' = d and q axes subtransient reactances in p.u.

X_t = Transformer leakage reactance.

X_c = Commutation reactance in p.u.

The connection of a generator to a 12-pulse bridge through converter transformers is called Double Block connection. The effective commutation reactance of the Double Block connection is given by :

$$X_{c\,(pu)} = \frac{x_d'' + x_q''}{4} + X_t \qquad (4.6.2)$$

The single line diagrams and equivalent circuits of Block and Double Block connections are shown in Figs. (4.21) and (4.22) respectively.

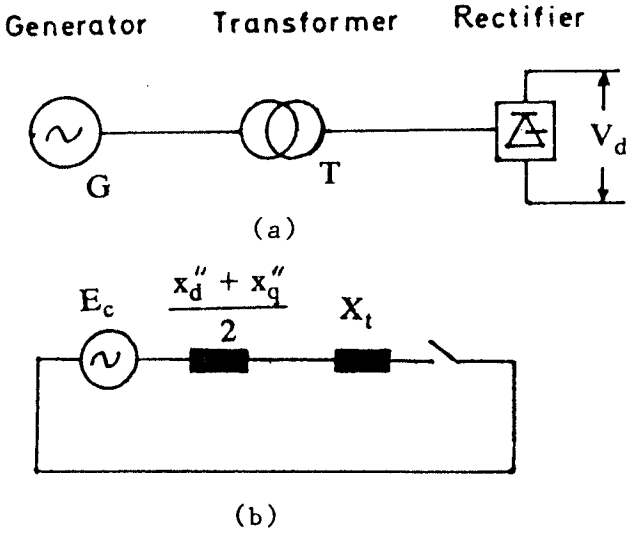

Fig. 4.22 : Block connection; (a) Single line diagram
(b) Equivalent circuit.

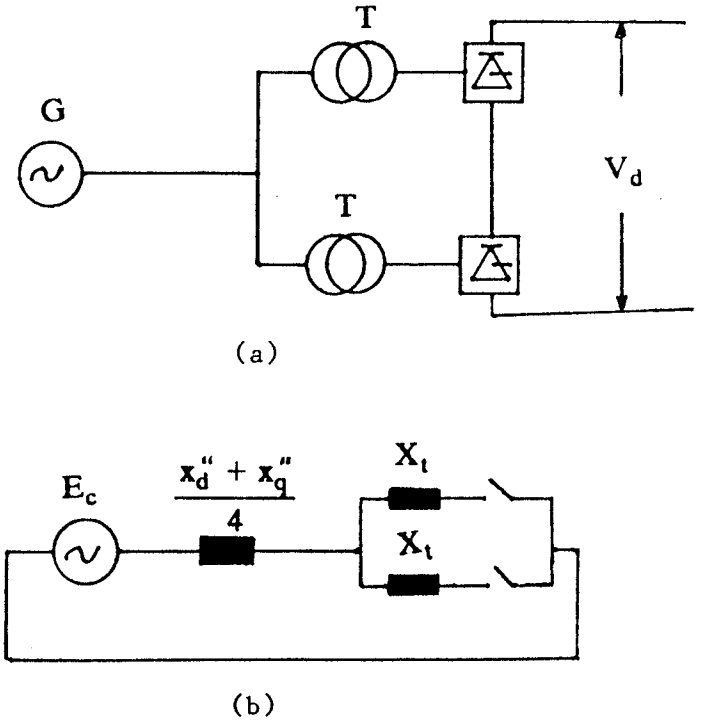

Fig. 4.23 : Double Block connection; (a) Single line diagram,
(b) Equivalent circuit.

4.6.2 Significance of commutation reactance on the generator performance

In the unit connection scheme, the subtransient reactances of the generator that form the major part of the commutation reactance, it intrinsically influences the performance of the system under different operating frequencies. Since unit connection schemes can be operated at higher base speeds or under variable speed operation, in both cases the frequency of operation deviates from the system frequency. It may be necessary to study the influence of the commutation reactance at different frequencies of operation with regard to the parameters a) overlap angle b) power factor and c) reactive power for 12- pulse operation.

Consider a typical 120 MVA, 13.8 kV, 81.8 rpm , 60 Hz synchronous generator for unit connection scheme. If the unit operates under variable speed operation, the generator operates at different frequency thereby effecting the commutation reactance. This in turn effects the overlap angle, power factor and reactive power requirement. In order to study these effects, consider the following parameters.

$$x_d'' = x_q'' = 0.23 \text{ p.u}$$

$$X_t = 0.13 \text{ p.u}$$

$$\alpha = 10^\circ - 20^\circ$$

(a) Overlap angle :

The overlap angle in terms of delay angle and commutation reactance is given by :

$$\mu = \cos^{-1} [\cos \alpha - X_c] - \alpha \qquad (4.6.3)$$

The variation of overlap angle at different frequencies for various delay angles is shown in Table 4.5.

α degrees	μ at 50 Hz degrees	μ at 60 Hz degrees	μ at 68 Hz degrees	μ at 70 Hz degrees
10	28.7	32.28	35.0	35.7
13	26.6	31.0	32.8	34.5
15	25.4	28.9	31.5	32.1
20	22.6	26.0	28.5	29.2

Table 4.5 : Variation of commutation angle at different frequencies for various delay angles with a hydrogenerator.

It can be observed from the above table that for 50 Hz operation (68 rpm), the overlap angle is within the limit of 30° for various values of α between 10° and 20° . For high speed/frequency operation α has to advance further to satisfy the overlap angle limit of 30° for satisfactory operation. At 70 Hz (95.4 rpm) for satisfactory operation, the delay angle should be around 20° for which the overlap angle is 29.2° . If the generators are designed for high base speed operation, special design measures are to be taken to minimize the commutation reactance.

In the case of thermal or nuclear stations, where generators are built with two or four pole rotors, higher base speed operation can reduce the

cost of turbines and generators. Since the poles of the generator are fixed, a high speed operation results in a high frequency operation.

Consider a typical 732.3 MVA, 2 pole, 24 kV, 60 Hz turbogenerator for unit connection scheme with the following parameters [24].

$$x_d'' = 0.218 \text{ p.u.}$$
$$x_q'' = 0.140 \text{ p.u.}$$

Assuming $X_t = 0.13$ p.u, the commutation reactance for Double Block connection is 0.2195 p.u. The variation of overlap angle for different values of delay angles is shown in Table (4.6).

α degrees	μ at 60 Hz degrees	μ at 68 Hz degrees	μ at 70 Hz degrees
10	30.0	32.6	33.2
13	28.0	30.5	31.0
15	26.7	29.1	29.8
20	23.9	26.3	26.9

Table 4.6 : Variation of commutation angle at different frequencies for various delay angles with a turbogenerator.

It can be observed from the Table 4.6 that for a 2-pole generator with the base speed of 4200 rpm which corresponds to 70 Hz operation, with the delay angle of 15° , the overlap angle is 29.8° , which is in the safe limit of

30° . Hence the base speed of turbines with 2-pole generators can be selected at 4200 rpm for economical advantage. In this analysis, it is assumed that the reactances such as x_d'' and x_q'' increase proportionaln to the frequency. However, special design procedures can be adopted to reduce the above reactances at high frequency of operation inorder to reduce the commutation reactance.

(b) Power factor :

The power factor of the generator connected to the converter is given by :

$$\cos \phi = \frac{1}{2} [\cos \alpha + \cos (\alpha + \mu)] \qquad (4.6.4)$$

For hydrogenerator, the variation of power factor for different frequencies of operation at different values of α is shown in Table 4.7.

α degrees	pf at 50 Hz	pf at 60 Hz	pf at 68 Hz	pf at 70 Hz
10	0.883	0.862	0.846	0.842
13	0.872	0.852	0.836	0.825
15	0.864	0.843	0.827	0.823
20	0.838	0.820	0.801	0.797

Table 4.7 : Variation of power factor at different frequencies for various delay angles with a hydrogenerator.

As seen from the above table, the power factor decreases as the frequency

of the operation increases. For $\alpha = 20^{\circ}$ at 70 Hz operation, the power factor is 0.797. For a 2- pole, 732.3 MVA generator the variation of the power factor for different base frequencies is shown in the Table 4.8.

α degrees	pf at 60 Hz	pf at 68 Hz	pf at 70 Hz
10	0.875	0.860	0.857
13	0.864	0.850	0.847
15	0.856	0.842	0.838
20	0.830	0.815	0.810

Table 4.8 : Variation of power factor at different base frequencies for various dealy angles with a turbogenerator.

For normal operating value of the delay angle of 15° , at the base frequency of 70 Hz corresponding to the base speed of 4200 rpm, the power factor is 0.838. But, if the base speed is selected at a lower value of 4080 rpm which corresponds to 68 Hz operation, the improvement in power factor is marginal (0.842). Hence it is advisable to select base speed of 4200 rpm for the turbine / generator in the case of nuclear or thermal stations in order to minimize the unit cost.

(c) Reactive power :

The reactive power required by the rectifier is given by :

$$Q = P_d \tan \phi \qquad (4.6.5)$$

Where :

P_d = DC power.

ϕ = Power factor angle.

In the case of the 120 MVA hydrogenerator operating at the nominal speed of 81.8 rpm (60 Hz) with delay angle of 15° , the reactive power requirement is 63.8% of the dc power. But, at 70 Hz operation (95.4 rpm), since it is required to operate at $\alpha = 20°$ such that $\mu = 20°$ for safe operation, the reactive power requirement is 75.8% of the dc power. There is 12% increase in the reactive power when the generator operates at 70 Hz (95.4 rpm).

In the case of a 2-pole 732.3 MVA generator, the reactive power requirement at 60 Hz operation (4200 rpm) for the delay angle of 13° is 58.3% of the dc power. Whereas at 70 Hz operation the unit has to operate at 15° delay angle for safe operation. In this case the requirement of the reactive power is 65.0% of the dc power which corresponds to 0.84 power factor of the generator. Since generators of this capacity are normally designed for 0.85 power factor, the above reactive power demand can be met by the generator with slight design modifications at marginal extra cost. As the frequency is increased if L_d'' and L_q'' parameters remain unchanged, the angle of overlap as well as the reactive power consumption of the converter increase to undesirable high values. However by redesigning the rotor slots it may be possible to reduce the values of L_d'' and L_q'' and therefore an optimum higher than the normal frequency.

4.7 Three phase generators

Three phase generators are commonly used in most of the power stations for power generation. In the case of unit connected dc transmission schemes, each generator is connected to a 12-pulse converter through Y-Y and Y- Δ transformers in order to achieve the required dc transmission voltage and also to minimize the characteristic harmonic currents which cause additional losses in the generator.

In this section, the additional losses in a typical 120 MVA, 13.8 kV hydrogenerator connected to a 12-pulse converter are calculated from the simulation results to evaluate the derating factor of the generator for 60 Hz and 70 Hz operation. The harmonic currents are computed for $\alpha = 13.7^{\circ}$, $I_{dc} = 2000A$, and shown in Table (4.9) for 60 Hz operation.

Harmonic number n	stator phase current I_{an} p.u	d-axis damper winding current I_{kdn} p.u	q-axis damper winding current I_{kqn} p.u	Field winding current I_{fn} p.u
0	-	-	-	2.747
1	1.0	-	-	-
11	0.02265	-	-	-
12	-	0.00896	0.003736	0.005404
13	0.01057	-	-	-
23	0.004323	-	-	
24	-	0.00363	0.001023	0.00427
25	0.002137	-	-	-

Table 4.9 : Magnitude of harmonic currents in the generator with 12-pulse converter load at $\alpha = 13.7^{\circ}$ for 60 Hz operation.

4.7.1 Additional losses and derating factor for 60 Hz operation

The parameters of the 120 MVA, 13.8 kV generator are given in Appendix IV.

(a) Losses under normal operation :

Stator copper losses = $I_a^2 r_a = (1)^2\ 0.0037 = 0.0037$ p.u.

Field copper losses = $(I_f)^2 r_f = (2.59)^2\ 0.0007 = 0.004696$ p.u.

Total losses = 0.0037 + 0.004696 = 0.008396 p.u.

The equivalent loss resistance of the generator, $r_e = 0.008396$ p.u.

(b) Losses under converter load operation :

Additional losses in the stator and rotor windings are calculated using Eqns. (4.4.18) and (4.4.19) respectively.

Additional losses in the stator = 0.000082 p.u.

Additional losses in the rotor = 0.0000015 p.u.

Total additional losses = 0.0000097 p.u.

The power factor of the generator is given by :

$$\cos \phi = \frac{1}{2} [\cos \alpha + \cos (\alpha + \mu)]$$

For $\alpha = 13.7°$, $\mu = 26.2°$, $\cos \phi = 0.87$

Field current required for the above power factor = 2.747 p.u.

Field copper losses = $(2.747)^2 r_f$ = 0.00528 p.u.

Total losses in the machine =

stator copper losses + field copper losses + additional losses

= 0.0037 + 0.00528 + 0.0000097 =0.00899 p.u.

The equivalent loss resistance of the generator, r_{eh}

$$= r_{eh} = 0.00899 \text{ p.u.}$$

The equivalent negative sequence current is calculated using Eqn. (4.4.20).

The equivalent negative sequence current = 0.02036 p.u.

But, the field current required to produce 1.0 p.u open circuit terminal voltage of the generator is given by :

$$I_{fo} = \frac{\sqrt{2}}{x_{md}} = \frac{\sqrt{2}}{0.936} = 1.51 \text{ p.u.}$$

If this field current is taken as 100% value, the equivalent negative sequence current due to 12-pulse rectifier load in the generator is 1.35%. Normally, hydrogenerators are designed to withstand 10% continuous negative sequence current. therefore, the above generator can easily withstand 1.35% negative sequence current due to the rectifier load.

(c) Derating factor :

For satisfactory operation of the generator the losses under converter load operation should not exceed that of the losses under normal operation

in order to avoid excessive heating of the generator. If the losses with converter load exceed the normal value, then the stator current has to be reduced to satisfy the above mentioned condition.

Therefore,

$$I_a^2 \; r_e = I_N^2 \; r_{eh}$$

Where:

I_N = New value of the generator current in p.u.

I_a = Rated value of the generator current in p.u.

$$I_N = \sqrt{\frac{r_e}{r_{eh}}} \cdot I_a$$

$$= \sqrt{\frac{0.008396}{0.00899}} \times 1 = 0.9664 \text{ p.u}$$

The new MW rating of the generator = $(MVA)_{rated} \cdot I_N \cdot \cos \phi$

The rated power factor of the generator = 0.927

The rated MW of the generator under normal load = 120 x 0.927

= 111.24 MW

$$\text{Derating factor} = \frac{\text{New MW rating}}{\text{Designed MW rating}}$$

$$= \frac{100.9}{111.24} = 0.907$$

It means that the generator can be loaded up to 90.7% of its rated capacity without causing excessive heating. Since hydrogenerators are normally designed to withstand 10% negative sequence current and the converter operation is balanced and symmetrical, the tolerance for the negative sequence load can be for the temperature rise in the rotor caused by the harmonic currents due to rectifier load. From the above calculations, it is shown that the negative sequence current due to 12-pulse converter load is only 1.35%. If the generator is designed for 0.84 power factor, then the normally designed generator can be used without derating when feeding into 12-pulse converter load for the unit connection schemes.

If the generator operates at large delay angles due to some unavoidable conditions, then it has to supply more reactive power which may result in additional burden on the generator field winding. For example, for the above machine at $\alpha = 20^{o}$, the power factor of the generator under rated load condition is 0.82. The field current required to meet the reactive power demand can be calculated from Eqn. (D.10) of the Appendix IV. Under this condition the derating factor of the generator can be calculated as follows :

At 0.82 pf, the required field current, $I_f = 2.82$ p.u.

Field copper losses = $I_f^2 r_f = (2.82)^2 \times 0.0007 = 0.00557$ p.u.

Total losses in the machine =

stator copper + field copper + additional losses. at 0.82 pf. + losses.

$= 0.0037 + 0.00557 + 0.0000097 = 0.009276$ p.u

The equivalent loss resistance of the machine, r_{eh}

$$= 0.009276 \text{ p.u}$$

But, $r_e = 0.008396$ p.u

The new value of the stator current, $I_N = \sqrt{\frac{r_e}{r_{eh}}}$

$$= \sqrt{\frac{0.008396}{0.009276}} = 0.9513 \text{ p.u}$$

The new MW rating of the machine = $(MVA)_{rated} \times I_N \cos \phi$

$$= 120 \times 0.9513 \times 0.82 = 93.61 \text{ MW}$$

The rated power factor = 0.927

The rated MW under normal load = 111.24

Derating factor at 0.82 pf load = $\frac{93.67}{111.24} = 0.8416$

If the generator is designed for 0.85 pf, then

The rated MW rating of the generator = 120 x 0.85 = 102.0 MW

The derating factor = $\frac{93.67}{102.0} = 0.9176$

Hence, if the generator is designed for 0.85 pf, it can be loaded up to 91.76% of its normal capacity without causing excessive heating in the machine.

4.7.2 Additional losses and derating factor for 70 Hz operation

Since hydroturbines in unit connection schemes can be operated under variable speed operation for maximizing the efficiency, the frequency of generators vary depending upon the speed. The 70 Hz operation is selected to evaluate the additional losses in the machine.

Harmonic currents at 70 Hz operation flowing into the stator and the rotor circuits of a 120 MVA generator designed for 60 Hz operation are shown in Table 4.10 for $\alpha = 19.5^{\circ}$ and $\mu = 29.8^{\circ}$.

Harmonic number n	stator phase current I_{an} p.u	d-axis damper winding current I_{kdn} p.u	q-axis damper winding current I_{kqn} p.u	Field winding current I_{fn} p.u
0	-	-	-	2.836
1	1.0	-	-	-
11	0.0203	-	-	-
12	-	0.007535	0.002973	0.005223
13	0.0112	-	-	-
23	0.00566	-	-	
24	-	0.004754	0.007776	0.004273
25	0.0026	-	-	-

Table 4.10 : Magnitude of harmonic currents in the generator with 12-pulse converter load at $\alpha = 19.5^{\circ}$ for 70 Hz operation.

The resistances of the stator and rotor circuits at 70 Hz frequency are calculated and given below based on the following relation.

$$r_{70\ Hz} = r_{60\ Hz} \cdot \sqrt{\frac{70}{60}}$$

Where :

$r_{70\ Hz}$ = Resistance at 70 Hz frequency.

$r_{60\ Hz}$ = Resistance at 60 Hz frequency.

r_a = 0.004 p.u

r_{kd} = 0.00378 p.u

r_{kq} = 0.00378 p.u

r_f = 0.00075 p.u

(a) Losses under normal operation at 60 Hz :

Stator copper losses = 0.0037 p.u

Field copper losses = 0.0047 p.u

Total losses = 0.0084 p.u

Equivalent loss resistance of the generator, r_e = 0.0084 p.u

(b) Losses under converter load at 70 Hz operation :

Additional losses in the stator =

$$0.0004\ [\ \sqrt{11}\ (0.0203)^2 + \sqrt{13}\ (0.0112)^2 + \sqrt{23}\ (0.00566)^2 + \sqrt{25}\ (0.0026)^2\ ]$$

$$= 0.000008 \text{ p.u}$$

Additional losses in the rotor =

$$0.00378\ [\ \sqrt{12}\ (0.007535)^2 + \sqrt{24}\ (0.004754)^2\ ]$$

$$0.00378\ [\ \sqrt{12}\ (0.02973)^2 + \sqrt{24}\ (0.007778)^2\ ]$$

$$0.000756\ [\ \sqrt{12}\ (0.005233)^2 + \sqrt{24}\ (0.004273)^2\ ]$$

$$= 0.000014 \text{ p.u}$$

Total additional losses in the machine = 0.000022 p.u

From the simulation results the measured value of $\mu = 29.8^{\circ}$, for $\alpha = 19.5^{\circ}$

The power factor of the generator under this condition is given by :

$$\cos \phi = \frac{1}{2} [\cos \alpha + \cos (\alpha + \mu)] = 0.8$$

The net field current required at 0.8 power factor under normal load at 70 Hz operation = 2.836 p.u.

Field copper losses = $(2.836)^2$ x 0.000756 = 0.006 p.u.
Stator copper loss under 70 Hz operation = 0.004 p.u.

Total losses under converter load at 70 Hz operation = 0.01 p.u.

Equivalent loss resistance of the generator, r_{eh} = 0.01 p.u.

The equivalent negative sequence current of the generator = 0.052 p.u

This corresponds to 3.5% negative sequence current of the generator which is with in the safe limit of design margin of 10%.

(c) Derating factor :

In order to keep the same power loss in the generator as under normal operation, the stator current of the generator has to be reduced under rectifier load in order to avoid excessive heating of the machine.

New value of the stator current, $I_N = \sqrt{\frac{r_e}{r_{eh}}}$

$= \sqrt{\frac{0.0084}{0.01}} = 0.9165$ p.u.

New MW rating of the machine = 120 x 0.9165 x 0.8 = 880 MW

Designed rating of the machine at 0.92 pf = 120 x 0.92 = 110.4 MW

Derating factor = $\frac{880.0}{110.4} = 0.8$

The generator has to be derated to 80% of its nominal capacity under this operation. But, normally generators are designed for 0.85 pf operation. With 0.85 nominal power factor, the derating factor of the generator is calculated as below.

The nominal rating of the machine at 0.85 pf = 120 x 0.85 = 102 MW

The derating factor under this condition = $\frac{880}{102} = 0.863$

Hence, if the generator is designed for 0.85 pf under 60 Hz operation, it can be loaded up to 86.3% of its designed rating when operating at 70 Hz with rectifier load. In order to load the generator to its rated capacity, special design and cooling requirements may be necessary.

4.8 Summary and conclusions

Six phase generators have economic advantages as compared to the conventional three phase generator for large rating machines. These can be used for unit connection schemes for nuclear or thermal stations. The Y-Y windings configuration is recommended as compared to the Y-Δ windings configuration for the above generators. Space harmonics generated by time harmonic currents in the air gap mmf are smaller in magnitude in the former case as compared with the later case.

Six phase generator directly connected to 12 pulse converter can be used under special circumstances where the generating station is to be connected to the existing nearby ac line through dc link to improve the system stability. These schemes can also be used to feed power to the existing ac line as dc taps. For HVDC transmission schemes, converter transformers are required to attain the required dc voltage to minimize the transmission line losses and also to isolate the generator from the dc system. It is shown that normally designed six phase generator can be used with 12-pulse converter without derating. For nuclear or thermal power stations higher base speed operation can be selected for turbines and generators to reduce their capital cost.

In the case of hydro power stations, turbines can be operated under variable speeds as discussed in the Chapter III to maximize the operating efficiency. Under these conditions generators operate under variable frequency. It is shown that if a three phase generator designed for 0.85 power factor at 60 Hz operation operates at 70 Hz, the machine has to be derated to 86.3% of its nominal rating. In order to load the generator to its rated capacity, special design and cooling requirements may be necessary.

CHAPTER V

DC SYSTEM ASPECTS OF UNIT CONNECTION SCHEMES

5.1 Introduction

If the unit connection scheme is adopted for a generating station, each generator in the station is connected to one or more twelve pulse converters depending up on the rating of the generator. For example, in the case of hydro station with 10 generators each of 100 MW capacity, one twelve pulse converter of 100 MW rating can be connected to each generator through a three windings transformer as one unit. In the case of nuclear power station, where a single generator capacity is about 1000 MW which can justify a bipole, the generator can be connected to four twelve pulse converters of 250 MW each through converter transformers. In all these cases the number of converters at the inverter side need not be same as on the rectifier side. It may be necessary to select the optimum number and ratings of converters and converter transformers on both rectifier and inverter sides for a given number of generators in a station. It should take all possible operating conditions and contingencies into account in order to minimize the cost of the terminal stations.

In this chapter, a 10X100 MW hydro power station and a 1000 MW nuclear station with single generator are considered to determine the ratings of converters and converter transformers taking all possible operating conditions into account. As discussed in Chapter III, hydro turbines can be operated under variable speed depending up on available water head and

loading conditions to maximize the operating efficiency. In the case of a unit connected nuclear power station, the cost of the turbines and generators can be reduced by selecting the higher base speed of the turbine generator sets. In all these cases generators operate at different frequencies. It is necessary to study the behavior of the unit connection schemes at different possible operating frequencies under different fault conditions to ascertain the possible stresses on the generators and converters. A typical 500 MW unit connection scheme is simulated in time domain using Electro Magnetic Transient Program (EMTDC) developed by Manitoba Hydro and the University of Manitoba, under different fault conditions to study the recovery of the system and stresses on the generator for 60Hz and 70 Hz operation. Additional losses in the generator are computed under these frequencies of operation to evaluate the derating factor of the generator.

In order to study the possible application of the diode rectifiers for unit connection scheme, a small signal model of the generator with diode rectifier is developed to control the dc voltage on the rectifier with generator field excitation. The influence of the controller gain on steady state stability is evaluated by using root locus technique and the system response is studied with unit step input. In order to improve the system response with reasonable gains of the controller and exciter, a compensator net work has been designed to incorporate in feed forward path of the dc voltage controller. The dynamic behaviour of a 500 MW, 250 kV diode rectifier scheme is studied in time domain by using EMTDC program to study the recovery of the system for the dc line fault.

5.2 Hydro power station interface with dc system

In view of minimizing the cost of the terminals it is required to select optimum number of converters and converter transformers on both terminals taking all possible operational contingencies into account in order to transmit maximum possible available power. A typical 10X100 MW hydrostation for point-to-point unit connection scheme is discussed in the section. This is a typical case of one of the stations on the Nelson River. The schematic diagram of the unit connected hydro station with 10 generators of 100 MW each is shown in Fig. (5.1). Each generator on the sending end is connected to one 12-pulse converter through converter transformers. If the transmission voltage is fixed at ± 500 kV, the required dc current is 1000 A. All converters of five units are connected in series per pole at the sending end in order to obtain 500 kV dc voltage. On the receiving end, two 12-pulse converters are connected in series per pole. Each 12-pulse converter is connected to the ac system through Y-Y and Y- Δ converter transformers.

Initially, it is assumed that each 12-pulse converter on the inverter side is rated for 250 kV and 250 MW. But, the final ratings of converters and converter transformers are determined after studying all possible operating conditions in order to maintain the required dc voltage in the event of the outage of some units on the sending end. The selection of the converter ratings and the need for the provision of taps on converter transformers are discussed in the following section.

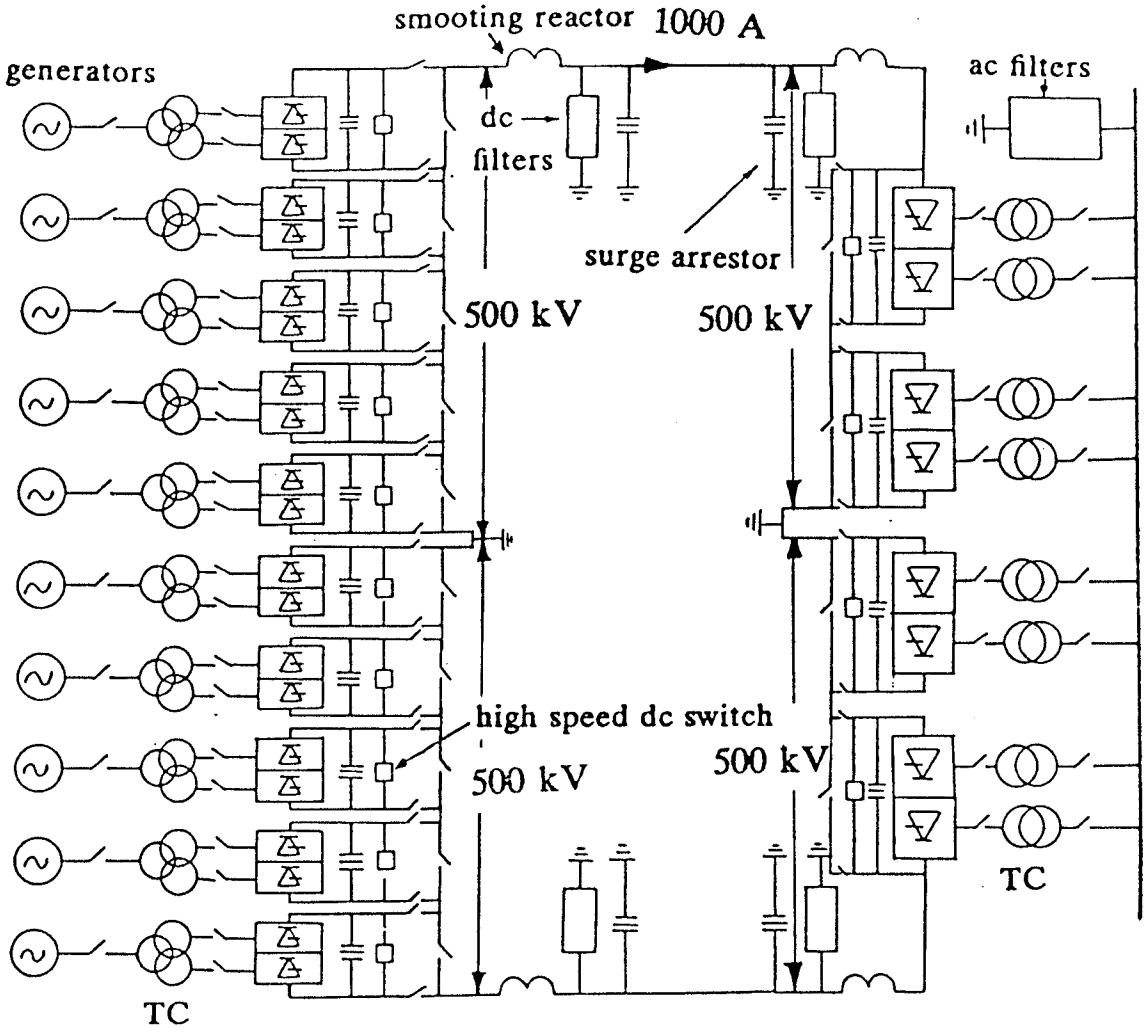

Fig. 5.1 : Interface of unit connected hydrostation with dc system.

5.2.1 Determination of the ratings of converters and converter transformers

In order to determine ratings of converters and converter transformers, initially two converters of equal ratings are assumed on the inverter side.

(a) Sending end under normal operation :

It is assumed that the dc line voltage drop and commutation voltage drop are neglected and the rectifier operates at the delay angle of 12° .

Generator ratings : 100 MW, 13.8 kV.

Total dc voltage per pole = 500 kV

Number of 12-pulse converters per pole = 5

Number of converter transformers per pole = 5

Rated dc current, I_{dc} = 1000 A

DC voltage per 12-pulse converter = 100 kV

$$V_{dc} = V_{do} \cos \alpha \tag{5.1}$$

$$V_{do} = \frac{6\sqrt{2}}{\pi} E_L \tag{5.2}$$

Where :

V_{dc} = DC voltage across the 12-pulse bridge.

V_{do} = No load dc voltage across the 12-pulse bridge.

E_L = Line-line ac voltage on the primary of the converter transformer.

From (5.1) and (5.2), E_L can be calculated.

The secondary side voltage of the transformer, E_L = 37.8 kV

The primary side voltage of the transformer = 13.8 kV

Transformer turns ratio = 1 : 2.74

MVA rating of the transformer = $\frac{\pi}{3} V_{do} I_{dc}$ = 107 MVA

(b) Receiving end under normal operation :

Number of 12-pulse converter bridges per pole = 2

DC voltage per 12-pulse bridge = 250 kV

But,

$$V_{dc} = V_{do} \cos \delta \qquad (5.3)$$

From (5.1) and (5.3) with the delay angle, $\delta = 18^o$

Secondary side voltage of the converter transformer, E_L = 97 kV

Primary side voltage of the converter transformer = 230 kV

Transformer turns ratio = 1 : 0.42

MVA rating of the transformer = $\frac{\pi}{3} V_{do} I_{dc}$ = 274 MVA

The above ratings of transformers and converters are modified taking into consideration of the following operating conditions. In this case only one pole of 500 MW capacity with five units are examined for the contingency evaluation.

(1) One unit on the sending end is out of service :

The net available power on the pole is 400 MW (80%) because only four units are under operation. Since the sending end dc voltage drops to 400 kV, the inverter side dc voltage has to be reduced to 400 kV. This can be achieved by providing +25% tap setting on the primary side of the converter transformers connected to the 230 kV ac bus. Under this condition, about 80% power of the pole can be transmitted.

(2) Two units on the sending end are out of service :

Under this condition only three units are in operation resulting in 300 MW (60%) available power on the pole. To transmit this power one 12-pulse bridge at the receiving end can be blocked keeping the other in operation. Since the dc voltage available at the sending end is only 300 kV, converter transformers at the receiving end should be provided with -17% tap on the primary side to increase the dc voltage to 300 kV. If each converter bridge is rated for 250 MW on the inverter side, the available 300 MW can not be transmitted through the available bridge. Under this condition two possible solutions can arise. These are as follows :

(i) Reduce the load on each unit by 16.7% which means that operating each generator at 83.3% of its rated capacity. Since the generator efficiency does not change appreciably under this load as shown in Table 5.1, the system can operate at 250 MW load which means a loss of 50 MW available power. In this case, one converter on the inverter side has to be rated for 300 kV which means that 20% more number of thyristors have to be connected in series as compared to that of the other bridge. Under this situation all three units can be loaded to their rated capacities to transmit 300 MW power.

(ii) If the inverter side bridges are selected with unequal ratings, one with 200 MW capacity for 200 kV and the other with 300 MW capacity for 300 kV, the available 300 MW power can be transmitted by operating 300 MW bridge and bypassing the other 200 MW converter. This configuration does not require over rating of converters and converter transformers. This arrangement is more attractive as compared to the former one. The detailed analysis of this scheme is discussed in the section 5.1.2.

% Load	115	105	100	90	80	75	50
% Efficiency	98.05	98.0	98.0	98.0	97.9	97.8	97.24

Table 5.1 : Efficiency variation of a 120 MVA, 0.85 pf salient pole synchronous generator with load.

(4) Four or five units on the sending end are out of service:

Under this condition the complete pole has to be shut down.

(5) One 12-pulse bridge on the inverter side is out of service :

If the bridge taken out of service is of 250 MW (50% capacity of the pole), then two units on the sending end have to be tripped. Under this condition only three units are in operation which can deliver 300 MW (60%) power at 300 kV. The inverter bridge rated for 300 MW capacity should be operated at -17% tap setting on the primary side of the transformer to transmit the above power.

If the inverter bridge, taken out of service, is of 300 MW capacity, then three units on the sending end should be operated at 83.3% rated capacity with inverter transformers tap settings at -17%. Only 250 MW (50%) power can be delivered under this situation.

If the two converter bridges are rated for 20% more than the nominal ratings initially specified, then in the event of the failure of the one converter bridge, 60% of the power can be delivered to the system instead of 50% power with the nominal rating converters. This configuration may increase the cost of the receiving end terminal station which may have to be compromised with 10% increase in power transfer capability. The required number of units at the sending end and the converter bridges and transformers on the receiving end for different loading conditions are shown in Table 5.2. For example, for 65% load condition (650 MW), four units can be operated at 100% load on one pole and three units at 83.3% load on other pole. The generators on the other pole at 83.3% load operate at 97.9% efficiency as shown in the Table 5.2. Since the change in the generator efficiency between 50% to 100% loading is not significant, the unit connection scheme for hydro power station has the flexibility of operating under all possible loading conditions. When the units are operating under partial loads depending up on the load demand, turbine efficiency under normal speed operation may decrease. If turbines are operated under variable speed depending upon the available water head and load demand, which is possible in the case of unit connection schemes, the turbine efficiency can be maintained at the maximum possible value as discussed in Chapter III.

If the number of units for the scheme shown in Fig. 5.1 are selected four instead of five per pole, the number of transformers can be reduced to

four on the sending end which may lead to saving in cost of the terminal. But the ratings of the converters and converter transformers on the sending end have to be increased to 25% more than the previous scheme for the same power transfer capability.

If two 12-pulse converters of 250 kV, 250 MW ratings are chosen per pole on the inverter side,+33% tap settings are to be provided on the primary side in order to transmit the maximum available power in the event of failure of one unit on a pole. If three units on a pole are taken out of service, complete pole has to be shut down, where as in the case of five units per pole, this situation may not happen if the converters on the inverter are selected with 200 MW, 200 kV and 300 MW, 300 kV ratings.

In the event of failure of one 12-pulse converter on the inverter side two units can be tripped in which case only 250 MW (50% pole capacity) can be transmitted. If one of the converter is rated 25% more than the other, then 375 MW power (75% pole capacity) can be transmitted. Table 5.3 shows the operation of 8X125 MW unit connection scheme for different loading conditions.

% load	Number of 100 MW units		Number of 250 MW bridges at the inverter terminal		%load on each unit		Efficiency of each generator		Total power in MW	
(MW)	pole1	pole2	pole1	pole2	pole1	pole2	pole1	pole2	pole1	pole2
100 (1000)	5	5	2	2	100	100	98.0	98.0	500	500
95 (950)	5	5	2	2	95	95	98.0	98.0	475	475
90 (900)	5	5	2	2	90	90	98.0	98.0	450	450
85 (850)	5	4	2 (+25% tap)	2	100	87.5	98.0	98.0	500	350
82 (820)	4	4	2 (+25% tap)	2 (+25% tap)	102	102	98.02	98.02	415	415
80 (800)	4	4	2 (+25% tap)	2 (+25% tap)	100	100	98.0	98.0	400	400
75 (750)	4	4	2 (+25% tap)	2 (+25% tap)	94	94	98.0	98.0	375	375
70 (700)	5	2	221	100 (+25% tap)	100	98.0	98.0	500	200	
65 (650)	4	3	2 (+25% tap)	1 (-17% tap)	100	83.3	98.0	97.9	400	250
63 (630)	3	3	2 (+25% tap)	2 (+25% tap)	105	105	98.04	98.04	315	315
60 (600)	3	3	2 (+25% tap)	2 (+25% tap)	100	100	98.0	98.0	300	300
55 (550)	3	3	2 (+25% tap)	2 (+25% tap)	91.7	91.7	98.0	98.0	275	275
50 (500)	5	-	2	-	100	-	98.0	-	500	-
45 (450)	5	-	2	-	90	-	98.0	-	450	-
40 (400)	4	-	2 (+25% tap)	-	100	-	98.0	-	400	-
35 (350)	4	-	2 (+25% tap)	-	87.5	-	97.9	-	350	-
30 (300)	3	-	1 (-17% tap and 25% over rating)	-	100	-	98.0	-	300	-
25 (250)	3	-	1 (-17% tap)	-	83.3	-	97.9	-	250	-
20 (200)	2	-	1 (+25% tap)	-	100	-	98.0	-	200	-
15 (150)	2	-	1 (+25% tap)	-	75	-	97.8	-	150	-
10 (100)	-	-	Total	bipole	shut	down	-	-	-	

Table 5.2 : Loading sequence of generators and converters of a 10X100 MW unit connected station depending up on the load demand.

% load	Number of 125 MW units		Number of 250 MW bridges at the inverter terminal		%load on each unit		Efficiency of each generator		Total power in MW	
(MW)	pole1	pole2	pole1	pole2	pole1	pole2	pole1	pole2	pole1	pole2
100 (1000)	4	4	2	2	100	100	98.0	98.0	500	500
95 (950)	4	4	2	2	95	95	98.0	98.0	475	475
90 (900)	4	4	2	2	90	90	98.0	98.0	450	450
85 (850)	4	4	2	2	85.0	85.0	98.0	98.0	425	425
79 (790)	4	4	2	2	79.0	79.0	97.9	97.9	395	395
78 (780)	3	3	2 (+33% tap)	2 (+33% tap)	104	104	98.0	98.0	390	390
75 (750)	3	3	2 (+33% tap)	2 (+33% tap)	100	100	98.0	98.0	375	375
70 (700)	3	3	2	2 (+33% tap)	93.3 (+33% tap)	93.3	98.0	98.0	350	350
65 (650)	3	2	2 (+33% tap)	1	105	105	98.04	98.04	325	325
60 (600)	3	2	2 (+33% tap)	1	100	90	98.0	98.0	300	300
55 (550)	3	2	2 (+33% tap)	1	88.0	88.0	98.0	98.0	275	275
50 (500)	4	-	2	-	100	-	98.0	-	500	-
45 (450)	4	-	2	-	90	-	98.0	-	450	-
40 (400)	4	-	2	-	80	-	97.9	-	400	-
39 (390)	3	-	2 (+33% tap)	-	105	-	98.04	-	390	-
35 (350)	3	-	2 (+33% tap)	-	93.4	-	98.0	-	350	-
30 (300)	3	-	2 (+33% tap	-	80	-	97.9	-	300	-
25 (250)	2	-	1	-	100	-	98.0	-	250	-
20 (200)	2	-	1	-	80	-	97.9	-	200	-
15 (150)	2	-	1	-	60	-	97.3	-	150	-
10 (100)	2	-	1	-	40	-	97	-	100	-

Table 5.3 : Loading sequence of generators and converters of a 8X125 MW unit connected station depending up on the load demand.

5.2.2 Determination of the ratings of converters and converter transformers with unequal bridge ratings at the inverter

It is assumed that the inverter terminal consists of two 12-pulse converters, one with 200 MW and 200 kV rating and the other with 300 MW and 300 kV rating per pole. There are five units of 100 MW capacity each per pole.

(a) Receiving end under normal operation :

Number of 12-pulse converter bridges per pole = 2

DC voltage across the 12-pulse bridge of 200 Mw capacity = 300 kV

But, From (5.1) and (5.3) with the delay angle, $\delta = 18^{o}$

Secondary side voltage of the converter transformer, E_L = 78 kV

Primary side voltage of the converter transformer = 230 kV

Transformer turns ration = 1 : 0.34

MVA rating of the tansformer $= \frac{\pi}{3} V_{do} I_{dc}$ = 211 MVA

DC voltage across the 12-pulse bridge of 300 MW capacity = 300 kV

Secondary side voltage of the converter transformer, E_L = 117 kV

Primary side voltage of the converter transformer = 230 kV

Transformer turns ration = 1 : 0.507

MVA rating of the tansformer $= \frac{\pi}{3} V_{do} I_{dc}$ = 316 MVA

The tap setting requirements on the converter transformers are determined after evaluating the system for all possible operating conditions taking all

possible contingencies into account.

(1) One unit on the sending end is out of service :

In this case the net available power is only 400 MW on the pole. Since the voltage on the sending end dropped to 400 kV, the inverter side voltage has to be reduced to this value. If the converters on the inverter side are provided with +20% tap setting on the primary side, then the dc voltage on the inverter side can be reduced to 400 kV. Under this condition 80% power on the pole can be transmitted.

(2) Two units on the sending end are out of service :

In this situation only 300 MW power is available for transmission at 300 kV. This power can be transmitted by operating only 300 MW bridge at 300 kV on the inverter side.

(3) Three units on the sending end are out of service :

Only 200 MW (40% of the pole capacity) is available for transmission. Since the voltage at the sending end is only 200 kV, by operating only 200 MW, 200 kV 12-pulse bridge on the inverter, 200 MW power can be transmitted.

(4) Four units on the sending end are out of service :

In this condition only one unit is in operation on the pole delivering 100 MW power at 100 kV. To transmit this power, the 200MW, 200 kV 12-pulse bridge on the inverter side can be operated as rectifier and the other

12-pulse converter of 300 MW can be operated at 300 kV. In this situations the losses for the 200 MW bridge operating as rectifier on the inverter side should be supplied from the receiving end.

(5) One 12-pulse bridge on the receiving end is out of service :

If the bridge taken out of service is of 200 MW capacity, two units on the sending end should be tripped thereby 300 MW (60%)power can be transmitted. If the bridge taken out of service is of 300 MW capacity, three units on the sending end have to be tripped. In this case only 200 MW (40%) power can be transmitted. But, in the previous case where the inverter side is equipped with two bridges of equal ratings, 50% power can be transmitted under this condition. Therefore the arrangement of the converter bridges with unequal ratings on the inverter side may be more economical and has the operational flexibility than that of the previous arrangement. Moreover tap settings are only required on the positive side to decrease the voltage in the event of outage of one unit. It has the operational flexibility to transmit maximum available power for different loading conditions as shown in Table 5.4.

% load	Number of 100 MW units		Number of bridges at the inverter				%load on each generator		Total power in MW	
			pole1		pole2					
(MW)	pole1	pole2	200 MW Bridge	300 MW Bridge	200 MW Bridge	300 MW Bridge	pole1	pole2	pole1	pole2
100 (1000)	5	5	1	1	1	1	100	100	500	500
95 (950)	5	5	1	1	1	1	95.0	95.0	475	475
90 (900)	5	5	1	1	1	1	90.0	90.0	450	450
85 (850)	5	5	1	1	1	1	85.0	85.0	425	425
82 (820)	5	5	1	1	1	1	82.0	82.0	410	410
80 (800)	5	3	1	1	-	1	100	100	500	300
75 (750)	5	3	1	1	-	1	100	83.3	500	250
70 (700)	5	2	1	1	1	-	100	100	500	200
65 (650)	5	2	1	1	1	-	100	75.0	500	150
60 (600)	3	3	-	1	-	1	100	83.3	300	250
55 (550)	3	3	-	1	-	1	100	83.3	300	250
50 (500)	5	-	1	1	-	-	100	-	500	-
45 (450)	5	-	1	1	-	-	90.0	-	450	-
40 (400)	4	-	1	1	-	-	80.0	-	400	-
35 (350)	2	2	1	-	1	-	100	75.0	200	150
30 (300)	3	-	-	1	-	-	100	-	300	-
25 (250)	3	-	-	1	-	-	83.3	-	250	-
20 (200)	2	-	1	-	-	-	100	-	200	-
15 (150)	2	-	1	-	-	-	75.0	-	150	-
10 (100)	1	-	1 (operates as rectifier)	1	-	-	100	-	100	-

Table 5.4 : Loading sequence of generators and converters of a 10X100 MW unit connected station depending up on the load demand.

5.3 Interface of 1000 MW nuclear power station with dc system

Nuclear power stations have the flexibility of choosing large rating generators and turbines. If the rating of the single generator is chosen as 1000 MW, it can justify a bipole. In this case two possible alternatives can arise in selecting the number of converters per pole on the sending end and the receiving end terminals. These are

(1) One converter of 500 MW, 500 kV per pole on each side.
(2) Two converters of 250 MW, 250 kV per pole on each side.

If the first alternative is selected for the station, in the event of outage of any converter on either side, the complete pole is lost. If the second alternative is chosen, then in the event of failure of one converter on either side only 50% capacity of the pole is lost. This alternative increases the power transfer capability as compared with the previous case. Hence second alternative with two 12-pulse converters per pole is selected due to aforesaid reasons. The generator is connected to each 12-pulse converter through Y-Y and Y- Δ transformers. The converters on both sides of the pole are connected in series to obtain 500 kV dc voltage. The transformers on the sending side are not provided with taps, since the generator terminal voltage can be kept at the preset value by its excitation control. The transformers on the receiving end are to be provided with tap settings in order to take care of ac voltage fluctuations as in the case of the conventional current collector scheme.

Since the efficiency of the generator would not change appreciably with the load up to 50% capacity as mentioned in the earlier section, the system can operate at any load up to 50% capacity without appreciable loss in the generator efficiency. The steam turbine efficiency also does not change appreciably with load up to 50% capacity. But, under very low load

conditions, say less than 40%, the steam in the Low Pressure stage of the turbine may saturate and cause corrosion on the turbine blades. Normally nuclear power stations are operated as base load stations in which the operation of the station under light load condition may be a remote possibility.

In conclusion, if unit connection scheme is adopted for nuclear power stations for transmitting power through HVDC link, the selection of converters and converter transformers is similar to that of a conventional current collector scheme. But, it has the advantage of operating the turbines and generators at higher base speed in order to minimize the capital cost of units.

5.4 Discussions

In the case of hydro power stations, if unit connection schemes are adopted, the ratings of converters and converter transformers are selected based on the number of generators and taking all possible operating conditions to transmit maximum available power. For example, in the case of 10X100 MW station with five units of each 100 MW capacity per pole, if two 12-pulse converters are chosen, each with three units capacity on the inverter side, in the event of outage of one converter, 60% of the power can be transmitted on the pole. However, this may increase the cost of the terminal station. On the other hand, if one of the converters is chosen with three units capacity and other one with two units capacity, in the event of outage of the lower capacity converter 60% power can be transmitted. But if the higher capacity converter is out of service, only 40% power can be transmitted on the pole. In this arrangement over ratings of converters are not required. Hence, this arrangement is preferred from an economical

point of view. It is shown that if the number of units are more in a power station, operational flexibility to transmit maximum available power increases under different loading and operational contingencies. The selection of the ratings of theconverters and converter transformers on the receiving end depends upon the possible operating conditions to transmit maximum available power taking economical aspects into account. For nuclear power stations the selection of converter and converter transformers rating on the receiving end is the same as in conventional schemes.

5.5 Digital simulation of the unit connection scheme

In order to evaluate the possible stresses on generators and converters and also to study the recovery of the system for different faults, a typical 250 kV, 500 MW, 2000 A, unit connection scheme has been simulated in time domain using the Electro-Magnetic Transient Program (EMTDC) which has been developed by Manitoba Hydro and the University of Manitoba. The schematic diagram of the system considered for digital simulation is shown in Fig. (5.2). As seen from the above figure, the total system is divided into four sub systems to improve the computational efficiency. A 556 miles long dc transmission line is modelled with frequency dependent parameters. The transformer is modelled as coupled circuits. The rectifier is equipped with constant current control and the inverter with minimum extinction angle control to minimize the reactive power consumption thereby minimizing the valve stresses.

The sending end station consists of five units each with 120 MVA generator connected to a 12-pulse bridge through Y-Y and Y- Δ transformers and the converter bridges are connected in series. The receiving end consists of two 12-pulse converters, connected in series, each one with 250 kV and 250 MW ratings. The generator is modelled in d-q-o components and the saturation is taken into account by modifying the magnetizing reactance as a function of the magnetizing current [25] with piecewise linearization of the saturation curve of the machine. Thyristor controlled excitation system along with the automatic voltage regulator model is used to keep the generator voltage constant. The pole controller and the valve group controllers models used in this simulation are shown in Figs. (5.3a) and (5.3b) respectively. The static excitation system with automatic voltage

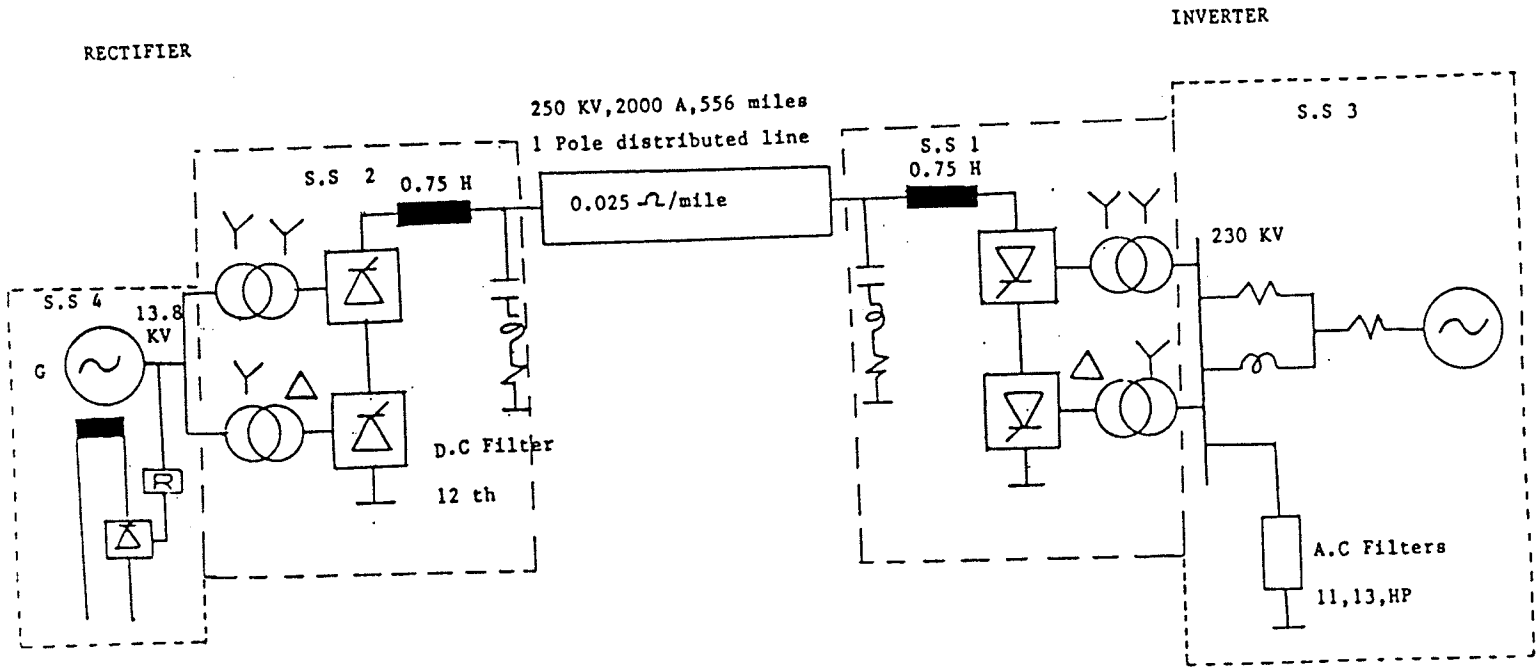

Fig. 5.2 : SCHEMATIC DIAGRAM FOR DIGITAL SIMULATION OF UNIT CONNECTION SCHEME

regulator model is shown in Fig. (5.3c).

5.5.1 DC controls

The block diagram of dc controls on the rectifier and the inverter terminals is shown in Fig. (5.4).

The pole controller shown in Fig. (5.3a) is a constant current controller. The measured dc current is compared with the input current order which is obtained by dividing the power order by the dc voltage. The master controller sends the current orders to the pole controllers of both rectifier and inverter. The current controller on the inverter side is provided with current margin so that it would not operate under normal operating conditions. The current error is passed through the proportional and integral controller to obtain the desired ignition angle, α, which is used as input to the valve group controller to keep the dc current at the set value. If the valve group controller shown in Fig. (5.3b) is in rectifier mode, the ' which ever is least ' block selects the α_{order} from the pole controller and delivers it to the firing control circuit. If the valve group is in the inverter operation with constant extinction angle control [26], then 'whichever is least' circuit selects α_{order} form the upper circuit. This circuit monitors the extinction angle, γ and selects the lowest value, $\gamma_{measured}$, over a period of a cycle to generate the $\gamma_{desired}$ order. The $\gamma_{desired}$ is equal to the γ_{min} if the $\gamma_{measured}$ is greater than the γ_{min}. However, if γ_{min} is greater than the $\gamma_{measured}$, the $\gamma_{desired}$ is advanced to $\gamma_{min} + (\gamma_{min} - \gamma_{measured})$, in order to avoid commutation failure. The actual firing angle $\alpha = \pi - \beta$, is determined by solving the following equation [26].

$$\cos \gamma = X_c I_{dc} + \cos \beta$$

Where, X_c is the net commutation reactance.

5.5.2 System startup - simulation

All the generators are brought to the rated voltage after blocking and by-passing both rectifier and inverter. In the EMTDC simulation, the generator can be brought to the steady state condition in shorter time (0.1 s) with proper steady state initial conditions in the program. At t=0 s with both rectifier and inverter under block and bypass condition, the firing angle at the rectifier is set to 5° and the the inverter to 57°, which means the inverter operates in rectifier mode. At t= 0.1 s, the inverter is deblocked and the bypass switch is opened. The dc current circulates in the line since the inverter operates in the rectifier mode at $\alpha = 57°$ and the rectifier at that time has been bypassed. During this period the current order is set to 0.3 p.u. At t=0.15 s, the rectifier is deblocked and the bypass switch is opened, and the inverter is forced into inversion mode by setting the firing angle to 110°. The dc current is ramped to 1.0 p.u with proper ramp rate. Under steady state the rectifier operates in constant current control and the inverter in constant extinction angle control mode with γ equal to 18°. A current controller is also provided at the inverter end with current margin of 0.1 p.u. If the dc voltage at the rectifier end falls below the value at the inverter, then the inverter takes over the current control and maintains the current at the set value (0.9 p.u) which means that the inverter brings down the dc voltage at its terminal below that of the rectifier such that the above set current is maintained. Under this condition the rectifier operates at minimum alpha ($\alpha = 5°$) and the

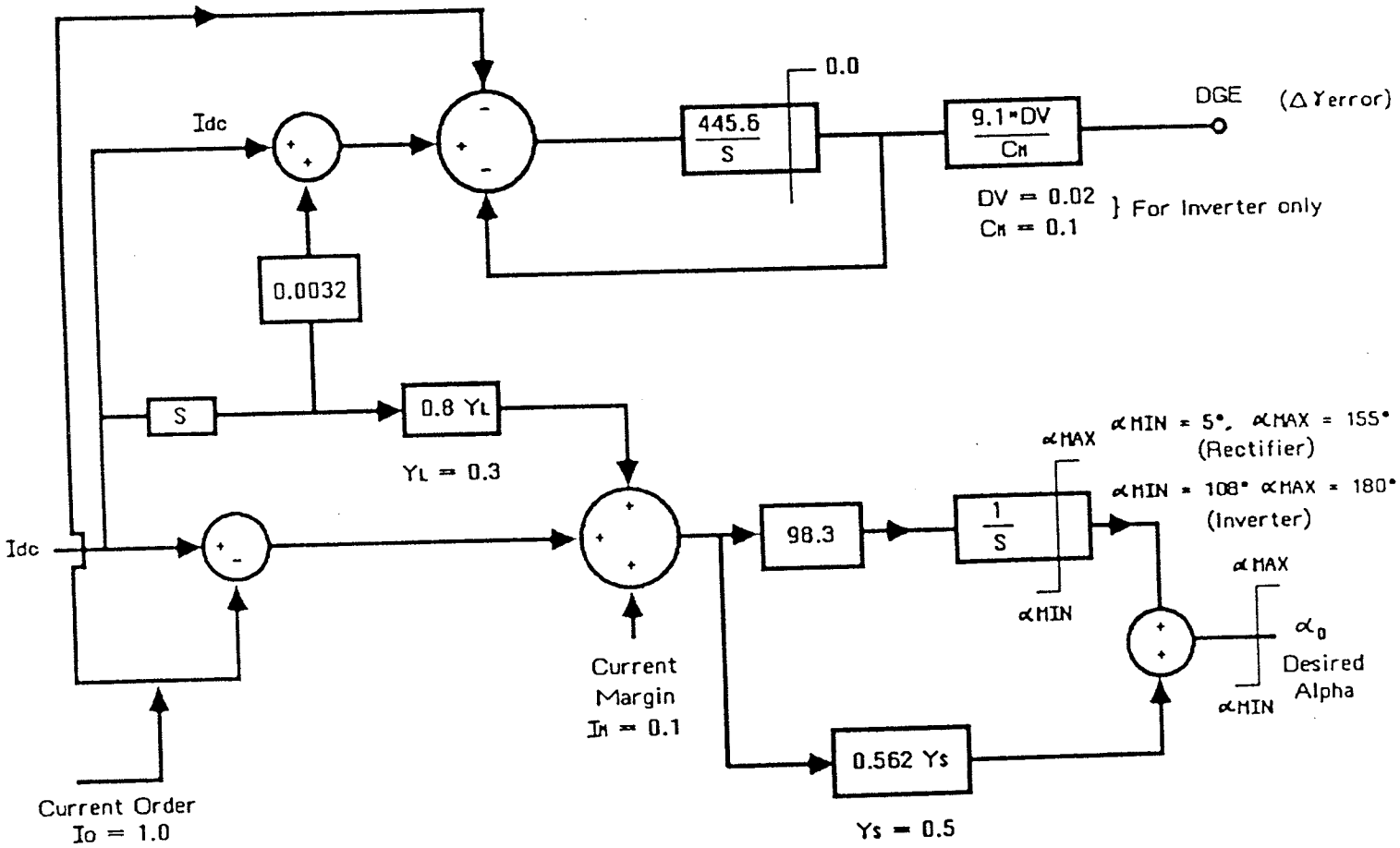

Fig. 5.3a : Block Diagram of Pole Controller (POL1C6)

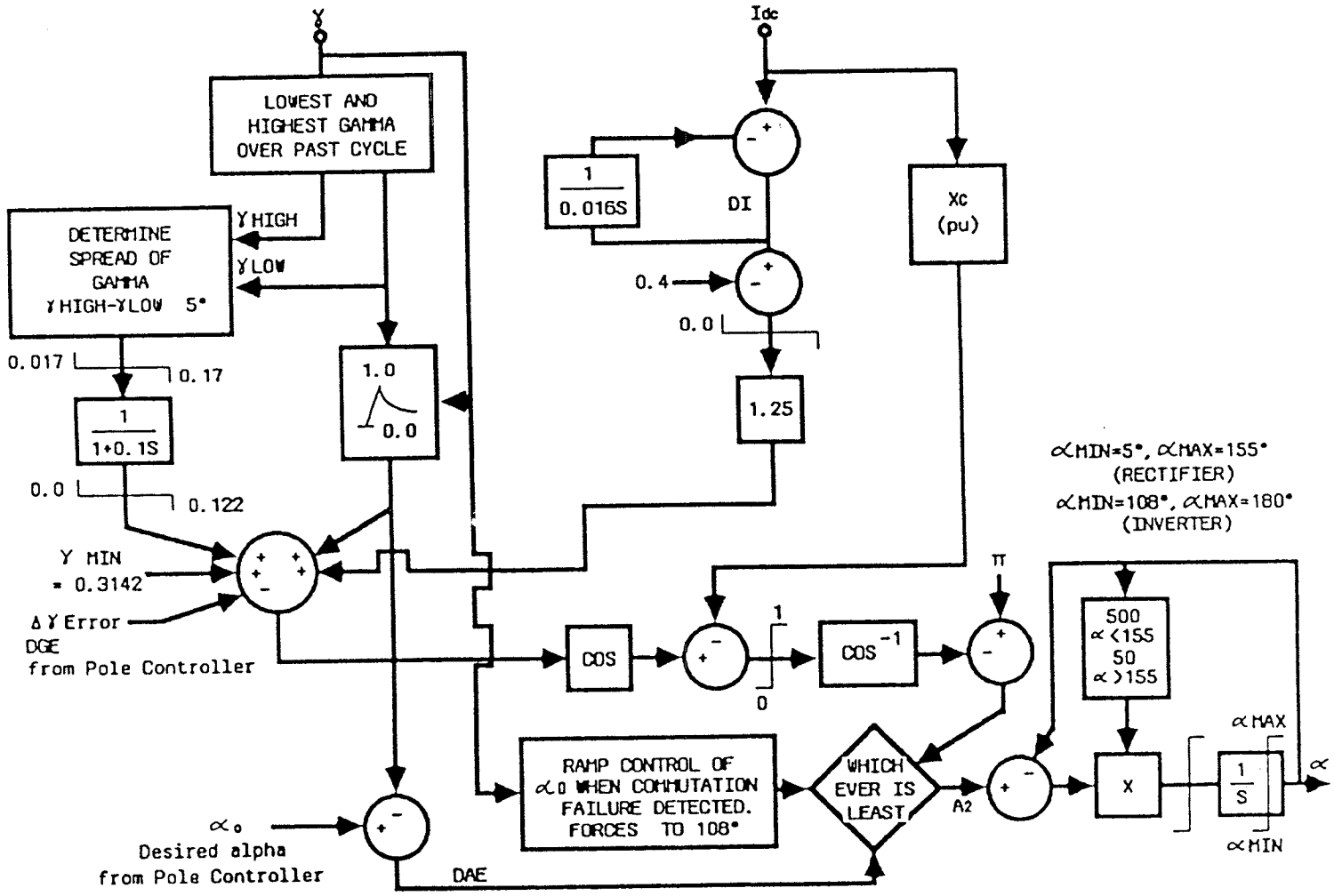

Fig. 5.3b : Block Diagram of Valve Group Controller (VG1C18)

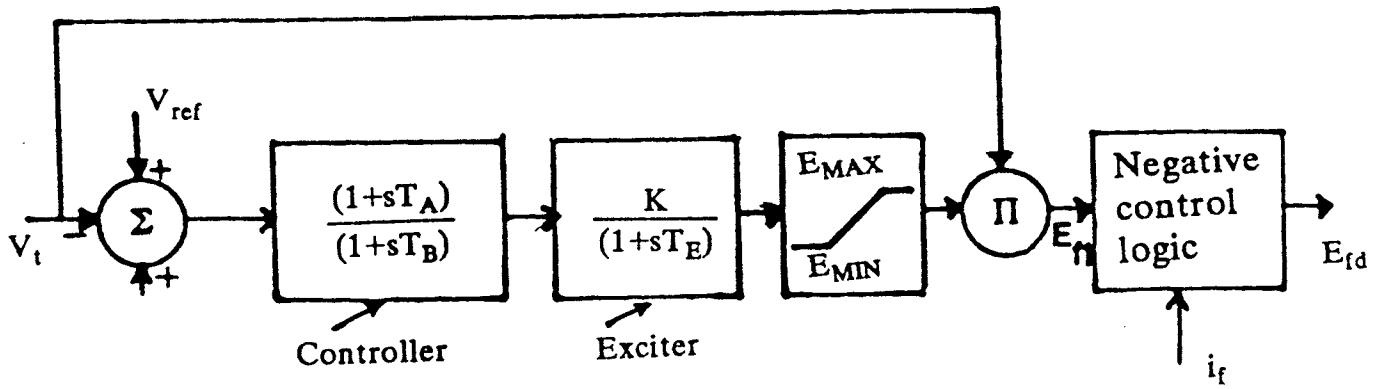

Fig. 5.3c : Block diagram of the static exciter model.

inverter at a large firing angle (β control). This situation may happen when some of the units on the rectifier end are taken out of service. Normal control modes can be restored by changing proper taps on inverter transformers or by blocking corresponding inverter bridges. Current control operation at the inverter is not recommended for operation for long time, since the reactive power consumption by the inverter bridges may increase which may lead to increase in voltage stress on valves.

5.5.3 Simulation results

In order to study the dynamic behavior of the unit connection scheme, under different fault conditions, the following faults are simulated on the system for 60 Hz and 70 Hz operations.

(1) DC line fault at the rectifier for 12 cycles.

(2) Permanent dc block

(3) Three phase to ground fault at the generator terminal for 5 cycles.

(4) Single line to ground fault on the generator terminals.

These faults have been studied with 2.5 short circuit ratio at the inverter end. The short circuit ratio is defined as the ratio of the short circuit capacity of the system to the dc power. The simulation results are shown in Table 5.5.

(1) : DC line fault at the rectifier :

The fault is created on the dc line at t=0.1 s and then cleared at t=0.3 s. The simulation results are shown in Figs. (5.5a) and (5.5b). It can be observed from the above results that immediately after clearing the fault, 2.8 p.u and 2.9 p.u peak values in dc voltage for 60 Hz and 70 Hz operation

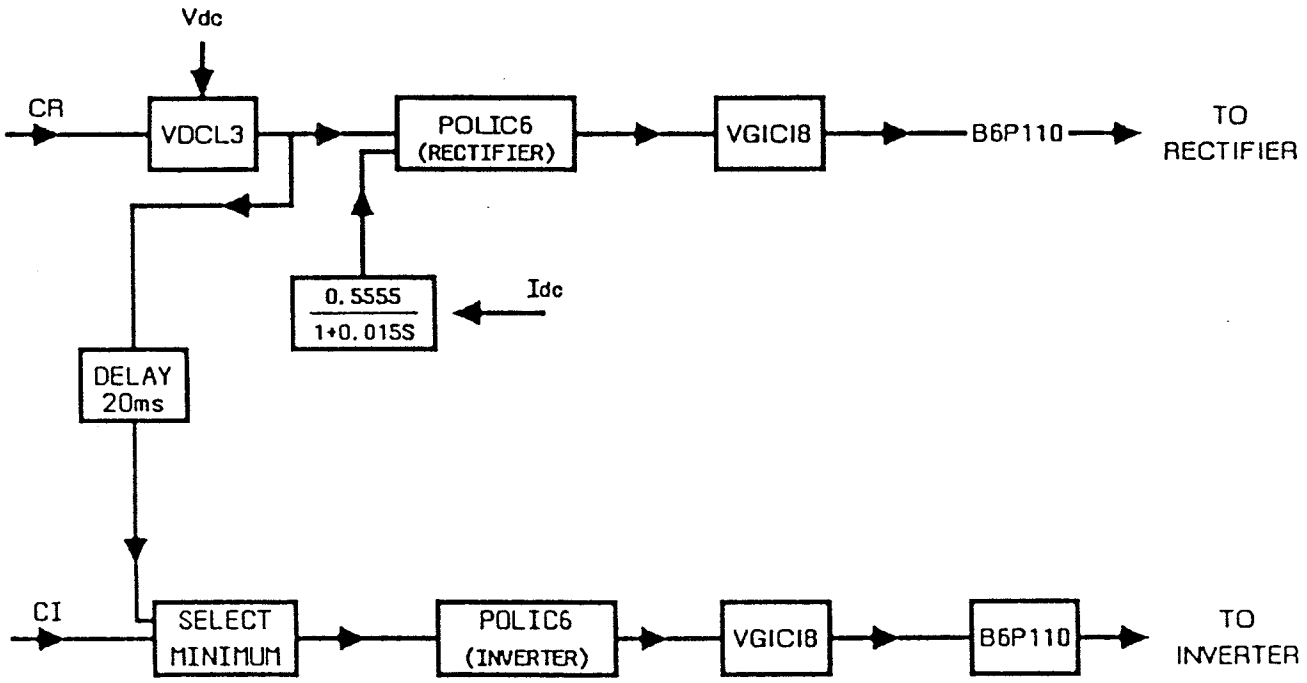

CR : current order at the rectifier

CI : current order at the inverter

Fig. 5.4 : Block Diagram of DC Controls

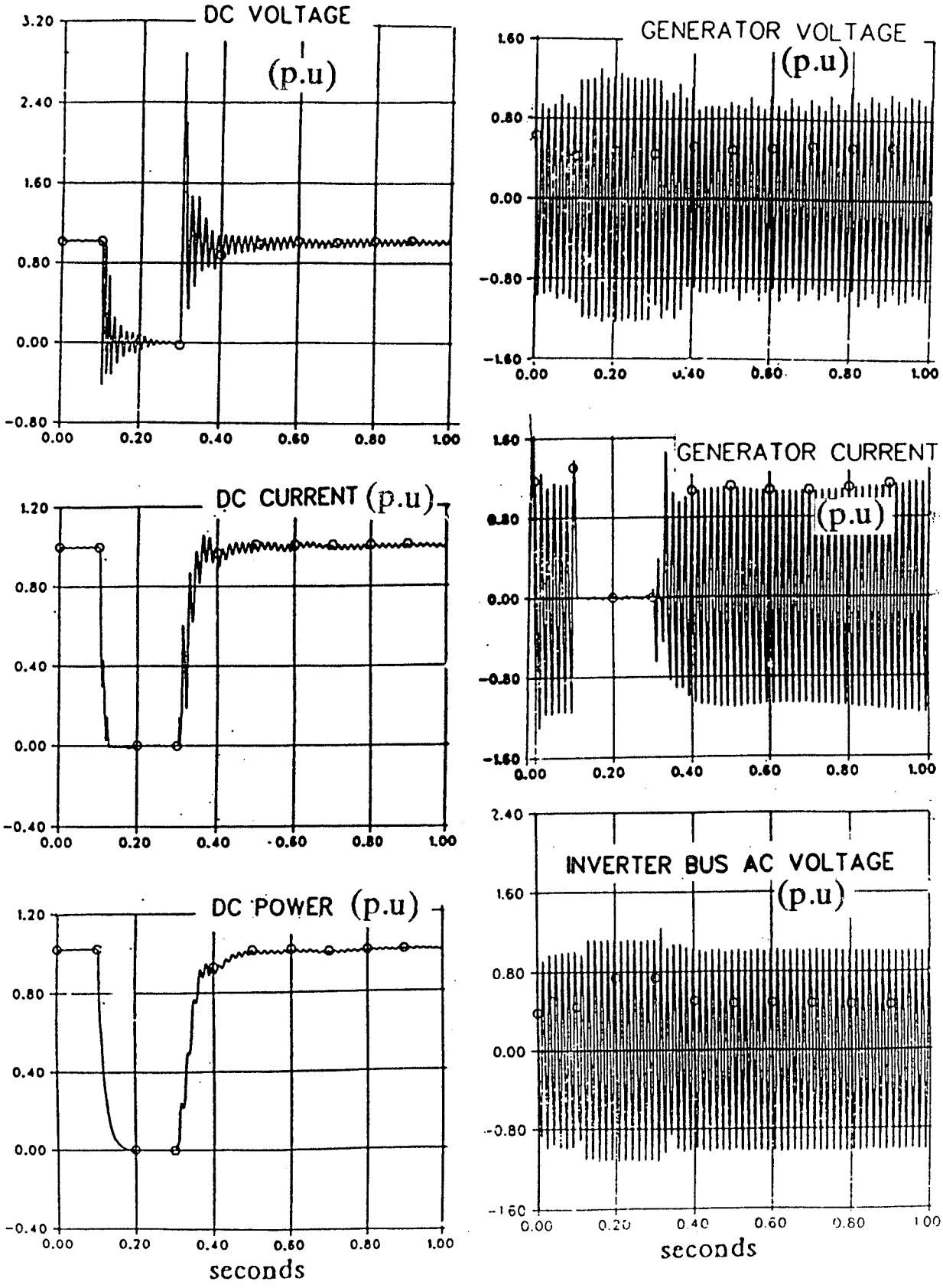

Fig. 5.5a : DC line fault at the rectifier (60 Hz operation)

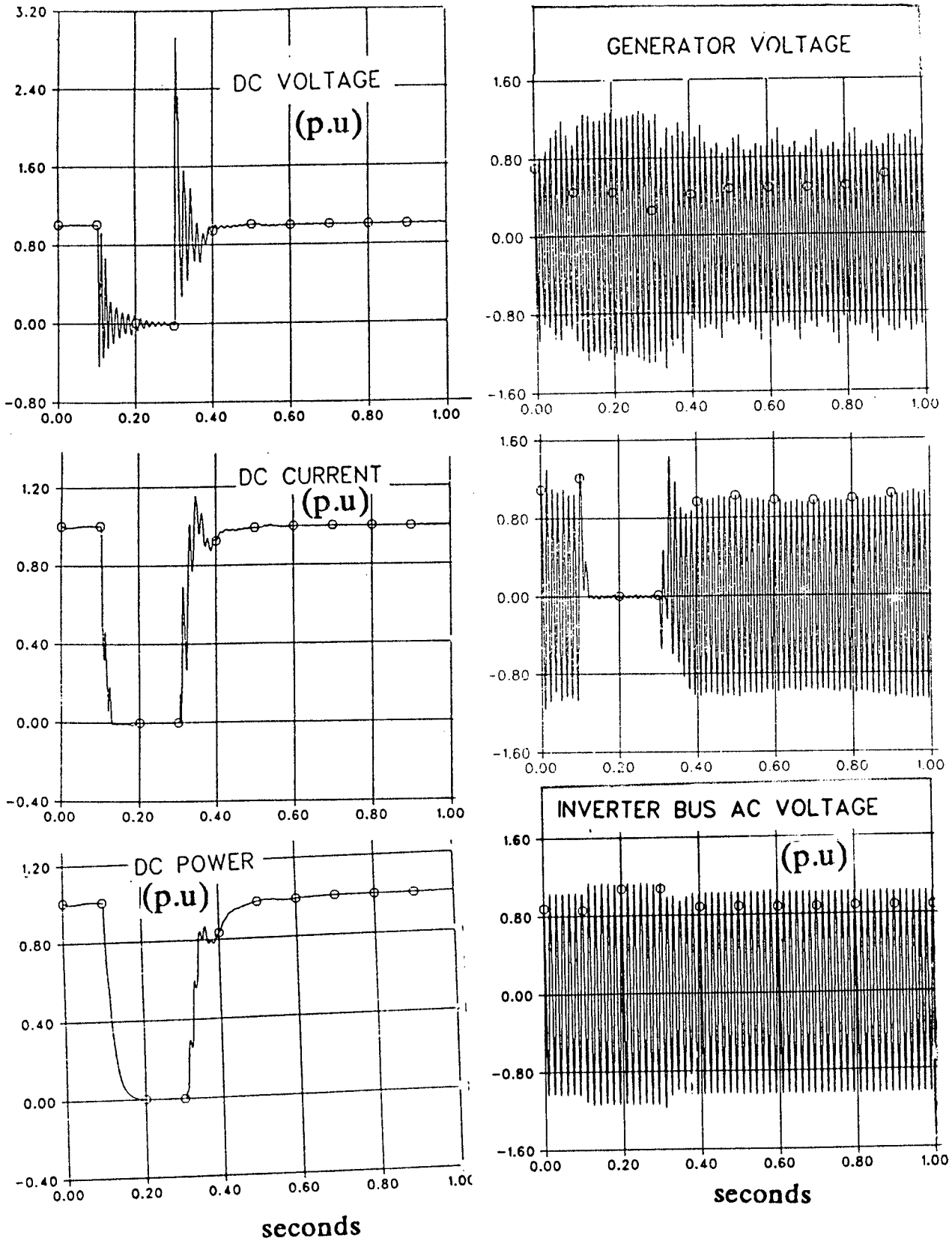

Fig. 5.5b : DC line fault at the rectifier (70Hz operation)

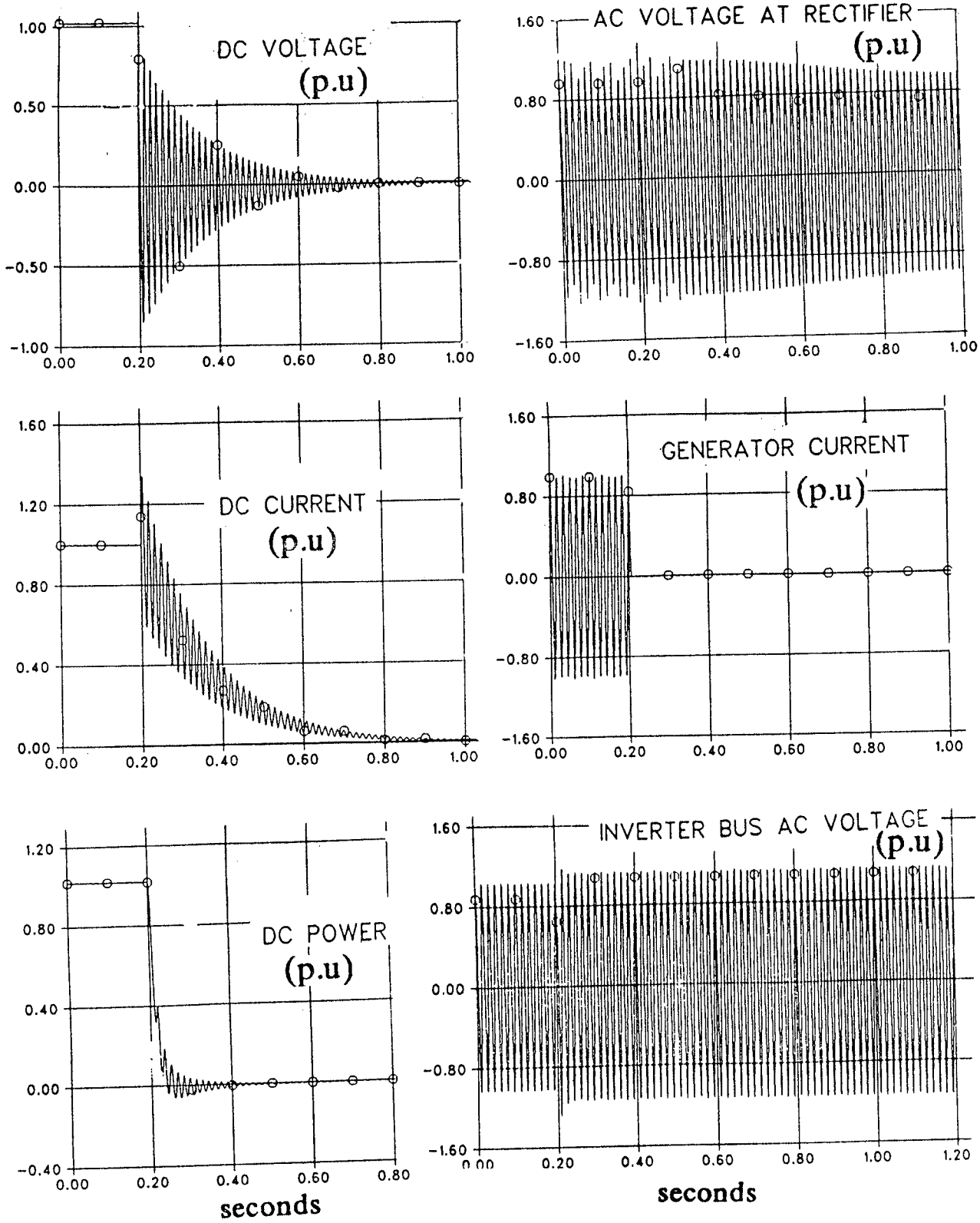

Fig. 5.6a : Permanent dc block (60 Hz operation)

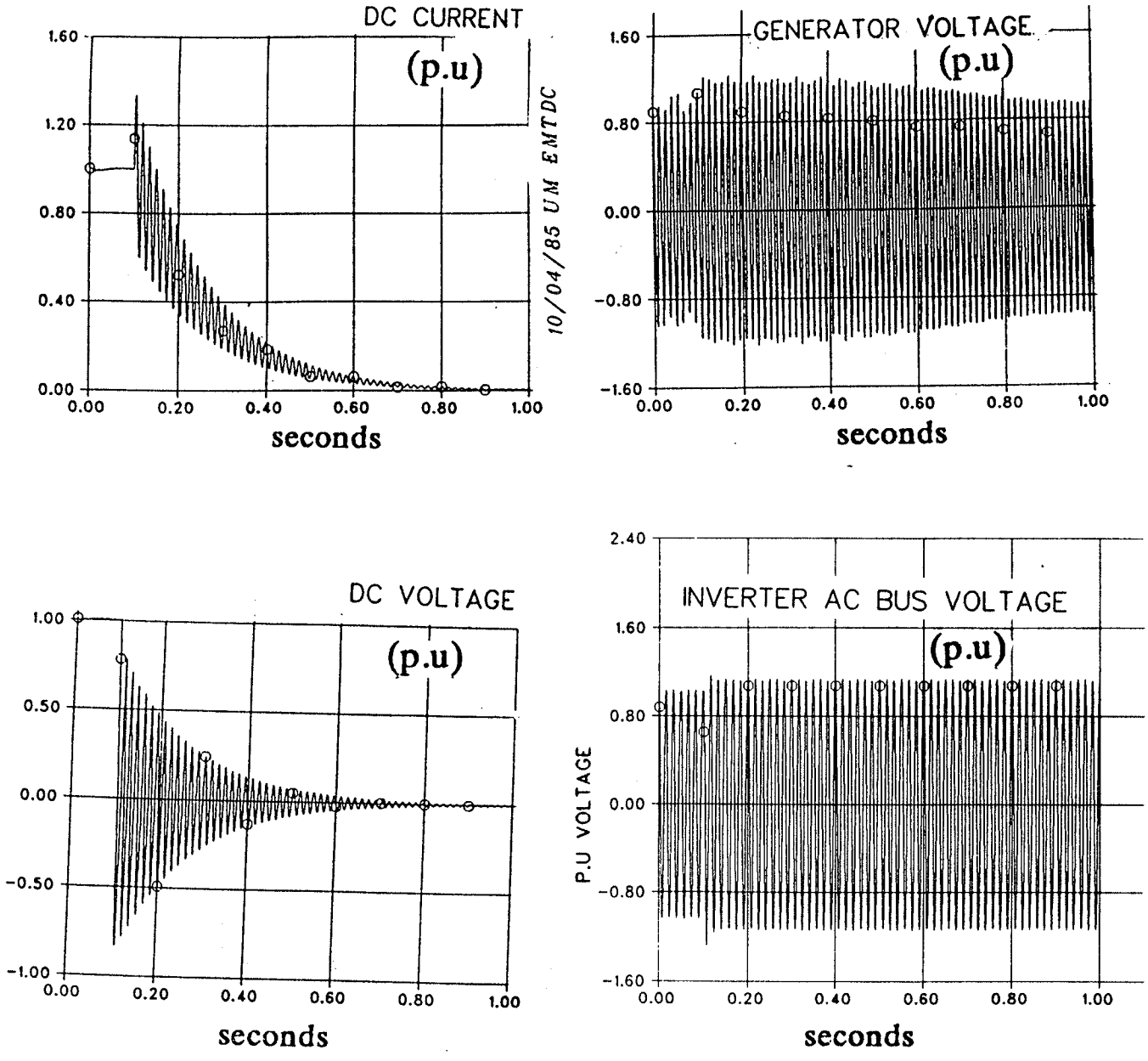

Fig. 5.6b : Permanent dc block (70 Hz operation)

respectively. But the voltage rose to 1.25 p.u and 1.30 p.u observed on the generator terminals during the fault period. No unusual dynamic overvoltages have been observed at the generator terminals after clearing the fault. The dc power and dc current recovered to 0.9 pu value in 200 ms.

(2) : Permanent dc block :

Converter valves on both rectifier and inverter are blocked by removing the firing pulses and by-pass valves are turned on at the same time in order to simulate the full load rejection. The simulation results are shown in Figs. (5.6a) and (5.6b).

The generator terminal voltage rose to 1.143 p.u and 1.2 p.u for 60 Hz and 70 Hz operation respectively after blocking both converters. These voltages are brought down to 1.0 p.u with the help of automatic voltage regulator after 0.7 s. The dc current decreased to zero in 0.6 s which depends on the dc line time constant. The inverter side ac voltage rose to 1.1 p.u and 1.16 p.u for 60 Hz and 70 Hz operations respectively. Dynamic overvoltages appeared on the ac side of converters which are within the acceptable limits.

(3) : Three phase to ground fault at the generator terminals :

The simulation results for the above fault for 5 periods are shown in Figs. (5.7a) and (5.7b) for 60 Hz and 70 Hz operation respectively. This fault is cleared by generator ac circuit breaker.

It can be observed from the simulation results, the generator is stressed to 4.0 p.u and 3.63 p.u short circuit currents for 60 Hz and 70 Hz operation. But, in the case of unit connection scheme, generators and converters are located in the close proximity, the probability of occurence of

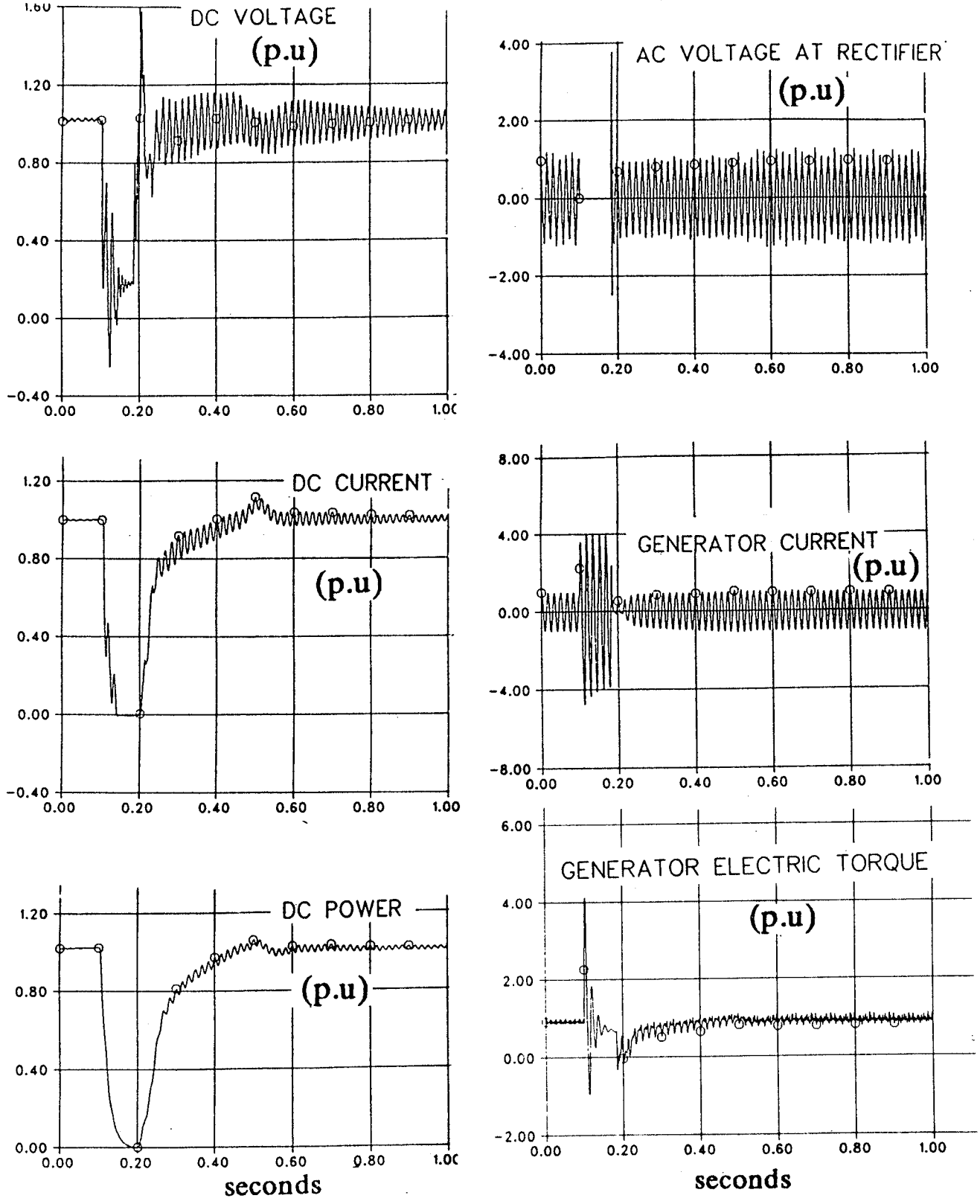

Fig. 5.7a : 3-phase to ground fault at the rectifier (60 Hz operation)

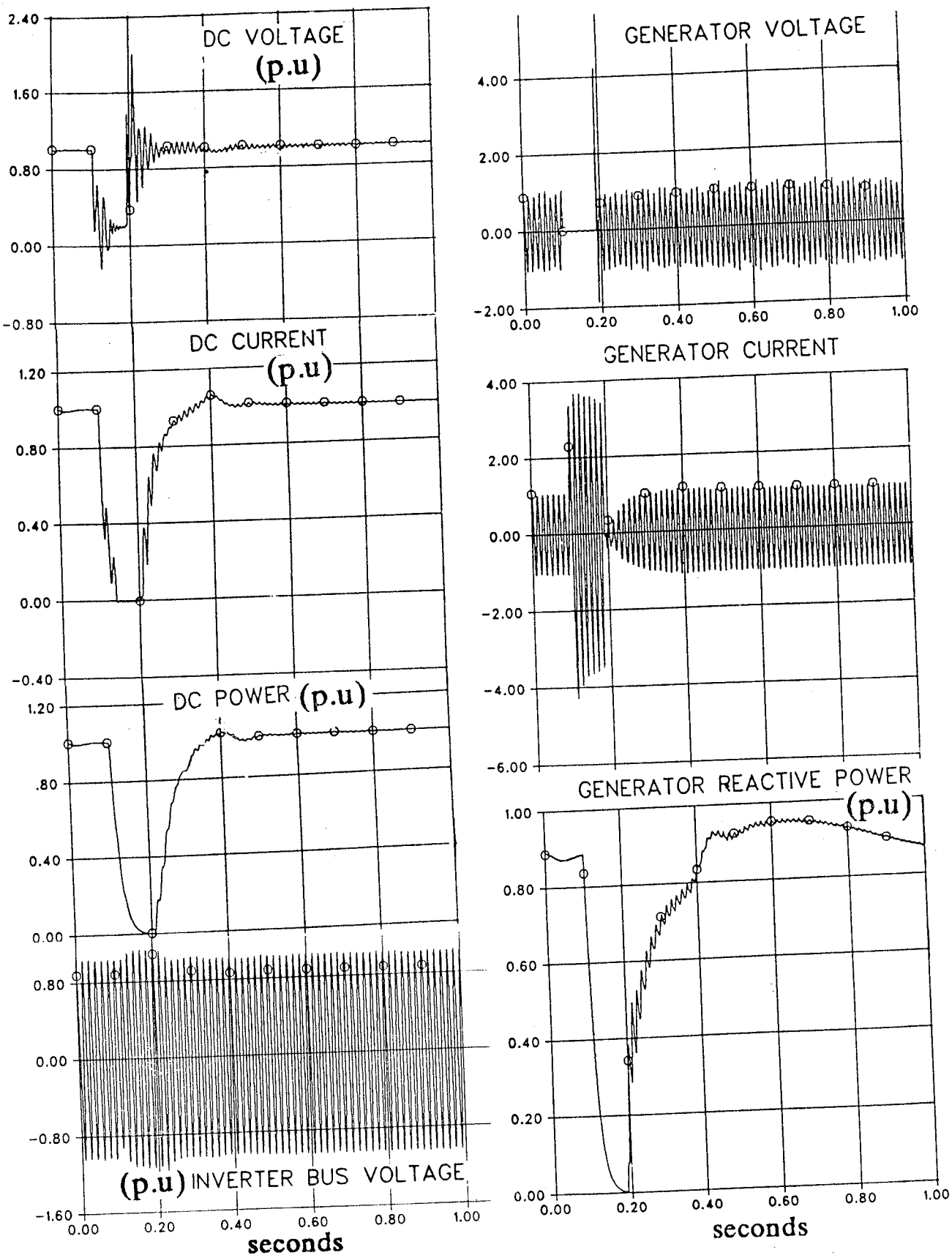

Fig. 5.7b : 3-phase to ground fault at the rectifier (70 Hz operation

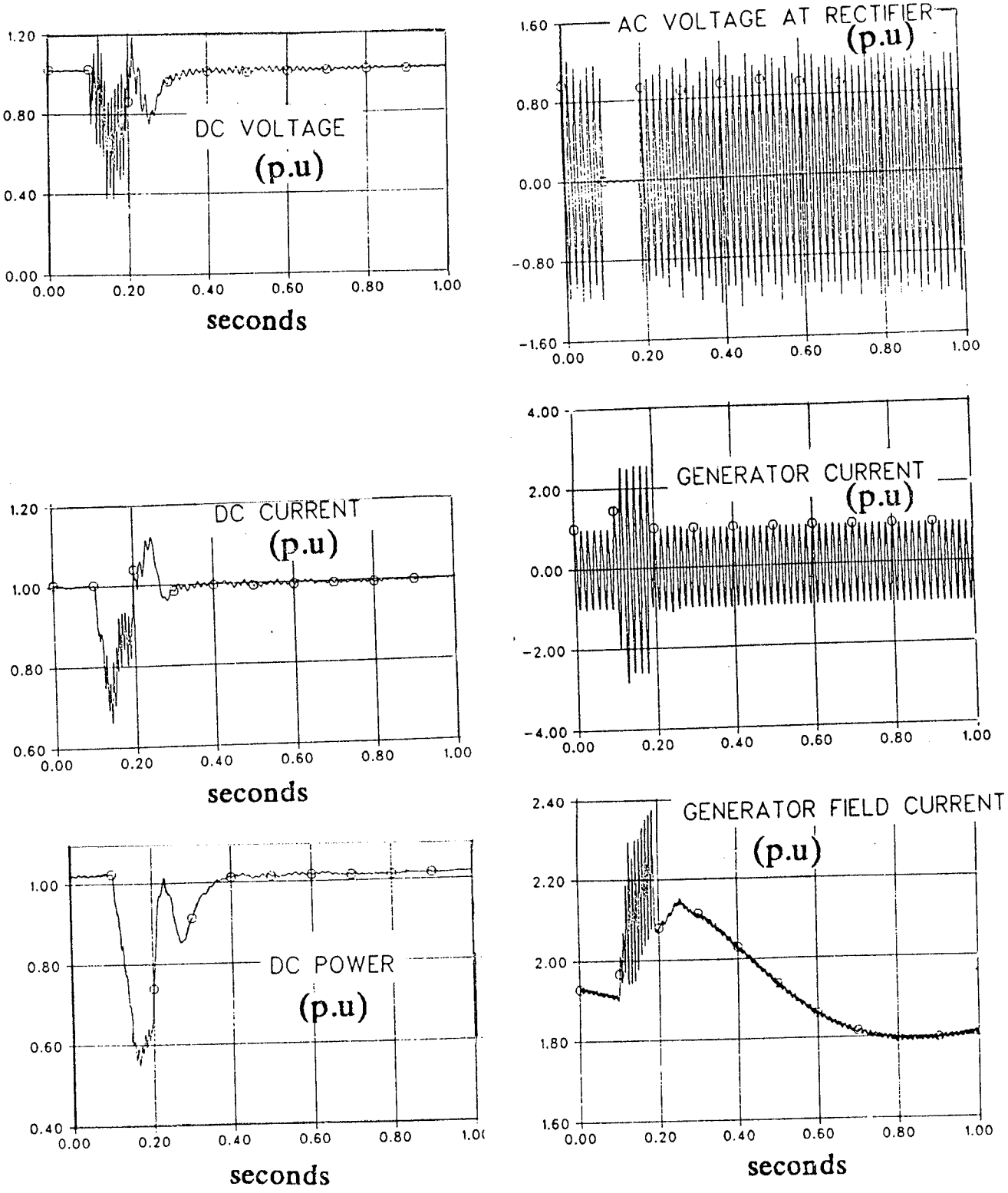

Fig. 5.8a : Single line to ground fault at the rectifier(60 Hz operation

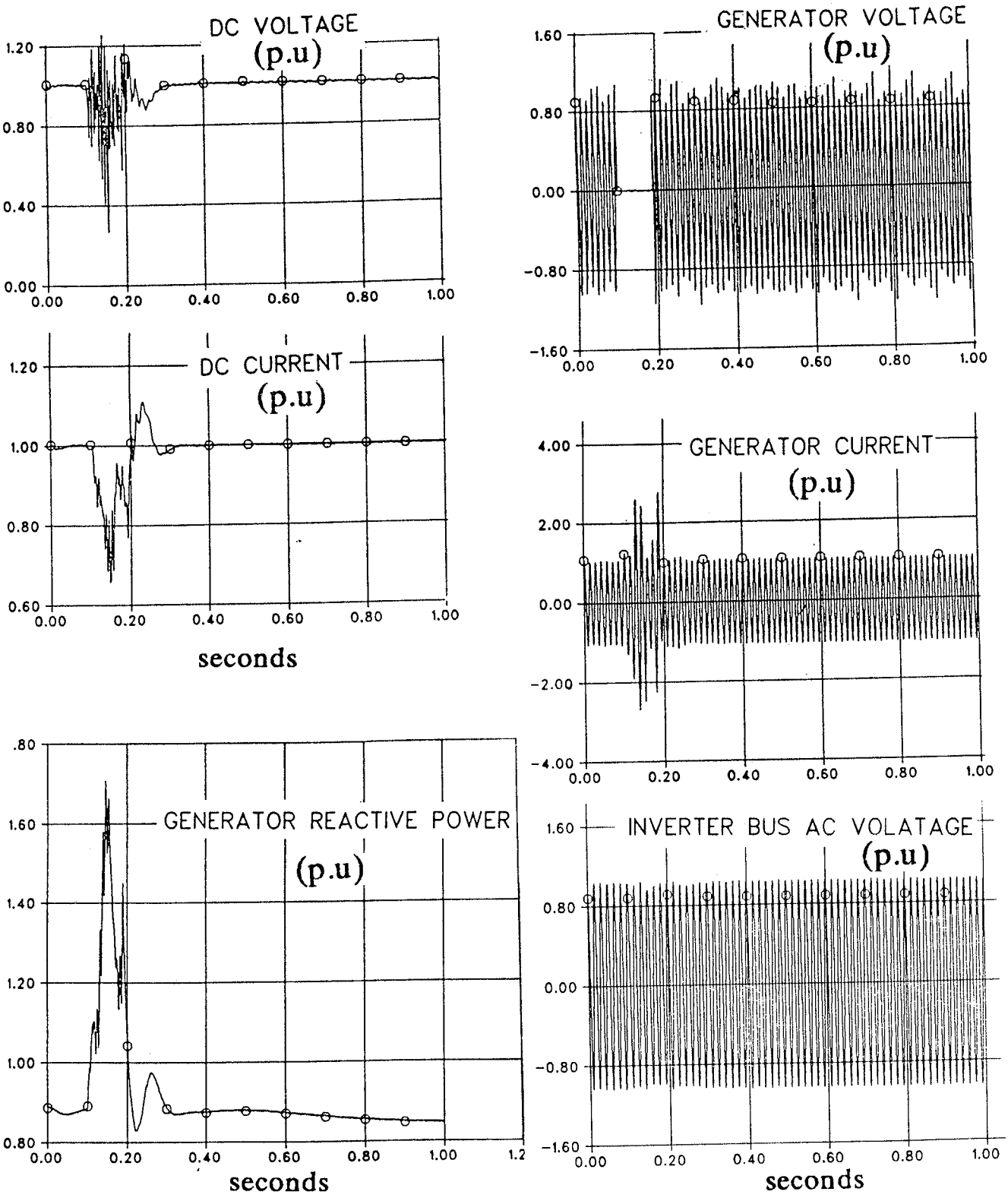

Fig. 5.8b : Single line to ground fault at the rectifier(70 Hz operation

this type of fault is remote and hence the generator breaker can be eliminated. In the event of incipient faults in the generator like interturn faults, core fault etc. the complete unit can be tripped by blocking the converters. The dc power and dc current recovered to 1.0 p.u in 415 ms and 259 ms for 60 Hz and 70 Hz respectively. The dc voltage spikes of 1.58 p.u and 2.0 pu have been observed immediately after clearing the fault for 60 Hz and 70 Hz operation. The dc voltage settled down in both cases to 1.0 p.u in 300 ms.

(4) : Single line to ground fault at the rectifier end :

The simulation results for the above fault for 5 periods are shown in Figs. (5.8a) and (5.8b) for 60 Hz and 70 Hz operation respectively. The maximum generator current of 2.82 p.u and 2.7 p.u is observed in the faulted phase for 60 Hz and 70 Hz operations, respectively. The dc current and the dc voltage recovered to 1.0 pu in 200 ms and 150 ms after clearing the fault for the above respective cases. But the peak dc voltages of 1.3 p.u and 1.21 p.u are observed immedietely after clearing the fault for the 60 Hz and 70 Hz operation.

5.5.4 Discussions

It can be observed from the simulation results that the dc power recovery is faster in the case of 70 Hz operation (300 ms) as compared to 60 Hz operation (400 ms). This is due to a decrease in short circuit ratio at the rectifier terminal at 70 Hz operation as compared to 60 Hz operation. Since high frequency operation increases the system impedance thereby reducing the short circuit ratio. Whereas the voltage stresses are more and the current stresses are less in the case of 70 Hz operation as compared to 60 Hz operation. In the event of permanent dc block (full load throw off

), the maximum voltage rise of 1.2 p.u is observed in the case of 70 Hz operation and 1.143 p.u in the case of 60 Hz operation for unit connection scheme. The overvoltages are higher in the case of 70 Hz operation because in order to meet a higher level of reactive power consumption of the converter, the generator is relatively over excited. In the case of conventional schemes where ac filters exists on ac converter bus, in the event of a load through off a danger of self excitation may occur. It can be observed that the pulsations in the air gap torque due to harmonic currents are not significant as compared to the average torque.

Type of the fault (60 Hz / 70 Hz) operation	Generator voltage V_a p.u max)	Generator current I_a p.u (max)	Field current I_f p.u (max)	DC current I_{dc} p.u (max)	DC voltage V_{dc} p.u (max)
DC Line fault at the rectifier (12 cycles)	1.25 / 1.30	1.27 / 1.27	2.2 / 2.42	1.08 / 1.18	2.67 / 2.9
Three phase to ground fault at the rectifier (5 cycles)	3.72 / 4.1	4.0 / 3.63	3.0 / 3.2	-	1.58 / 2.0
SLG fault at the rectifier (5cycles)	1.0 / 1.1	2.81 / 2.7	2.38 / 2.7	1.1 / 1.1	1.3 / 1.21
Permanent dc block	1.143 / 1.2	-	2.0 / 2.1	-	-

Table 5.5 : System parameters under fault conditions for 60 Hz/70 Hz operation.

5.6 Unit connection schemes with diode bridge rectifiers

5.6.1 Introduction

If the diode bridge converters are chosen instead of thyristor converters at the sending end terminal for unit connection scheme, the cost of the sending end terminal can be reduced. The advantages of the diode rectifier schemes are as follows.

(1) Diodes are cheaper as compared to thyristors for a given rating.

(2) Non existence of grid control circuitry at the sending end may result in further savings.

(3) Fast telecommunication link between sending and receiving ends can be eliminated.

(4) Increased reliability and easier maintenance.

(5) Reduction in the operating cost.

(6) Harmonic currents flowing into the generator are minimum.

However, the diode rectifiers schemes have the following disadvantages.

(1) Requirement of dc or ac circuit breakers to protect the system under dc line faults due to the absence of grid control action for diodes.

(2) Diode bridges are to be rated to withstand fault currents for at least 5 cycles which is the time required to open the ac circuit breaker.

(3) Since the inverter under constant current control mode operates at large firing angles, the reactive power consumption by the inverter is greater and hence more voltage stresses on converter valves. This may lead to an increase in the ratings of valves on the inverter side.

In view of the above mentioned pros and cons of the diode rectifier unit connection scheme, a detailed study may be required in order to asses whether in overall terms the above scheme is cost effective as compared to the thyristor rectifiers scheme.

A small signal model of the generator with diode rectifier bridges is developed to derive a transfer function between dc voltage and the generator field voltage in order to control dc voltage through generator field cxcitation. A controller is designed with proper compensation in order to obtain the optimum response through root locus technique as shown in Appendix V. A 500 MW, 250 kV diode rectifier scheme is simulated in time domain using the EMTDC program to study the recovery of the system for dc line faults and evaluate the possible stress on the converter valves and the generator.

5.7 Digital simulation of diode rectifier unit connection scheme

The simulation set up shown in Fig. (5.20) represents one pole of 500 MW capacity at 250 kV. Five generators of 120 MVA are represented by a single generator of 5X120 MVA capacity and connected to a 12-pulse diode bridge converter through Y-Y and Y-Δ transformers. Due to the absence of control action of diode rectifiers, the system must be protected against the dc line fault by means of a dc circuit breaker in the dc line or a generator ac circuit breaker. In this simulation generator ac circuit breaker is used to protect the system for dc line faults. The recovery of the system for the dc line fault is studied by simulating the above system in time domain using the EMTDC program. Generator excitation control is used to control the dc voltage at the rectifier end and constant current control is used on the inverter side. The exciter ceiling voltage is limited to ± 5.0 p.u.

5.7.1 System startup:

Before starting the system, the inverter is blocked and by passed and the generator circuit breaker is open. The generator is brought to the steady state condition with its rated terminal voltage in shorter time in the simulation by inputing proper initial conditions. At t=0.1 s the generator breaker is closed at the same time the inverter is forced into rectifier mode by setting the firing angle to 57° to build up the dc current in the line. At t= 0.15 s, the inverter is brought in to inversion mode by setting α to 110°. The system reached steady state condition in 0.4 s as shown in Fig. (5.20).

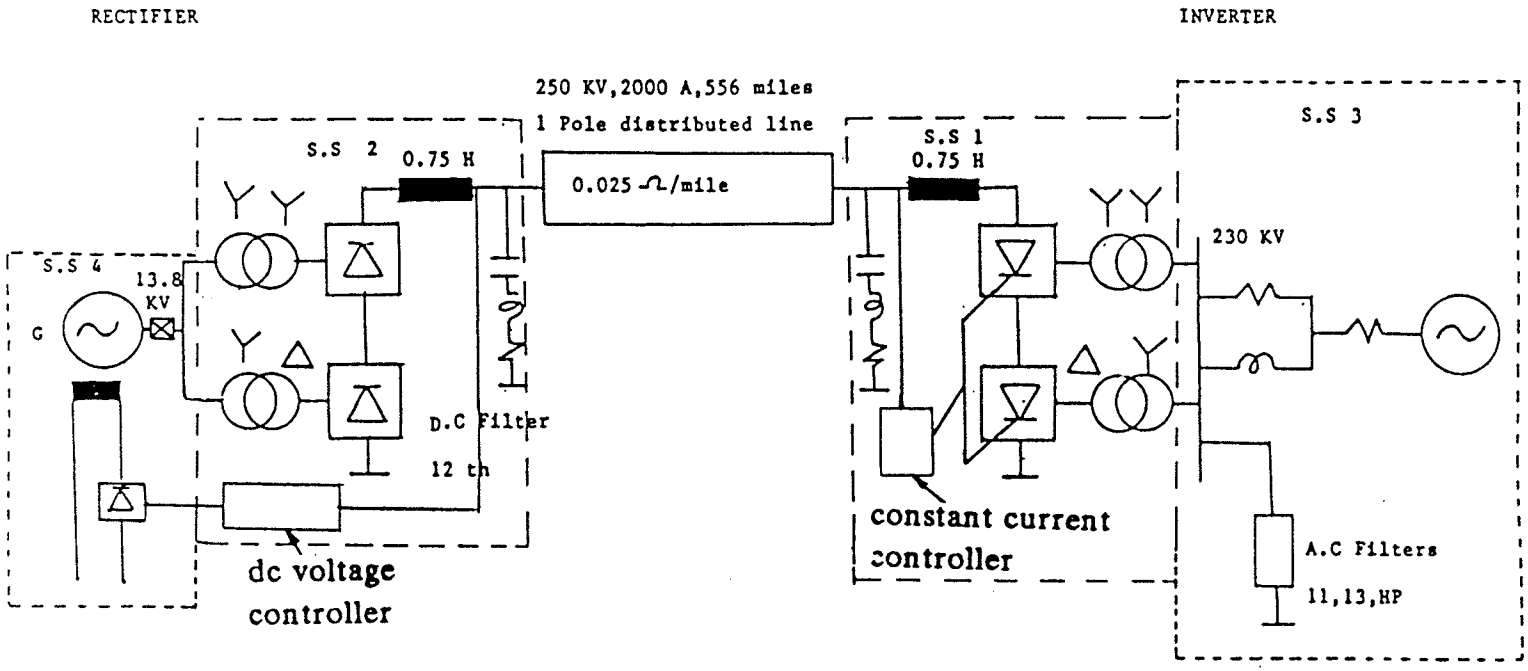

Fig. 5.19 : Simulation setup with diode bridge rectifiers for unit connection scheme.

5.7.2 Simulation results:

When the system is under steady state, at t=0.2 s, the dc line fault at the rectifier terminal is created. After 5 cycles delay which is normally the total opening time of the ac circuit breaker, the generator breaker is opened and the field voltage is forced to - 5.0 p.u and the inverter is blocked and by passed. The rectifier is also by passed so that the stored energy in the dc line decays rapidly which depends upon the time constant of the dc line. The current in the dc line reduced to zero in 0.8 s after the inception of the fault. At t=1.0 s, the generator breaker is closed and at the same time the the rectifier and inverter bypass switches are opened. The inverter is forced into rectifier mode by setting $\alpha = 57^{o}$ for 0.05 s and then into inversion mode by setting $\alpha = 110^{o}$. The dc current is ramped at 9 p.u/s. The dc power recovered to 1.0 p.u in 2.2 s after the instant of restarting. The peak dc voltage of 1.37 p.u has been observed immediately after restaring at the rectifier terminal and 1.24 p.u at the inverter side. The generator current reached to 2.05 p.u immedietely after the fault. The diodes have to withstand this current stress at least for 5 cycles. The total recovery time to restore the system after the occurence of the dc line fault is 3.0 s. This long time is due to large generator field time constant. The simulation results for dc current, dc voltage, dc power, field current and reactive power are shown in Fig. (5.22a). The other parameters like generator current, generator voltage, field voltage and generator electric torque are shown in Fig. (5.22b). The system recovered without any oscillations, in 3.0 s. This is a very long time as compared to the thyristor converter schemes in which case the recovery time is 200 ms for the same fault.

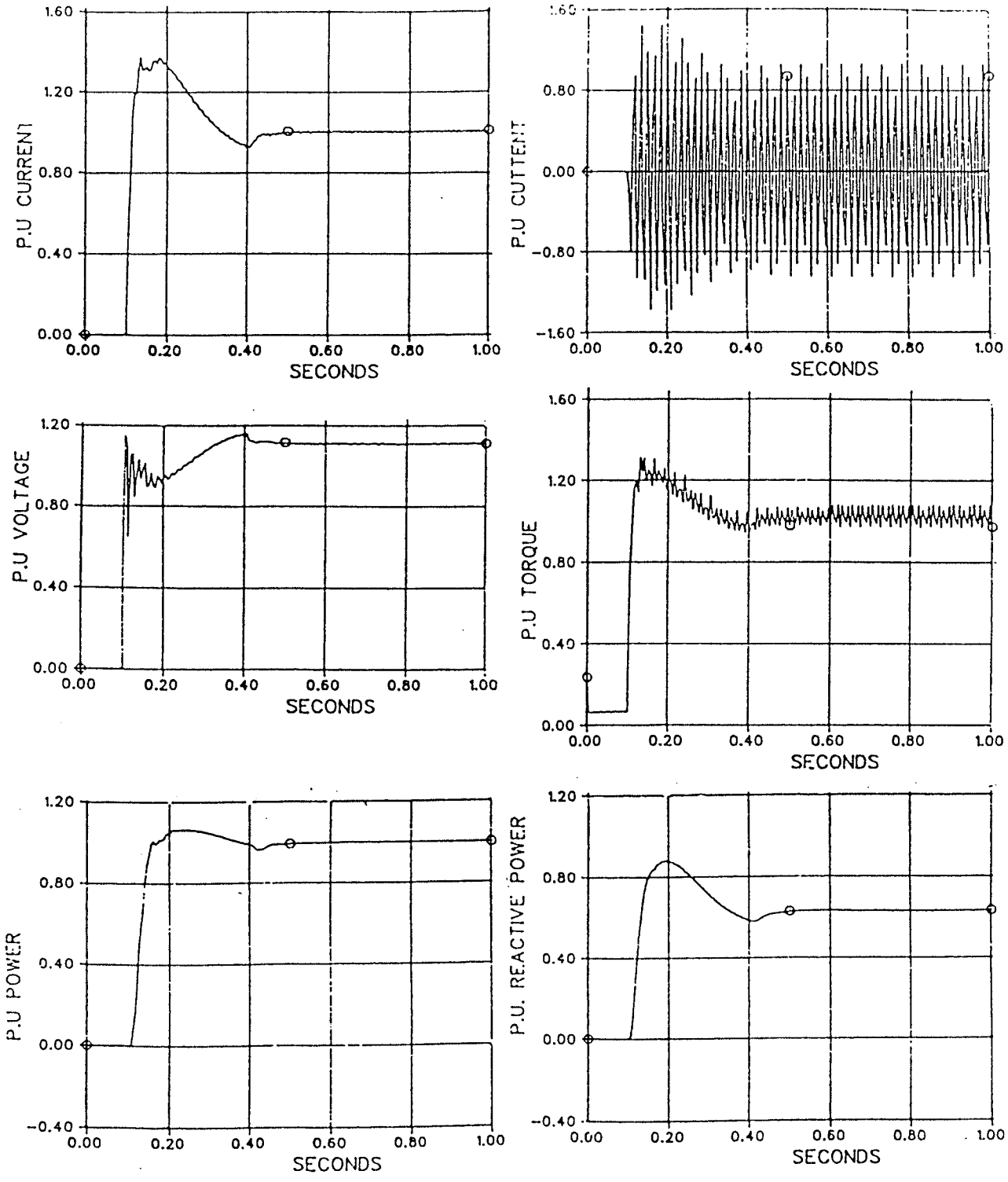

Fig. 5.20 : Steady state performance of the diode bridge rectifier unit connection scheme.

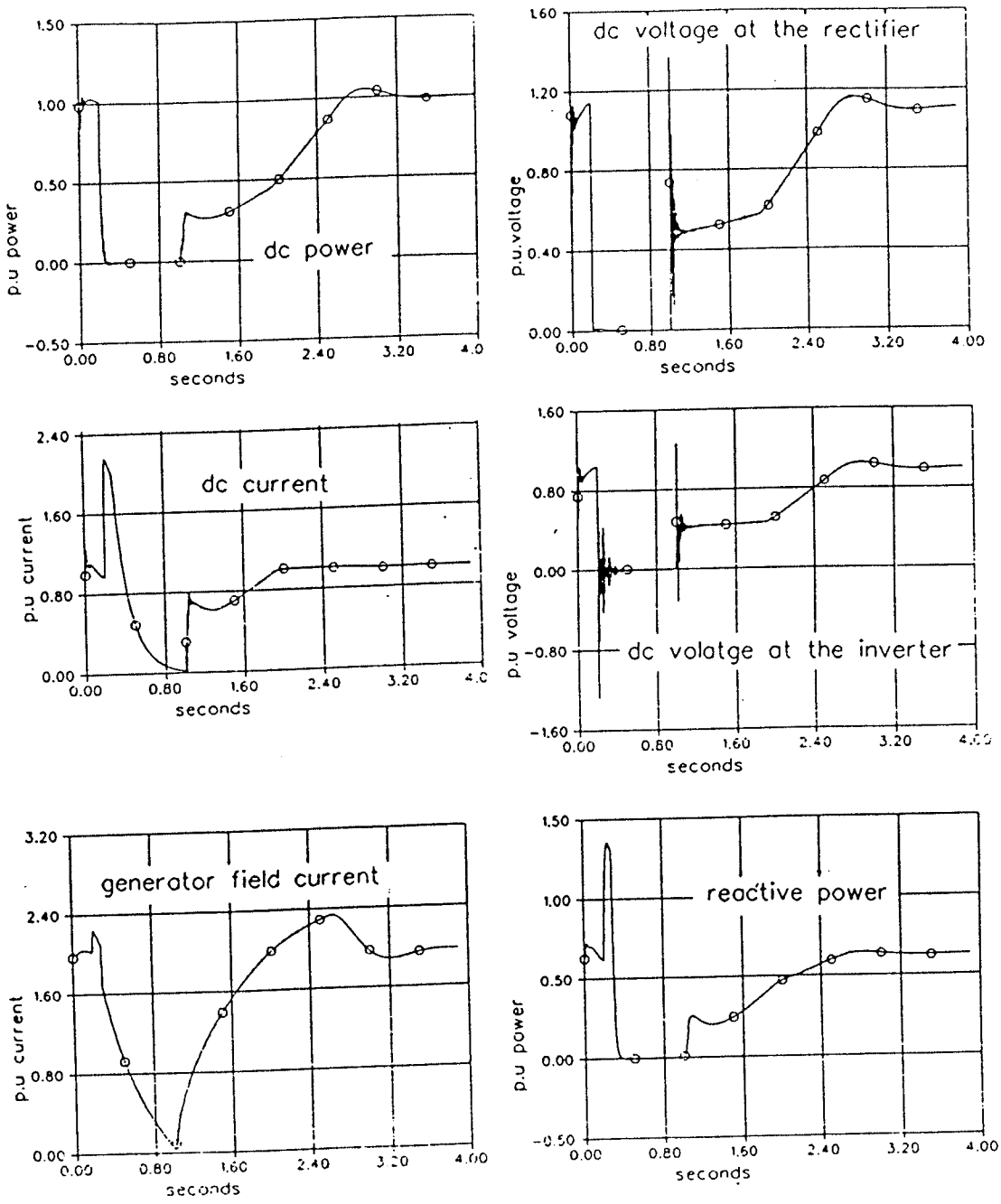

Fig. 5.21a : Performance of the diode rectifier unit connection scheme for dc line fault.

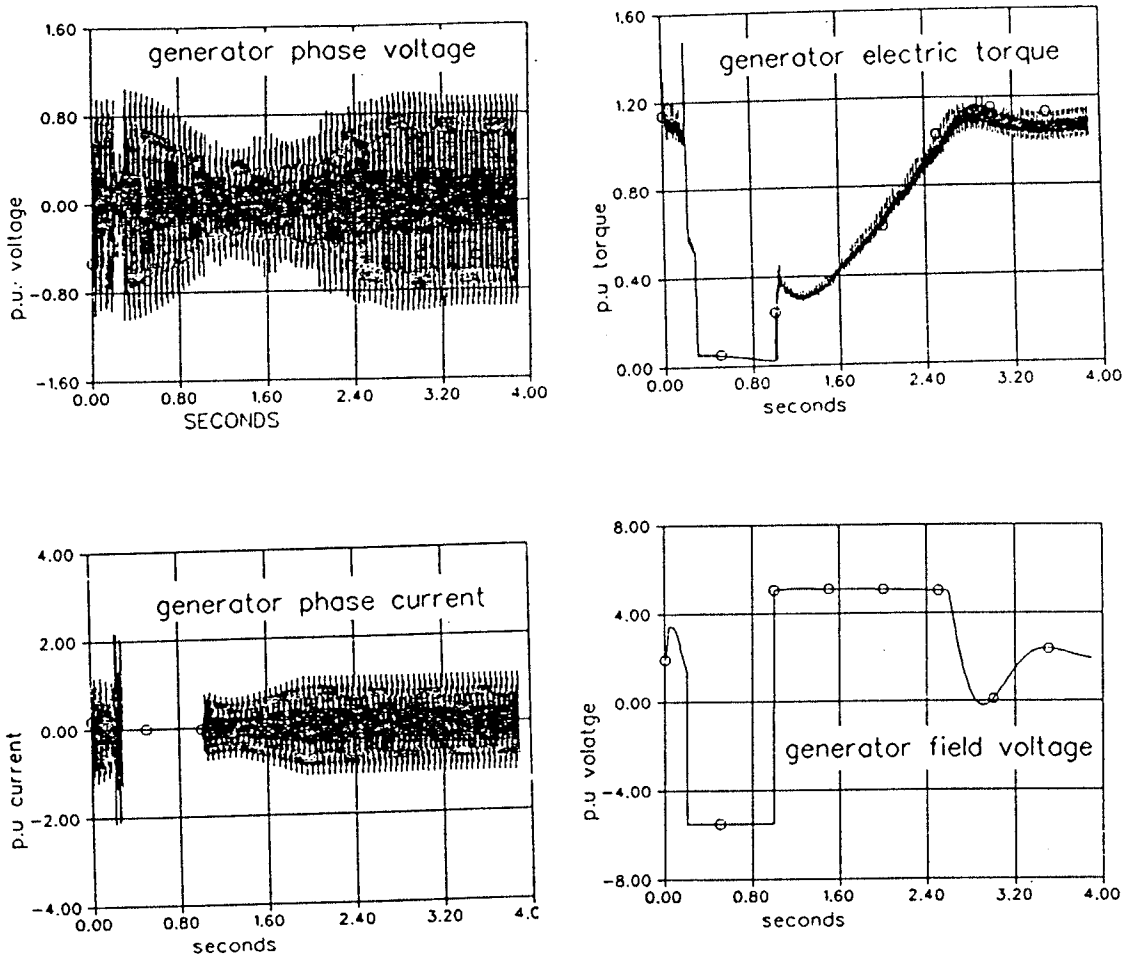

Fig. 5.21b : **Performance** of the diode bridge rectifier unit connection **scheme for** dc line fault.

5.7.3 Conclusions

Diode rectifier unit connection schemes have economic advantages as compared to thyristor schemes. Eventhough the sytem recovered smoothly after clearing the dc line fault, the long recovery time may not be acceptable from the system point of view. Detailed engineering evaluation will therefore be required to implement such scheme.

CHAPTER VI

ECONOMIC EVALUATION OF UNIT CONNECTION SCHEMES

6.1 Introduction

The crux of this investigation is to ascertain the possibility of unit connection schemes as viable alternatives to that of conventional current collector schemes. The technical analysis of unit connection schemes have been covered in the previous chapters. It is therefore necessary at this juncture to carry out the cost analysis of both schemes for relative comparison. In this chapter, a typical 10X100 MW hydro power station and a 1000 MW nuclear power station with single generator are analyzed for economic evaluation for both conventional current collector schemes and unit connection schemes with the available cost figures of the connected equipment from Manitoba Hydro and some manufacturers. This analysis gives approximate cost of the terminal stations for relative comparison of the two types of schemes. In order to evaluate the accurate cost of the station, the most recent cost of the equipment from the manufactures is required.

6.2 A 10X100 MW hydro power station with conventional current collector scheme

The single line diagram of a typical 10X100 MW hydro power station with conventional current collector scheme with bipolar arrangement is

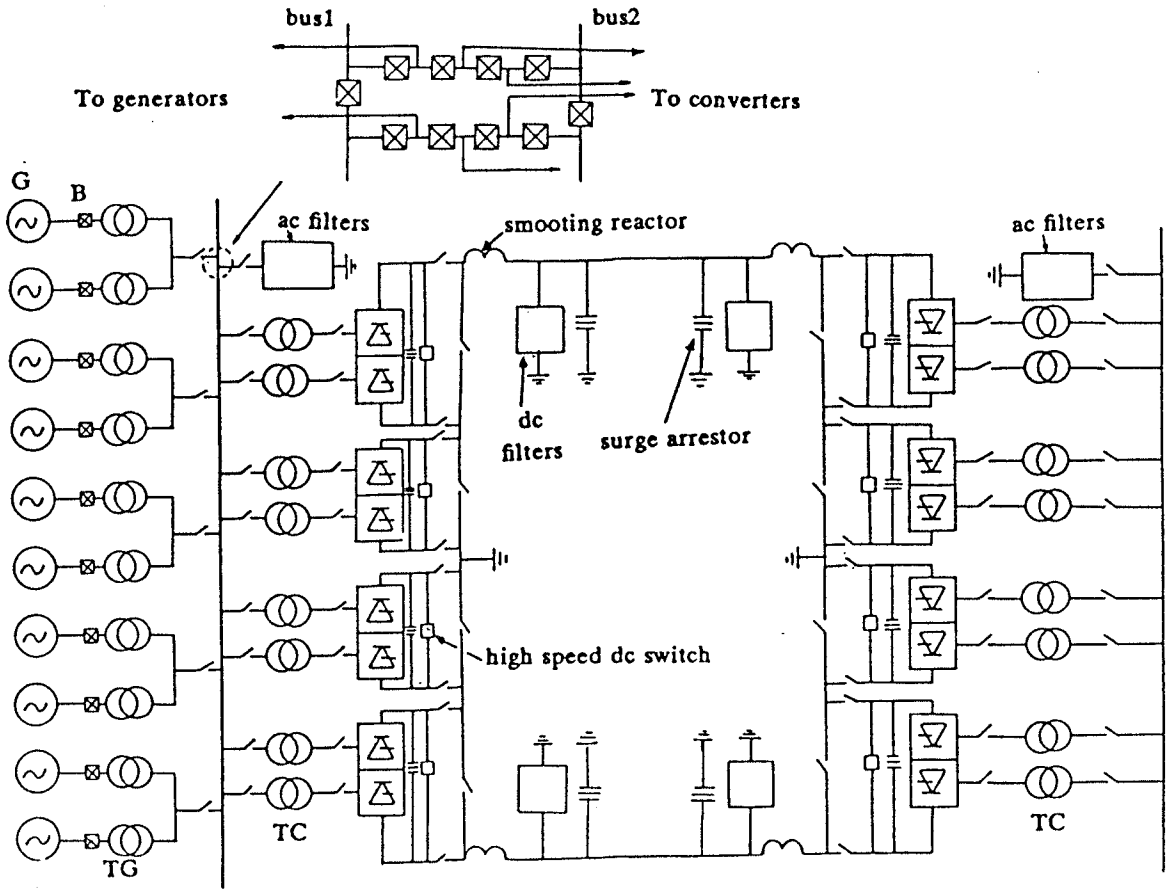

Fig. 6.1 : Single line diagram of a 10X100 MW hydro power station with conventional current collector scheme.

shown in Fig. (6.1). As seen from this figure, each generator equipped with the generator breaker and generator transformer is connected to the converter ac bus through short transmission line. The ac switch yard consists of a double bus structure with four breakers per bay serving three elements in a breaker-and-a-third scheme. This arrangement is selected for reliable operation. Tuned ac filters of 11th, 13th and high pass are connected to the ac bus. Two sets of these filters are usually connected to the bus for reliable operation in the event of failure of one set. The sending station consists of four 250 MW, 250 kV, 12-pulse converters with two bridges connected in series per pole to obtain 500 kV dc voltage. Two coverter transformers each with 150 MVA capacity with Y-Y and Y-Δ configuration are connected to each 12-pulse converter. Each 12-pulse bridge is provided with high speed by-pass switch and a surge arrestor. The dc switch yard consist of dc reactors one on each pole with 12 th and high pass filters. The dc switches and surge arrestors at different positions are not fully shown in the single line diagram. The receiving end station consists of four 12-pulse bridges with two winding transformers and ac tuned filters similar to the sending end.

The cost break down of the terminal equipment in Canadian dollars per kW based on the available data from the Manitoba Hydro is shown in Table 6.1.

6.2.1 Economic evaluation of a 10X100 MW conventional current collector scheme

Based on the available cost figures of the terminal station from Manitoba Hydro, a 10X100 MW hydro power station is analyzed for economic evaluation. The Limestone generating station on the Nelson River is one of

the typical examples of such scheme.

DC System : ± 500 kV, 1000 MW AC System : 230 kV.		
Item	C$ per kW	Remarks
Generator transformer	10.0	100 MW capacity
Generator Breaker	3.5	1500 MVA breaking capacity at 13.8 kV
230 kV ac switch yard	20.0	Breaker-and-a-third scheme
ac filters	3.5	
Converter transformers	8.4	
Converter Value groups	16.0	12-pulse converters.
Valve controls	6.0	
Valve cooling	2.8	
Converter building	2.0	

Table 6.1 : Cost break down in C$ per kW of HVDC terminal equipment.

The cost break down in Canadian dollars of the sending end station of the conventional current collector scheme shown in Fig. (6.1) is given below.

(1) : 10 - 13.8 kV, 1500 MVA breaking capacity
generator breakers. @ C$ 0.35 x 10^6 = $ 3.5 x 10^6

(2) : 10 - 13.8 kV/138 kV, generator transformers
each 100 MW capacity @ C$ 1.0 x 10^6 = $ 10 x 10^6

(3) : 5 - Breaker- and-a-third circuit breaker
positions for 230 kV, ac switch yard @ $ 4 x 10^6 = $20 x 10^6

(4) : 2 - 200 MVAR filter banks, @ $ 3.5 x 10^6 = $ 7 x 10^6

(5) : 4 - Converter transformers, each 300 MVA
capacity @ $ 2.1 x 10^6 = $ 8.4x10^6

(6) : 4 - 12-pulse converter valve groups
each 250 kV, 250 MW @ $ 4 x 10^6 = $ 16 x 10^6

(7) : Valve controls = $ 6 x 10^6

]8) : Valve cooling = $ 2.8 x 10^6

(9) : Other HV equipment = $ 1.2 x 10^6

(10) : 2 Nos. Smoothing Reactors @ $ 1.6x10^6 = $ 3.2 x 10^6

(11) : DC filters @ $ 0.8 x 10^6 per pole = $ 1.6 x 10^6

(12) : Other dc equipment = $ 1.3 x 10^6

(13) : Electrode station and line = $ 1.2 x 10^6

(14) : Land and sight development = $ 0.8 x 10^6

Sub total 1 = $ 83 x 10^6

(15) : Construction and Labour cost (10% sub total 1) = $ 8.3 x 10^6

Sub total 2 = $ 91.3 x 10^6

(16) : Engineering and Supervision (15% of sub total 2) = $ 13.7 x 10^6

Sub total 3 = $ 105.0 x 10^6

(17) Contingency (10% of sub total 3) = $ 10.5x 10^6

TOTAL COST OF THE SENDING END TERMINAL = $ 115.5 x 10^6

From the above analysis, the cost of the sending end terminal of a 10X100 MW hydro power station for conventional current collector scheme is C$ 115.5 x 10^6 which amounts to C$ 115.5.0 per kW. These cost figures are based on the approximate available data. But, the exact cost analysis can be performed after obtaining the equipment cost from the manufacturers for a given scheme.

6.2.2 Economic evaluation of a 10X100 MW unit connection scheme

In the case of the unit connection scheme, generator breakers, generator transformers, ac filters and ac switch yard can be eliminated thereby the cost of the sending end terminal can be minimized. The single line diagram of the 10X100 MW unit connected hydro power station is shown in Fig. (6.2). The approximate cost of the sending end station of the above scheme is given herewith.

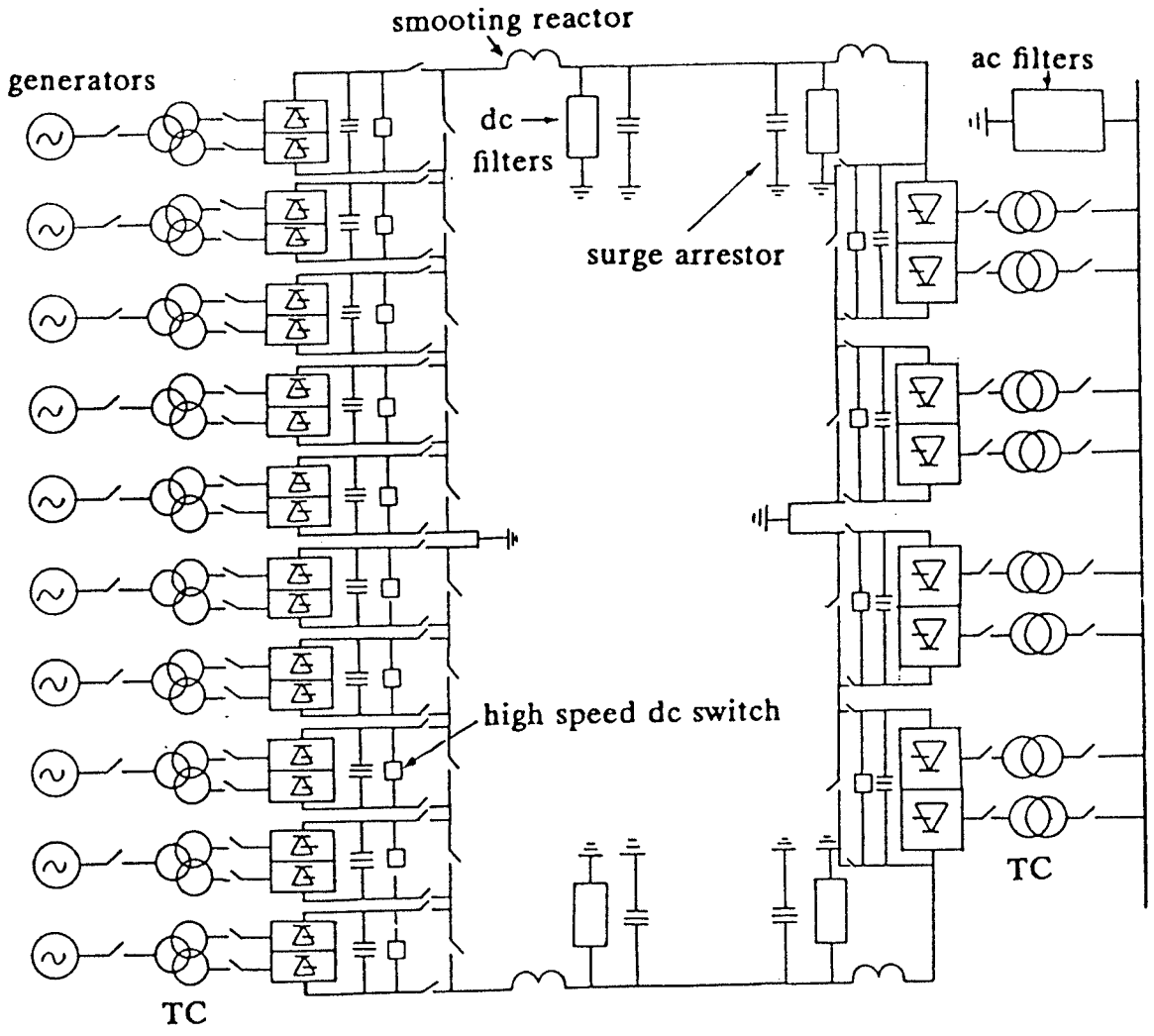

Fig. 6.2 : Single line diagram of a 10X100 MW hydro power station with unit connection scheme.

(1) : 10 - Converter transformers, each 120 MVA capacity @ $ 1.1 x 10^6	= $ 11.0 x10^6
(2) : 10 - 12-pulse converter valve groups each 100 kV, 100 MW @ $ 1.6 x 10^6	= $ 16 x 10^6
(3) : Valve controls	= $ 8 x 10^6
(4) : Valve cooling	= $ 3.0 x 10^6
(5) : Other HV equipment	= $ 1.2 x 10^6
(6) : 2 - Smoothing Reactors @ $ 1.6x10^6	= $ 3.2 x 10^6
(7) : DC filters @ $ 0.8 x 10^6 per pole	= $ 1.6 x 10^6
(8) : Other dc equipment	= $ 1.3 x 10^6
(9) : Electrode station and line	= $ 1.2 x 10^6
(10) : Land and sight development	= $ 0.5 x 10^6
Sub total 1	= $ 47.0 x 10^6
(11) : Construction and Labour cost (10% sub total 1)	= $ 4.7 x 10^6
Sub total 2	= $ 51.7 x 10^6
(16) : Engineering and Supervision (15% of sub total 2)	= $ 7.8 x 10^6
Sub total 3	= $ 59.5 x 10^6
(17) : Contingency (10% of sub total 3)	= $ 6.0 x 10^6
TOTAL COST OF THE SENDING END TERMINAL	= $ 65.5 x 10^6

DC System : 500 kV, 2500 MW AC System : 345 kV.		
Item	US $ per kW (1977)	%
Transformers	5.74	23.7
Reactors	1.28	5.3
Valves	7.75	32.0
Auxiliaries	2.0	8.3
Filters	2.0	8.3
Buildings	1.0	4.2
Total Equipment	19.8	81.8
Installation	3.2	13.2
Project design and Management	1.2	5.0
Total Terminal	24.2	100.0

SOURCE : Progress report LA-7116-PR, dc super conducting power transmission line project at Los Almos Scientific Laboratory, January 1978.

Table 6.2 : Cost break down in US $ per Terminal per kW.

If the unit connection scheme is adopted for the above hydro power station, the cost of the sending end terminal station is only C$ 65.5x 10^6. In order to give the feel of the cost figures of the HVDC equipment, the cost break down per terminal of 600 kV, 2500 MW station with 230 kV ac switch yard based on the 1978 prices is shown in Table 6.2. This data differs marginally from the cost data shown in Table 6.1 which is based on 1985 prices, due to the price escalation from 1978 to 1985. Another interst-ing curve which gives the turn-key cost of the HVDC terminal station has been published in 1980 is shown in Fig. (6.5) [40]. As per this curve, the total cost of the terminal station is about US $ 50 per kW (C$ 65 per kW) of the installed capacity. This figure does not include generator breakers, generator transformers and ac switch yard. From the above analysis, the installed capacity of the sending end terminal station without generator breakers and generator transformers is about C$ 76/kW. It may be reasonable figure taking five years inflation into account.

It can be clearly seen from the above cost analysis that a net amount of C$ 50.0 X 10^6 (56.7%) can be saved in the sending end terminal station by adopting unit connection scheme for the above mentioned station instead of conventional current collector scheme. Apart from the savings in minimizing the terminal equipment, further operational savings can be added for the above, since the hydro power station can be operated under variable speed depending upon the available water head and load for maximizing the efficiency of the turbines. It has been shown in Chapter III that based on the annual water head variation and load curves of 10X100 MW Longspruce generating station on the Nelson River, the expected annual gains under this operation is about C$ 2X 10^6. This operation alone can save about C$ 100 x 10^6 for a period of 50 years, if the same period is taken as the expected life of the station.

6.3 Economic evaluation of a 1000 MW nuclear power station

In the case of nuclear power station, the size of the turbine and the generator can be selected to match the converter ratings unlike in the case of hydro power station where the size and the speed of the turbine and the generator depends upon the available water head. One of the possible configurations with two converter bridges per pole is chosen for economic evaluation. The cost figures of some of the equipment for the nuclear power station based on 1983 prices are given below [17].

(1) : Turbogenerator	12-15 US $/kVA (C$ 16-20)
(2) : Steam turbines	20-15 US $/kVA (C$ 25-40)
(3) : HVDC short connection	50 US $/kW (C$ 65)
(4) : Fossile fuel plant	800-900 US $/kW (C$ 1050-1175)

6.3.1 Economic evaluation of a 1000 MW point-to-point conventional current collector scheme for nuclear power station

The single line diagram of a 1000 MW nuclear station with current collector scheme for power transmission is shown in Fig. (6.3). The cost break down of the sending end terminal station of a 1000 MW nuclear power station with conventional current collector scheme is given below.

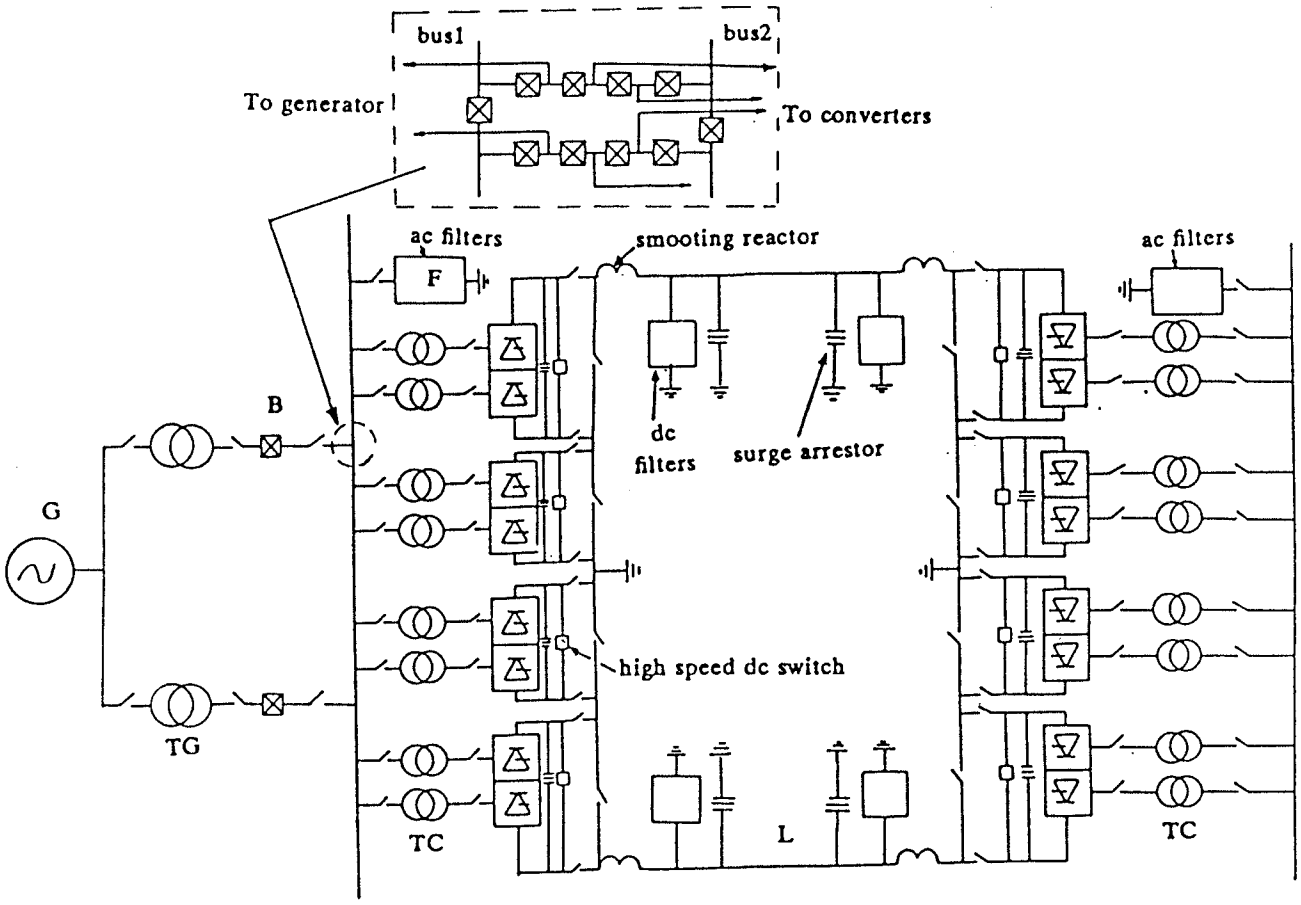

Fig. 6.3 : Single line diagram of a 1000 MW nuclear power station with conventional current collector scheme.

(1) : 2 - 22.0 kV, 500 MW rating generator
circuit breakers. = \$ 3.0 x 10^6

(2) : 2 - 525 MVA, generator transformers = \$ 5.0 x 10^6

(3) : 5 - Breaker- and-a-third circuit breaker
positions for 230 kV, ac switch yard @ \$ 4 x 10^6 = \$20 x 10^6

(4) : 2 - 200 MVAR filter banks, @ \$ 3.5 x 10^6 = \$ 7 x 10^6

(5) : 4 - Converter transformers, each 300 MVA capacity
@ \$ 2.1 x 10^6 = \$ 8.4x10^6

(6) : 4 - 12-pulse converter valve groups
each 250 kV, 250 MW @ \$ 4 x 10^6 = \$ 16 x 10^6

(7) : Valve controls = \$ 6 x 10^6

(8) : Valve cooling = \$ 2.8 x 10^6

(9) : Other HV equipment = \$ 1.2 x 10^6

(10) : 2 - Smoothing Reactors @ \$ 1.6 x10^6 = \$ 3.2 x 10^6

(11) : DC filters @ \$ 0.8 x 10^6 per pole = \$ 1.6 x 10^6

(12) : Other dc equipment = \$ 1.3 x 10^6

(13) : Electrode station and line = \$ 1.2 x 10^6

(14) : Land and sight development = \$ 0.8 x 10^6

Sub total 1 = \$ 83.0 10^6

(15) : Construction and Labour cost (10% sub total 1) = \$ 8.3 x 10^6

Sub total 2 = \$ 91.3 x 10^6

(16) : Engineering and Supervision (15% of sub total 2) = \$ 13.7 x 10^6

Sub total 3 = \$ 105.0 x 10^6

(17) Contingency (10% of sub total 3) = \$ 10.5 x 10^6

TOTAL COST OF THE SENDING END TERMINAL = \$ 115.5 x 10^6

From the above cost analysis, the cost of the sending end station for 1000 MW nuclear power station with conventional HVDC scheme is approximately C$ 115.5 x 10^6. be C$ 115.5 per kW.

6.3.2 Economic evaluation of a 1000 MW nuclear power station with unit connection scheme

The single line diagram of the unit connected 1000 MW nuclear power station with single generator is shown in Fig. (6.4). The cost break down of the sending end station in Canadian dollars is as follows:

(1) : 4 - Converter transformers, each 300 MVA capacity
250 kV, @ $ 2.1 x 10^6 = $ 8.4 x 10^6

(2) : 4 - 12-pulse converter valve groups
each 250 kV, 250 MW @ $ 4.0 x 10^6 = $ 16 x 10^6

(3) : Valve controls = $ 6 x 10^6

(4) : Valve cooling = $ 2.8 x 10^6

(5) : Other HV equipment = $ 0.6 x 10^6

(6) : 2 Nos. Smoothing Reactors @ $ 1.6x10^6 = $ 3.2 x 10^6

(7) : DC filters @ $ 0.8 x 10^6 per pole = $ 1.6 x 10^6

(8) : Other dc equipment = $ 1.3 x 10^6

(9) : Electrode station and line = $ 1.2 x 10^6

(10) : Land and sight development	= \$ 0.5 x 10^6
Sub total 1	= \$ 44.4 x 10^6
(11) : Construction and Labour cost (10% sub total 1)	= \$ 4.5 x 10^6
Sub total 2	= \$ 48.9 x 10^6
(16) : Engineering and Supervision (15% of sub total 2)	= \$ 7.3 x 10^6
Sub total 3	= \$ 56.2 x 10^6
(17) Contingency (10% of sub total 3)	= \$ 5.6 x 10^6
TOTAL COST OF THE SENDING END TERMINAL	= \$ 61.8 x 10^6

Therefore, the total cost of the sending terminal station of 1000 MW nuclear station with unit connection scheme is about \$ 62.0 x 10^6. The expected savings in adopting the unit connection scheme instead of the conventional current collector scheme is \$ 53.5 x 10^6.

If the higher base speed of the turbine is selected, further savings can be expected in the capital cost of the turbine and the generator.

6.4 Economic evaluation of a 1000 MW nuclear power station with back-to-back schemes

If the system stability is the main criteria, then back-to-back asynchronous dc link can be adopted. In this section the cost of the following schemes are evaluated.

(1) A 1000 MW conventional generating station with turbine, generator and step up transformer connected to a ac bus.

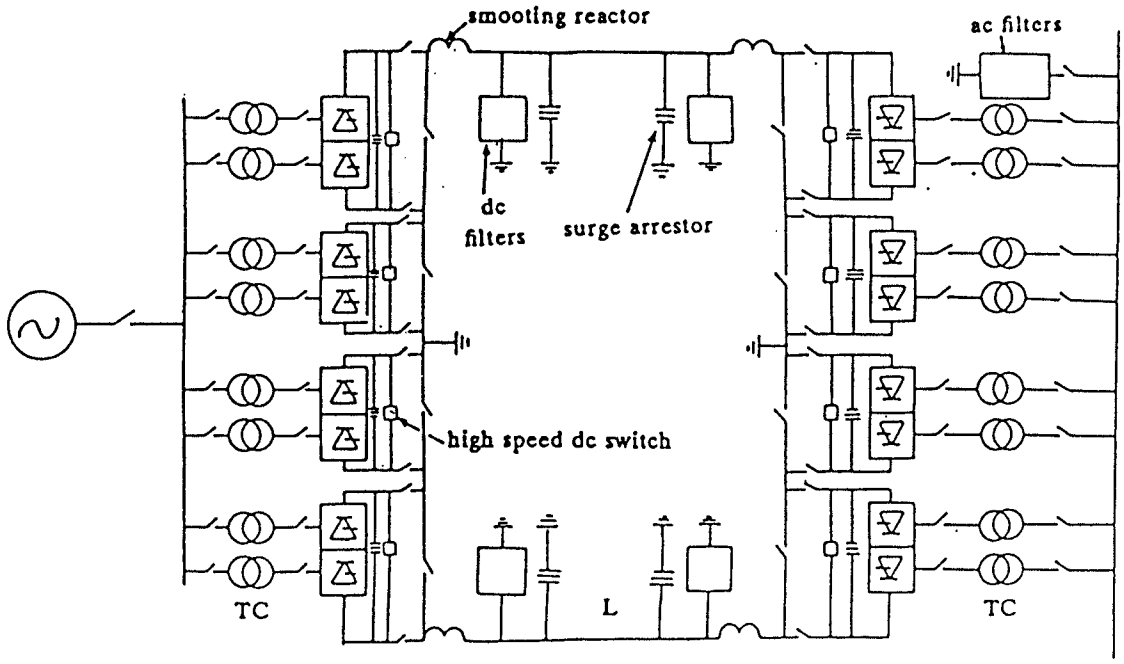

Fig. 6.4 : Single line diagram of a 1000 MW nuclear power station with unit connection scheme.

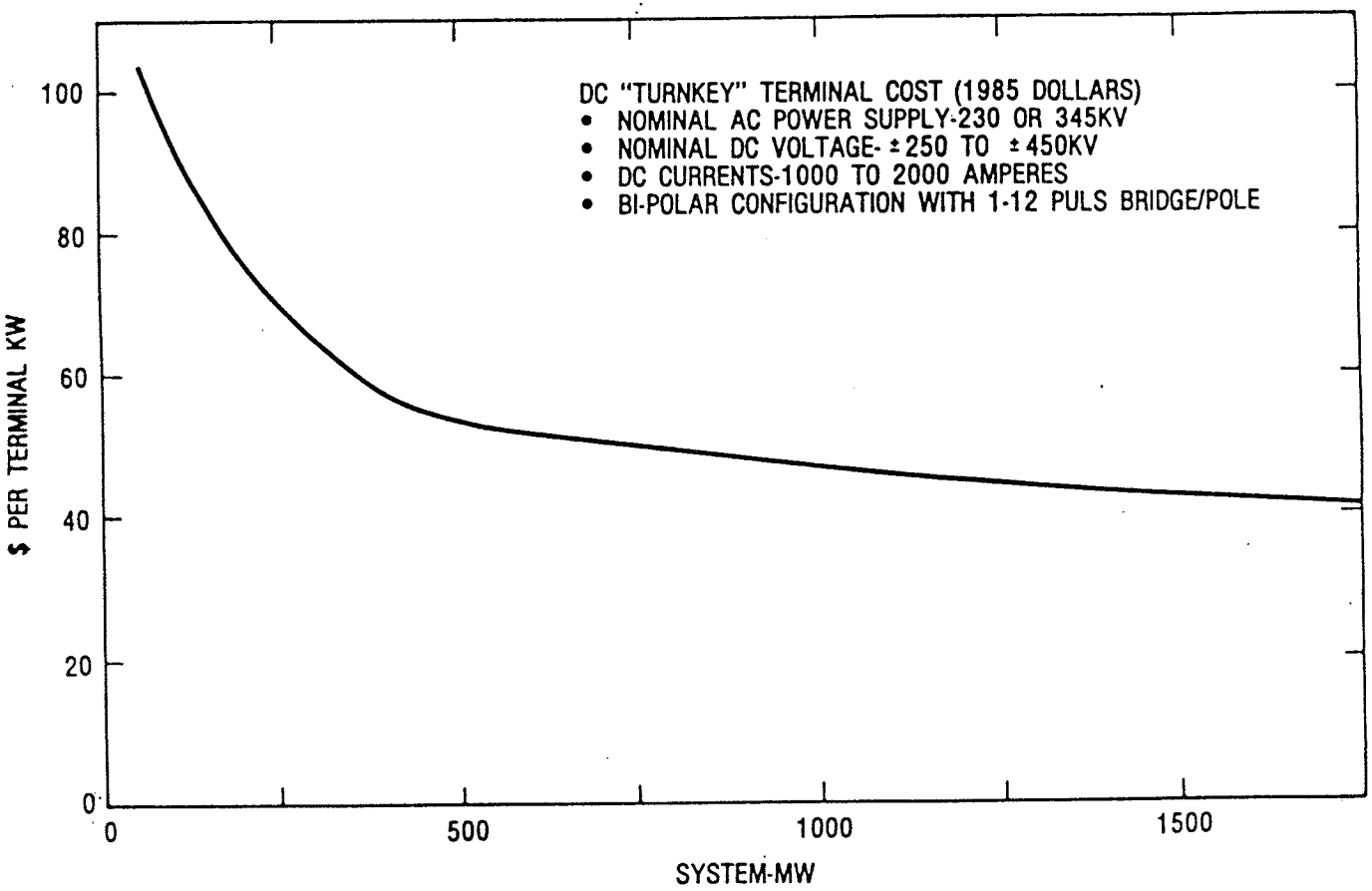

Fig. 6.5 : PRICE/TERMINAL/KW VS DC TERMINAL SIZE

(2) A 1000 MW conventional HVDC back-to-back scheme.

(3) A 1000 MW unit connected back-to-back scheme.

6.4.1 Economic evaluation of a 1000 MW conventional nuclear power station

A single line diagram of 1000 MW generating station with a turbine and a generator connected to the ac bus through step up transformer is shown in Fig. (6.6). Out of the total cost of the system, the cost of the turbine is about 50%, the cost of the generator is about 30% , the transformer cost is 10% and the circuit breaker cost is around 6% . The remaining 4% is for supervision and control. The cost break down of the above station is as follows in US dollars.

(1) : 1000 MW Turbine cost, @ US $ 25/ kW = $ 25 x 10^6 (C$ 33 x 10^6)
(2) : 1000 MW Turbogenerator, @ US $ 15/ kW = $ 15 x 10^6 (C$ 20 x 10^6)
(3) : 1000 MW Transformer, @ US $ 5/ kW = $ 5 x 10^6 (C$ 6.5 x 10^6)
(4) : 6000 MVA, 22 kV Breaker, @ US $ 2/ kW = $ 2 x 10^6 (C$ 2.5 x 10^6)

The total cost of the station is US $ 47 x 10^6, which amounts to US $ 47/kW (C$ 61 /kW).

6.4.2 Economic evaluation of a 1000 MW nuclear station with conventional back-to-back scheme

The single line diagram of this scheme is shown in Fig. (6.7). The cost of this scheme in US dollars is as follows.

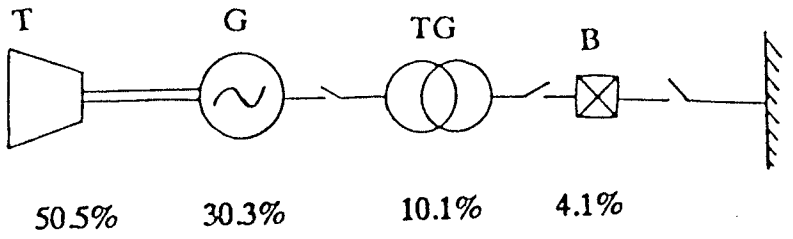

Fig. 6.6 : 1000 MW conventional nuclear generating station with a three phase generator.

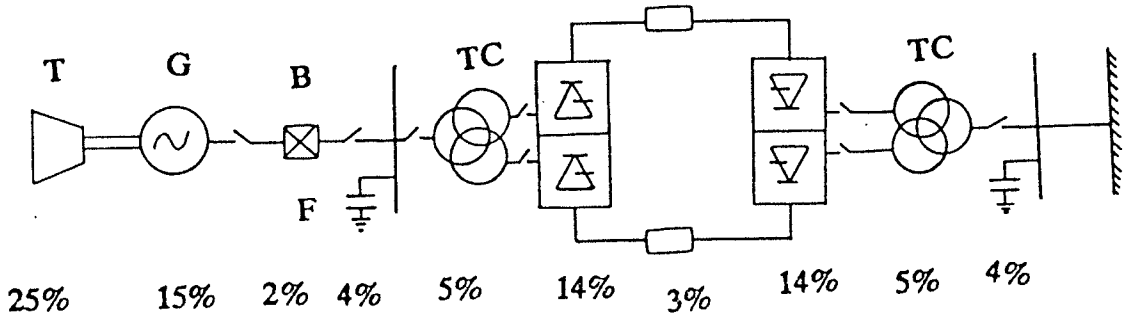

Fig. 6.7 : 1000 MW conventional HVDC back-to-back scheme for nuclear power station.

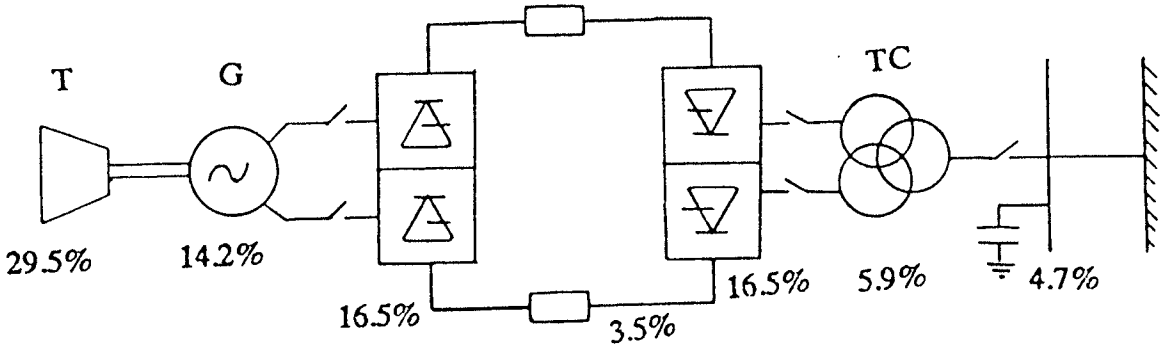

Fig. 6.8 : 1000 MW unit connected back-to back scheme with a six phase generator for nuclear power station.

(1) : 1000 MW turbine = US $ 25 x 10^6

(2) : 1000 MW turbogenerator = $ 15 x 10^6

(3) : Generator breaker position = $ 2 x 10^6

(4) : 1000 MW converter transformer = $ 5 x 10^6

(5) : AC filters and compensators = $ 4 x 10^6

(6) : Rectifier Valves and cooling = $ 14 x 10^6

(7) : DC choke = $ 3 x 10^6

(8) : Inverter Valves and cooling = $ 14 x 10^6

(9) : Receiving end converter
transformers+ Filters+ compensators = $ 9 x 10^6

(10): Supervisory control and
structural equipment = $ 9 x 10^6

TOTAL COST = $ 100 x 10^6

The total cost of the 1000 MW nuclear power station the sending and the receiving end terminals for the conventional HVDC back-to-back scheme is US $ 100 x 10^6 (C$ 130 x 10^6).

6.4.3 Economic evaluation of a 1000 MW unit connected nuclear power station with back-to-back scheme

The single line diagram of the unit connected back-to-back scheme for the 1000 MW nuclear station with six phase generator is shown in Fig. (6.8). The cost break down of the complete station in US dollars is as follows.

(1) : 1000 MW turbine = US $ 25 x 10^6

(2) : 1000 MW six phase generator = $ 12 x 10^6

(3) : Rectifier Valves and cooling = $ 14 x 10^6

(4) : DC choke = $ 3 x 10^6

(5) : Inverter Valves and cooling = $ 14 x 10^6

(6) : Receiving end converter transformers+ Filters+ compensators = $ 9 x 10^6

(7) : Supervisory control and structural equipment (10%) = $ 9 x 10^6

TOTAL COST = $ 84.7 x 10^6

The total cost of this scheme is about US $ 85 x 10^6 which amounts to US $ 85/kW (C$ 110/kW). In this analysis the cost of the six phase generator is taken approximately as the cost of the conventional three phase generator less the cost of the transformer. It has been reported in the CIGRE paper in 1968 by Robert. P et al. that the cost of the 1200 MW six phase generator with a three winding transformer is cheaper than that of a conventional three phase generator of the same rating [18] . Based on this, the six phase generator cost is taken as US $ 12 x 10^6 which is the cost of the three phase generator less the converter transformer. Additional one million dollars are added to its cost due the requirement of more insulation for the stator windings. By adopting unit connection scheme for the above station, about US $ 15 x 10^6 (C$ 20 x 10^6) can be saved as compared to the conventional back-to-back scheme. In the case of point-to-point scheme, the expected savings may be around US $ 10 x 10^6 (C$ 13 x 10^6).

6.4.4 Discussions

With normal ac generating scheme, the 1000 MW generating station cost is about C$ 61 x 10^6, which is 2.1 times cheaper than that of the

conventional HVDC back-to-back scheme and 1.8 times cheaper than unit connected back-to-back scheme. However, if the HVDC scheme is essential for system stability point of view, then unit connected back-to-back HVDC scheme with six phase generator offers about C$ 20 x 10^6 saving as compared to the conventional back-to-back scheme.

6.5 Summary and conclusions

The economic evaluation of conventional HVDC schemes and unit connection schemes has been performed for 1000 MW hydro power station and nuclear power station based on the available cost data. It is found that in the case of 10X100 MW hydro power station the cost of the sending end terminal with conventional current collector scheme is about C$ 115.5 x 10^6, whereas if the unit connection scheme is adopted, the sending end station cost has been reduced to C$ 65.5 x 10^6. There is a remarkable saving of C$ 50 x 10^6 by adopting unit connection scheme. In addition to this saving, annual savings due to increase in turbine efficiency can be added due to variable speed operation of turbines. This feature is only possible in the case of unit connection schemes.

In the case of nuclear power stations the cost of the back-to-back conventional HVDC scheme is around C$ 130 x 10^6. By adopting unit connection scheme with six phase generator the cost of the total scheme is reduced to C$ 110 x 10^6 which amounts to a net saving of C$ 20 x 10^6. However, these HVDC schemes are expensive as compared to the conventional generating station which cost only C$ 61 x 10^6. When stability of the system is a major criteria which warrants the use of HVDC asynchronous link, then unit connection scheme offers economical advantage as compared to the conventional back-to-back scheme.

CHAPTER VII

CONCLUSIONS AND RECOMMENDATIONS

7.1 Major conclusions

The major conclusions resulting from this investigation are as follows:

(1) It has been demonstrated that considerable gains can be obtained by operating hydraulic turbines at variable speeds so as to keep the operating efficiency at the highest attainable values.

(2) Application of multiphase generators for unit connection schemes are studied and found that six phase generators are more suitable as compared to five phase or seven phase generators. It has been shown that the six phase generator has more advantages as compared to the three phase generator for a given rating, if the size of the generator is above 1000 MW. A six phase generator designed for operation at 0.85 pf and a three phase generator designed for 60 Hz operation at 0.87 pf can be operated without derating when feeding 12-pulse rectifier load. If the three phase generator designed at 0.85 pf at 60 Hz is to be operated at 70 Hz, it must be derated to 86.3%. It is also found from the simulation results that the effective commutation reactance of the generator directly connected to the 12-pulse converter can be best represented as the arithmetic mean of the d-axis and q-axis subtransient reactances.

(3) It has been found that a 10X100 MW hydrostation has more operational flexibility as compared to a 8X125 MW station. If the converter bridges on the inverter station are selected with unequal ratings (200 kV, 200 MW + 300 kV, 300 MW), considerable operational flexibility can be achieved without tap settings on the converter transformers at the receiving end.

(4) It has been found from the simulation results that the current stress on the generator for 70 Hz operation is less than that of 60 Hz operation, but the voltages stresses on the valves are more in the former case than in the latter. The system recovered for most of the faults within 200 ms, even though the recovery under 70 Hz operation is little faster than 60 Hz operation due to relatively low short circuit ratio at the sending end for 70 Hz operation.

(5) From the digital simulation results of a 500 MW, 250 kV, unit connected diode bridge rectifier scheme, it has been found that the total recovery time of the system from the dc line fault is 3.0 s, hence may not be acceptable from system view point.

(6) Based on the economic comparison performed for the hydro and nuclear power stations with the available data from the Manitoba Hydro, it is found that if the unit connection scheme is adopted for a 10X100 MW hydrostation instead of conventional current collector scheme, the expected savings is about C$ 50 x 10^6 . In addition to this further gains can be expected due to variable speed operation of the turbines and reduction in maintenance manpower. In the case of nuclear power station for back-to-back scheme, the expected saving in

adopting unit connection scheme is around C$ 20 x 10^6. Whereas in the case of point-to-point scheme the expected savings may be about C$ 13 x 10^6. Further saving in the capital cost of the turbine and generator can be expected if higher base speed operation is selected.

(7) From the above investigation, it is found that unit connection schemes are viable economic alternatives to the conventional current collector schemes if the power is to be transmitted from remote generating stations to the load centre.

7.2 Recommendations for future work

(1) Conduct an estimation of iron losses in the generator when fed with 12-pulse rectifier load using finite element technique in order to find the derating factor of the generator under fixed and variable speed operation.

(2) Study the effect of dc load on the hydraulic turbine characteristics under variable speed operation with variable loads.

(3) Perform economic evaluation of unit connection schemes for thermal power stations.

(4) Study the behavior of turbine generator units for nuclear power stations at higher base speed operation with respect to critical speeds, variable dc loads etc.,

(5) Study to minimize the harmonic currents entering into the generator by injecting proper harmonic currents in the generator field current in order to cancel the harmonics in the air gap mmf.

REFERENCES

1. Kauferle, J. : " Infeed from Power Stations with Generators and Static Converters in Unit Connection", Brown Boveri Review, Vol. 60, No. 5, pp. 205-211, May 1973.

2. Calverly, T.E., Ottaway, C.H. and Tufnell, D.H.A. : " Concept of a Unit Generator Converter Transmission System", International Conference on High Voltage DC and / or Ac Power Transmission", IEE Conf. Publication 107, 19-23, November 1973.

3. Hausler, M. and Kanngiesser, K.W. : " Generator Converter Unit Connection with Thyristor and Diode Rectifiers ", USDOE Conference on " Incorporating HVDC Power Transmission into System Planning ", Phoenix, Arizona, 1980.

4. Kanngiesser, K.W. : " Unit Connection of Generator Converter to be Integrated in HVDC or HVAC Energy Transmission ", International Symposium on HVDC Technology, Rio de Janeiro, Brazil, 1983.

5. Krishnayya, P.C.S. : " Block and Double Block Connections for HVDC Power Station Infeed ", a paper presented at IEEE/PES Winter Meeting, Paper No. C 73 227-6, New York, Feb. 1973.

6. Bajwa, D.S. and Mathur, R.M. : " Re-rating of synchronous generators supplying HVDC converters with special reference to unit-connections ", IEEE- Canadian Conference on Communications and Power, Montreal, 1976.

7. Arrilaga, J., Campos Barros, I.G. and Al-Khashali, H.J. : " Dynamic Modelling of Single generator connected to HVDC converters ", IEEE- PES Summer Meeting, Paper No. F 77 647-1, Mexico City, July 1977.

8. El-Serafi, A.M. amd Sehata, S.A. : " Digital Simulation of a AC/DC System in Direct-Phase quantities ", IEEE Trans., Vol. Pas-95, No. 2, pp. 731-742, March/ April 1976.

9. Bowles, J.P. : " Un Conventional Systems and Control techniques for HVDC Transmission ", a paper presented at the Canadian Electrical Association, Spring Meeting, Toronto, March 1984.

10. Arabi, S. and Tarnawecky, M.J. : " A diode rectifier series tap on a HVDC line ", a paper presented in IEEE-PES Winter Meeting, Paper No. 85 WM 217-5, New York, 1985.

11. Machida, T., Ishikawa, I., Okada, E. and Karasawa, E. : " Control and Protection Systemss for DC Transmission System with diode valve converter ", a paper presented in IEEE International Semiconductor Power Converter Conference, Orlando, Florida, March 1977.

12. Choudary, M.M. and Singh, L.P. : " Operating Point stability analysis of a six phase synchronous machine ", IFAC Conference on Instrumentation and control for Power Plants, Bangolore, India, December 1986.

13. Sheldon, L.H. : " An analysis of the applicability and benefits of variable speed generation for hydro power ", a paper presented in ASME Winter Meeting, New Oleans, Louisiana, December 1984.

14. Chaplygina, E.N. : " Variable speed hydraulic turbines ", Gidrotechnicheskoe Stroitel' Stvo, No. 4, 1969.

15. William P. Creager and Joel D. Justin : " Hydro Electric Hand Book ", John Wily and sons Inc., 1968.

16. Shepherd, D.G. : " Principles of Turbomachinery ", Macmillian Book Company, New York, 1956.

17. Ammanns, C., Richert, K. and Joho, R. : " Coverter fed Synchronous generator system for medium and large power plants ", a paper presented in IEEE / PES, No. 85 WM 104-5, Winter Meeting, New York, Feb. 3-8, 1985.

18. Robert, R., Dispaux, J. and Daur, J. : " Improvement of Turbogenerator Efficiency ", CIGRE, Vol. II, paper No. 124, 1966.

19. Adamson, C. and Hingorani, N.G. : " High Voltage Direct Current Power Transmission ", Garraway Limited, London, England 1960.

20. Gole, A.M., Turanli, H.M. and Woodford, D.A. : " Improved Interface of Electrical Machine Models to Electro Magnetic Transient Programs ", " IEEE Transactions on Power Apparatus and Systems, Vol. PAS-103, No.9, September 1984.

21. Badaway, E.H. : " Performance of Synchronous Generators with Bridge Rectifier output ", Electric Power Systems Research, No.8, pp. 1-7, 1985.

22. Abolins, A., Archenback, H. and Lambercht, D. : " Design and Performance of large four pole turbogenerators with Semiconductor excitation for nuclear power stations ", CIGRE, paper 11-04, 1972.

23. Kouskoff, G., Therby, M., Coustere, A. and Herouard, M. : " factors limiting the unit capacity of turbogenerators ", CIGRE, paper 11-08, 1974.

24. De Melloo, F. P. and Harnnett, L.H. : " Validation of Synchronous Machine Models and Derivation of Model Parameters from Tests ", IEEE Transactions on Power Apparatus and Systems, Vol. PAS-100, No. 2, pp. 662-672, February 1981.

25. Gole, A.M. : " Exciter Stresses in Capacitively loaded Synchronous Generator ", Ph.D Thesis, The University of Manitoba, Winnipeg, Canada, 1982.

26. Ainsworth, J.D. : " The Phase Locked Oscillator- A New Control System for Controlled Static Converters ", IEEE Transactions on PAS, PAS-87, No. 3, March 1968.

27. Clade, Jaques. J. : " Calculation of dynamic behaviuor of generators connected to a DC Link ", IEEE Transactions on PAS, PAS-87, No. 7, July 1968.

28. Adkins, B. and Harley, R.G. : " The General Theory of Alternating Current Machines ", Chapman and Hall, LOndon, 1970.

29. Ogata, K. : " Modern Control Engineering ", Printice-Hall, 1970.

30. Naidu, M. and Mathur, R.M. : " Unit connection of HVDC convertors ", IEE Conference on AC and DC Power Transmission, London, Sept. 1985.

31. Naidu, M. and Mathur, R.M. : " Unit connection of double three phase generator to HVDC converters ", MONTECH '86, IEEE Conference on HVDC Power Transmission, Montreal, October 1986.

32. Naidu, M. and Mathur, R.M. : " Analysis of the armature m.m.f of the double phase synchronous generator connected to the HVDC converters for unit connection scheme ", International Conference on Harmonics in Power Systems, Winnipeg, Canada, October 1986.

33. Glebov, I.A. : " Additional losses in Synchronous Generator Rotor and its Electromagnetic Moment Under Rectifier Load Operation ", Electra No. 17, pp. 14-27, 1971.

34. Becker, W. and Hochsletter, W. : " HVDC Transmission system connected to an Isolated Hydro Power Station ", IEE Conference on High Voltage DC and/or AC Power transmission, London, November 1973.

35. Kimbark, K.W. : " Direct Current Transmission ", Vol. I, Wiley Interscience, New York, 1971.

36. Uhlmann. : " Power transmission by DC ", Springer Verlag, 1975.

37. Arrilaga, J. : " Direct Current Transmission ", John Wiley & Company Inc., 1984.

38. Estrom, A. and Liss, G. : " Basic problems of control and protection of multiterminal HVDC schemes with and without d.c switching devices ", CIGRE, paper 14-08, 1972.

39. Carlos, A.O. Peixoto. : " Itaipu 6300 MW HVDC Transmission System Feasibility and Planning Aspects ", HVDC Symposium on " Incorporating Power Transmission into System Planning ", Phoenix, Arizona, March 1980.

40. Lindh, C.B. : " Power transfer uprating by conversion of ac lines to dc ", HVDC symposium on " Incorporating HVDC Power Transmission into System Planning", Phoenix, Arizona, March 1980.

41. Tarnawecky, M.Z. : " HVDC Graduate Course Notes ", University of Manitoba, Winnipeg, Canada, 1985.

42. Woodford, D.A. : " The incomplete book on Power system Simulation using Electro Magnetic Transients Direct Current Program (EMTDC) ", Manitoba Hydro, Winnipeg, Canada, 1983.

43. Last, F.H., Jarret, G.S.H., Huddart, K.W.,Brewer, G.L. and Watson,W.G. : " Isolated Generator- D.C.Link Feasibility Trails", IEE Conference on High Voltage DC Transmission, Part 1, pp. 58-65, London, 1966.

44. Ino. T., Mathur, R.M., Irvani. M.R. and Sasaki.S. : " Validation of digital simulation of DC links - Part II ", IEEE transactions on Power Apparatus and Systems, Vol. PAS-104, No.9, pp. 2596-2603, September 1985.

APPENDIX I

A : SIMILARITY CRITERIA FOR HYDROTURBINES

The important parameters governing the performance of a hydraulic turbine are :

(a) Water head (H), ft.

(b) Volume flow rate (Q), ft^3/s.

(c) Speed (N), rpm.

(d) Rotor diameter (D), ft.

Since most of the literature and the available data for hydraulic turbines are in British Systems, in this chapter the same is adopted. Flow similarities occur in turbomachines when geometric, kinematic and dynamic similarities between its model and large prototype exists [13]. These are :

(1) The ratio dimensions of corresponding points in flow field are the same throughout.

(2) Velocity triangles at corresponding points are also similar.

For example, similar velocity triangles imply equal flow coefficients. Similarity flow in hydrodynamics require a constant ratio between fluid velocity and peripheral velocity of the runner at all geometrically similar points of the machines compared. It means that

$$\frac{\tilde{V}}{\tilde{U}} = \text{Constant}$$

Where :

$\tilde{V}$ = Fluid Velocity, ft/s.

$\tilde{U}$ = Peripheral Velocity, ft/s.

But

$$H \alpha \frac{\tilde{V}^2}{2g}, \text{ ft.}$$

Volume flow rate, $Q = \tilde{V} . A$, ft^3/s

Where :

A = Area of cross section of Fluid flow.

αD^2

$Q \alpha \tilde{V} . D^2$

$$\tilde{V} \alpha \frac{Q}{D^2}$$

Peripheral speed of the runner , $\tilde{U} = \frac{\pi D N}{60}$, ft/s

Therefore :

$$\xi = \frac{\tilde{V}}{\tilde{U}}$$

$$= \frac{Q}{D^3 . N} \qquad \text{(A.1)}$$

Where ξ called the ' Flow Coefficient '.

Dynamic relation :

$$H \alpha \frac{\tilde{V}^2}{2g}$$

and also

$$H \alpha \frac{\tilde{V}^2}{2g}$$

Therefore :

$$\frac{g \cdot H}{\tilde{V}^2} = \text{Constant} \qquad (A.2)$$

$$\frac{g \cdot H}{\tilde{U}^2} = \text{Constant} \qquad (A.3)$$

From the Eqns. (A.2) and (A.3)

$$\psi = \frac{g \cdot H}{D^2 \cdot N^2} = \text{Constant} \qquad (A.4)$$

The Power Coefficient C_p is defined as :

$$C_p = \xi \cdot \psi$$

$$= \frac{Q}{N \cdot D^3} \cdot \frac{g \cdot H}{N^2 \cdot D^2}$$

$$= \frac{g \cdot P \cdot 550}{\rho \cdot N^3 \cdot D^5} \qquad (A.5)$$

Where :

$$P = \frac{Q \cdot H \cdot \rho}{550} \quad \text{(power input in hp)}$$

ρ = Density of the water, lb/ft^3.

By similarity condition, we can arrive at :

$$\frac{C_p^{1/2}}{\psi^{5/4}} = \text{Constant}$$

i.e.

$$\frac{(500\,P)^{1/2} \cdot g^{1/2}}{\rho^{1/2} \cdot N^{3/2} \cdot D^{5/2}} \cdot \frac{N^{5/2} \cdot D^{5/2}}{H^{5/4} \cdot g^{5/4}} = \text{Constant}$$

This constant is called the ' Specific speed of the turbine ' and is denoted by N_s'.

Where :

$$N_s' = \frac{P^{1/2} \cdot N \cdot (500)^{1/2}}{H^{5/4} \cdot g^{3/4} \cdot \rho^{1/2}}$$

This is the dimensionless quantity. But,

$$N_s' = K \cdot N_s$$

Where :

$$K = \frac{(550)^{1/2}}{g^{3/4} \cdot \rho^{1/2}} = \text{Constant}$$

$$N_s = \frac{N \cdot P^{1/2}}{H^{5/4}} \qquad \text{(A.6)}$$

N_s also can be defined as specific speed which is not a dimensionless quantity. This is used in this thesis.

APPENDIX II

I : AN ANALYSIS OF AIR GAP MMF OF Y-Y CONNECTED ARMATURE WINDINGS WITH 30^0 PHASE SHIFT

The generator with Y-Y windings configuration with 30^0 phase shift between winding axes is connected directly to two six pulse bridge rectifiers as shown in Fig. (4.5). The armature phase currents are shown in Fig. (4.6).

The armature current in phase a is given by :

$$i_a(t) = \frac{2\sqrt{3}\, I_{dc}}{\pi}\left\{ \cos(\omega t) - \frac{1}{5}\cos(5\omega t) + \frac{1}{7}\cos(7\omega t) - \frac{1}{11}\cos(11\omega t) + \frac{1}{13}\cos(13\omega t) - \cdots \right\} \qquad (B.1)$$

The conductor distribution of the armature winding of phase a is given by

$$n_a(\theta) = \frac{4}{\pi} N_a[\, kw_1 \cos(\theta) - kw_3 \cos(3\,\theta) + kw_5 \cos(5\,\theta) - kw_7 \cos(7\,\theta) + ..] \qquad (B.2)$$

The armature m.m.f distribution per pole of phase a due to current i_a is :

$$F_a(\,\theta\,,t\,) = 8\sqrt{3}\,\frac{N_a}{\pi^2}\, I_{dc} \cdot \left\{ \sum_{h=0}^{h=\infty} \sum_{k=0}^{k=\infty} \delta \left[\frac{\cos(6k+1)\omega t}{(6k+1)} - \frac{\cos(6k-1)\omega t}{(6k-1)} \right] \cdot \left[kw_{(2h+1)}\,(-1)^h \frac{\cos(2h+1)\theta}{(2h+1)} \right] \right\} \qquad (B.3)$$

Where k and δ are integers resulting in time and space harmonics respectively.

$$\delta = \frac{1}{2} \quad \text{for } k = 1$$

$$= 1 \quad \text{for other values of } k$$

After simplification the above equation can be written as :

$$F_a(\theta, t) = \frac{4\sqrt{3}\, N_a\, I_{dc}}{\pi^2} \left\{ \sum_{h=0}^{h=\infty} \sum_{k=0}^{k=\infty} (-1)^h\, \delta\, \frac{kw_{(2h+1)}}{(2h+1)} \cdot \right.$$

$$\left(\frac{1}{(6k+1)} \left\{ \cos\left[(6k+1)\omega t - (2h+1)\theta \right] + \cos\left[(6k+1)\omega t + (2h+1)\theta \right] \right\} \right.$$

$$- \frac{1}{(6k-1)} \left\{ \cos\left[(6k-1)\omega t - (2h-1)\theta \right] \right.$$

$$\left. \left. \left. + \cos\left[(6k-1)\omega t + (2h+1)\theta \right] \right\} \right) \right\} \qquad \text{(B.4)}$$

Where :

$m = (2h+1)$

N_a = Number of turns per phase

m the harmonic winding factor, $K_{wm} = K_{dm} \cdot K_{pm}$ m th harmonic distribution factor, $k_{dm} = \dfrac{\sin(\frac{m \gamma q}{2})}{q \cdot \sin(\frac{m \gamma}{2})}$

m th harmonic pitch factor, $k_{pm} = \cos(\frac{m \epsilon}{2})$

q = Slots per pole per phase.

γ = Slot angle in electrical degrees.

ϵ = Chording angle in electrical degrees.

Since the windings of phase b and phase c are displaced in space by $2\frac{\pi}{3}$ and $4\frac{\pi}{3}$ radians, respectively from phase a, the currents in the above phases are displaced by the same magnitude in time respectively with respect to the phase a.

The m.m.f distribution of phase b due to the current i_b is given by :

$$F_b(\theta, t) = \frac{4\sqrt{3}N_a I_{dc}}{\pi^2} \left\{ \sum_{h=0}^{h=\infty} \sum_{k=0}^{k=\infty} (-1)^h \delta \frac{kw_{(2h+1)}}{(2h+1)} \cdot \right.$$

$$\left(\frac{1}{(6k+1)} \left\{ \cos\left[(6k+1)(\omega t - 2\frac{\pi}{3}) - (2h+1)(\theta - 2\pi/3) \right] \right.\right.$$

$$\left.\left. + \cos\left[(6k+1)(\omega t - 2\frac{\pi}{3}) + (2h+1)(\theta - 2\frac{\pi}{3}) \right] \right\}$$

$$- \frac{1}{(6k-1)} \left\{ \cos\left[(6k-1)(\omega t - 2\frac{\pi}{3}) - (2h+1)(\theta - 2\frac{\pi}{3}) \right] \right.$$

$$\left.\left.\left. + \cos\left[(6k-1)(\omega t - 2\frac{\pi}{3}) + (2h+1)(\theta - 2\frac{\pi}{3}) \right] \right\} \right) \right\} \quad \text{(B.5)}$$

Similarly the armature m.m.f distribution of phase c due to current i_c is :

$$F_c(\theta, t) = \frac{4\sqrt{3}N_a I_{dc}}{\pi^2} \left\{ \sum_{h=0}^{h=\infty} \sum_{k=0}^{k=\infty} (-1)^h \delta \frac{kw_{(2h+1)}}{(2h+1)} \cdot \right.$$

$$\left(\frac{1}{(6k+1)} \left\{ \cos\left[(6k+1)(\omega t + 2\frac{\pi}{3}) - (2h+1)(\theta + 2\frac{\pi}{3}) \right] \right.\right.$$

$$+ \cos[\,(6k+1)(\omega t + 2\tfrac{\pi}{3}) + (2h+1)(\theta + 2\tfrac{\pi}{3})\,]\Big\}$$

$$-\frac{1}{(6k-1)}\Big\{\cos[\,(6k-1)(\omega t + 2\tfrac{\pi}{3}) - (2h+1)(\theta + 2\tfrac{\pi}{3})]$$

$$+ \cos[\,(6k-1)(\omega t + 2\tfrac{\pi}{3}) + (2h+1)(\theta + 2\tfrac{\pi}{3})\,]\Big\}\Big)\Big)\Big\} \qquad (B.6)$$

The resultant armature m.m.f of phases a, b and c is given by :

$$F_{abc}(\theta, t) = F_a(\theta, t) + F_b(\theta, t) + F_c(\theta, t)$$

After simplification the above expression yields to :

$$F_{abc}(\theta, t) = F \sum_{m=odd}^{m=\infty} \cdot \sum_{k=0}^{k=\infty} \delta \frac{kw_1}{m} \cdot \left(\frac{1}{(6k+1)} \cdot \cos[\,(6k+1)\omega t - \theta] - \frac{1}{(6k-1)} \cdot \cos[\,(6k-1)\omega t - \theta]\right)$$

$$\pm F \sum_{m=odd}^{m=\infty} \cdot \sum_{k=0}^{k=\infty} \delta \frac{kw_m}{m} \cdot \left(\frac{1}{(6k+1)} \cdot \cos[\,(6k+1)\omega t + m\theta] - \frac{1}{(6k-1)} \cdot \cos[\,(6k-1)\omega t \pm m\theta]\right) \qquad (B.7)$$

Where :

$$F_{abc} = \frac{12\sqrt{3}\, N_a\, I_{dc}}{\pi^2}$$

$$F_{(m,n)} = F \cdot \frac{kw_m}{m.n}$$

$F_{(m,n)}$ is the magnitude of the the m th armature m.m.f space harmonic caused by the n th current time harmonic in the windings.

The terms corresponding to m = 3 and its multiples equate to zero.

II : ARMATURE M.M.F OF Y- WINDING WITH 30^0 PHASE SHIFT

The armature current in phase i_x is given by :

$$i_x(t) = \frac{2\sqrt{3}\, I_{dc}}{\pi}\left(\cos(\omega t-\frac{\pi}{6}) - \frac{1}{5}\cos 5(\omega t-\frac{\pi}{6}) + \frac{1}{7}\cos 7(\omega t-\frac{\pi}{6}) - \frac{1}{11}\cos 11(\omega t-\frac{\pi}{6}) + \frac{1}{13}\cos 13(\omega t-\frac{\pi}{6}) \right) \qquad (B.8)$$

The conductors distribution of phase x is given by :

$$n_x(\theta) = \frac{4}{\pi}N_a\left(\cos(\theta-\frac{\pi}{6}) - \frac{1}{3}\cos 3(\theta-\frac{\pi}{6}) + \frac{1}{5}\cos 5(\theta-\frac{\pi}{6}) - \frac{1}{7}\cos 7(\theta-\frac{\pi}{6}) + \frac{1}{11}\cos 11(\theta-\frac{\pi}{6}) - \frac{1}{13}\cos 13(\theta-\frac{\pi}{6}) \right) \qquad (B.9)$$

The m.m.f of phase x due to current i_x is given by :

$$F_x(\theta, t) = i_x \cdot n_x(\theta)$$

$$= \frac{8\sqrt{3}}{\pi^2} N_a I_{dc} \left(\sum_{h=0}^{h=\infty} \delta \left(\frac{1}{(6k+1)} \cos[\,(6k+1)(\omega t-\frac{\pi}{6})\,] \right. \right.$$

$$- \frac{1}{(6k-1)} \cos\left[(6k-1)\left(\omega t - \frac{\pi}{6}\right) \right] \Bigg)$$

$$\cdot \left(\frac{kw_{(2h+1)}}{(2h+1)} \cdot (-1)^h \cdot \cos\left[(2h+1)\left(\theta - \frac{\pi}{6}\right) \right] \right) \Bigg) \qquad \text{(B.10)}$$

The y and z phase windings are displaced by $2\frac{\pi}{3}$ and $4\frac{\pi}{3}$ radians respectively the from phase x. The currents in the above windings are displaced by the same magnitude in time with respect to the phase x.

The m.m.f of phase y due to current i_y is :

$$F_y(\theta, t) = \frac{8\sqrt{3}}{\pi^2} N_a I_{dc} \left[\sum_{h=0}^{h=\infty} \delta \left(\frac{1}{(6k+1)} \cos\left[(6k+1)\left(\omega t - \frac{\pi}{6} - \frac{2\pi}{3}\right) \right] \right.\right.$$

$$\left. - \frac{1}{(6k-1)} \cos\left[(6k-1)\left(\omega t - \frac{\pi}{6} - \frac{2\pi}{3}\right) \right] \right)$$

$$\cdot \left(\frac{kw_{(2h+1)}}{(2h+1)} \cdot (-1)^h \cdot \cos\left[(2h+1)\left(\theta - \frac{\pi}{6} - \frac{2\pi}{3}\right) \right] \right) \Bigg) \qquad \text{(B.11)}$$

Similarly the m.m.f of phase z due to the current i_z is :

$$F_z(\theta, t) = \frac{8\sqrt{3}}{\pi^2} N_a I_{dc} \left[\sum_{h=0}^{h=\infty} \delta \left(\frac{1}{(6k+1)} \cos\left[(6k+1)\left(\omega t - \frac{\pi}{6} + \frac{2\pi}{3}\right) \right] \right.\right.$$

$$\left. - \frac{1}{(6k-1)} \cos\left[(6k-1)\left(\omega t - \frac{\pi}{6} + \frac{2\pi}{3}\right) \right] \right)$$

$$\cdot \left(\frac{kw_{(2h+1)}}{(2h+1)} \cdot (-1)^h \cdot \cos\left[(2h+1)\left(\theta - \frac{\pi}{6} + \frac{2\pi}{3}\right) \right] \right) \Bigg) \qquad \text{(B.12)}$$

The resultant m.m.f of x, y and z phases is :

$$F_{xyz}(\theta, t) = F_x + F_y + F_z$$

$$= F \cdot kw_1 \sum_{k=0}^{k=\infty} (-1)^k \cdot \delta \left\{ \left(\frac{1}{(6k+1)} \cos [\, (6k+1)\omega t - \theta \,] \right. \right.$$

$$\left. - \frac{1}{(6k-1)} \cos[\, (6k-1)\omega t + \theta \,] \right)$$

$$- F \cdot \frac{kw_5}{5} \sum_{k=0}^{k=\infty} (-1)^k \cdot \delta \left(\frac{1}{(6k+1)} \cos [\, (6k+1)\omega t + 5\theta \,] \right.$$

$$\left. - \frac{1}{(6k-1)} \cos [\, (6k-1)\omega t - 5\theta \,] \right)$$

$$+ F \cdot \frac{kw_7}{7} \sum_{k=0}^{k=\infty} (-1)^k \cdot \delta \left(\frac{1}{(6k+1)} \cos [\, (6k+1)\omega t - 7\theta \,] \right.$$

$$\left. - \frac{1}{(6k-1)} \cos[\, (6k-1)\omega t + 7\theta \,] \right)$$

$$+ F \cdot \frac{kw_{11}}{11} \sum_{k=0}^{k=\infty} (-1)^k \cdot \delta \left(\frac{1}{(6k+1)} \cos [\, (6k+1)\omega t + 11\theta \,] \right.$$

$$\left. - \frac{1}{(6k-1)} \cos [\, (6k-1)\omega t - 11\theta \,] \right)$$

$$- F \cdot \frac{kw_{13}}{13} \sum_{k=0}^{k=\infty} (-1)^k \cdot \delta \left(\frac{1}{(6k+1)} \cos [\, (6k+1)\omega t - 13\theta \,] \right.$$

$$\left. \left. - \frac{1}{(6k-1)} \cos [\, (6k-1)\omega t + 13\theta \,] \right) \right\} \qquad \text{(B.13)}$$

Where :

$$F = \frac{12\sqrt{3}}{\pi^2} I_{dc} N_a$$

The magnitude of F_{xyz} is zero for m = 3 and all its multiples.

The total armature m.m.f due to currents in two sets of three phase Y-Y windings displaced in space by 30 degrees is given by :

$$F_{Y-Y}(\theta, t) = F_{abc} + F_{xyz}$$

$$= \frac{24\sqrt{3}}{\pi^2} N_a I_{dc} \left(kw_1 [\cos(\omega t-\theta) - \frac{1}{11}\cos(11\omega+\theta) + \frac{1}{13}\cos(13\omega t-\theta) - \cdots] \right.$$

$$+ \frac{kw_5}{5} [- \frac{1}{5}\cos(5\omega t-5\theta) + \frac{1}{7}\cos(7\omega t+5\theta)]$$

$$- \frac{kw_7}{7} [\cos(- \frac{1}{5}\cos(5\omega t+7\theta) + \frac{1}{7}\cos(7\omega t-7\theta)]$$

$$+ \frac{kw_{11}}{11} [\cos(\omega t+11\theta) _ \frac{1}{11}\cos(11\omega t-11\theta) + \frac{1}{13}\cos(13\omega t+11\theta) - ..]$$

$$- \frac{kw_{13}}{13} [\cos(\omega t-13\theta) _ \frac{1}{11}\cos(11\omega t+13\theta)]$$

$$\left. + \frac{1}{13}\cos(13\omega t-13\theta) - \cdots] \right) \qquad (B.14)$$

II : ARMATURE M.M.F OF Y- Δ WINDINGS CONFIGURATION.

The generator with Y- Δ windings connected to two six pulse rectifier bridges is shown in Fig. (4.6). The armature phase currents are shown in

Fig. (4.7). The number of turns per phase in Δ connected windings is taken as $\sqrt{3}$ times the number of turns per phase of Y connected windings.

The Fourier analysis of the current wave form i_p shown in Fig. (4.7) is given by :

$$i_p(t) = \frac{2}{\pi} I_{dc} \left(\cos(\omega t) + \frac{1}{5}\cos(5\omega t) - \frac{1}{7}\cos(7\omega t) + \frac{1}{11}\cos(11\omega t) - \frac{1}{13}\cos(13\omega t) + .. \right)$$

$$= \frac{2}{\pi} I_{dc} \sum_{k=0}^{k=\infty} \delta\, (-1)^k \left(\frac{1}{(6k+1)}\cos(6k+1)\omega t \right.$$

$$\left. - \frac{1}{(6k-1)}\cos(6k-1)\omega t \right) \qquad \text{(B.15)}$$

The turns distribution of phase winding p is given by :

$$n_p(\theta) = \frac{4}{\pi} N_a \sqrt{3} \left[kw_1 \cos(\theta) - kw_3 \cos(3\,\theta) + kw_5 \cos(5\,\theta) - kw_7 \cos(7\,\theta) + .. \right]$$

$$= \frac{4}{\pi} N_a \sqrt{3} \sum_{h=0}^{h=\infty} \frac{1}{(2h+1)} kw_{(2h+1)} \cdot (-1)^h \cdot \cos\left[(2h+1)\theta \right] \qquad \text{(B.16)}$$

The armature m.m.f distribution per pole of phase p due to current i_p is :

$$F_p(\theta\ ,\ t) = 8\frac{\sqrt{3}}{\pi^2} N_a I_{dc} \cdot \left(\sum_{h=0}^{h=\infty} \sum_{k=0}^{k=\infty} \delta(-1)^k \left[\frac{\cos(6k+1)\omega t}{(6k+1)} - \frac{\cos(6k-1)\omega t}{(6k-1)} \right.\right.$$

$$\left.\left. \left[kw_{(2h+1)} (-1)^h \frac{\cos(2h+1)\theta}{(2h+1)} \right] \right) \qquad \text{(B.17)}$$

After simplification the above equation can be written as:

$$F_p(\theta, t) = \frac{4\sqrt{3}\, N_a\, I_{dc}}{\pi^2} \left\{ \sum_{h=0}^{h=\infty} \sum_{k=0}^{k=\infty} (-1)^h (-1)^k\, \delta\, \frac{kw_{(2h+1)}}{(2h+1)} \cdot \right.$$

$$\left(\frac{1}{(6k+1)} \left\{ \cos\left[(6k+1)\omega t - (2h+1)\theta \right] + \cos\left[(6k+1)\omega t + (2h+1)\theta \right] \right\} \right.$$

$$- \frac{1}{(6k-1)} \left\{ \cos\left[(6k-1)\omega t - (2h-1)\theta \right] \right.$$

$$\left. \left. \left. + \cos\left[(6k-1)\omega t + (2h+1)\theta \right] \right\} \right) \right\} \qquad \text{(B.18)}$$

Where :

$$\delta = \frac{1}{2} \quad \text{for } k = 1$$

$$= 1 \quad \text{for other values of } k$$

Since the windings of phase q and phase r are displaced in space by $2\frac{\pi}{3}$ and $4\frac{\pi}{3}$ radians respectively from phase p, the currents in the above phases are displaced by same angles in time with respect to phase p.

The m.m.f distribution of phase q due to the current i_q is :

$$F_q(\theta, t) = \frac{4\sqrt{3}\, N_a\, I_{dc}}{\pi^2} \left\{ \sum_{h=0}^{h=\infty} \sum_{k=0}^{k=\infty} (-1)^h (-1)^k\, \delta\, \frac{kw_{(2h+1)}}{(2h+1)} \cdot \right.$$

$$\left(\frac{1}{(6k+1)} \left\{ \cos\left[(6k+1)(\omega t - 2\frac{\pi}{3}) - (2h+1)(\theta - 2\pi/3) \right] \right.\right.$$

$$\left.\left. + \cos\left[(6k+1)(\omega t - 2\frac{\pi}{3}) + (2h+1)(\theta - 2\frac{\pi}{3}) \right] \right\}$$

$$- \frac{1}{(6k-1)} \left\{ \cos \left[(6k-1)(\omega t - 2\frac{\pi}{3}) - (2h-1)(\theta - 2\frac{\pi}{3}) \right] \right.$$

$$\left. + \cos \left[(6k-1)(\omega t - 2\frac{\pi}{3}) + (2h+1)(\theta - 2\frac{\pi}{3}) \right] \right\} \Bigg) \Bigg) \Bigg\} \qquad \text{(B.19)}$$

The armature m.m.f distribution of phase r due to the current i_r is :

$$F_r(\theta, t) = \frac{4\sqrt{3}\, N_a\, I_{dc}}{\pi^2} \left\{ \sum_{h=0}^{h=\infty} \sum_{k=0}^{k=\infty} (-1)^h (-1)^k \delta \frac{kw_{(2h+1)}}{(2h+1)} \cdot \right.$$

$$\left(\frac{1}{(6k+1)} \left\{ \cos \left[(6k+1)(\omega t + 2\frac{\pi}{3}) - (2h+1)(\theta + 2\pi/3) \right] \right. \right.$$

$$\left. \left. + \cos \left[(6k+1)(\omega t + 2\frac{\pi}{3}) + (2h+1)(\theta + 2\frac{\pi}{3}) \right] \right\} \right.$$

$$- \frac{1}{(6k-1)} \left\{ \cos \left[(6k-1)(\omega t + 2\frac{\pi}{3}) - (2h-1)(\theta + 2\frac{\pi}{3}) \right] \right.$$

$$\left. \left. \left. + \cos \left[(6k-1)(\omega t + 2\frac{\pi}{3}) + (2h+1)(\theta + 2\frac{\pi}{3}) \right] \right\} \right) \right) \Bigg\} \qquad \text{(B.20)}$$

The resultant armature m.m.f of p, q and r phases is given by :

$$F_{pqr}(\theta, t) = F_p(\theta, t) + F_q(\theta, t) + F_r(\theta, t)$$

After simplification, the above expression yields to :

$$F_{pqr}(\theta, t) = F \sum_{m=odd}^{m=\infty} \sum_{k=0}^{k=\infty} \delta (-1)^k \frac{kw_m}{m} \left\{ \frac{1}{(6k+1)} \cos \left[(6k+1)\omega t - m\theta \right] \right.$$

$$- \frac{1}{(6k-1)} \cdot \cos [\, (6k-1)\omega t + m\theta] \Bigg\} \qquad \text{(B.21)}$$

Where :

$$F = \frac{12\sqrt{3}\, N_a\, I_{dc}}{\pi^2}$$

The value of F_{pqr} becomes zero for m = 3 and its all multiples.

The armature mmf of a, b and c phase windings due to currents i_a , i_b and i_c is given by the equation (A.7).

Therefore, the resultant air gap m.m.f of Y- Δ windings is :

$$F_{Y-\Delta} = \frac{24\sqrt{3}}{\pi^2} I_{dc}\, N_a \sum_{m=odd}^{m=\infty} \cdot \sum_{m=odd}^{m=\infty} \frac{kw_m}{m} \cdot$$

$$\Bigg\{ \frac{1}{(\,12k+1\,)} \cdot \cos [\,(\,12k+1\,)\omega t + m\theta\,]$$

$$\frac{1}{(\,12k-1\,)} \cdot \cos [\,(\,12k-1\,)\omega t \pm m\theta\,] \Bigg\} \qquad \text{(B.22)}$$

IV : Machine data

MVA	125.0
Voltage	11.0 kV
Poles	2
Number of slots	72
Pole pitch	36 slots
Coil pitch	33 slots
Slots/pole/phase	6

APPENDIX III

A : SIX PHASE SYNCHRONOUS GENERATOR DATA

2 X 588 MVA, 22 kV, 0.85 pf, 3600 rpm round rotor machine.

(a) Reactances:

x_a = 0.113 p.u

x_{12} = 0.113 p.u

x_{md} = 1.153 p.u

x_{kf} = 0.0 p.u

x_f = 0.12 p.u

x_{kd} = 0.027 p.u

x_{mq} = 0.94 p.u

x_{kq} = 0.032 p.u

x_d = 0.2467 p.u

x_q = 0.227 p.u

x_d'' = 0.2476 p.u

x_q'' = 0.227 p.u

Resistances:

r_a = 0.0008 p.u

r_{kd} = 0.0044 p.u

r_f = 0.00035 p.u

r_{kq} = 0.002 p.u

Current regulator:

T_1 = 0.015 s

T_a = 0.1 s

K_p = 1500

R_N = 2.0 ohms

(b) Generator base quantities:

I_{base} = 15.1 kA

V_{base} = 12.7 kV

Z_{base} = 0.841 Ω

I_f = 1.23 p.u (to produce 1.0 p.u open circuit voltage)

(c) DC system quantities:

I_{dc} = 18.5 kA

V_{dc} = 56.0 kV

P_d = 1036 MW

E_c = 24.4 kV

$$\text{Base MVA} = \frac{\pi}{3} V_0 I_{dc}$$

$$= \frac{\pi}{3} \times 2 (1.35 \times 42.4) \times 18.5$$

$$= 1276 \text{ MVA}$$

$$Z_{sb} = \text{Base impedance of the system} = \frac{E_c^2}{(MVA)_{base}}$$

$$= \frac{(24.4)^2}{1276} = 0.466 \Omega$$

B : SIX PHASE GENERATOR EQUATIONS

(a) Induced voltages in the armature windings displaced by 30°:

$$v_a = p\,(\psi_{md}\cos\theta + \psi_{mq}\sin\theta) + (r_a + L_1 p)\,i_a$$
$$- L_{m1}\,p i_b - L_{m1}\,p i_c + L_{m2}\,p i_x - L_{m2}\,p i_y \qquad \text{(C.1)}$$

$$v_x = p\psi_{md}\cos\left(\theta-\frac{\pi}{6}\right) + \psi_{mq}\sin\left(\theta-\frac{\pi}{6}\right) + (r_a+L_1 p)\,i_x$$
$$-L_{m1}\,p i_y - L_{m1}\,p i_z + L_{m2}\,p i_a - L_{m2}\,p i_c \qquad \text{(C.2)}$$

Where :

L_1 = Leakage inductance of an armature coil without coupling with other coils.

$+L_{m2}$ = Mutual inductance between coils displaced by ± 30° due to the part of the flux which does not crossthe air gap.

$-L_{m2}$ = Mutual inductance between coils displaced by ± 150° due to the part of the flux which does not crossthe air gap.

$-L_{m1}$ = Mutual inductance between coils displaced by ± 120° due to the part of the flux which does not crossthe air gap.

L_1, L_{m1} and L_{m2} are assumed to be independent of the rotor position.

(1) : d-q-o axis equations for armature winding set 1 :

$$v_a = v_{d1}\cos\theta + v_{q1}\sin\theta + v_{o1} \qquad \text{(C.3)}$$

$$i_a = i_{d1}\cos\theta + i_{q1}\sin\theta + i_{o1} \qquad \text{(C.4)}$$

$$i_x = i_{d2}\cos(\theta-\frac{\pi}{6}) + i_{q2}\sin(\theta-\frac{\pi}{6}) + i_{o2} \qquad (C.5)$$

$$i_y = i_{d2}\cos(\theta-\frac{\pi}{6}-\frac{2\pi}{3}) + i_{q2}\sin(\theta-\frac{\pi}{6}-\frac{4\pi}{3}) + i_{o2} \qquad (C.6)$$

$$i_{o1} = \frac{1}{3}(i_a + i_b + i_c) \qquad (C.7)$$

From (C.5) and (C.6)

$$(i_x - i_y) = \sqrt{3}\, i_{d2}\cos\theta + \sqrt{3}\, i_{q2}\sin\theta \qquad (C.8)$$

Equating (C.1) and (C.3) using (C.4) to (C.7)

$$v_{d1} = p\psi_{md} + p(L_1 + L_{m1})\, i_{d1} + p\sqrt{3}\, L_{m2}\, i_{d2}$$
$$+ \omega\, \psi_{mq} + \omega\, (L_1 + L_{m1})\, i_{q1} + \sqrt{3}\, L_{m2}\, i_{q2} + r_a\, i_{d1} \qquad (C.9)$$

$$v_{q1} = p\psi_{mq} + p(L_1 + L_{m1})\, i_{q1} + p\sqrt{3}\, L_{m2}\, i_{q2}$$
$$- \omega\, \psi_{md} - \omega\, (L_1 + L_{m1})\, i_{d1} - \omega\sqrt{3}\, L_{m2}\, i_{d2} + r_a\, i_{q1} \qquad (C.10)$$

$$v_{o1} = r_a\, i_{o1} + p(L_1 - 2\, L_{m1})\, i_{o1} \qquad (C.11)$$

(2) : d-q-o axis equations for winding set 2 :

$$v_{d2} = p\psi_{md} + p(L_1 + L_{m1})\, i_{d2} + p\sqrt{3}\, L_{m2}\, i_{d1}$$
$$+ \omega\, \psi_{mq} + \omega\, (L_1 + L_{m1})\, i_{q2} + \sqrt{3}\, L_{m2}\, i_{q1} + r_a\, i_{d2} \qquad (C.12)$$

$$v_{q2} = p\psi_{mq} + p(L_1 + L_{m1})\, i_{q2} + p\sqrt{3}\, L_{m2}\, i_{q1}$$
$$- \omega\, \psi_{md} - \omega\, (L_1 + L_{m1})\, i_{d2} - \omega\sqrt{3}\, L_{m2}\, i_{d1} + r_a\, i_{q2} \qquad (C.13)$$

$$v_{o2} = r_a\, i_{o2} + p(L_1 - 2\, L_{m1})\, i_{o2} \qquad (C.14)$$

The eqations from (C.9) to (C.14) can be simplified as :

$$v_{d1} = p\,\psi_{d1} + \omega\,\psi_{q1} + r_a\,i_{d1} \tag{C.15}$$

$$v_{q1} = p\,\psi_{q1} - \omega\,\psi_{d1} + r_a\,i_{d1} \tag{C.16}$$

$$v_{o1} = (p\,L_o + r_a)\,i_{o1} \tag{C.17}$$

$$v_{d2} = p\,\psi_{d2} + \omega\,\psi_{q2} + r_a\,i_{d2} \tag{C.18}$$

$$v_{q2} = p\,\psi_{q2} - \omega\,\psi_{d2} + r_a\,i_{d2} \tag{C.19}$$

$$v_{o2} = (p\,L_o + r_a)\,i_{o2} \tag{C.20}$$

Where :

$$\psi_{d1} = \psi_{md} + L_a\,i_{d1} + L_{12}\,(i_{d1} + i_{d2}) \tag{C.21}$$

$$\psi_{q1} = \psi_{mq} + L_a\,i_{q1} + L_{12}\,(i_{q1} + i_{q2}) \tag{C.22}$$

$$\psi_{d2} = \psi_{md} + L_a\,i_{d2} + L_{12}\,(i_{d1} + i_{d2}) \tag{C.23}$$

$$\psi_{q2} = \psi_{mq} + L_a\,i_{q2} + L_{12}\,(i_{q1} + i_{q2}) \tag{C.24}$$

$$\psi_{md} = L_{md}\,(i_{d1} + i_{d2} + i_f + i_{kd}) \tag{C.25}$$

$$\psi_{mq} = L_{mq}\,(i_{q1} + i_{q2} + i_{kq}) \tag{C.26}$$

$$L_{12} = \sqrt{3}\,L_{m2} \tag{C.27}$$

$$L_a = L_1 + L_{m1} - L_{12} \tag{C.28}$$

$$L_o = L_1 - 2\,L_{m1} \tag{C.29}$$

(b) Simplified equations for deriving equivalent circuits :

Direct axis equations :

$$\psi_{d1} = (L_{md} + L_a + L_{12}) i_{d1} + (L_{md} + L_{12}) i_{d2} + L_{md} i_{kd} + L_{md} i_f \quad \text{(C.30)}$$

$$\psi_{d2} = (L_{md} + L_{12}) i_{d1} + (L_{md} + L_a + L_{12}) i_{d2} + L_{md} i_{kd} + L_{md} i_f \quad \text{(C.31)}$$

$$v_f = L_{md} p i_{d1} + L_{md} i_{d2} i_{d2} + (L_{md} + L_{kf}) p i_{kd} + [r_f + (L_{md} + L_k + L_{kf}) p] i_f \quad \text{(C.32)}$$

$$0 = L_{md} p i_{d1} + L_{md} p i_{d2} + (L_{md} + L_{kf}) p i_f + [r_{kd} + (L_{md} + L_{kd} + L_{kf}) p] i_{kd} \quad \text{(C.33)}$$

Quadrature axis equations :

$$\psi_{q1} = (L_{mq} + L_a + L_{12}) i_{q1} + (L_{mq} + L_{12}) i_{q2} + L_{mq} i_{kq} \quad \text{(C.34)}$$

$$\psi_{q2} = (L_{mq} + L_{12}) i_{q1} + (L_{mq} + L_a + L_{12}) i_{q2} + L_{mq} i_{kq} \quad \text{(C.35)}$$

$$0 = L_{mq} p i_{q1} + L_{mq} p i_{q2} + (L_{mq} + L_{kq}) p i_{kq} \quad \text{(C.36)}$$

APPENDIX IV

(A) : GENERATOR PARAMETERS AT 60 HZ OPERATION:

Ratings: 120 MVA, 13.8 kV, 0.927 pf, three phase synchronous generator.

(a) Reactances:

x_a = 0.170 p.u

x_{md} = 0.936 p.u

x_{kf} = 0.002 p.u

x_f = 0.152 p.u

x_{kd} = 0.122 p.u

x_{mq} = 0.472 p.u

x_{kq} = 0.0835 p.u

x_d'' = 0.24 p.u

x_q'' = 0.23 p.u

Resistances:

r_a = 0.0037 p.u

r_f = 0.00035 p.u

r_{kd} = 0.0035 p.u

r_{kq} = 0.0035 p.u

The field current required for 1.0 p.u open circuit voltage, $I_{fo} = \frac{\sqrt{2}}{x_{md}} = 1.51$ p.u

Rated full load field current, I_f = 2.59 p.u

(B) : Calculation of generator field current under steady state normal operation :

Under steady state condition, $i_{kd} = I_{kq} = 0$

The voltage equations can be written as :

$$V_d = V_o \cos \omega t \tag{D.1}$$

$$V_q = I_o \cos (\omega t + \phi) \tag{D.2}$$

But,

$$V_a = V_o \cos \omega t \tag{D.3}$$

$$I_a = I_o \cos (\omega t + \phi) \tag{D.4}$$

Therefore :

$$V_d = V_o \cos \theta_o \tag{D.5}$$

$$V_q = V_o \sin \theta_o \tag{D.6}$$

$$I_d = I_o \cos (\theta_o - \phi) \tag{D.7}$$

$$I_q = I_o \sin (\theta_o - \phi) \tag{D.8}$$

By substituting (D.5) to (D.8) into (D.1) and (D.2)

$$\theta_o = \tan^{-1} \left[\frac{V_o - r_a I_a \cos \phi + (x_{md} + x_a) I_a \sin \phi}{r_a I_o \sin \phi + (x_{mq} + x_a) I_o \cos \phi} \right] \tag{D.9}$$

From (D.2)

$$I_f = \frac{-V_o \sin \theta_o + r_a I_o \sin (\theta_o - \phi) - (x_{md} + x_a) I_o \cos (\theta_o - \phi)}{x_{md}} \tag{D.10}$$

Initial conditions :

$V_o = 1.414$ p.u

$I_o = 1.414$ p.u

$\cos \phi = 0.927,$

$\phi = 22.0^\circ$ or 158°

$\phi = 158^\circ$ (Motor convention is used)

$\theta_o = -64.55^\circ$

Where θ_o is the initial angle of phase a with d-axis.

$I_{fo} = 2.59$ p.u

$E_{fd} = 1.72$ p.u

Static Exciter data :

$T_A = 1.43$ s

$T_B = 7.04$ s

$K = 289$

$T_E = 0.012$ s

$E_{max} = 5.0$ p.u

$E_{min} = -3.5$ p.u

APPENDIX V

5.6.2 : Small signal analysis of a three phase generator connected to a 12-pulse diode bridge rectifier

The schematic diagram of a generator connected to a 12-pulse diode bridge rectifier through converter transformers is shown in Fig. (5.9). The no load dc voltage on the inverter side is assumed to be constant. The current in the dc link is kept constant by the current controller on the inverter.

5.6.2.1 Generator equations :

Assumptions:

(1) Armature windings of the generator are sinusoidally distributed around the periphery of the armature.

(2) Saturation in the machine is neglected.

(3) One damper winding in each axis is considered.

Since the purpose of this study is to find the dc voltage regulation, 0-5 Hz frequency range of operation is considered. This range is more than sufficient to study the regulation problems considering the relatively large time constants which governs the dynamic behaviour of the alternator[27]. Under this condition transformer voltages in the machine can be neglected relative to rotational voltages. It is also assumed in this analysis that the converters are continuously controlled under these frequencies. The

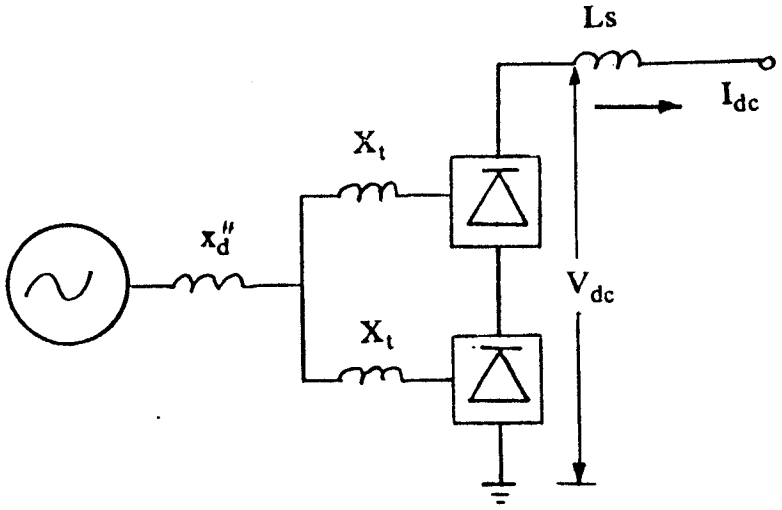

Fig. 5.9 : Schematic diagram of a generator connected to a 12-pulse diode bridge rectifier.

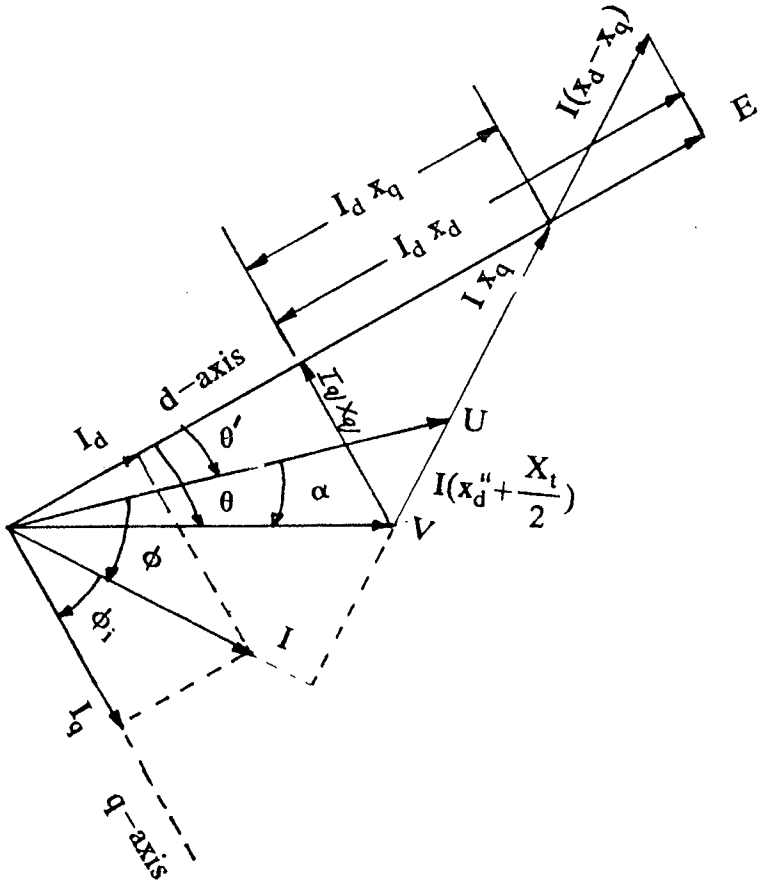

Fig. 5.10 : Steady state phasor diagram of the generator with 12-pulse rectifier load.

generalized Park's equations are used for evaluating the machine performance. The steady state phasor diagram of the generator connected to the rectifier load is shown in Fig. (5.10). For a given field voltage, the steady state of the machine is completely characterized by the vector $\frac{E}{V}$ which is stated being equal to [27].

$$\frac{E}{V} = \rho\, e^{j\theta} \tag{5.6.1}$$

Where :

$$\rho = \left| \frac{E}{V} \right|$$

E = Electromotive force

V = Terminal voltage of the generator per phase

The normalized incremental Park's equations in terms of operational impedances can be written as [28] :

$$\Delta V_d = H(p)\, \Delta I_d + \Delta N \tag{5.6.2}$$

$$\Delta V_q = \frac{(\cos\theta - \rho)}{\cos\theta} F(p)\, \Delta I_d + \frac{\rho}{\cos\theta} G(p)\, \Delta e_f + \Delta N \tag{5.6.3}$$

The incremental values are normalized with respect to the steady state values. Subscripts d and q apply to direct and quadrature axes components; E_f and N are generator field voltage and speed respectively and p is the Laplace operator. The expression for operational impedances H(p), F(p) and G(p) are given by :

$$H(p) = \frac{(1 + T_q'' p)}{(1 + T_{qo}'' p)} \tag{5.6.4}$$

$$F(p) = \frac{(1 + T_d' p) . (1 + T_d'' p)}{(1 + T_{do}' p) . (1 + T_{do}'' p)} \tag{5.6.5}$$

$$G(p) = \frac{(1 + T_{kd} p)}{(1 + T_{do}' p) . (1 + T_{do}'' p)} \tag{5.6.6}$$

Internal commutation voltage :

When the generator is connected to the bridge rectifier, it is subjected to periodic two phase short circuit at the terminals due to commutation phenomena. The voltage which remains constant during commutation period is the voltage behind the subtransient reactance under the reasonable assumption that constant flux linkage theorem is applicable to the synchronous machine. This voltage is called commutation voltage where the ideal no load voltage is proportional to it. It is therefore necessary to calculate the components of this voltage as a function of current components I_d and I_q.

Assuming $x_d'' \approx x_q''$ from Fig. (5.10)

$$U_d = V_d - jx_d'' I_q \tag{5.6.7}$$

$$U_q = V_q + jx_d'' I_d \tag{5.6.8}$$

Where, U is the voltage behind the subtransient reactance per phase.

By defining $\frac{E}{U} = \rho' e^{j\theta'}$, then the normalized incremental equations for ΔU_d and ΔU_q can be written by differentiating (5.6.7) and (5.6.8) and using (5.6.4) to (5.6.6)

$$\Delta U_d = [\, 1 - (\, 1 - H(p) \frac{\rho' \sin \theta}{\rho \sin \theta'} \,] \Delta I_q + \Delta N \tag{5.6.9}$$

$$\Delta U_q = \left[1 + \frac{(\rho' \cos\theta - \rho)}{\rho \cos\theta'} F(p) - \frac{\rho' \cos\theta}{\rho \cos\theta'} \right] \Delta I_d$$

$$+ \frac{\rho'}{\cos\theta'} G(p)\, \Delta e_f + \Delta N \qquad (5.6.10)$$

If the inertia of the rotating mass is large, the speed variations around the operating point can be neglected. The signal flow graph of the alternator with $\Delta N = 0$ is shown in Fig. (5.11).

By using Mason's gain formula, the overall gain between the input Δe_f and the output ΔU is given by [29]

$$G = \frac{1}{\Delta} \sum_k G_k \Delta_k$$

Where :

G_k = Path gain of kth forward path

Δ = Determinant of graph

= 1 - (Sum of all different loop gains)

+ (Sum of gain products of all possible combinations of two non touching loops)

- (Sum of gain products of all possible combinations of three non touching loops)

+ . . . . .

$$= 1 - \sum_a L_a + \sum_{b,c} L_b L_c - \sum_{d,e,f} L_d L_e L_f + \cdots$$

Where :

$\sum_{a} L_a$ = Sum of all different loop gains.

$\sum_{b,c} L_b L_c$ = Sum of gain products of all possible combinations of two non touching loops.

$\sum_{d,e,f} L_d L_e L_f$ = Sum of gain products of all possible combinations of three non touching loops.

Δ_k = Co-factor of the k th forward path determinant of the graph with loops touching the k th forward path removed.

From the signal flow graph shown in Fig. (5.11)

$$\Delta = 1 - h_3 h_7 h_8 + h_3 h_5 h_6$$

$$\Delta_1 = 1 + h_3 h_5 h_6$$

$$\Delta_2 = 1$$

$$G_1 = h_1 h_2$$

$$G_2 = h_1 h_3 h_4 h_5 h_6$$

$$G = \frac{h_1 [h_2 + h_3 h_5 h_6 (h_2 + h_4)]}{1 - h_3 (h_7 h_8 - h_5 h_6)}$$

Where :

$$h_1 = \frac{\rho'}{\cos \theta'} G(p)$$

$$h_2 = \cos^2 \theta'$$

$$h_3 = \sin \theta' \cos \theta'$$

$$h_4 = \sin^2 \theta'$$

$$h_5 = \tan (\theta' + \phi)$$

$$h_6 = 1 - [1+H(p)] \frac{\rho' \sin \theta}{\rho \sin \theta'}$$

$$h_7 = - \cot (\theta' + \phi)$$

$$h_8 = 1 + \frac{\rho' (\cos \theta - \rho)}{\rho \cos \theta'} F(p) - \frac{\rho' \cos \theta}{\rho \cos \theta'}$$

Therefore :

$$G = \frac{\Delta U}{\Delta e_f} = \text{Transfer function between } \Delta U \text{ and } \Delta e_f$$

$$\left[\frac{\rho'}{\cos \theta} G(p) \left\{ \cos^2 \theta' + \sin \theta' \cos \theta' \tan (\theta' + \phi) . \left(1 - (1 - H(p) \frac{\rho' \sin \theta}{\rho \sin \theta} \right) . [\sin^2 \theta' + \cos^2 \theta'] \right\} \right]$$

$$\frac{\Delta U}{\Delta e_f} = \frac{}{}$$

$$\left[1 + \sin \theta' \cos \theta' \left\{ \cot (\theta' + \phi) \left(1 + \frac{\rho' (\cos \theta - \rho)}{\rho \cos \theta'} F(p) - \frac{\rho' \cos \theta}{\rho \cos \theta'} \right) + \tan (\theta' + \phi) \left[(1 - (1 - H(p)) \frac{\rho' \sin \theta}{\rho \sin \theta'} \right] \right\} \right] \qquad (5.6.11)$$

If the influence of subtransient behaviour which occurs only at frequencies of more than or around 5 Hz is neglected, then equations (5.6.4) to (5.6.6) are simplified by letting

$$T_d'' = T_q'' = T_{do}'' = T_{qo}'' = 0$$

Therefore the simplified equations can be written as :

$$H(p) = 1$$

$$F(p) = \frac{1 + T_d'' p}{1 + T_{do}''}$$

$$G(p) = \frac{1 + T_{kd} p}{1 + T_{do}'' p}$$

The simplified transfer function can be written as :

$$\frac{\Delta U}{\Delta e_f} = \frac{K_1 G(p)}{1 + k_6 [k_5 (1+k_2 F(p)-k_3) + K_4]} \qquad (5.6.12)$$

Where :

$$K_1 = \rho' [\cos\theta' + \sin \theta'] \tan (\theta' + \phi)$$

$$K_2 = \frac{\rho (\cos \theta - \rho)}{\rho \cos \theta''}$$

$$K_3 = \frac{\rho'' \cos \theta}{\rho \cos \theta''}$$

$$K_4 = \tan (\theta'' + \phi)$$

$$K_5 = \cot (\theta'' + \phi)$$

$$K_6 = \sin \theta'' \cos \theta''$$

It can be further simplified as :

$$\frac{\Delta U}{\Delta e_f} = \frac{K_1 G(p)}{K_7 + K_8 F(p)}$$

Where :

$$K_7 = 1 - K_5 K_6 K_3 + K_4 K_6 + K_6 K_5$$

$$K_8 = K_5 K_6 K_2$$

Further simplification of the above transfer function yields to :

$$\frac{\Delta U}{\Delta e_f} = \frac{K_9 G(p)}{(K_{10} + F(p))}$$

Where :

$$K_9 = \frac{K_1}{K_8} \text{ and } K_{10} = \frac{K_7}{K_8}$$

The final form of the transfer function is :

$$\frac{\Delta U}{\Delta e_f} = K_v \frac{(1+T_{kd} p)}{(1+T_d^{\bullet} p)} \qquad (5.6.13)$$

Where :

$$K_v = \frac{K_9}{(1+K_{10})}$$

$$T_d^{\bullet} = \frac{(K_{10} T_{do}'' + T_d'')}{(1+K_{10})}$$

To take the subtransient effect into account for considering the system behaviour at 5 Hz or above, the time constant T_{do}'' should be added to the above transfer function since $(1+T_{do}'' s)$ term is contained in G(p) which occurs as a multiplier term in the transfer function. This term will introduce marginal phase shift at 5 Hz.

The transfer function taking subtransient effect of the machine into account is given by :

$$\frac{\Delta U}{\Delta e_f} = K_v \frac{(1+T_{kd} p)}{(1+T_{do}'' p) (1+T_d^{\bullet} p)} \qquad (5.6.14)$$

If the current in the dc link is kept constant by means of current regulator at the inverter, then the variation in dc current is assumed to be zero. In this case the incremental dc voltage, ΔV_{dc} is given by :

$$\Delta V_{dc} = \frac{3\sqrt{6}}{\pi} \left(\frac{U}{V_{dc}} \right) \Delta U \qquad (5.6.15)$$

Where :

$$h_9 = \frac{3\sqrt{6}}{\pi} \frac{U}{V_{dc}}$$

The transfer function between field voltage and dc voltage is given by

$$\frac{\Delta V_{dc}}{\Delta e_f} = \frac{K (1+T_{kd} p)}{(1+T_{do}'' p) (1+T_d^{\bullet} p)} \qquad (5.6.16)$$

Where :

$$K = K_v . K_9$$

T_{kd} = Direct-axis damper leakage time constant

T_{do}'' = Direct-axis subtransient short circuit time constant

The parameters of the transfer function are calculated in Appendix V for the system with a 120 MVA generator connected to a 12-pulse diode bridge rectifier for unit connection scheme as shown in Fig. (5.9).

5.6.2.2 DC voltage regulation :

In order to control the dc voltage by means of generator field excitation, the measured dc voltage is compared with the reference value and the error signal is amplified and fed to the exciter as shown in Fig. (5.12). The

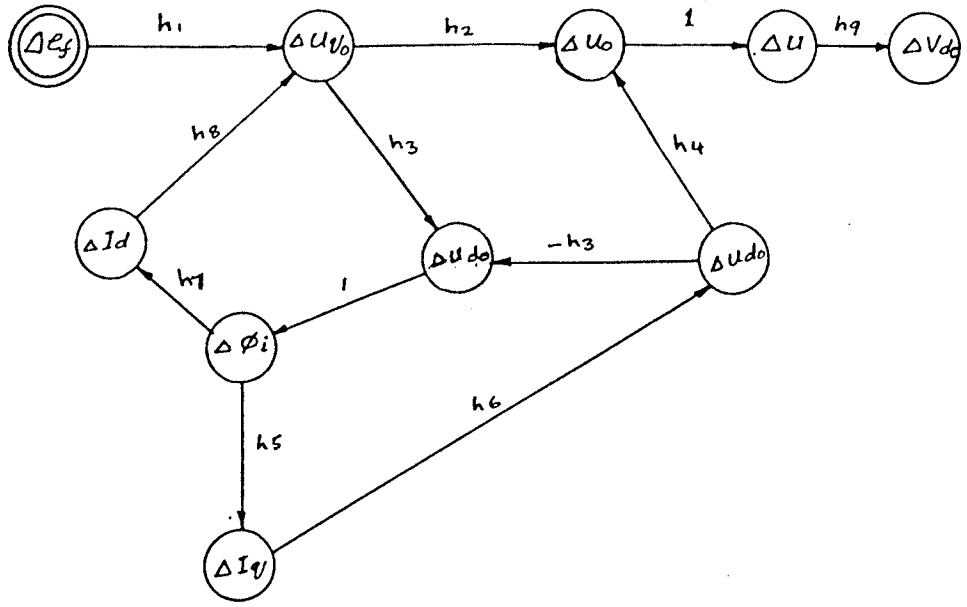

Fig. 5.11 : Signal flow graph of the alternator with rectifier load.

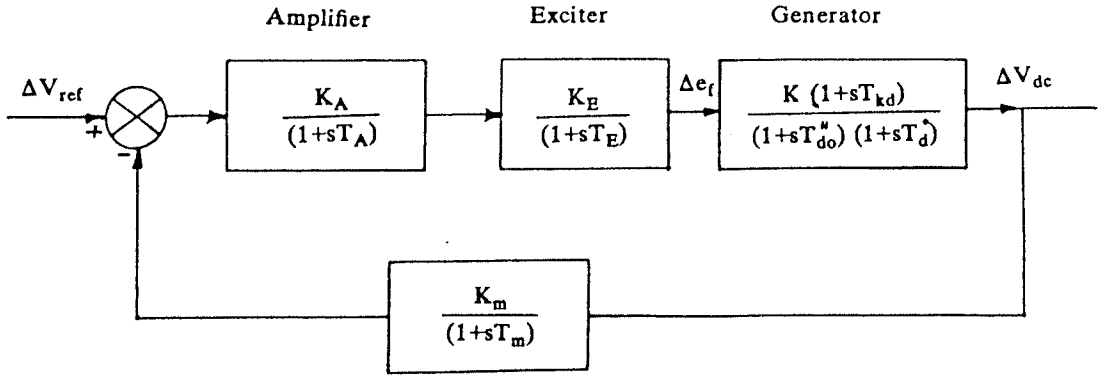

Fig. 5.12 : Block diagram of dc voltage control without compensator.

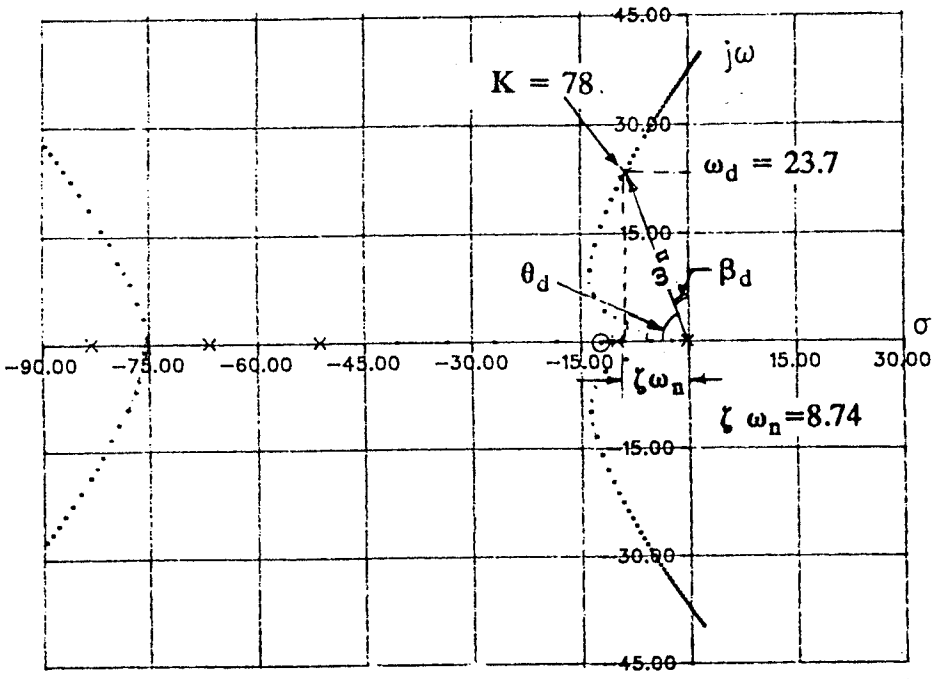

Fig. 5.13 : Root locus of the system without compensator.

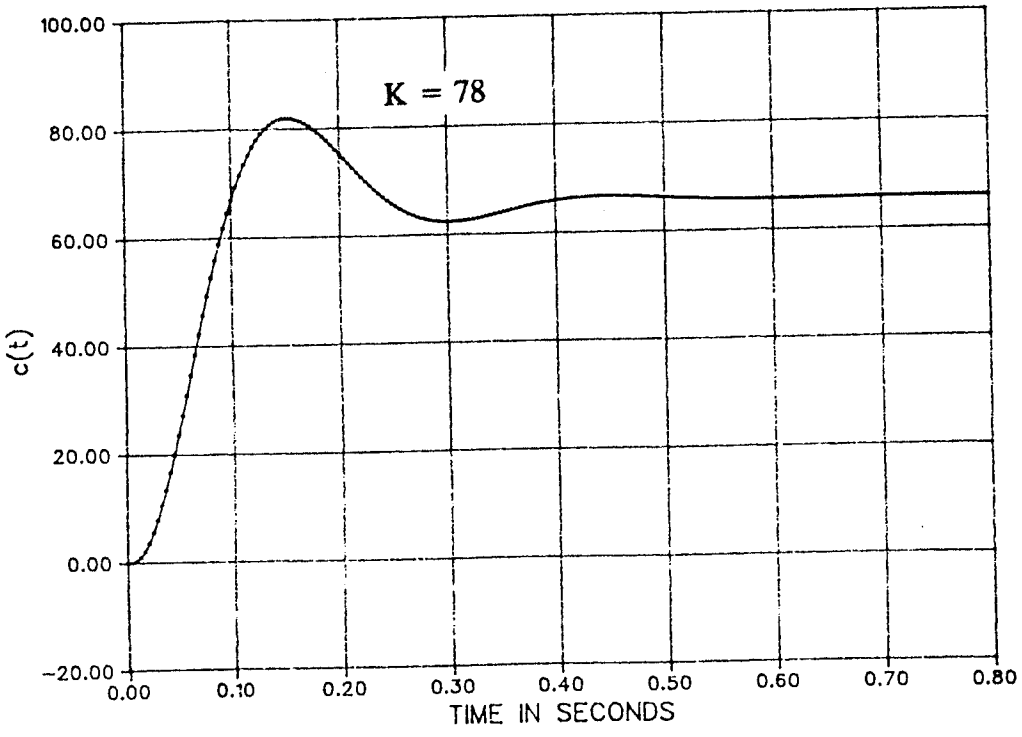

Fig. 5.14 : System response for the step input without compensator.

characteristic equation of the transfer function of Fig. (5.12) is given by :

$$1 + G(s)\,H(s) = K\,(1+0.095s) + (1+sT_A)\,(1+0.012s)\,(1+0.195s)\,(1+6.17s) = 0$$

The root locus of the of the open loop transfer function G(s) H(s) is shown in Fig. (5.13) for T_A = 0.1 s. It can be seen from the root locus that the dominant poles at s = -0.162 and at s = -10 tend to move the locus towards jω axis and crosses the imaginary axis for a gain, K equals to 246. But, in order to achieve proper response of the system, the gain should not exceed 78 as seen from the step response shown in Fig.(5.14). The dominant roots are located at -8.74 ± j 23.7 for the above value of gain. The settling time, t_s, for ± 2% tolerance band of the final value can be measured in terms of the time constant, T.

i.e $\quad t_s = 4\,T$

Where :

$$T = \frac{1}{\zeta\,\omega_n}$$

$\zeta\,\omega_n = \sigma$ = Real part pf the dominant root at a given damping ζ

From the Fig. (5.14), the damping factor ζ is found to be

$$\zeta = \cos\theta_d = \frac{\zeta\,\omega_n}{\omega_n} = 0.37$$

The undamped natural frequency, ω_n = 25.3 radians/s.

The damped natural frequency, ω_d = 23.7 radians/s.

The settling time, t_s = 0.46 s.

The maximum over shoot, M_p = 21%

The rise time, t_r is given by :

$$t_r = = \frac{\pi - \beta_d}{\omega_d} = 0.12s.$$

The system performance is satisfactory for the gain of 78, beyond which the system response overshoots with oscillations as shown in Fig. (5.15).

In order to increase the system gain to a reasonable value, say 100, the dominant poles near the imaginary axis in s-plane have to be moved away from it to the left of s-plane. This is achieved by means of a lead compensator. The transfer function of the compensator is given by

$$G_c = \frac{(1+s\,T_A)}{(1+s\,T_B)}$$

The controller block diagram with compensator is shown in Fig. (5.15). The time constants T_A and T_B are selected such that the root locus moves away from $j\omega$ axis towards left side of the s-plane. The zero is selected nearer to the dominant pole and the pole is selected five times away from the zero such that its effect is non-dominant at high frequency range. For T_A = 0.05 s and T_B = 0.01 s, the zero and the pole of the compensator are located at s = -20 and s = -100. The root locus of the system with the compensator is shown in Fig. (5.17). The system has optimum response with the above compensator in feed forward path as shown in Fig. (5.18). It has been tried for other pole zero combination of the compensator, but the system response did not improve for higher values of gain.

Parameters of the system with gain of 93 is calculated from the root locus shown in Fig. (5.17) and from the step response shown in Fig. (5.18) are given below :

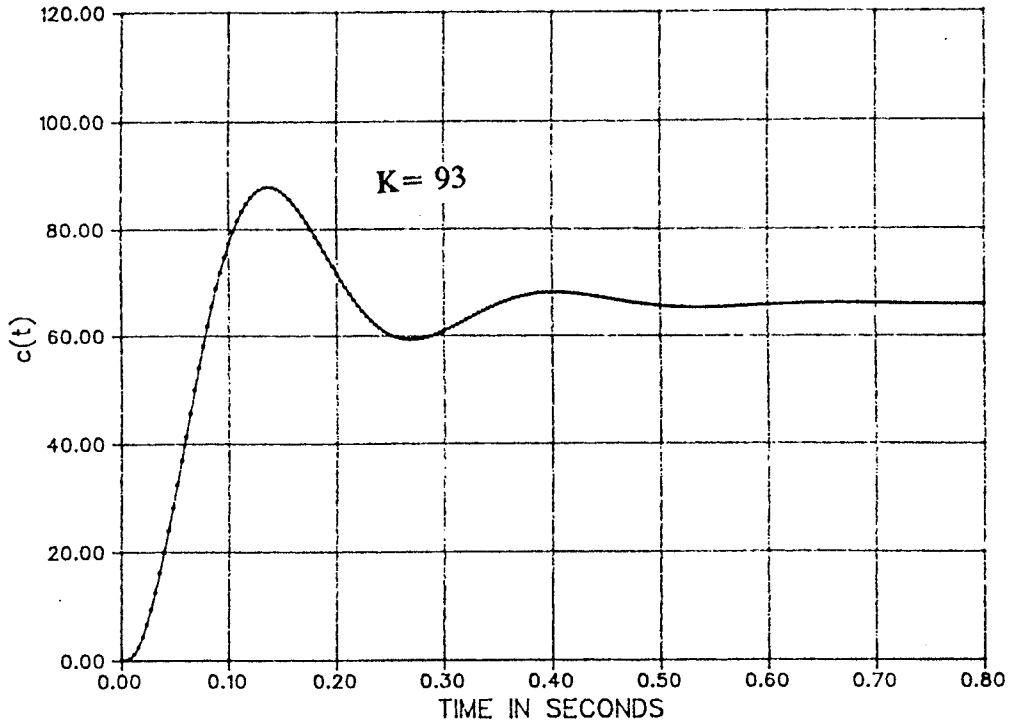

Fig. 5.15 : System response without compensation at higher gain.

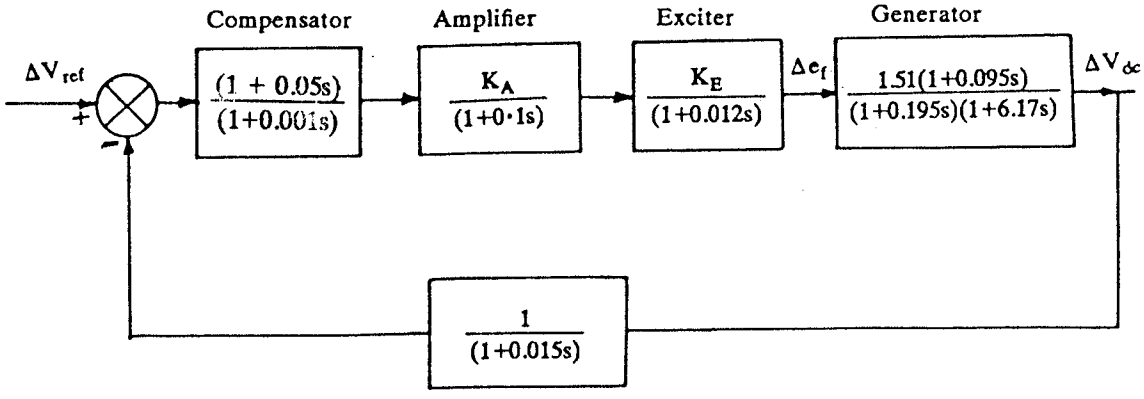

Fig. 5.16 : Block diagram of the controller with compensator.

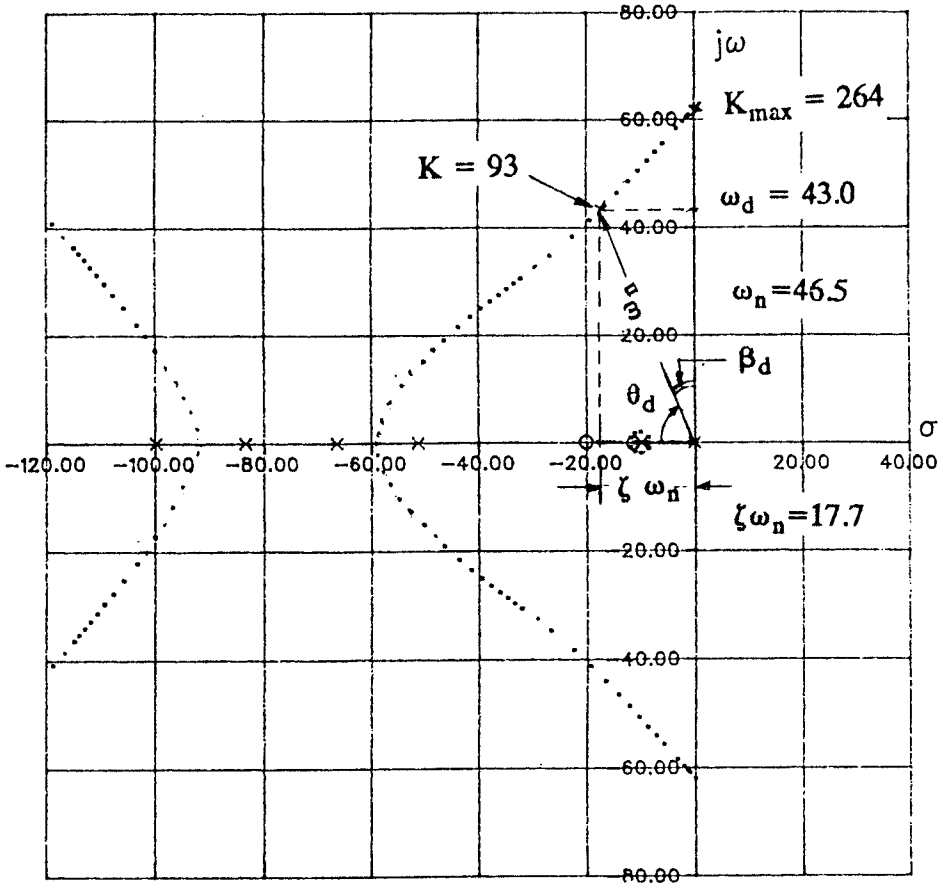

Fig. 5.17 : Root locus of the system with compensator.

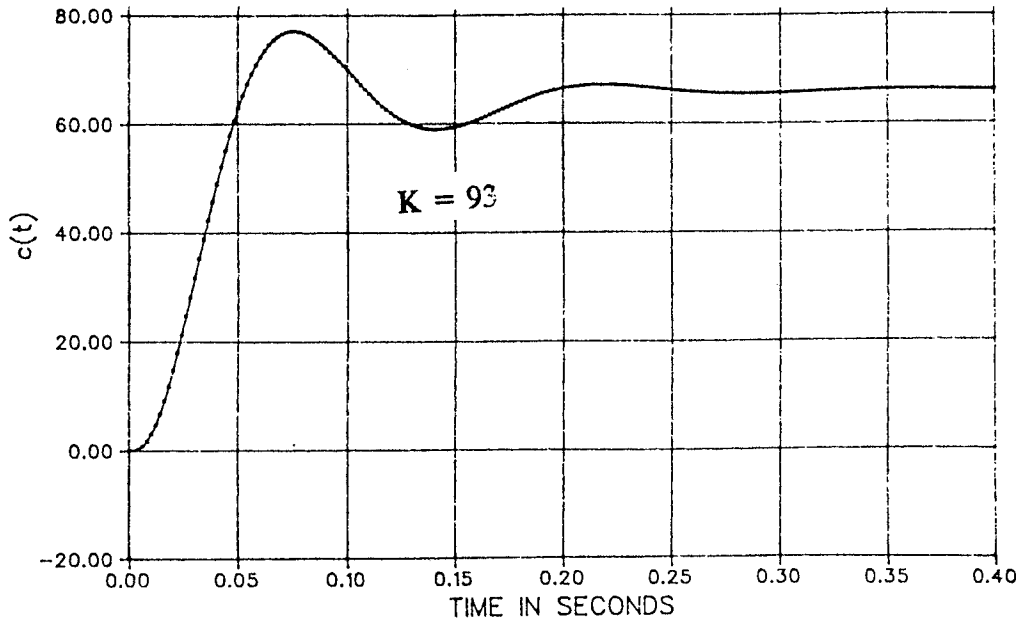

Fig. 5.18 : System response for step input with compensator.

Location of dominant poles = $-17.7 \pm j\ 43.0$

Damped natural frequency, ω_d = 43.0 radians/s.

Un damped natural frequency, ω_n = 46.5 radians/s.

Damping factor, $\zeta = \frac{\zeta\ \omega_n}{\omega_n} = 0.38$

Settling time, t_s = 0.23 s.

Rise time, $t_r = \pi - \beta_d$ = 0.06 s.

Maximum over shoot, M_p = 10.9%

It can be observed that by selecting T_A = 0.05 s and T_B = 0.01 s, of the compensator the response of the system has been improved at reasonably large values of the system gain as compared to the uncompensated system.

In conclusion, the dc voltage can be regulated with generator field excitation by properly selecting the regulator time constants for optimum response at reasonable system gain.

5.6.3 : Calculation of parameters of diode bridge rectifier scheme

DC System ratings : 500 MW, 500kV, 1000 A per pole

Number of generators per pole = 5

Length of dc line = 556 miles

DC line resistance/ mile = 0.025 Ω

Total resistance of the dc line, r = 13.9 Ω

DC voltage per pole at the inverter = 500 kV

DC voltage per pole at the rectifier = $500 + I_{dc}\ r$

$= 500 + 1.0\ (13.9) = 513.9$ kV

DC voltage per 12-pulse rectifier bridge = 103 kV

Transformer leakage reactance, X_t = 0.13 p.u

Generator subtransient reactance, x_d'' = 0.232 p.u

Commutation reactance, $X_{c2} = \frac{x_d''}{2} + X_t = 0.246$ p.u

(for $\mu \leq 30^\circ$)

For 12-pulse operation the overlap angle, μ should not exceede 30°. If the overlap angle exceeds 30°, then the effective commutation reactance is given by [3] :

$$X_c = \frac{[\,(\mu-30)\,X_{c1} + (60-\mu)\,X_{c2}\,]}{30} \qquad \text{(E.1)}$$

Where :

$$X_{c1} = x_d'' + X_t \qquad \text{(E.2)}$$

$$X_{c2} = \frac{x_d''}{2} + X_t \qquad \text{(E.3)}$$

Therefore :

$$X_{c1} = 0.362 \text{ p.u}$$

$$X_{c2} = 0.246 \text{ p.u}$$

The overlap angle can be calculated by :

$$X_c = \cos\alpha - \cos(\alpha + \mu) \qquad \text{(E.4)}$$

With $X_c = X_{c2} = 0.246$ p.u, assuming $\mu < 30^\circ$ the actual value of the overlap angle calculated from (E.4) is 41° Since the overlap angle exceeded 30°, the effective commutation reactance is calculated using Eqn. (E.1) as given below :

$$X_c = \frac{[\,(41-30)\,0.362 + (60-41)\,0.246\,]}{30} = 0.284 \text{ p.u}$$

With the above commutation reactance, the commutation line voltage E_c is calculated by using :

$$V_{dc} = \frac{6\sqrt{2}}{\pi} E_c \left(1 - \frac{X_c}{2}\right) \qquad \text{(E.5)}$$

The commutation voltage, E_c = 44.6 kV. Therefore the commutation voltage per phase, U = 25.75 kV.

The secondary current of the transformer, $I_L = \sqrt{\frac{2}{3}}\, I_{dc} = 816.5$ A

The no load ideal voltage, $V_o = \frac{6\sqrt{2}}{\pi} E_c$

The MVA rating of each transformer = $\frac{\pi}{3} V_o I_{dc} = 63$ MVA

Since two two-winding transformers are connected to the generator, the rating of the generator should be 2X63 = 126 MVA.

The generator phase voltage, V_p = 7.97 k V

(i) : Derivation of transfer function parameters :

Referring to the phasor diagram of the generator with rectifier load as shown in Fig. (10), the angles can be calculated as follows :

$$\cos \phi = \frac{\cos \alpha + \cos \mu}{2}$$

$$= \frac{1 + \cos 41}{2} = 0.877$$

Therefore, $\phi = 28.7^{o}$

Generator phase current, I = 5.27 kA

Generator base current, I_{base} = 5.27 kA

Generator base voltage, V_{base} = 7.97 kV

Base impedance, Z_{base} = 1.51 Ω

With, X_c = 0.289 p.u = 0.436 Ω

$$\tan \beta = \frac{U \phi - I X_c}{U \cos \phi} \qquad \text{(E.6)}$$

$$= \frac{U \sin(28.7) - 5.27\ (0.436)}{U \cos(28.7)}$$

From the above realtion the generator phase voltage is given by :

$$V_p = \frac{U \cos \phi}{\cos \beta} = 7.97 \qquad \text{(E.7)}$$

From (E.6) and (E.7), β can be solved by trail and error method by initially guessing the value of U.

$\beta = 14^{o}$

U = 8.8 kV

$\alpha = \phi - \beta = 14.7^{o}$

$$\tan \theta = \frac{I x_q \cos \beta}{V_p + I X_q \sin \beta}$$

With X_q = 0.642 p.u = 0.69 Ω

$\tan \theta = 0.578$, therefore, $\theta = 30^{o}$

$$\theta' = \theta - \alpha = 30 - 14.7 = 15.3^{o}$$

$$\phi_i = 90 - (\theta + \beta) = 46^\circ$$

$$\phi_u = \alpha + \beta = 14.7 + 14.0 = 28.7^\circ$$

(ii) : Calculation of E :

$$I_{dc} = I \cos \phi_i = 3.66 \text{ kA}$$

$$E = V_p \cos \theta + I_{dc} + x_d$$

With $x_d = 1.106$ p.u $= 1.67\ \Omega$ the value of E = 13.0 kV.

(iii) : Calculation of constants :

$$\left|\frac{E}{V_p}\right| = \rho = \frac{13.0}{7.97} = 1.633$$

$$\left|\frac{E}{U}\right| = \rho' = \frac{13.0}{8.8} = 1.477$$

$$K_1 = \rho' [\cos \theta' + \sin \theta' \tan (\theta'+\phi)] = 1.8$$

$$K_2 = \frac{\rho' \cos \theta - \rho}{\rho \cos \theta'} = -0.224$$

$$K_3 = \frac{\rho' \cos \theta}{\rho \cos \theta'} = 0.812$$

$$K_4 = \tan (\theta'+\phi) = 0.966$$

$$K_5 = \cot (\theta'+\phi) = 1.035$$

$$K_6 = \sin \theta' \cos \theta' = 0.2545$$

$$K_7 = 1 - k_5 K_6 K_3 + K_4 K_6 + K_6 K_5 = 0.277$$

$$K_8 = K_5 K_6 K_2 = -0.059$$

$$K_9 = \frac{K_1}{K_8} = -30.5$$

$$K_{10} = \frac{K_7}{K_8} = -3.47$$

$$K_v = \frac{K_9}{(1+K_{10})} = 12.35$$

$$T_d^* = \frac{K_{10}\, T_{do}' + T_d'}{1 + K_{10}}$$

With $T_{do}' = 4.1$s and $T_d' = 1.123$ s, $T_d^* = 6.17$ s

$$T_{kd} = 0.0925 \text{ s}$$

$$K = K_v \frac{3\sqrt{6}}{\pi} \frac{U}{V_{dc}} = 4.94$$

The transfer function time constants are given below :

T_{kd} = Damper leakage time constant = 0.0925 s

T_{do}'' = 0.0195 s

T_d^* = 6.17 s

T_E = Exciter time constant = 0.012 s

T_m = Measurement time constant = 0.015 s